DETECTOR BACKGROUNDS

Fast Neutron and **Gamma-ray** Sensitivity
of **Helium-3** and **Boron-10** Detectors
and Effect of Window and Cosmic Neutrons

Francesco Piscitelli
on behalf of the ESS Detector Group

IKON18
Lund
2020/02/25

DETECTOR BACKGROUND

- Cosmic neutrons
- Gamma-rays
- Fast Neutrons
- Scattered Neutrons

He-3 vs B-10

DETECTOR BACKGROUND

- Cosmic neutrons
- Gamma-rays
- Fast Neutrons
- Scattered Neutrons

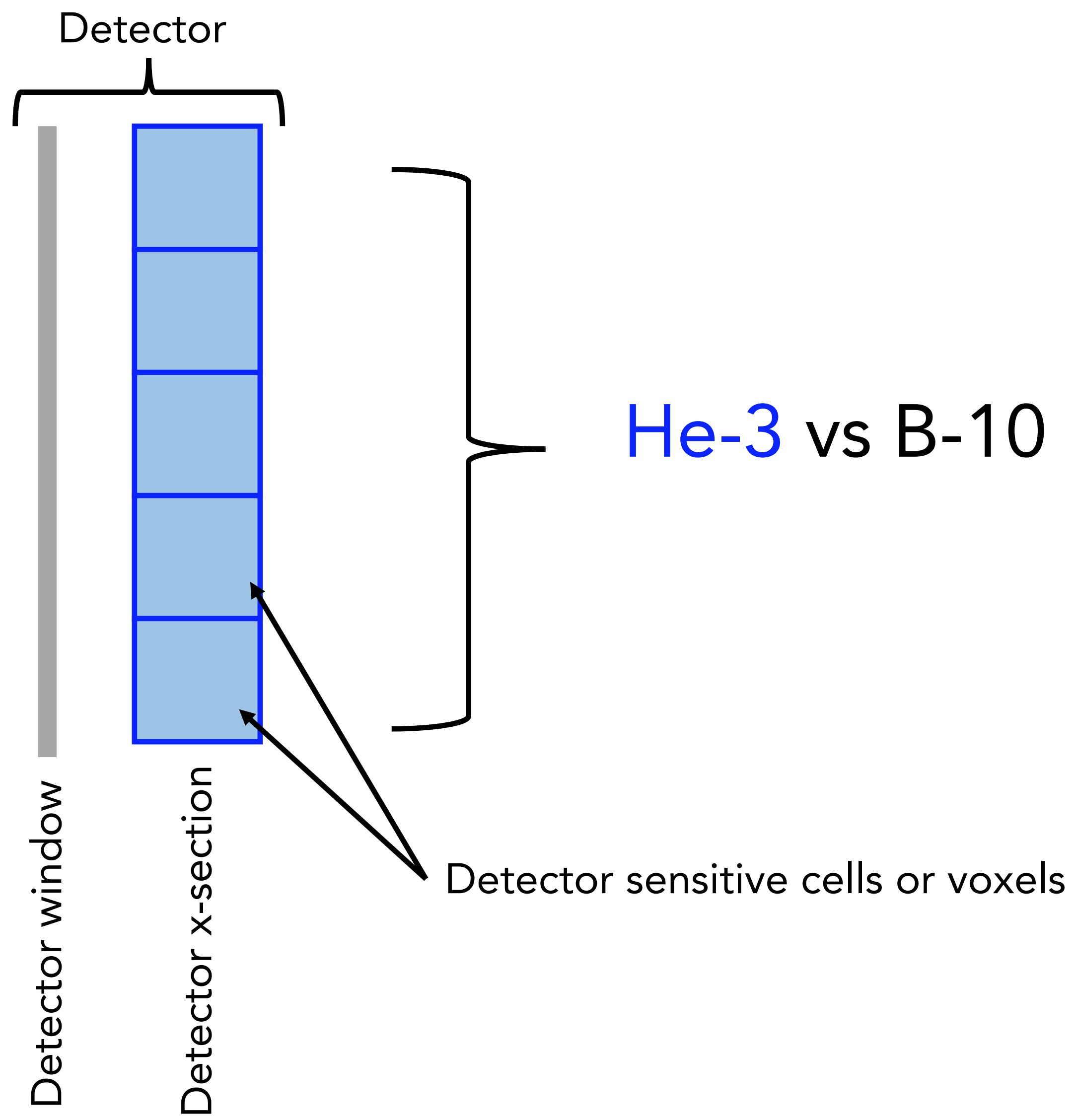

DETECTOR BACKGROUND

- Cosmic neutrons
- Gamma-rays
- Fast Neutrons
- Scattered Neutrons

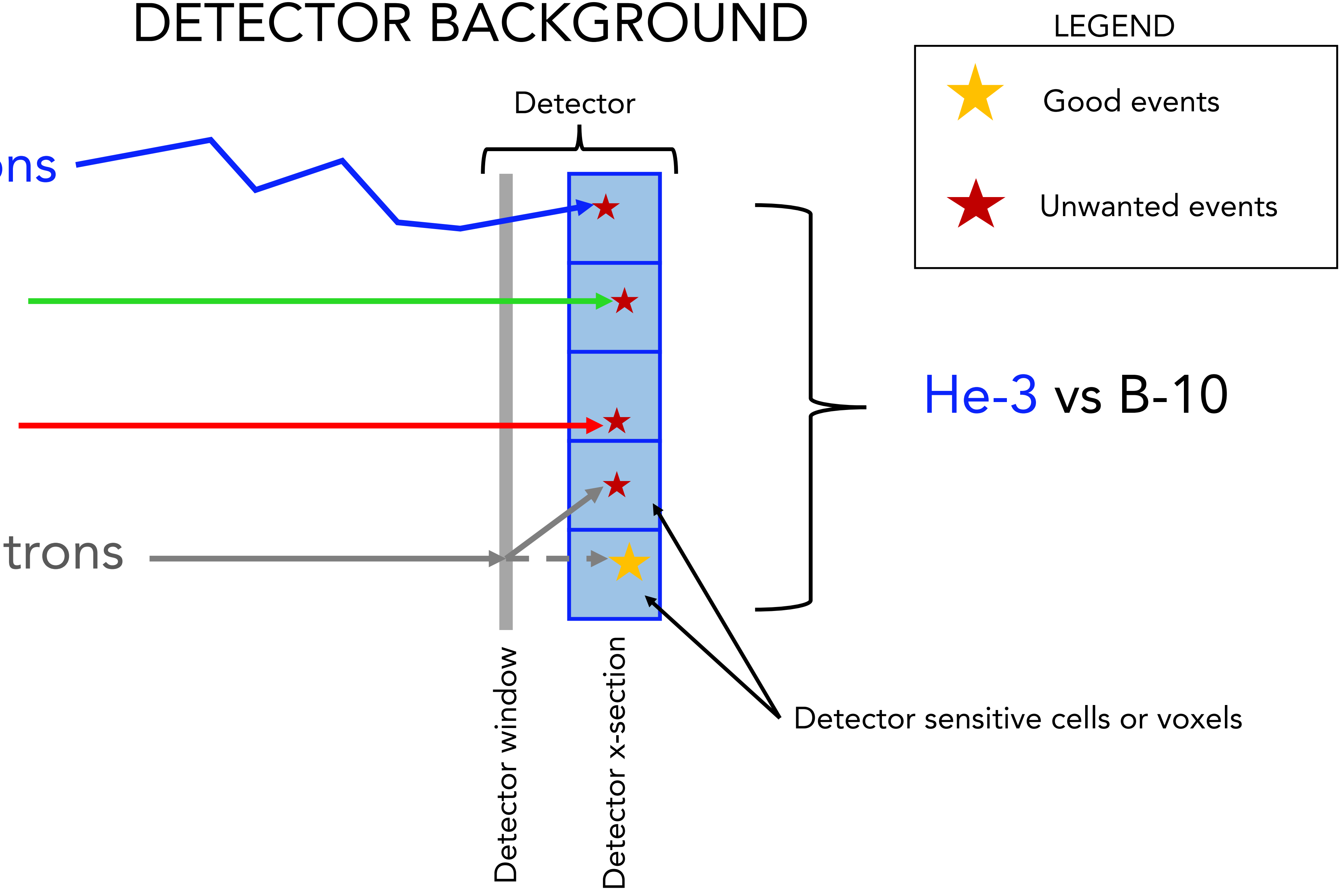

COSMIC NEUTRON BACKGROUND

BACKGROUND: cosmic neutrons

Neutrons are created by cosmic ray spallation in the high atmosphere.
Energies from 10^{-9} to 10^{3} MeV

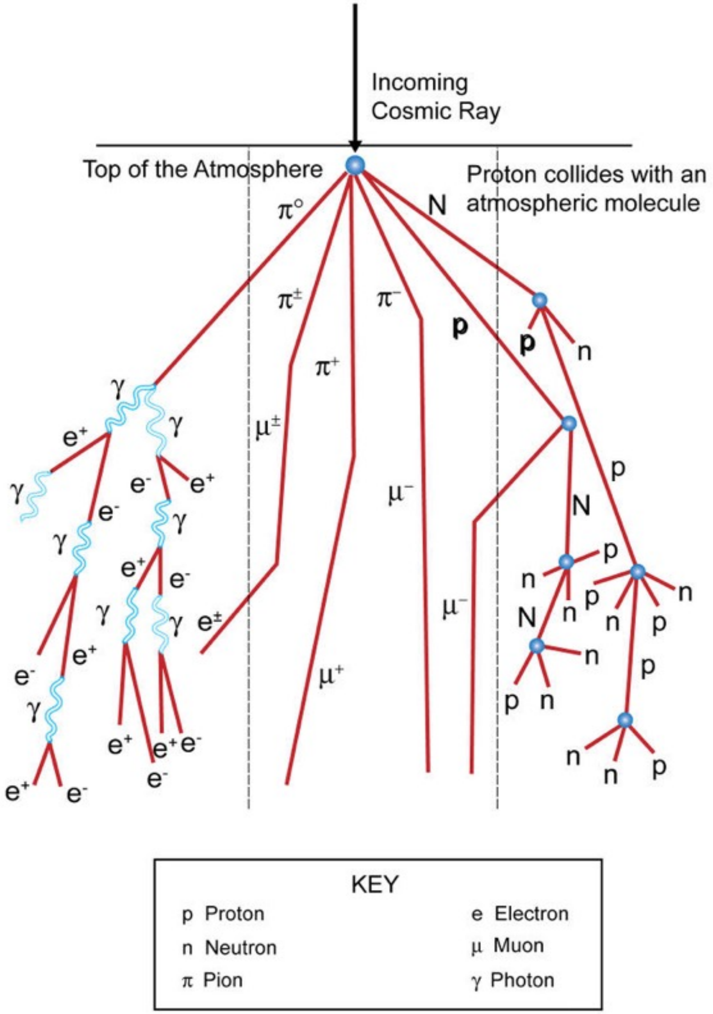

BACKGROUND: cosmic neutrons

Neutrons are created by cosmic ray spallation in the high atmosphere.
Energies from 10^{-9} to 10^{3} MeV

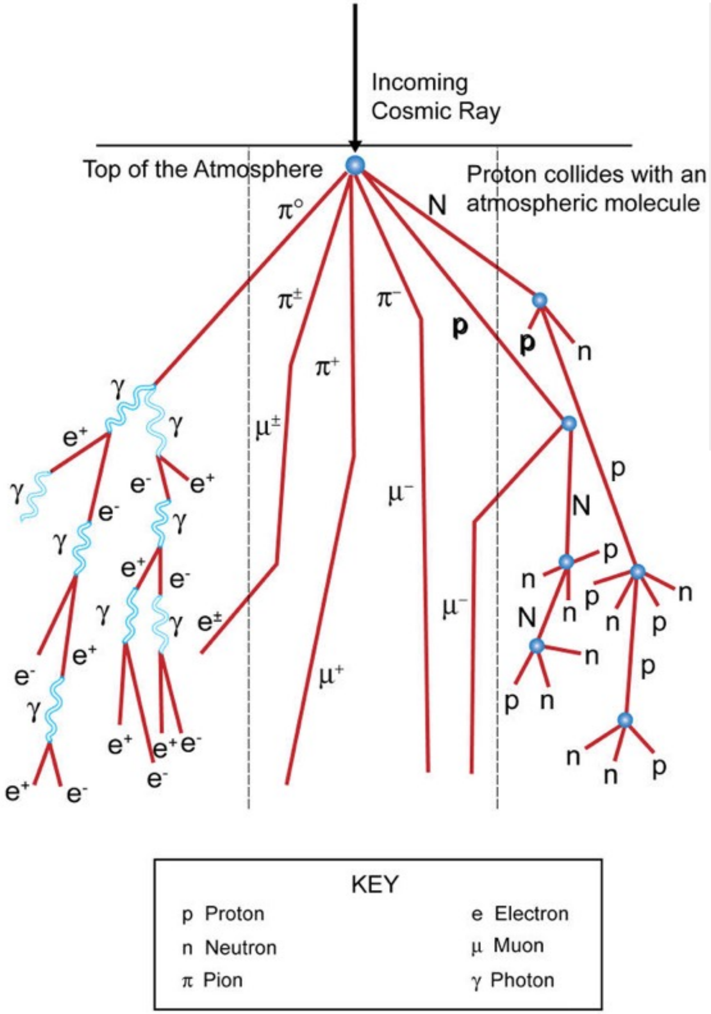

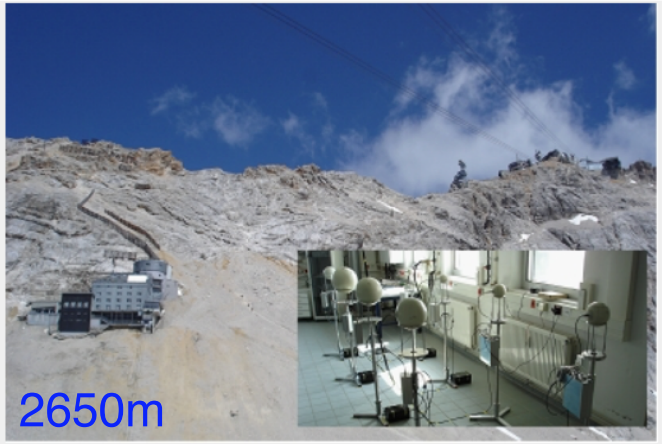

Measured with Bonner spheres in the whole eneregy spectrum

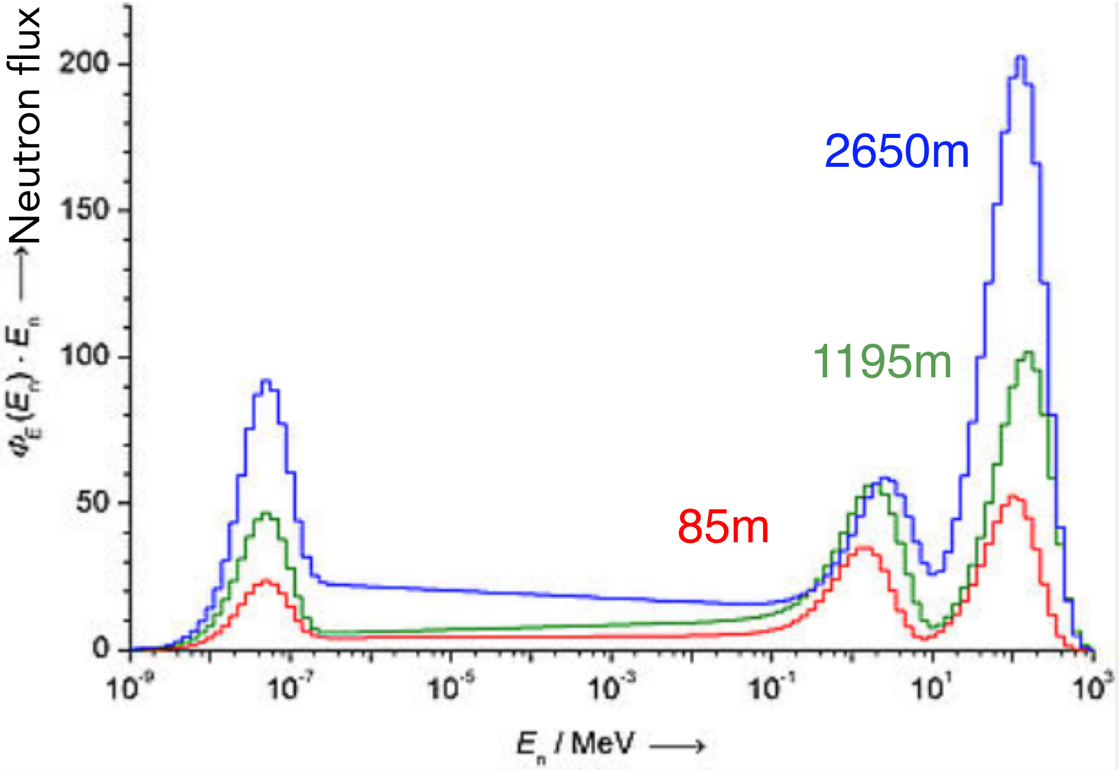

Physikalisch-Technische Bundesanstalt (PTB) - Measurements of Neutron Spectra Induced by Cosmic Radiation at Altitudes of 85m, 1195m and 2650m (2010)

BACKGROUND: cosmic neutrons

Neutrons are created by cosmic ray spallation in the high atmosphere.
Energies from 10^{-9} to 10^{3} MeV

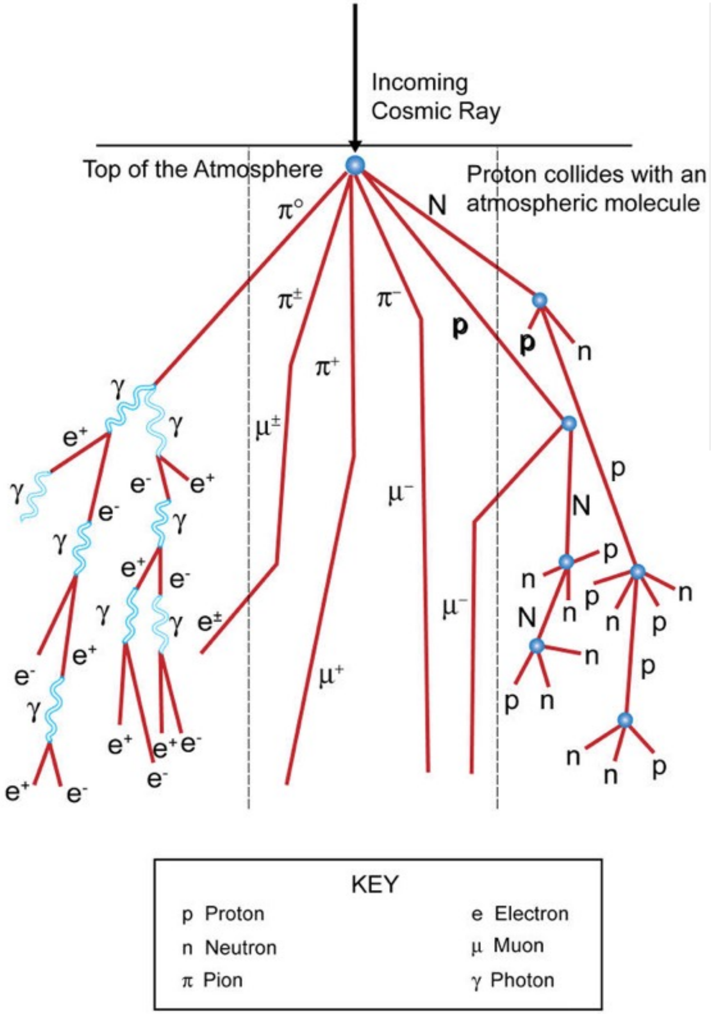

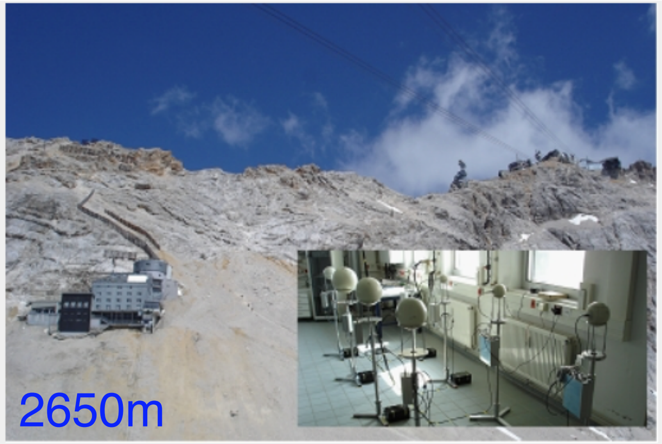

Measured with Bonner spheres in the whole eneregy spectrum

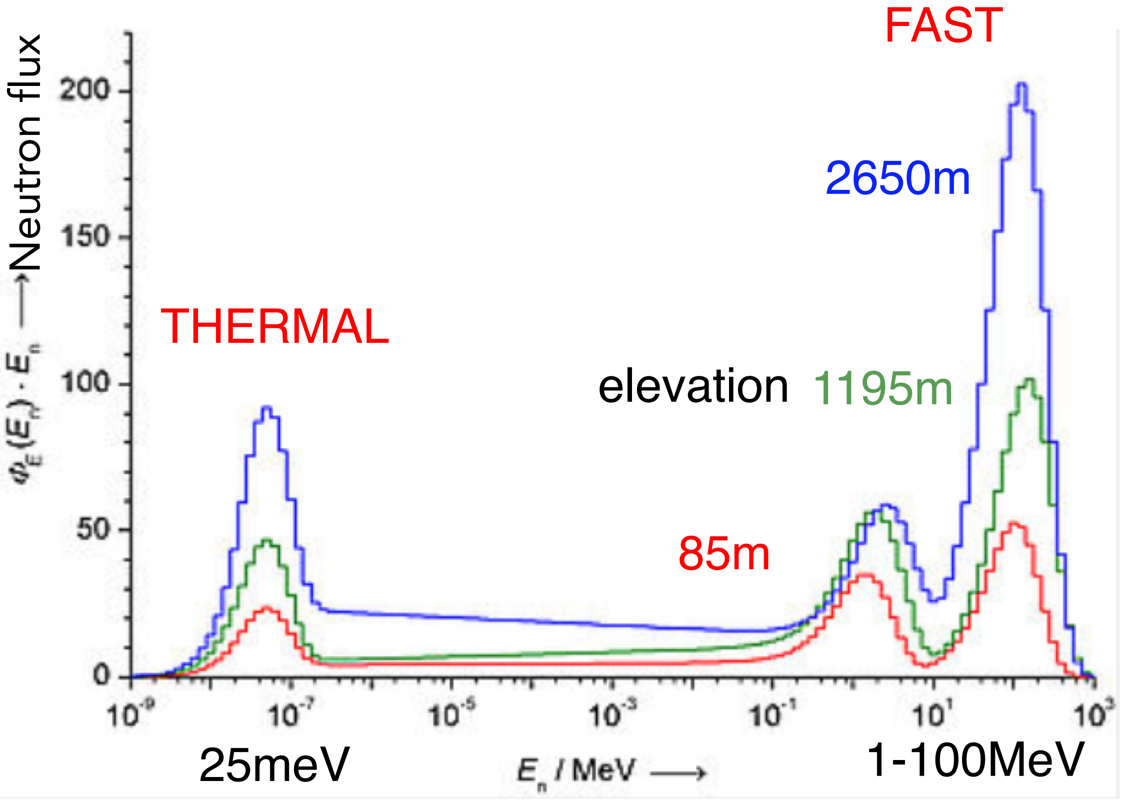

Physikalisch-Technische Bundesanstalt (PTB) - Measurements of Neutron Spectra Induced by Cosmic Radiation at Altitudes of 85m, 1195m and 2650m (2010)

BACKGROUND: cosmic neutrons

Neutrons are created by cosmic ray spallation in the high atmosphere.
Energies from 10^{-9} to 10^{3} MeV

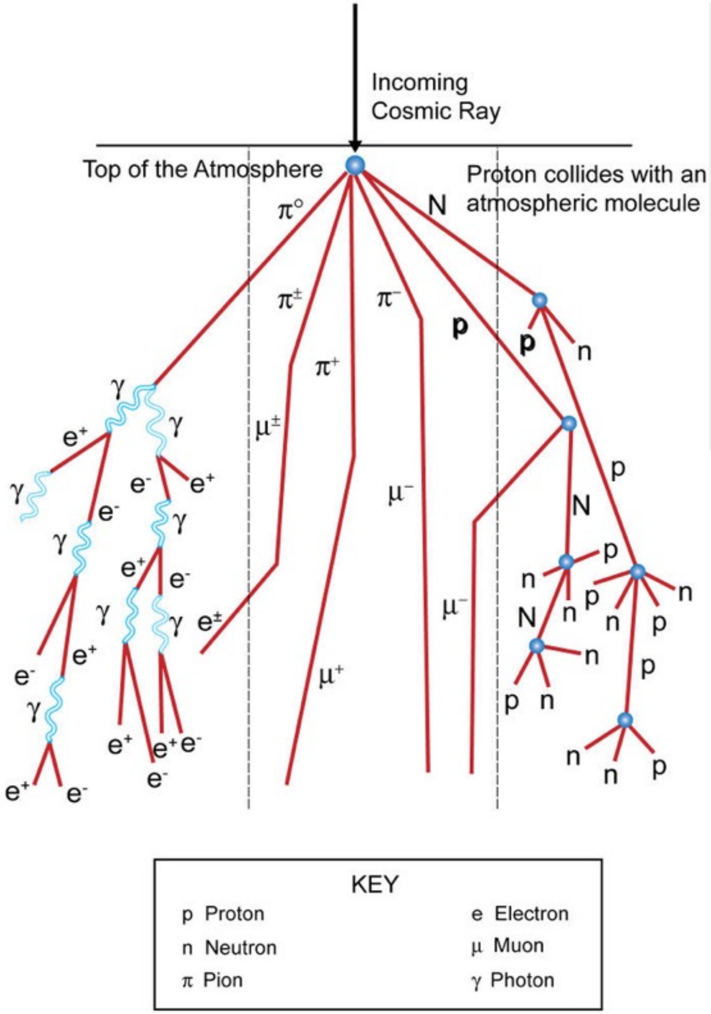

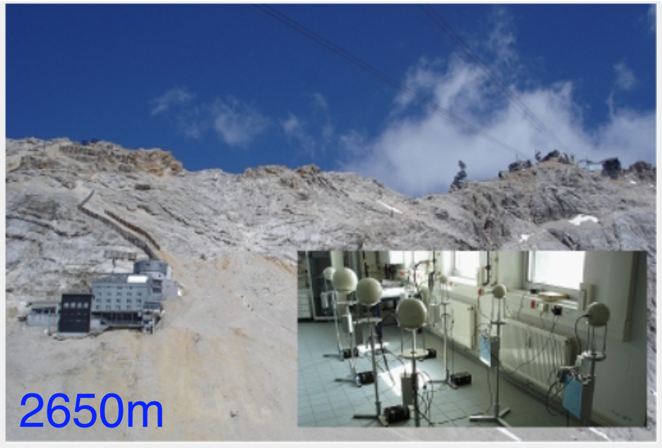

Measured with Bonner spheres in the whole eneregy spectrum

elevation 85m ~ ESS
135 Hz/m^2 (10^{-9} to 10^{3} MeV) by PTB

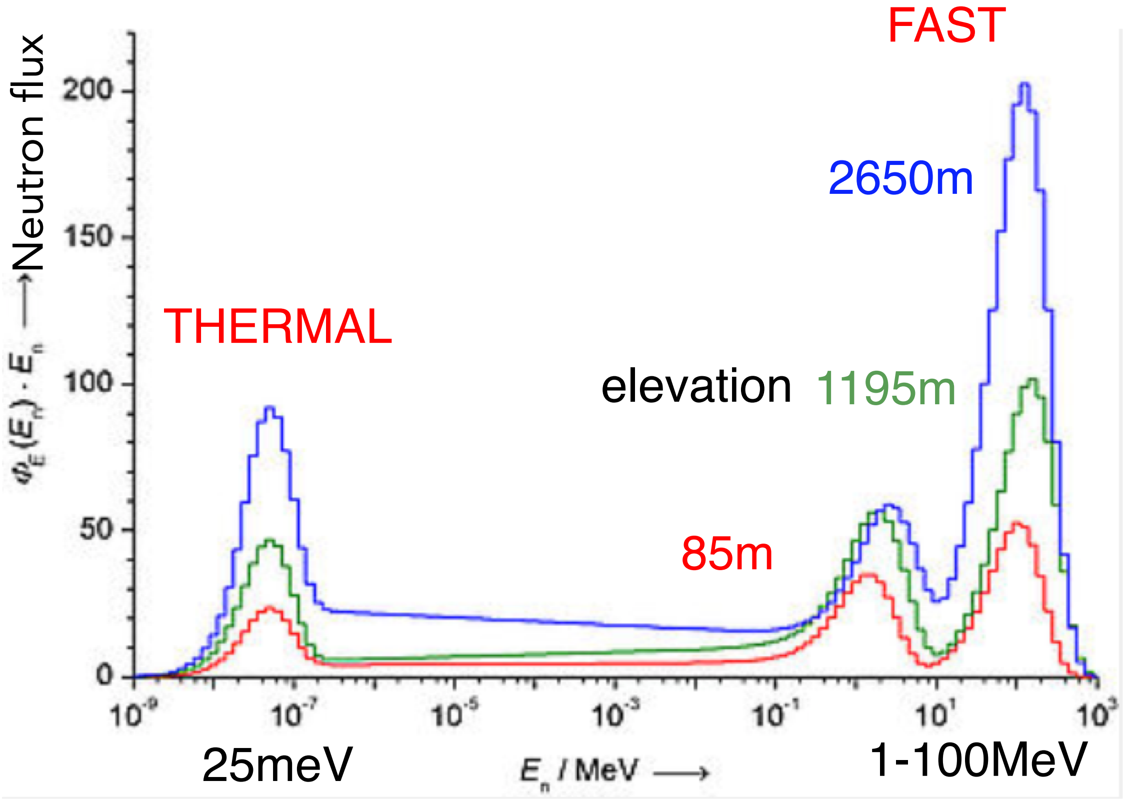

Physikalisch-Technische Bundesanstalt (PTB) - Measurements of Neutron Spectra Induced by Cosmic Radiation at Altitudes of 85m, 1195m and 2650m (2010)

BACKGROUND: cosmic neutrons

Neutrons are created by cosmic ray spallation in the high atmosphere.
Energies from 10^{-9} to 10^{3} MeV

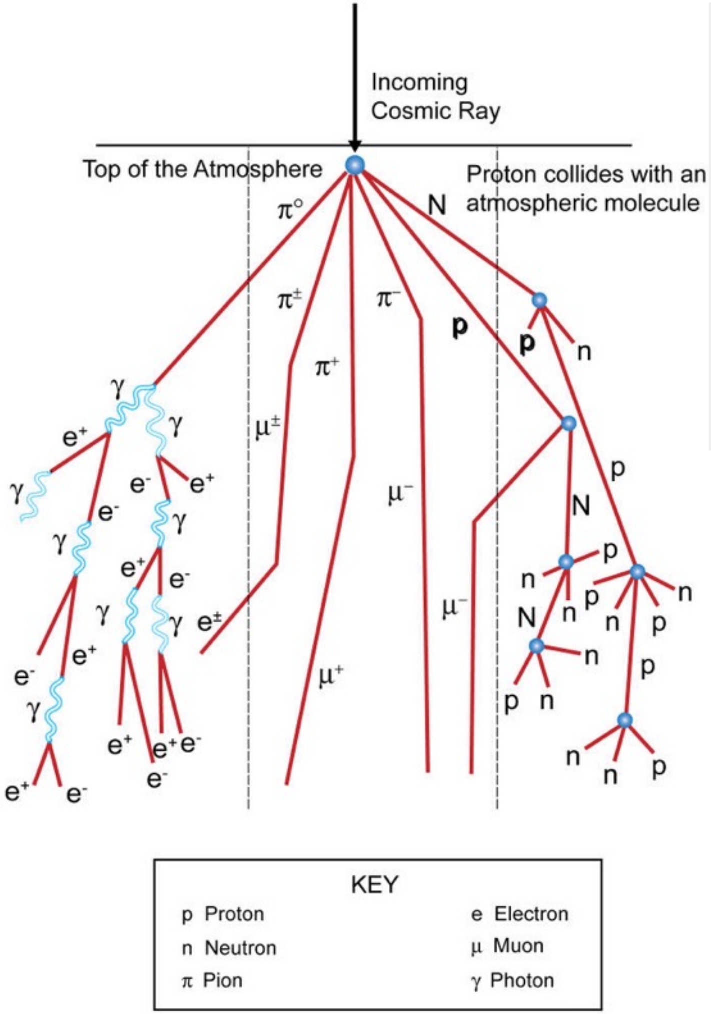

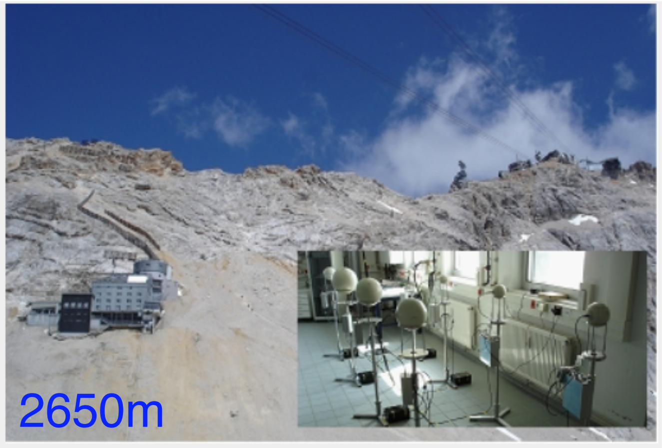

Measured with Bonner spheres in the whole eneregy spectrum

elevation 85m ~ ESS
135 Hz/m^2 (10^{-9} to 10^3 MeV) by PTB

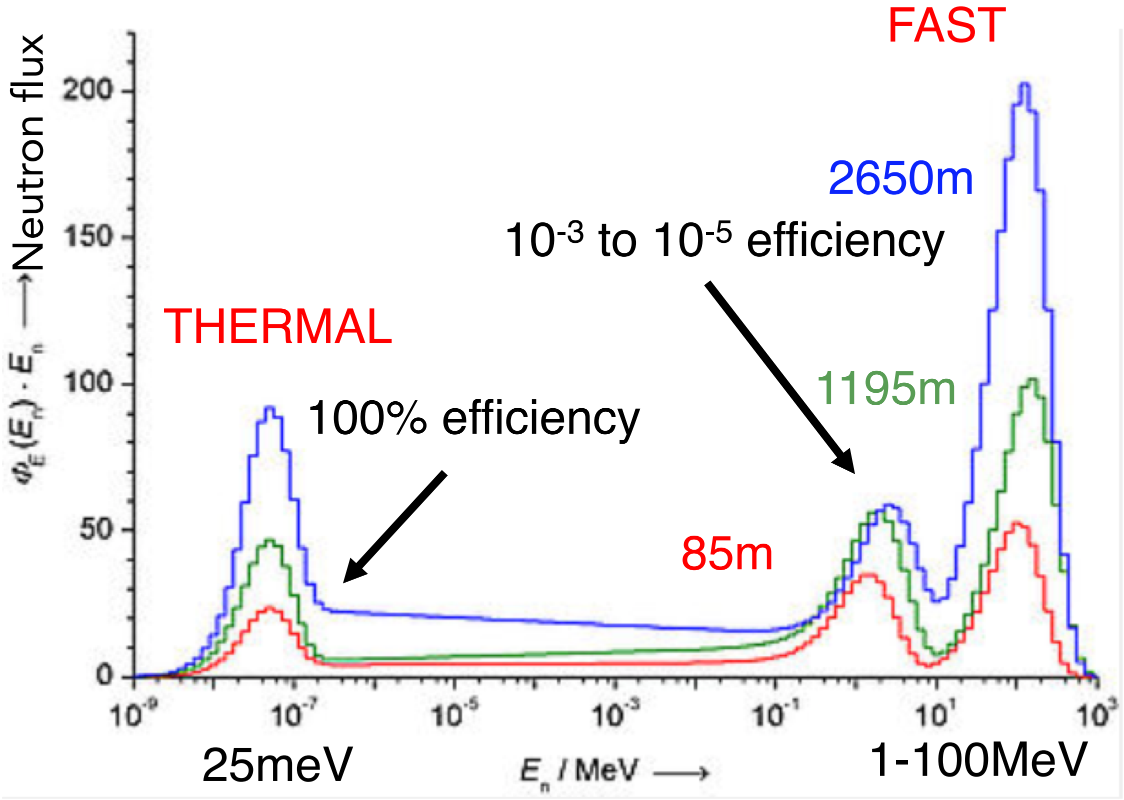

Physikalisch-Technische Bundesanstalt (PTB) - Measurements of Neutron Spectra Induced by Cosmic Radiation at Altitudes of 85m, 1195m and 2650m (2010)

BACKGROUND: cosmic neutrons

Measurements done in Utgård

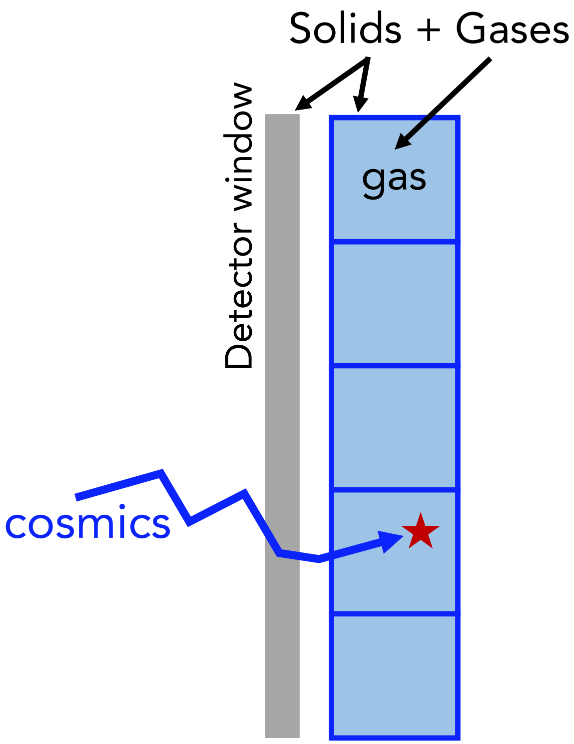

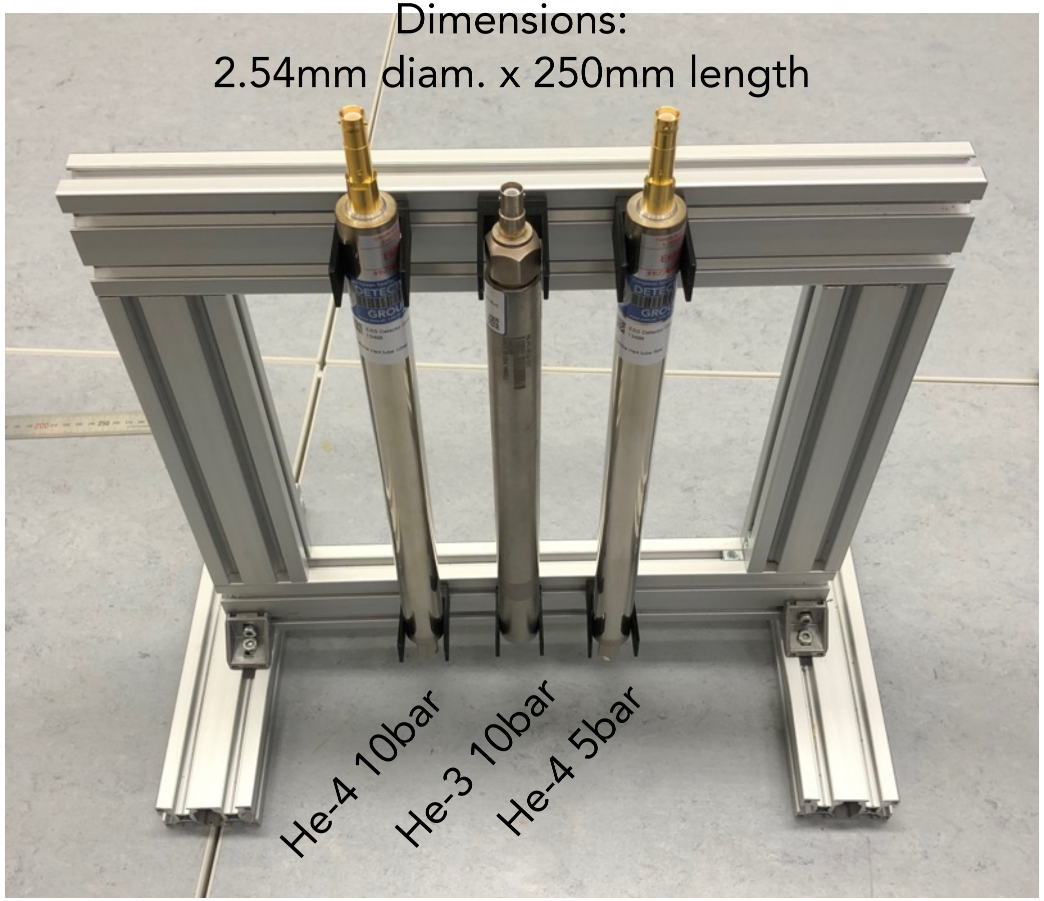

He-3 and He-4 detectors

*Thanks to Toshiba/Canon Electron Tubes & Devices Co. LTD for the He-4 tubes.

F. Piscitelli et al., Verification of He-3 proportional counters fast neutron sensitivity through a comparison with He-4 detectors, sub. to EPJ Plus (2020) (arxiv: 2002.08153)

BACKGROUND: cosmic neutrons

Bare tubes

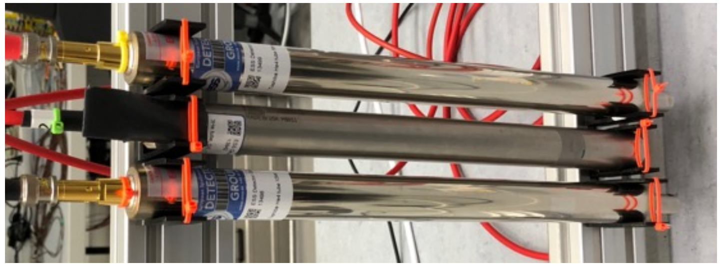

He-4 5 bar
He-3 10 bar
He-4 10 bar

Pulse-Height-Spectrum

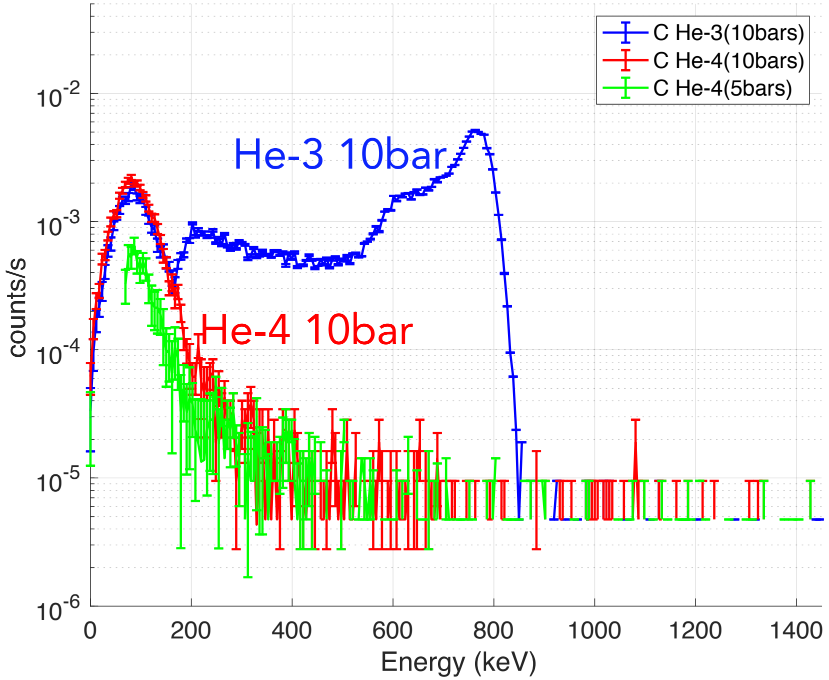

F. Piscitelli et al., Verification of He-3 proportional counters fast neutron sensitivity through a comparison with He-4 detectors, sub. to EPJ Plus (2020) (arxiv: 2002.08153)

BACKGROUND: cosmic neutrons

Bare tubes

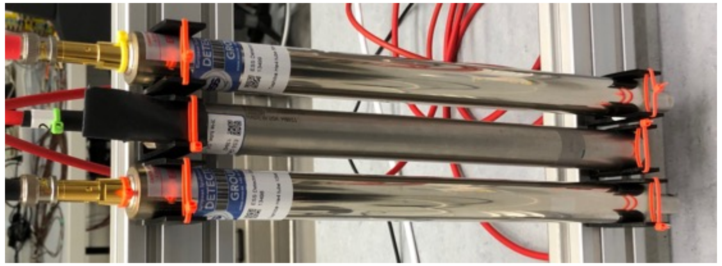

He-4 5 bar
He-3 10 bar
He-4 10 bar

Covered with 2mm Mirrobor

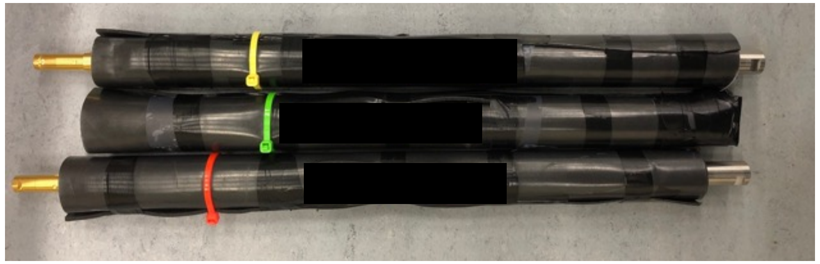

Pulse-Height-Spectrum

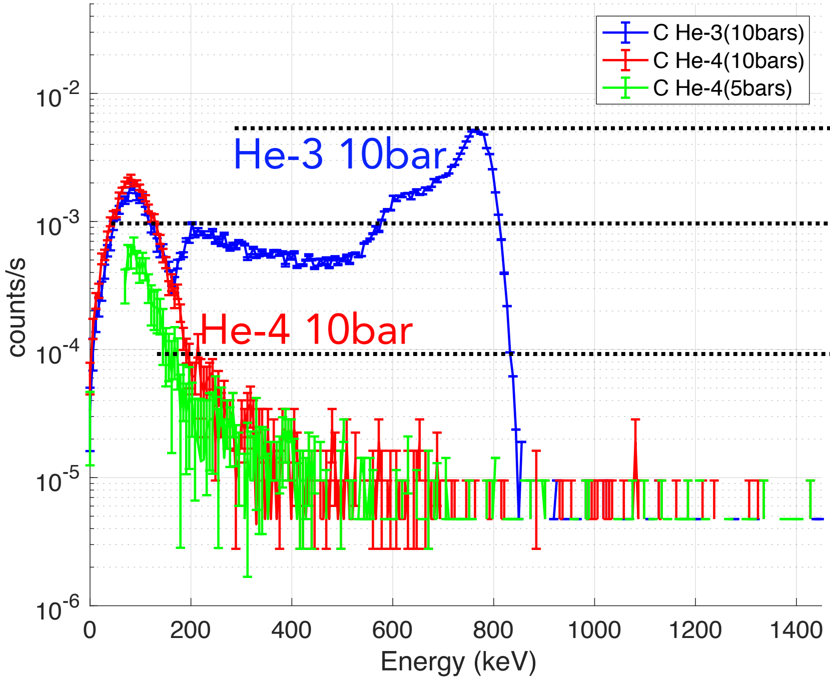

Pulse-Height-Spectrum

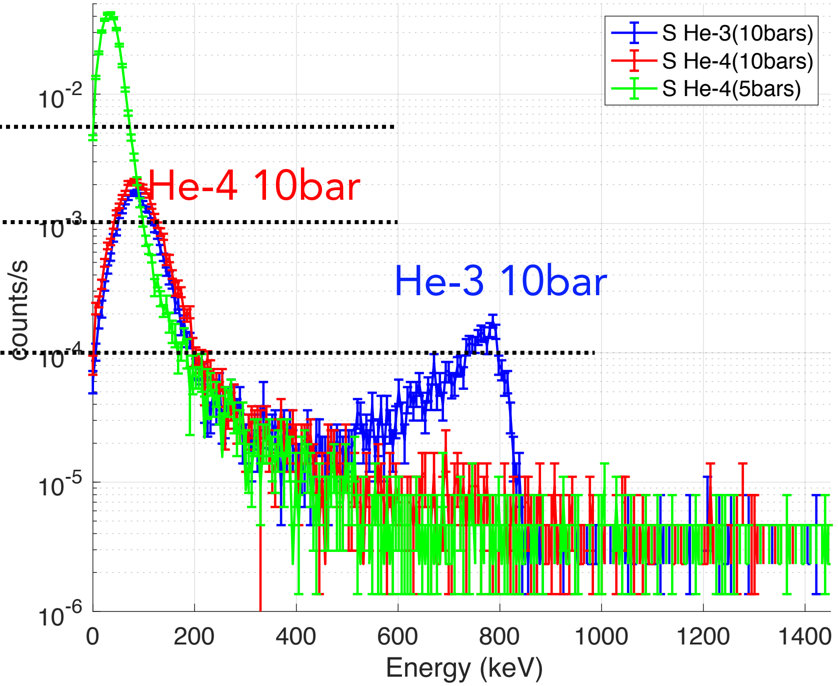

F. Piscitelli et al., Verification of He-3 proportional counters fast neutron sensitivity through a comparison with He-4 detectors, sub. to EPJ Plus (2020) (arxiv: 2002.08153)

BACKGROUND: cosmic neutrons

Bare tubes

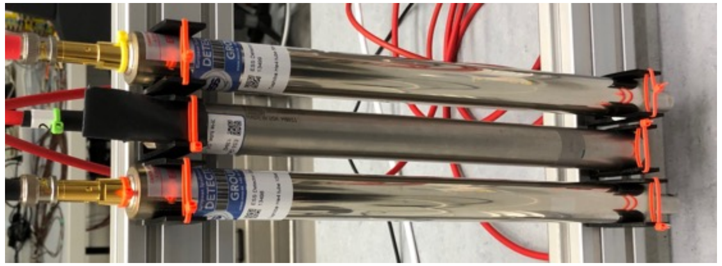

He-4 5 bar
He-3 10 bar
He-4 10 bar

Covered with 2mm Mirrobor

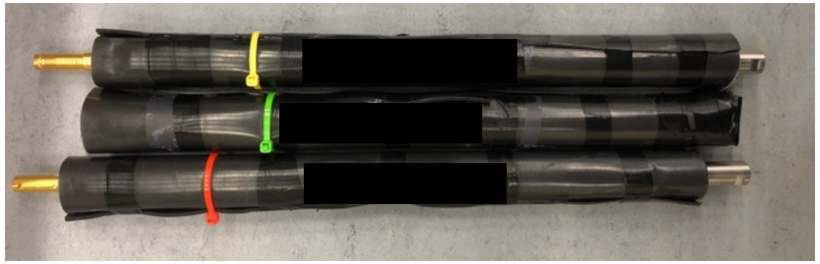

Pulse-Height-Spectrum

Pulse-Height-Spectrum

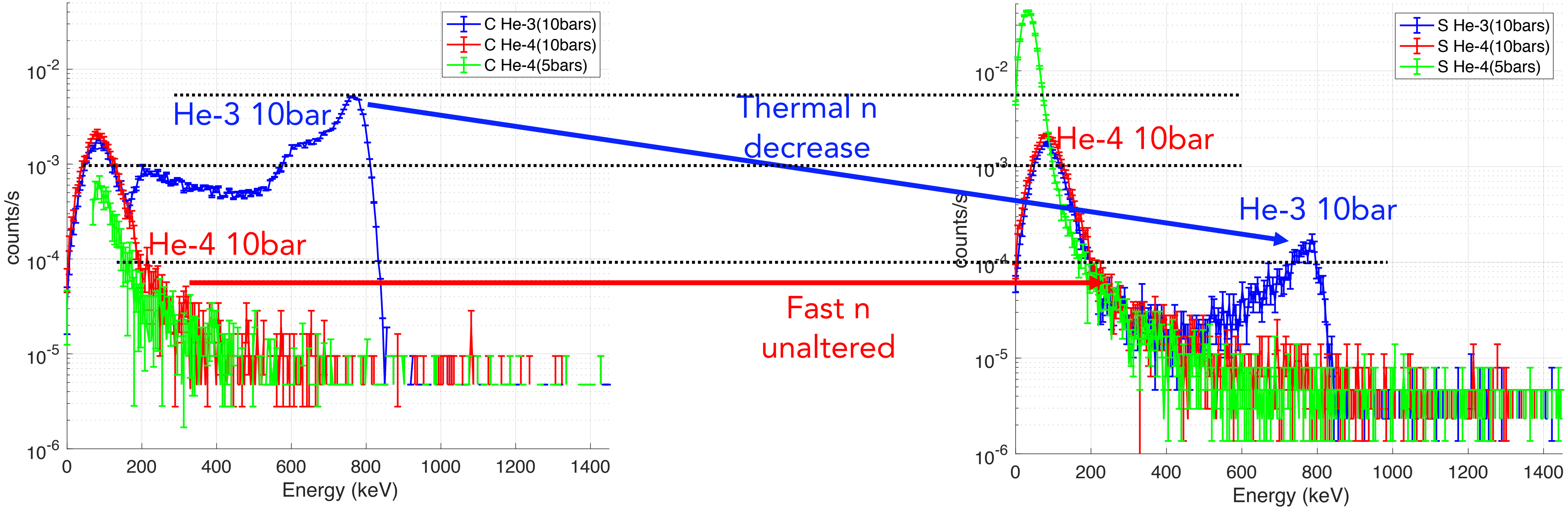

F. Piscitelli et al., Verification of He-3 proportional counters fast neutron sensitivity through a comparison with He-4 detectors, sub. to EPJ Plus (2020) (arxiv: 2002.08153)

BACKGROUND: cosmic neutrons

Bare tubes

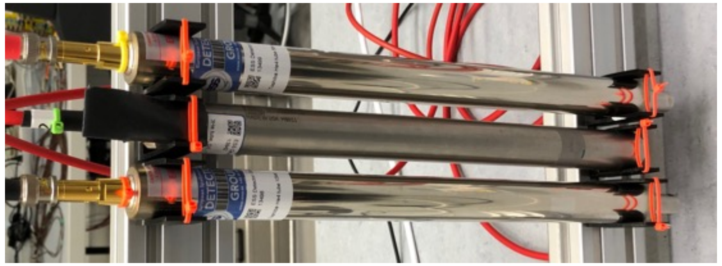

He-4   5 bar
He-3 10 bar
He-4 10 bar

Covered with 2mm Mirrobor

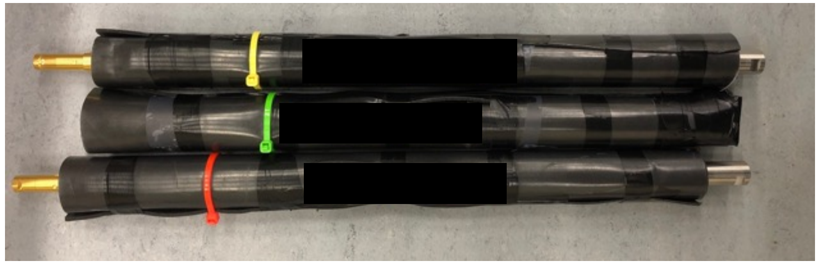

Bare tubes				Covered with 2mm Mirrobor		
Rate Hz	rate per area Hz/m^2	rate per volume Hz/m^3	detector	Rate Hz	rate per area Hz/m^2	rate per volume Hz/m^3
0.148	23	292	He-3 10bar	0.007	1	14
0.0043	0.7	8.5	He-4 10bar	0.005	0.8	10

0.029 Hz / (bar · litre) of He3

0.0014 Hz / (bar · litre) of He3

F. Piscitelli et al., Verification of He-3 proportional counters fast neutron sensitivity through a comparison with He-4 detectors, sub. to EPJ Plus (2020) (arxiv: 2002.08153)

BACKGROUND: cosmic neutrons

Bare tubes

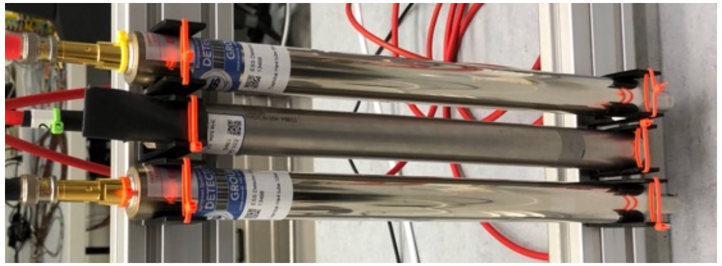

He-4 5 bar
He-3 10 bar
He-4 10 bar

Covered with 2mm Mirrobor

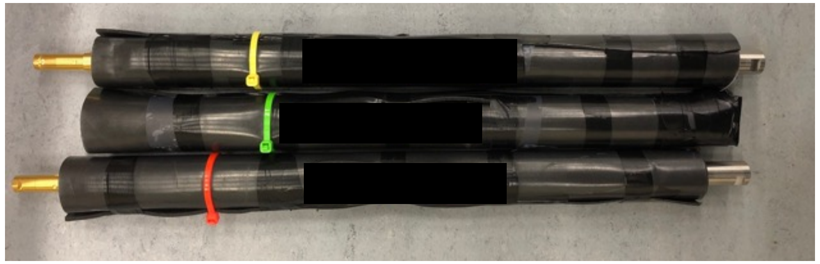

Bare tubes: Rate Hz	Bare tubes: rate per area Hz/m^2	Bare tubes: rate per volume Hz/m^3	detector	Covered with 2mm Mirrobor: Rate Hz	Covered with 2mm Mirrobor: rate per area Hz/m^2	Covered with 2mm Mirrobor: rate per volume Hz/m^3
0.148	23	292	He-3 10bar	0.007	1	14
0.0043	0.7	8.5	He-4 10bar	0.005	0.8	10

0.029 Hz / (bar · litre) of He3

0.0014 Hz / (bar · litre) of He3

elevation 85m ~ ESS
135 Hz/m^2 (10^{-9} to 10^{3} MeV) by PTB

Agreement with rates at FRMII
K. Zeitelhack – private communication

Agreement with rates measured with MG at Utgård (See next talk from Alex)

F. Piscitelli et al., Verification of He-3 proportional counters fast neutron sensitivity through a comparison with He-4 detectors, sub. to EPJ Plus (2020) (arxiv: 2002.08153)

GAMMA-RAY BACKGROUND

BACKGROUND: gamma-rays

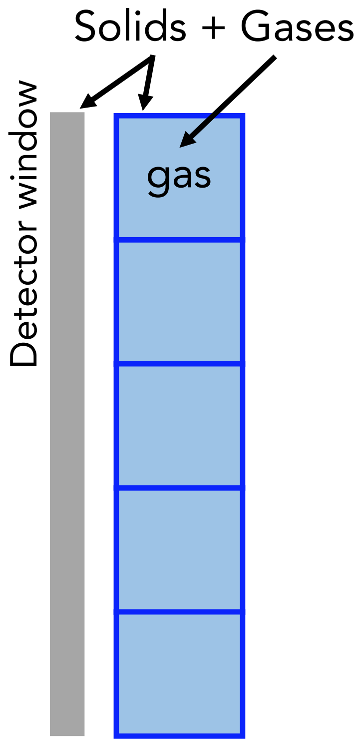

BACKGROUND: gamma-rays

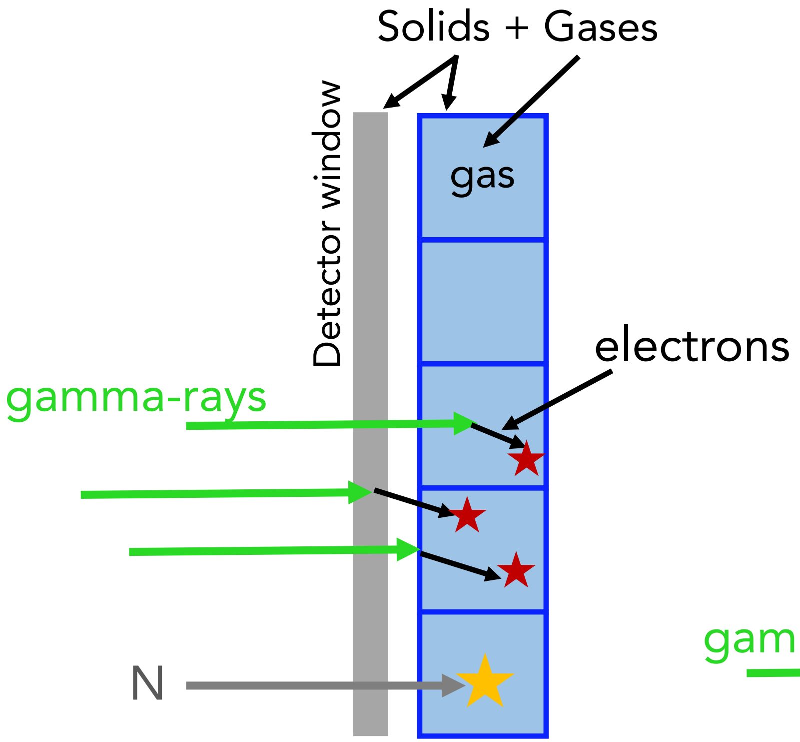

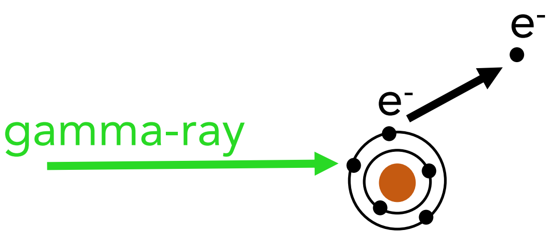

Photoelectric / Compton

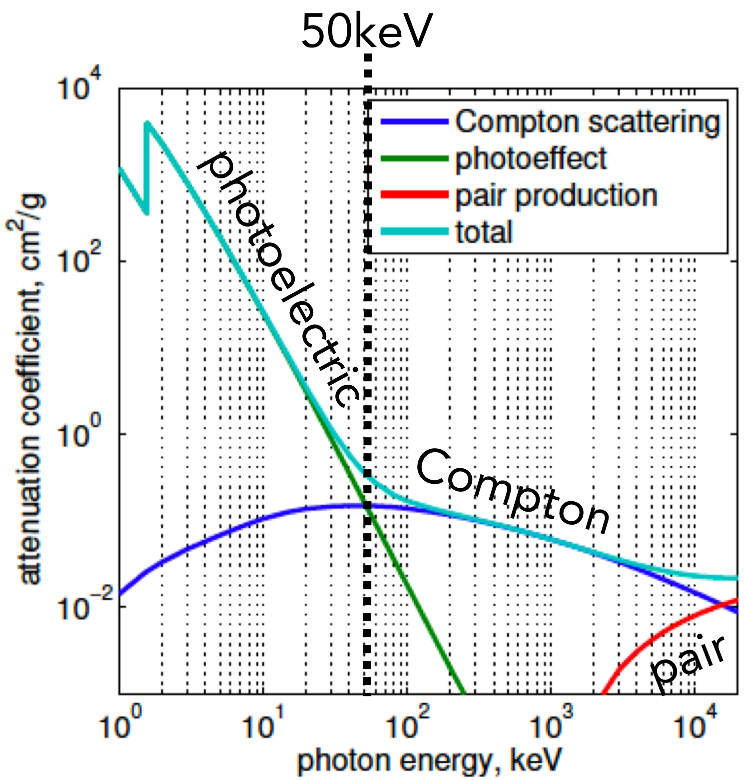

Photoelectric interaction most probable at low energy, Compton scattering is the majority of the background

A. Khaplanov et al., Investigation of gamma-ray sensitivity of neutron detectors based on thin converter films, JINST 8 P10025 (2013) (arxiv: 1306:6247)

BACKGROUND: gamma-rays

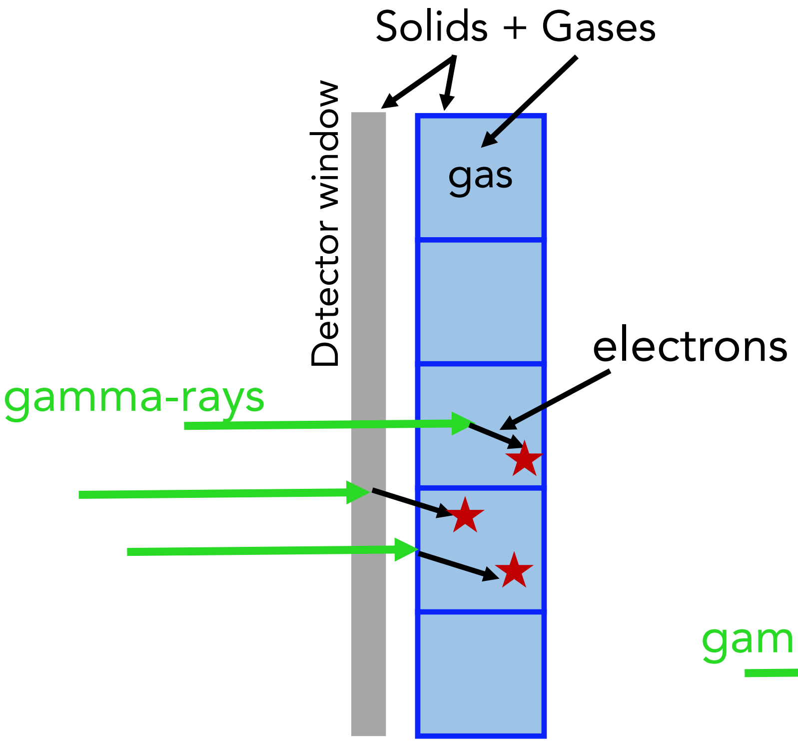

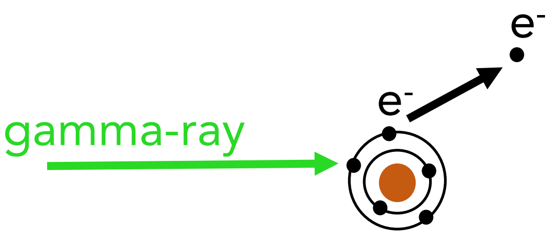

Photoelectric / Compton

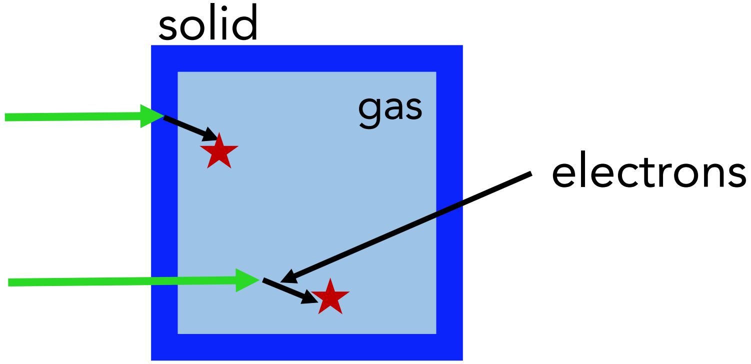

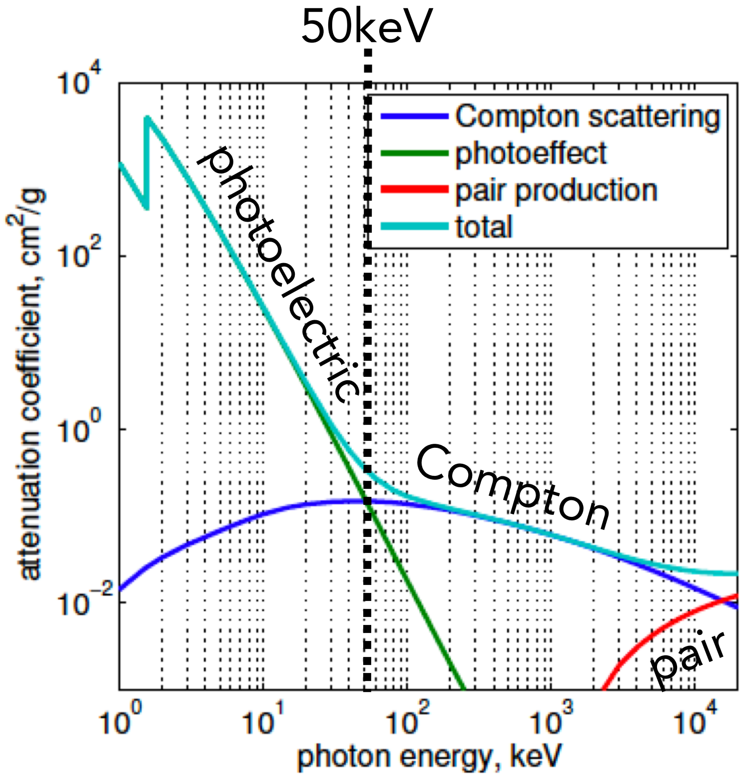

Photoelectric interaction most probable at low energy,
Compton scattering is the majority of the background

A. Khaplanov et al., Investigation of gamma-ray sensitivity of neutron detectors based on thin converter films, JINST 8 P10025 (2013) (arxiv: 1306:6247)

BACKGROUND: gamma-rays

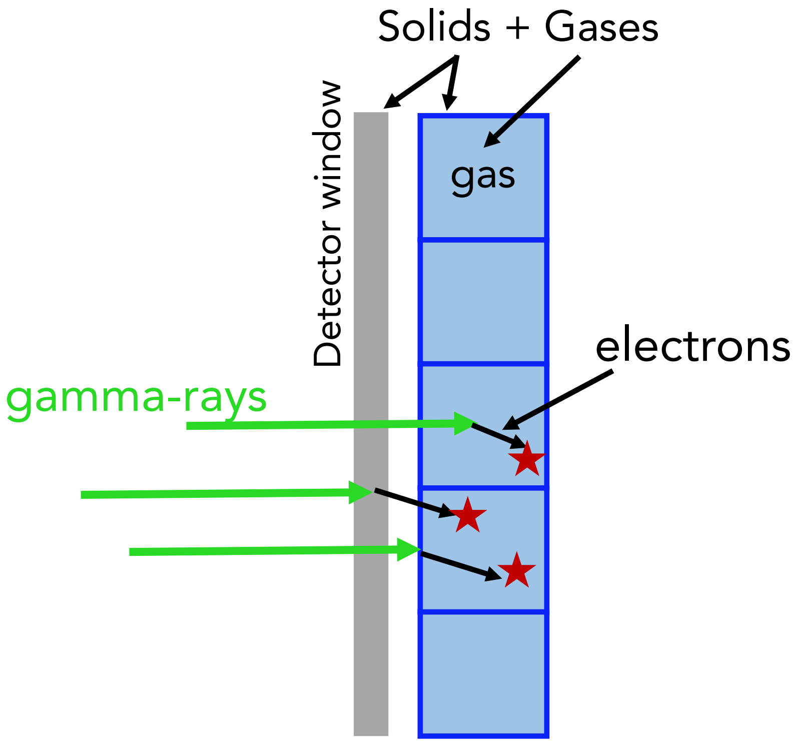

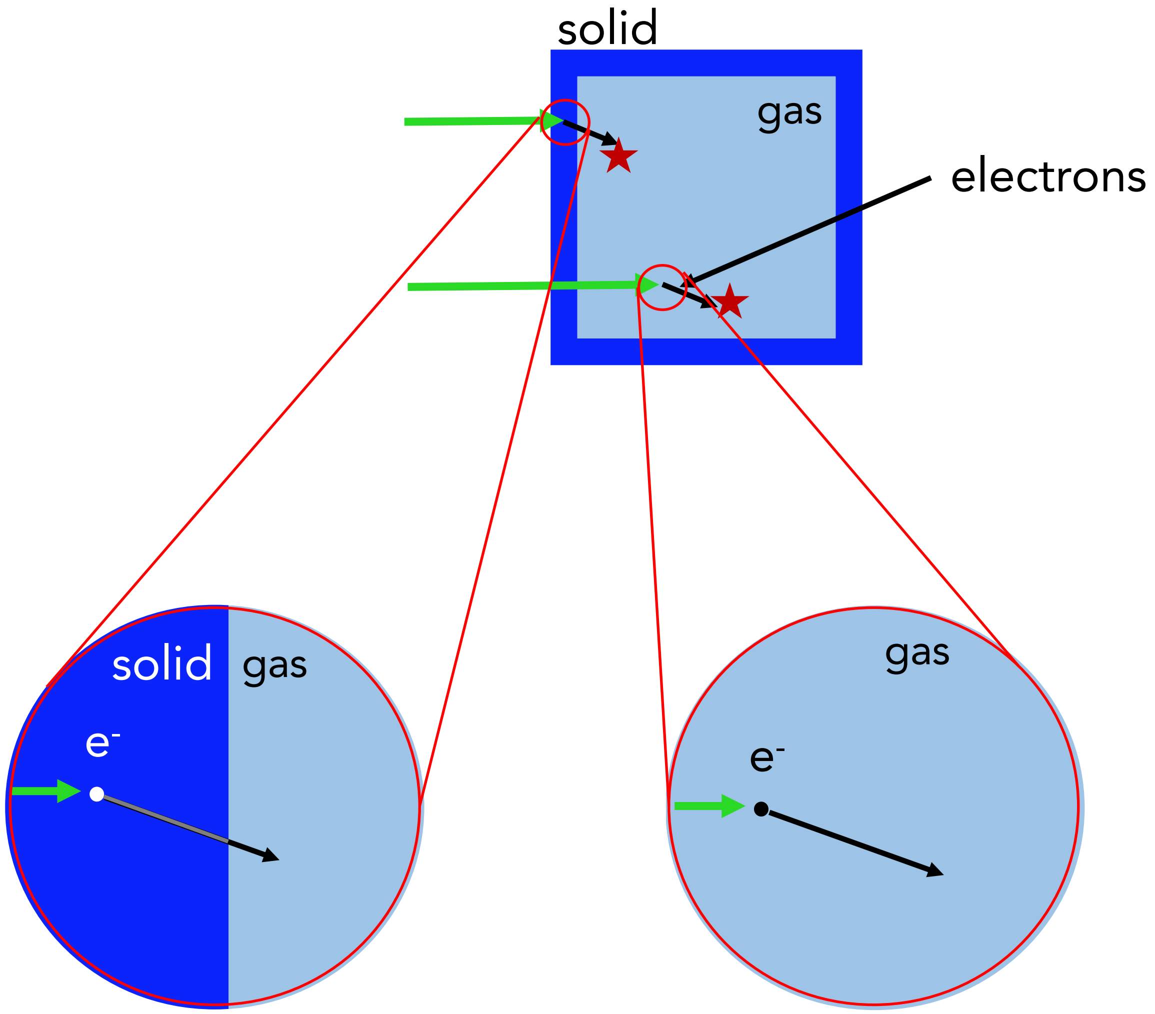

gammas in the walls can only result in a signal if the electron reaches the gas

photons interacting with the gas are guaranteed to generate a signal

Gas vs Solid

A. Khaplanov et al., Investigation of gamma-ray sensitivity of neutron detectors based on thin converter films, JINST 8 P10025 (2013) (arxiv: 1306:6247)

BACKGROUND: gamma-rays

(Simulations)

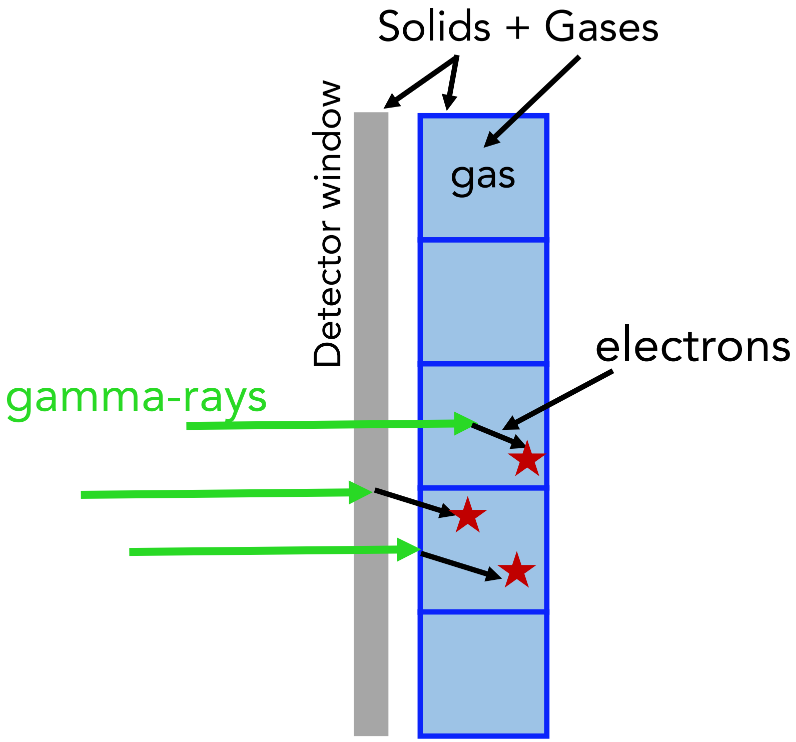

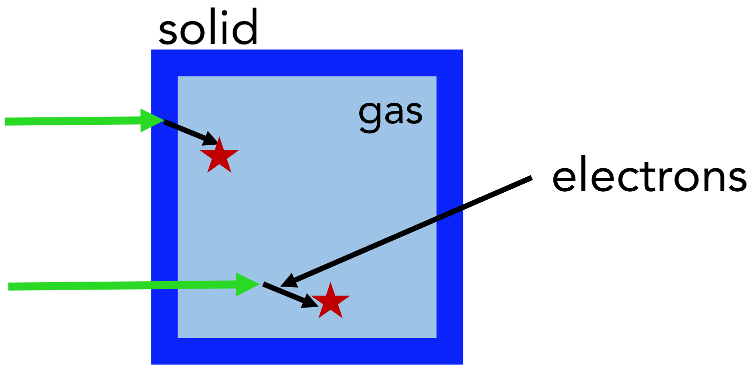

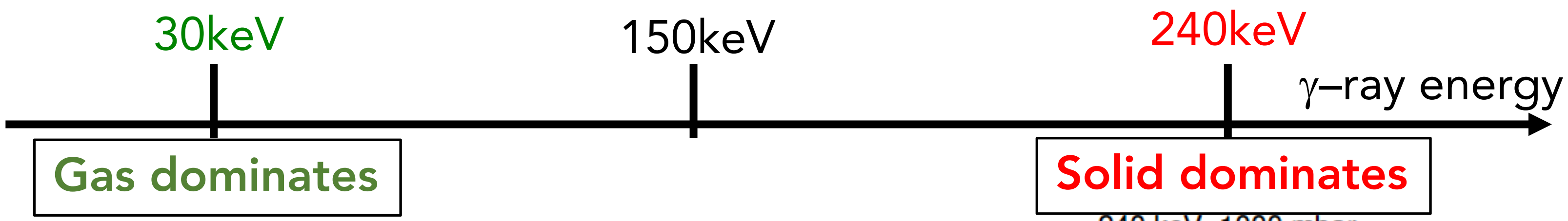

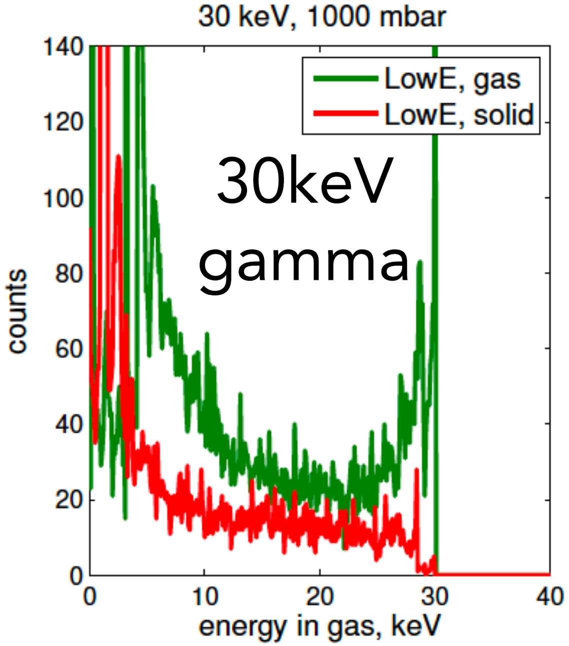

150 keV for
1 atm of ArCO2
and Al walls
is 50/50

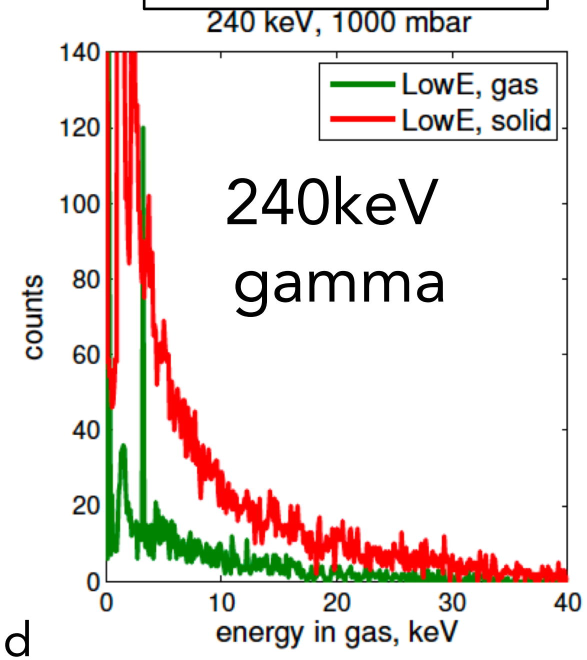

Gas vs Solid

A. Khaplanov et al., Investigation of gamma-ray sensitivity of neutron detectors based on thin converter films, JINST 8 P10025 (2013) (arxiv: 1306:6247)

BACKGROUND: gamma-rays

(Simulations)

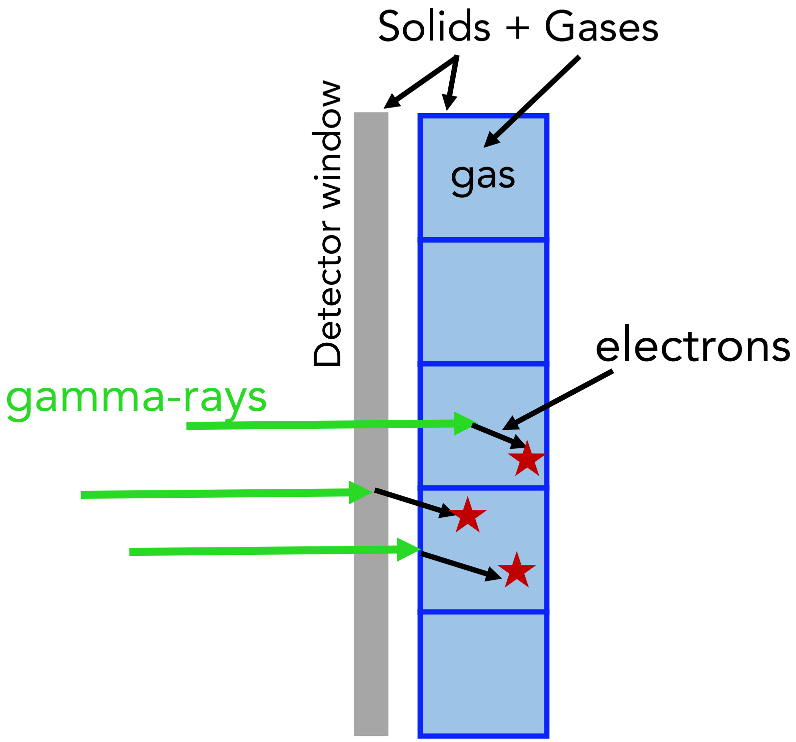

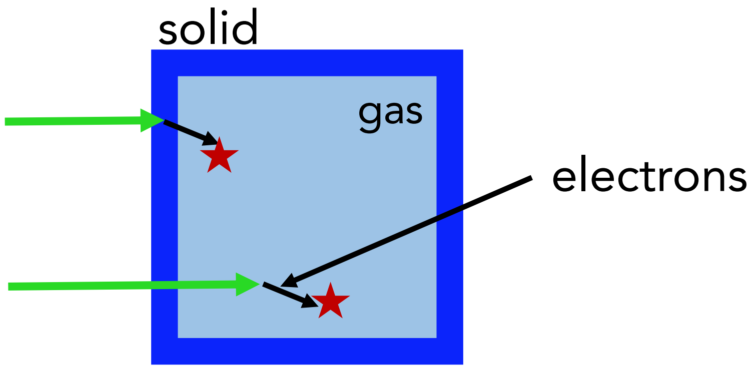

Gas dominates

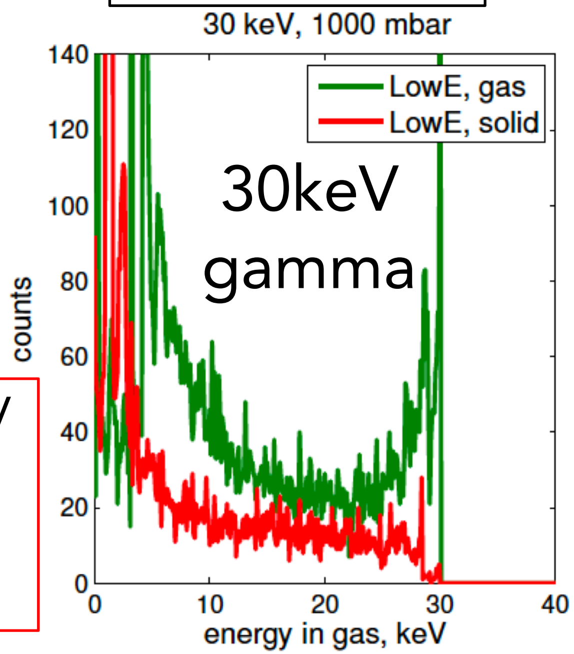

150 keV for
1 atm of ArCO2
and Al walls
is 50/50

Solid dominates

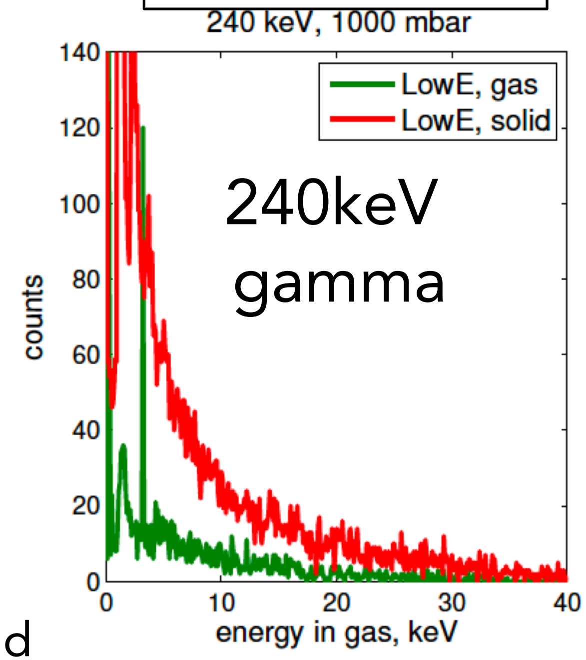

Gas vs Solid

Energy threshold generally 100-200keV

↓

Solid dominates

A. Khaplanov et al., Investigation of gamma-ray sensitivity of neutron detectors based on thin converter films, JINST 8 P10025 (2013) (arxiv: 1306:6247)

BACKGROUND: gamma-rays

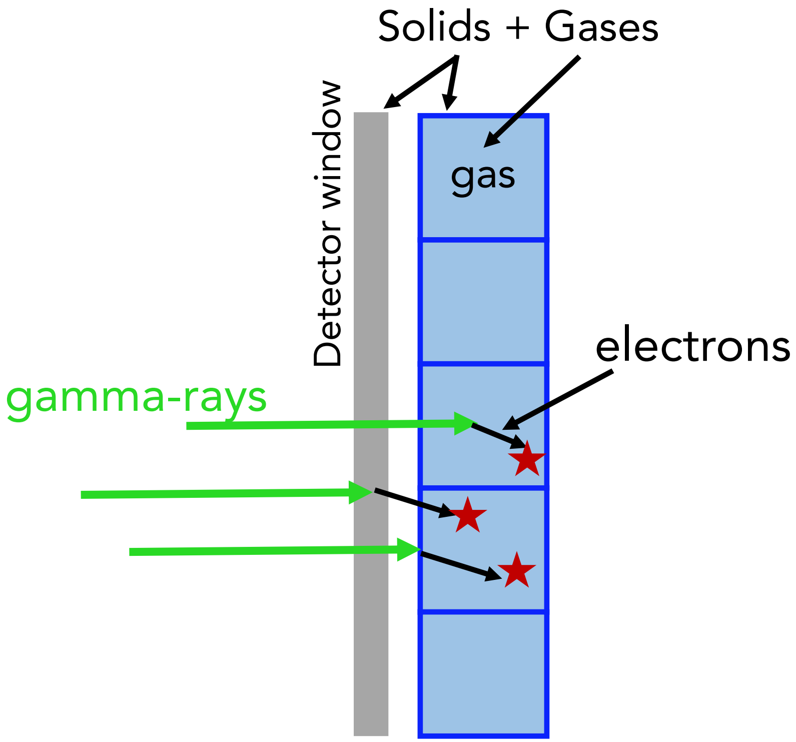

Higher pressure = higher energy deposition

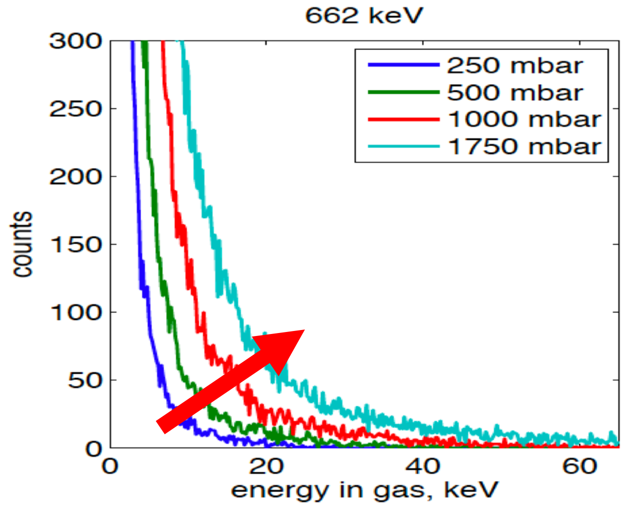

(Simulations)

A. Khaplanov et al., Investigation of gamma-ray sensitivity of neutron detectors based on thin converter films, JINST 8 P10025 (2013) (arxiv: 1306:6247)

BACKGROUND: gamma-rays

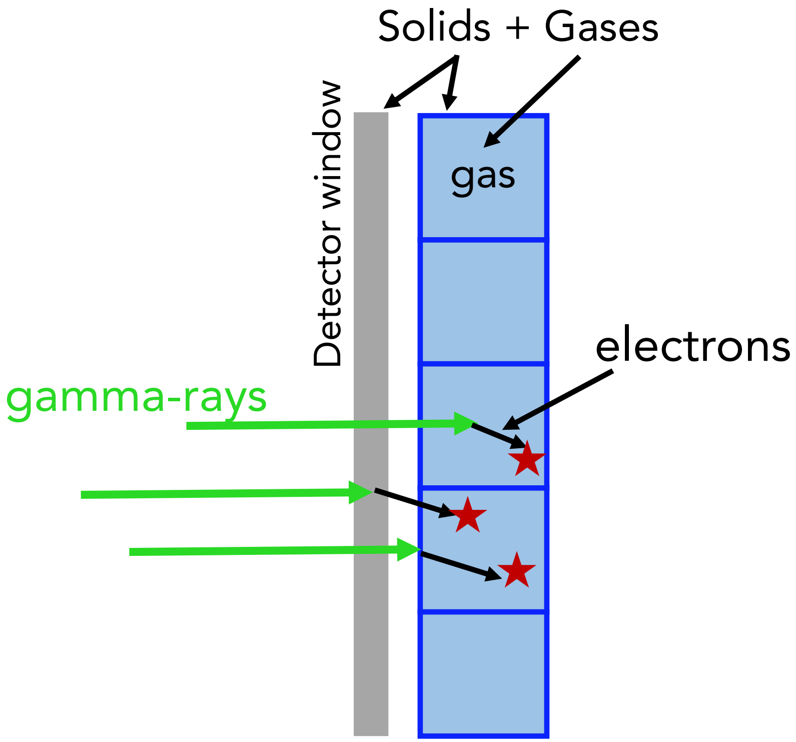

Higher pressure = higher energy deposition

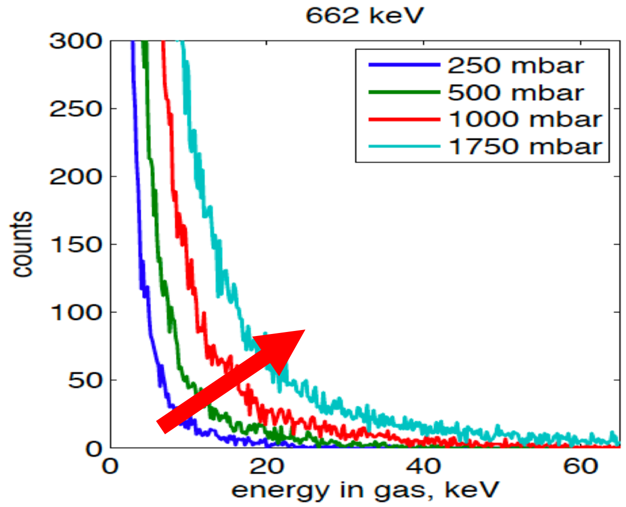

Higher gamma energy = higher energy deposition

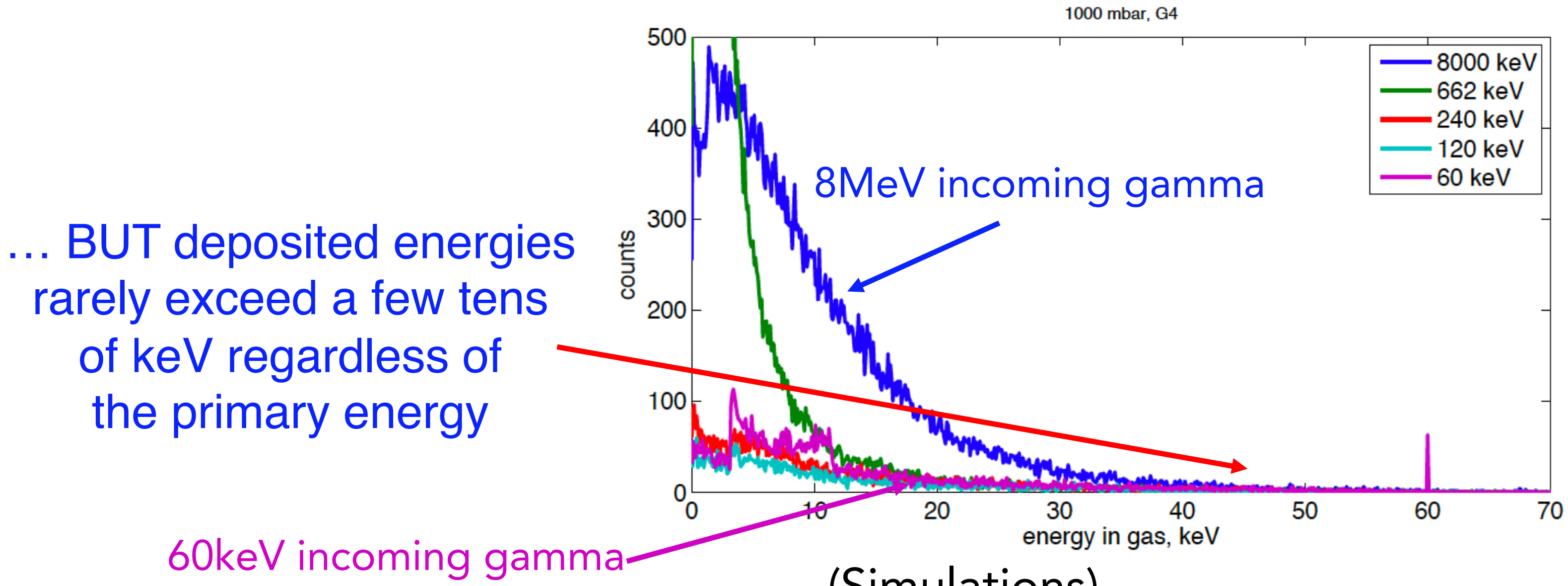

(Simulations)

A. Khaplanov et al., Investigation of gamma-ray sensitivity of neutron detectors based on thin converter films, JINST 8 P10025 (2013) (arxiv: 1306:6247)

BACKGROUND: gamma-rays

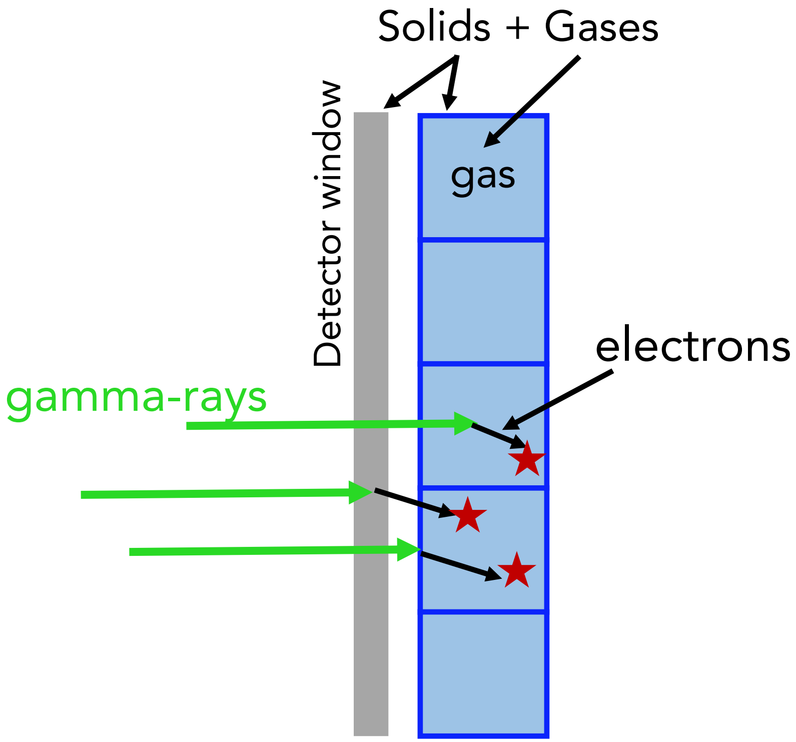

Solid dominates no matter if He-3 or B-10

Measurements

He-3/He-4 detectors

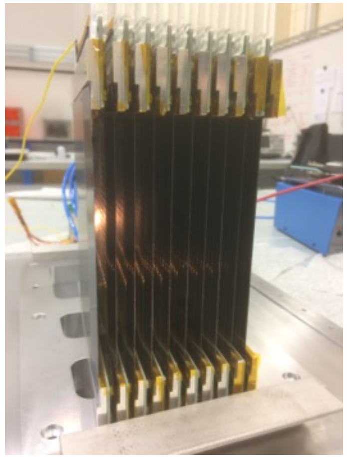

Multi-Blade B-10
(reflectometers)

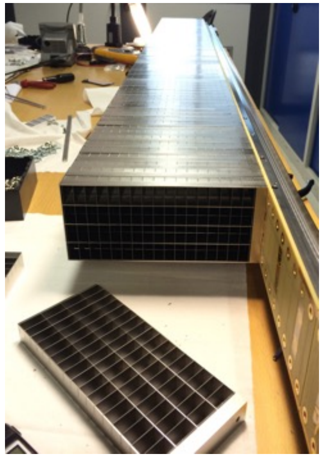

Multi-Grid B-10
(spectrometers)

Solid dominates no matter if He-3 or B-10

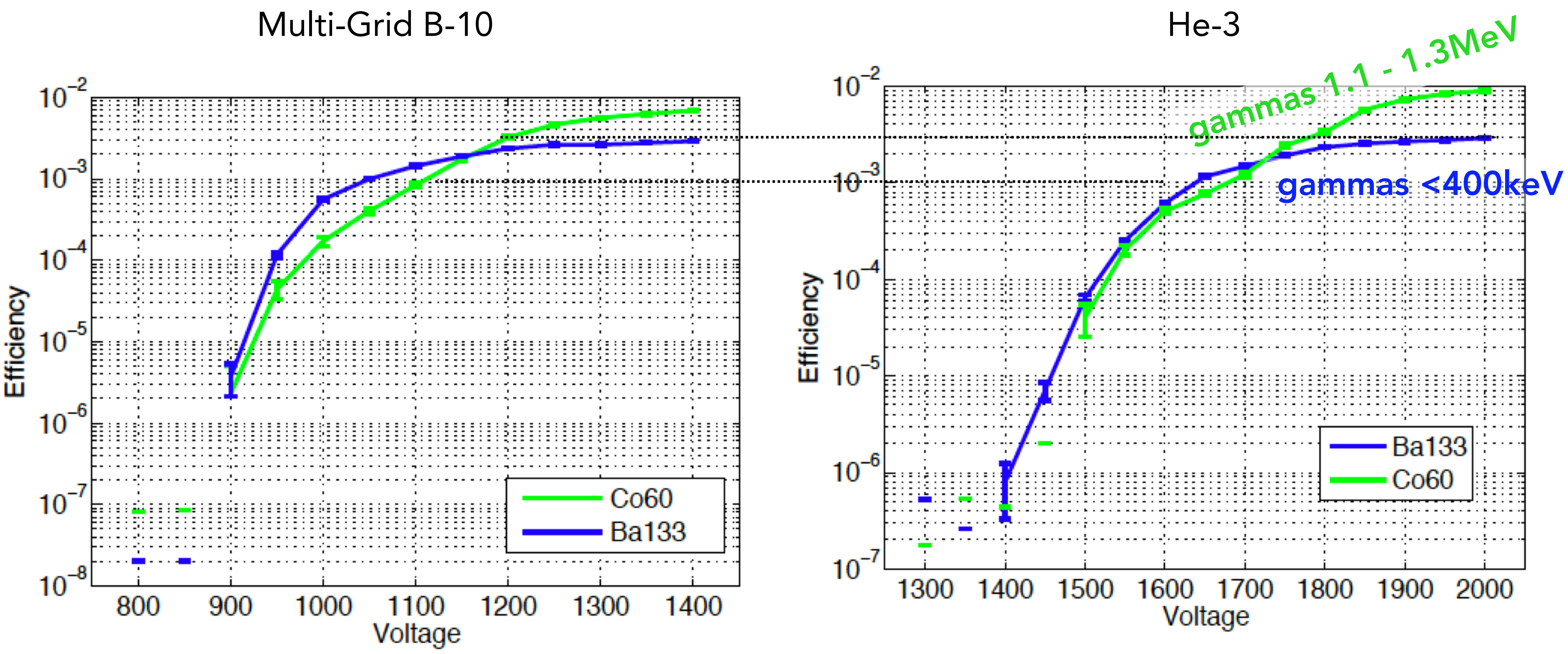

A. Khaplanov et al., Investigation of gamma-ray sensitivity of neutron detectors based on thin converter films, JINST 8 P10025 (2013) (arxiv: 1306:6247)

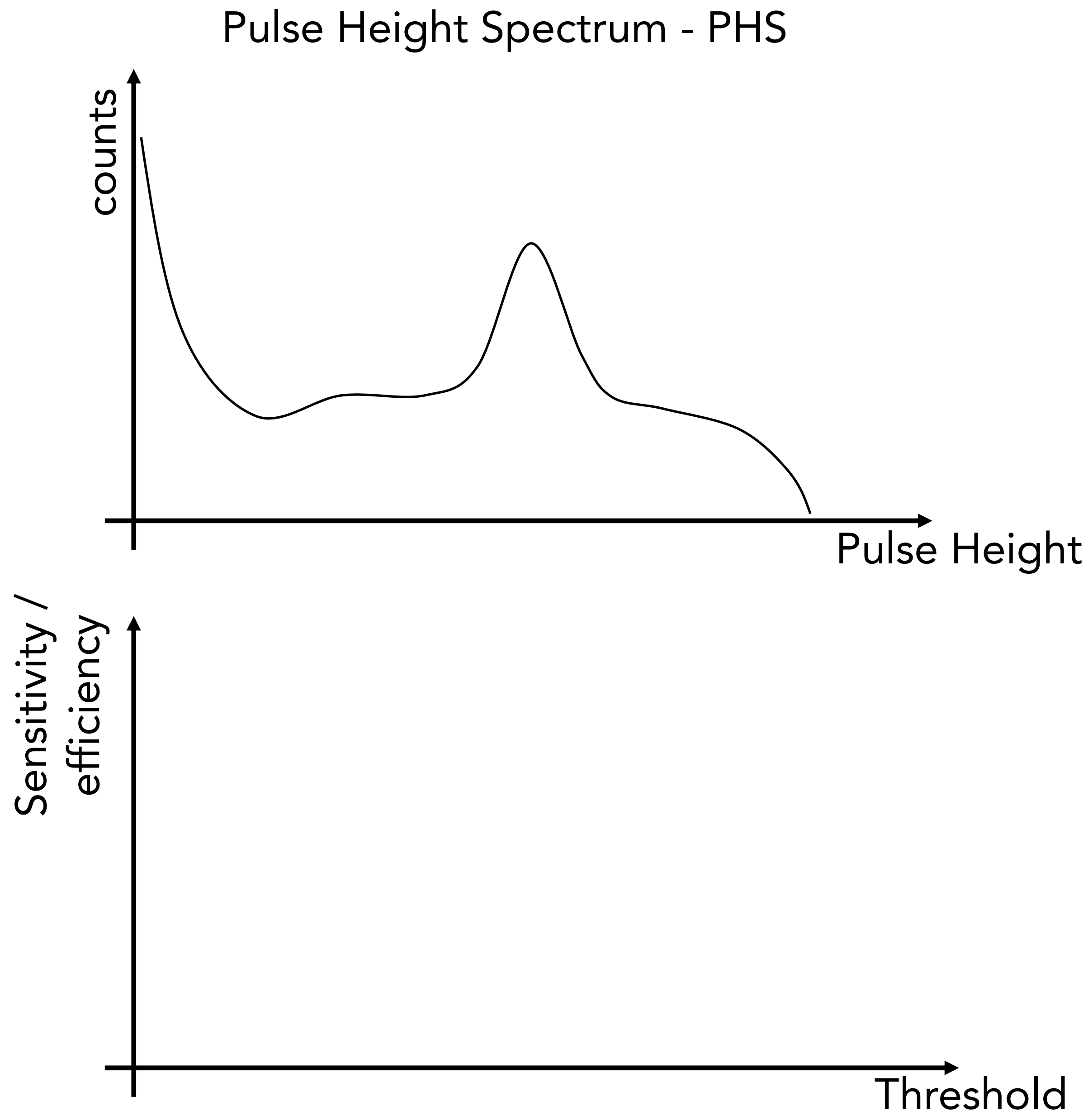
Pulse Height Spectrum - PHS
counts
Pulse Height
Sensitivity /
efficiency
Threshold

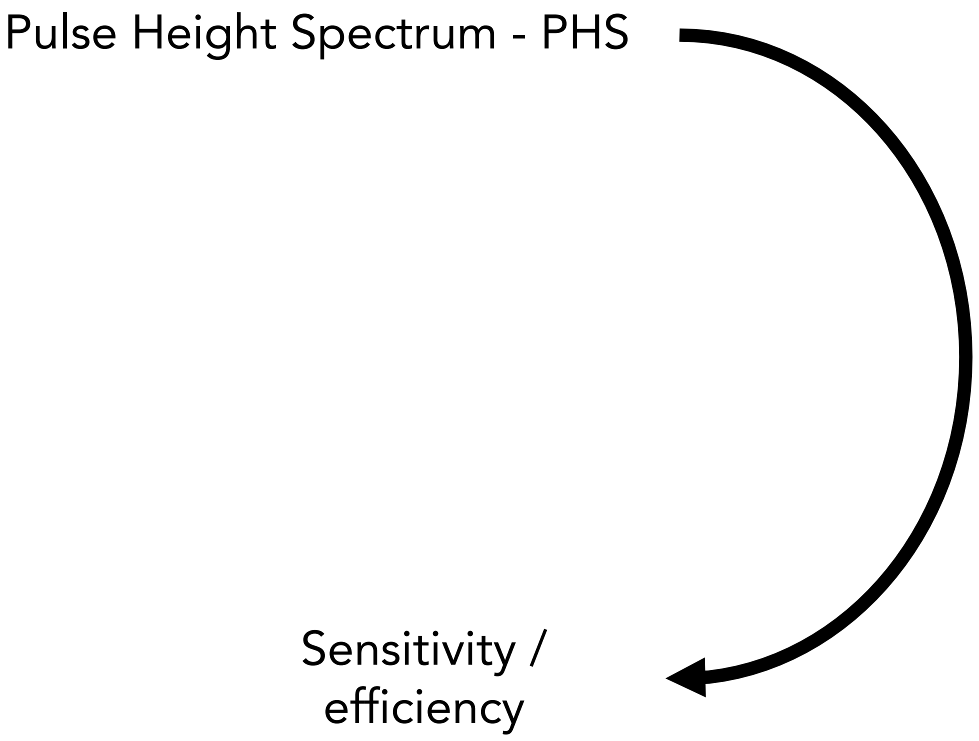
Pulse Height Spectrum - PHS
Sensitivity /
efficiency

Pulse Height Spectrum - PHS

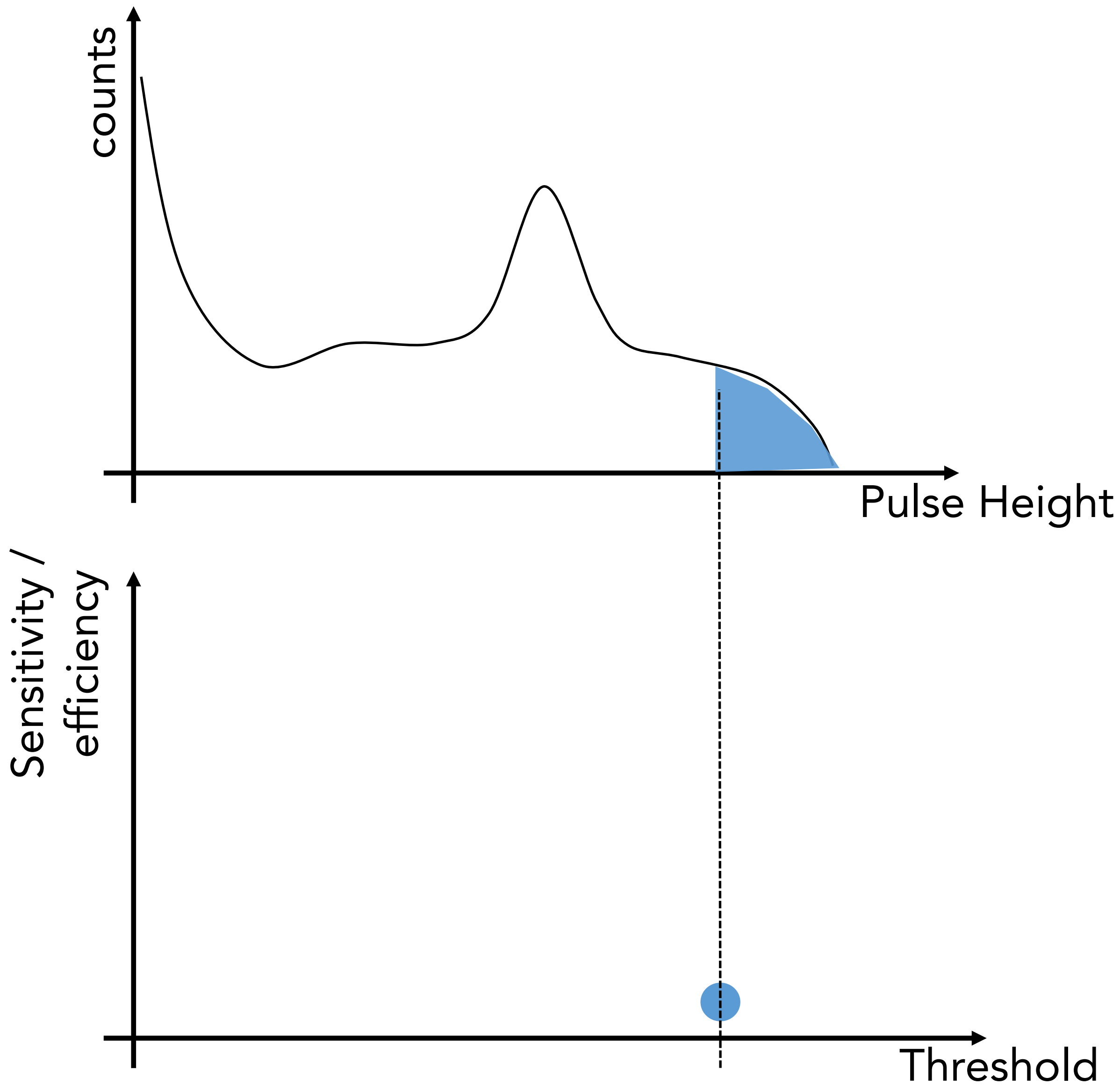

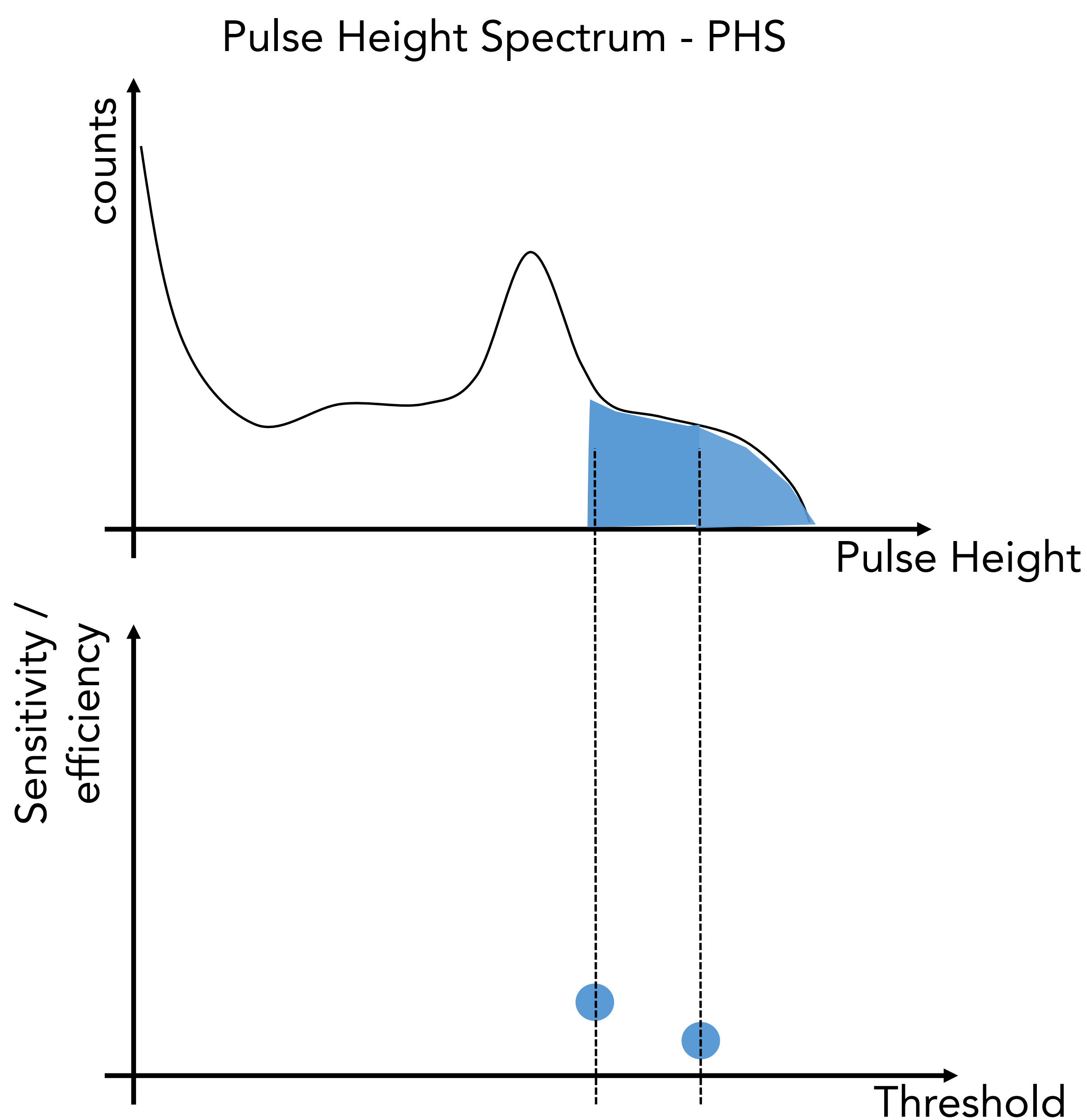

Pulse Height Spectrum - PHS
counts
Pulse Height
Sensitivity / efficiency
Threshold

Pulse Height Spectrum - PHS

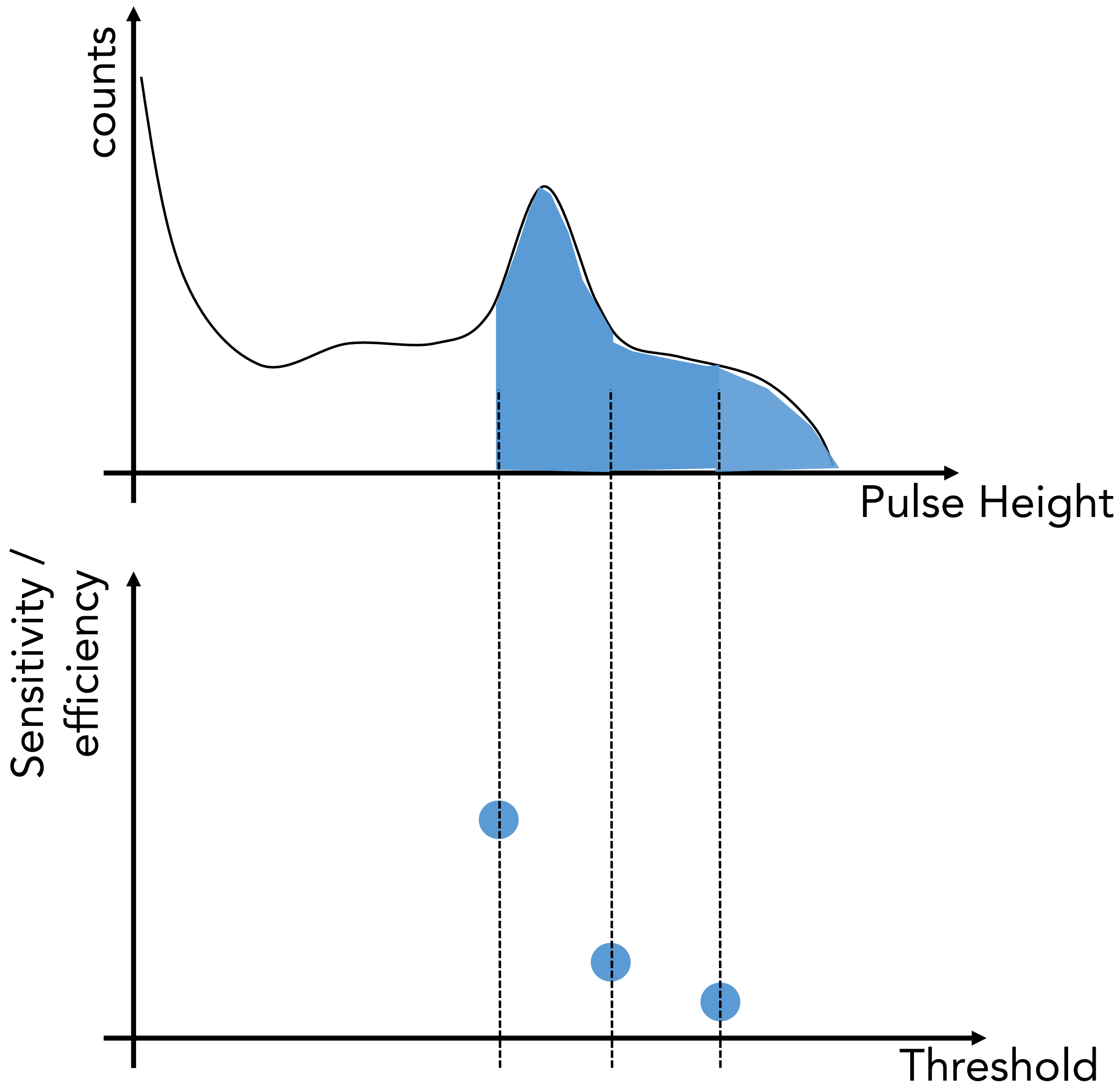

Pulse Height Spectrum - PHS

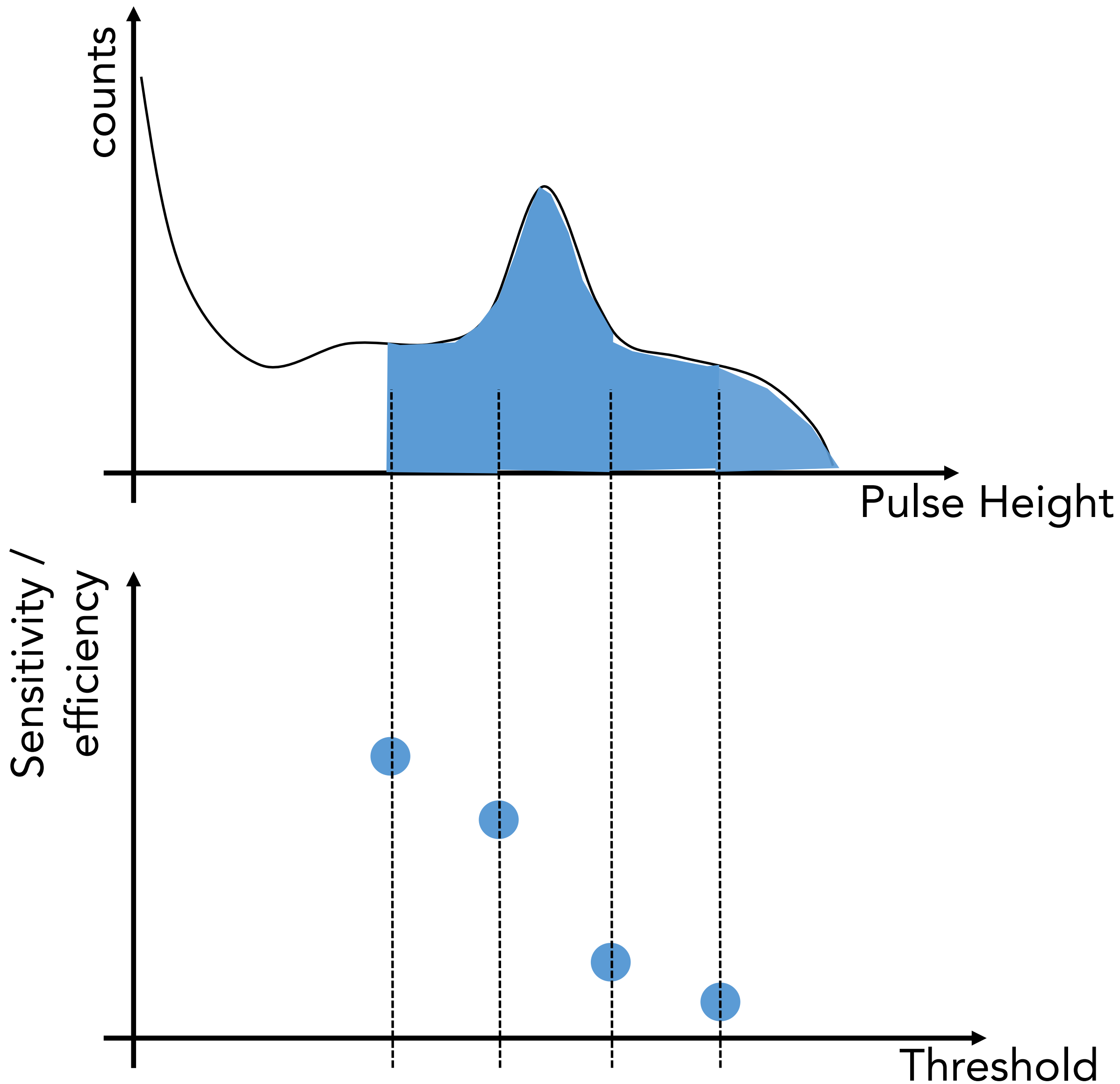

Pulse Height Spectrum - PHS

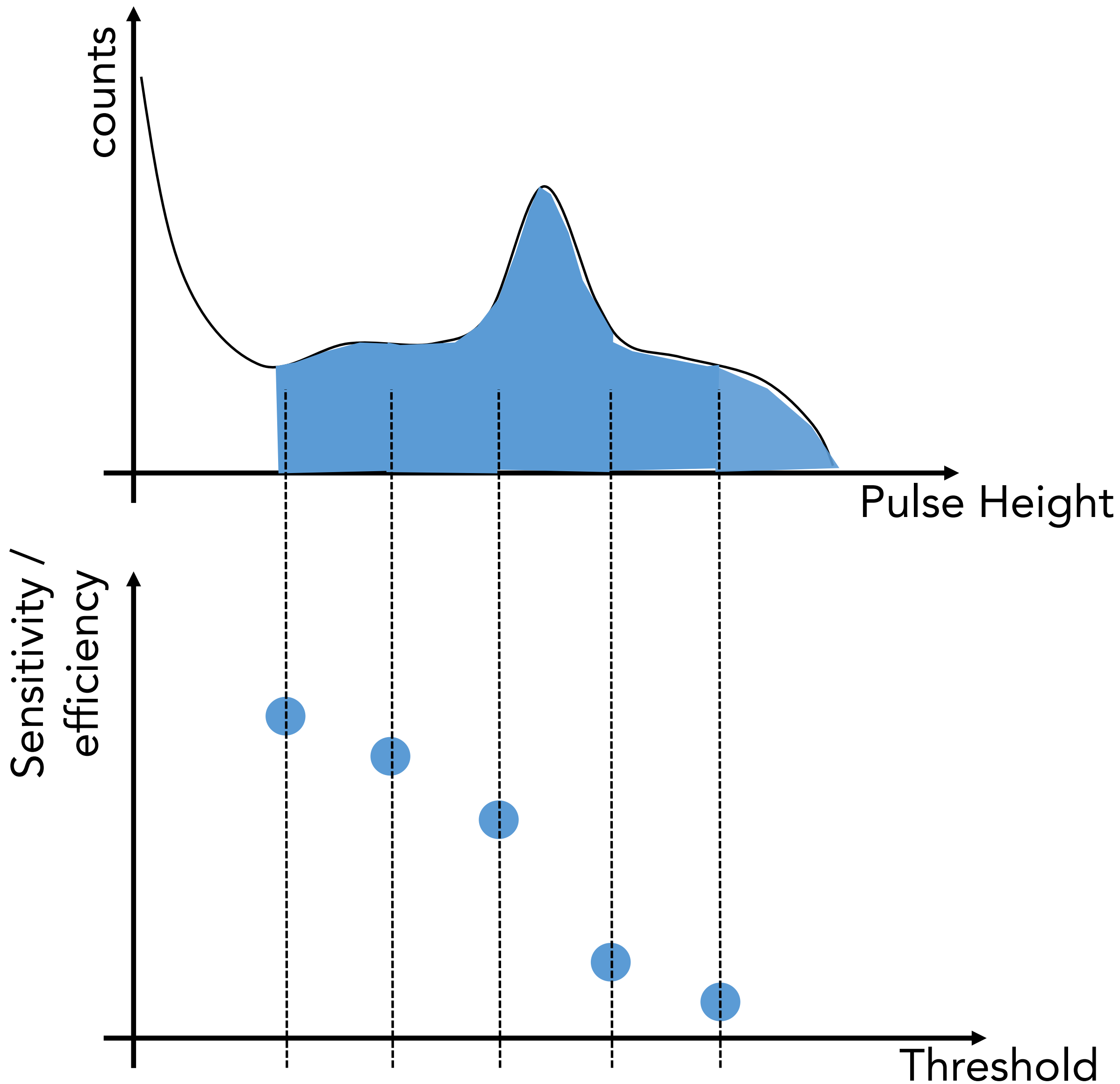

Pulse Height Spectrum - PHS

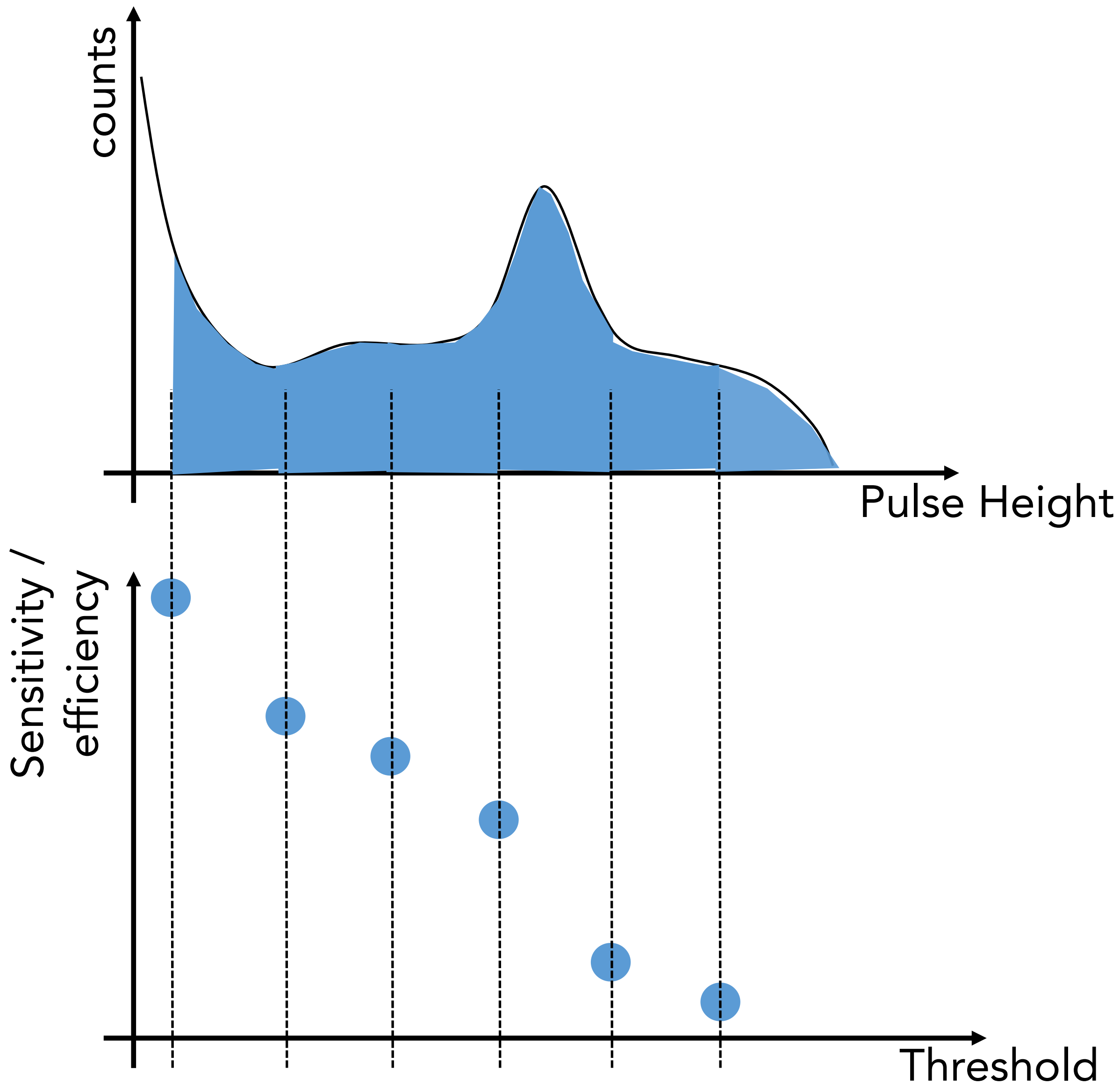

Pulse Height Spectrum - PHS

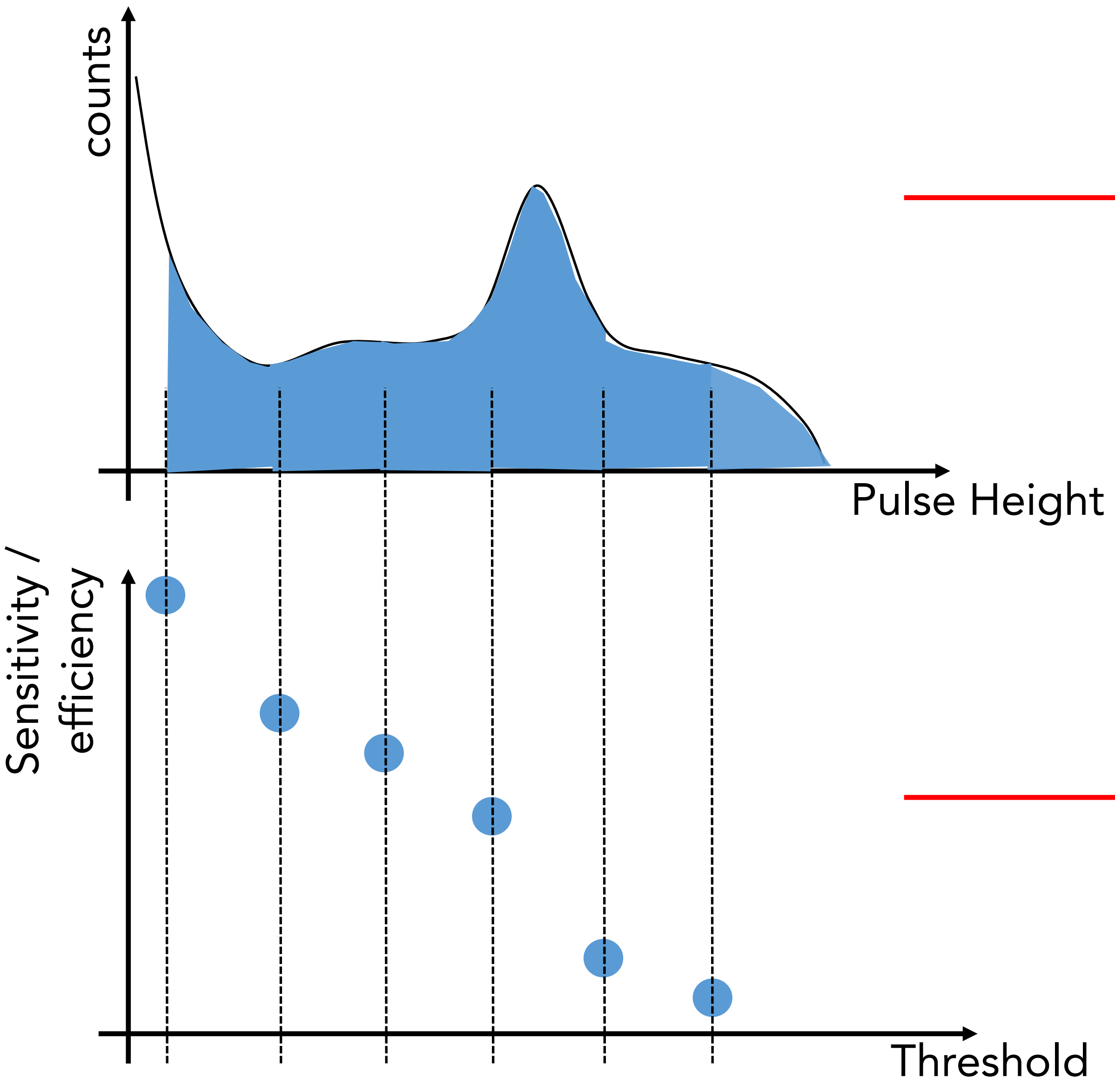

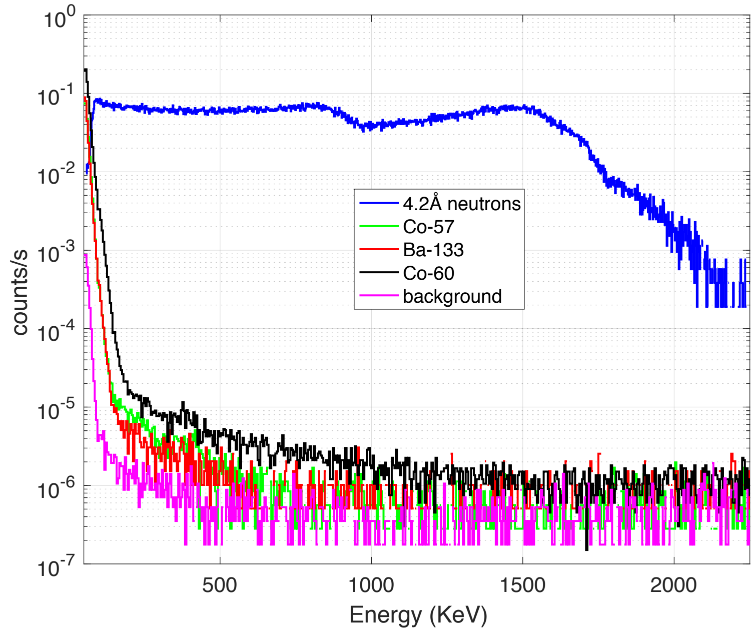

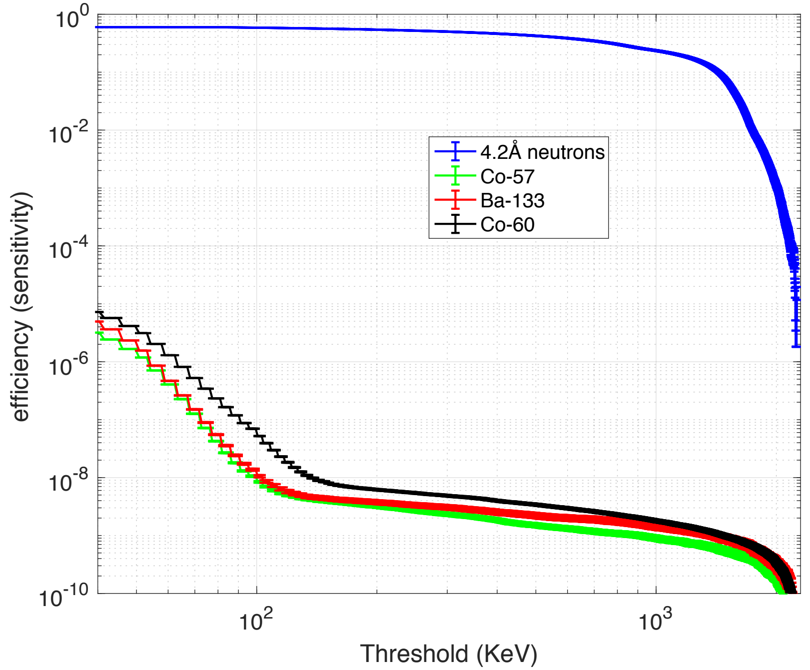

F. Piscitelli et al., The Multi-Blade Boron-10-based Neutron Detector for high intensity Neutron Reflectometry at ESS, JINST 12 P03013 (2017) (arxiv: 1701.07623)

Measured with Multi-Blade B-10

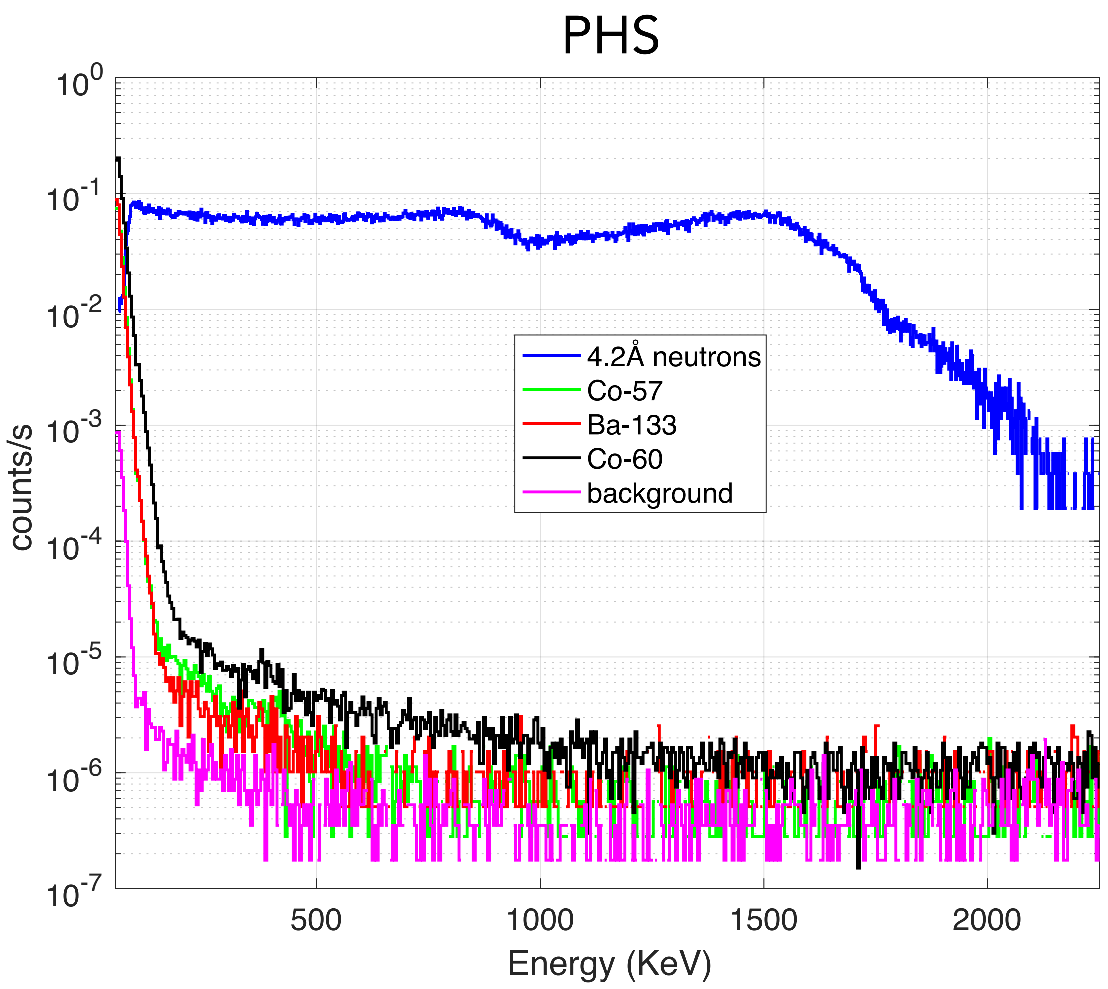

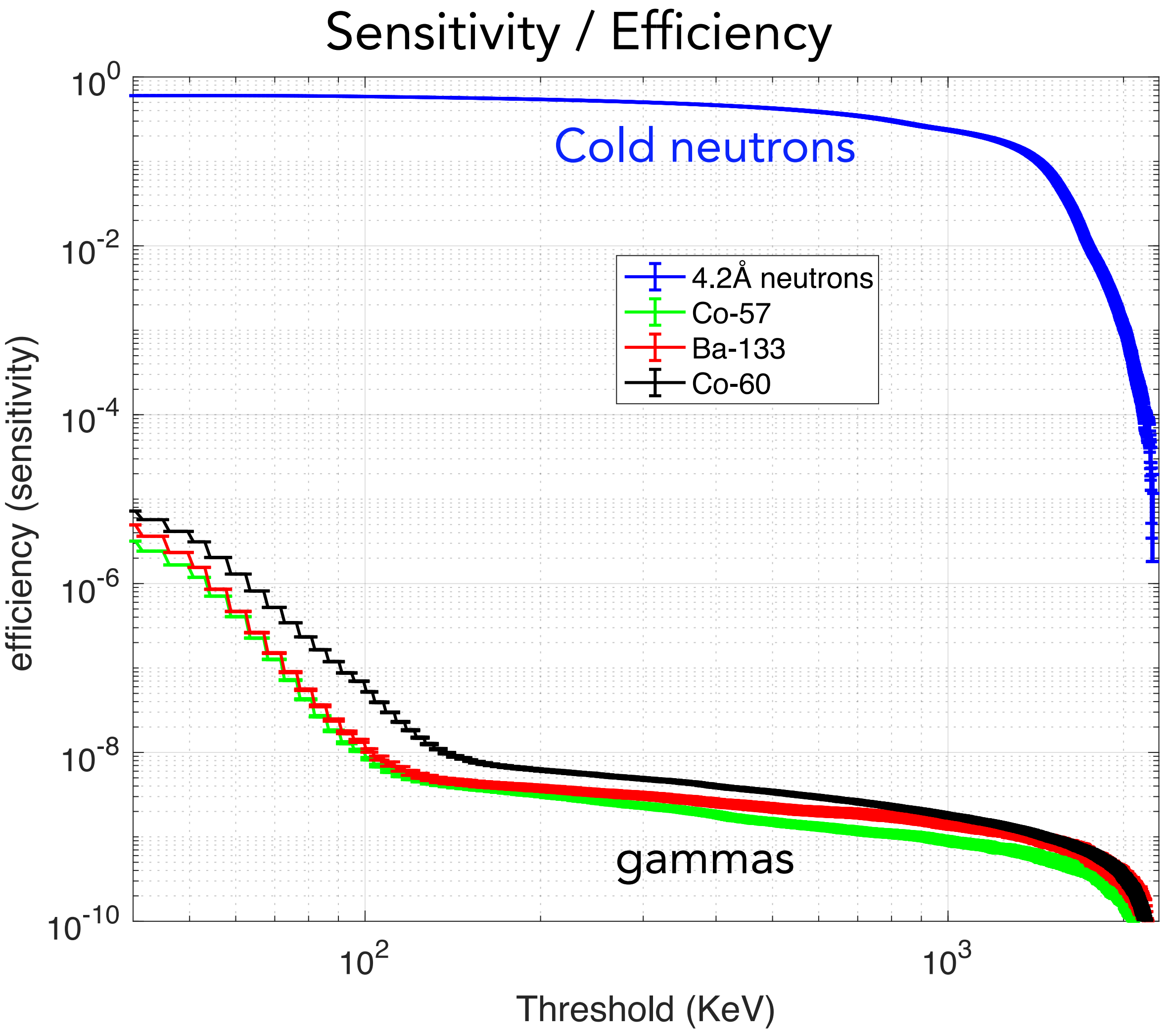

F. Piscitelli et al., The Multi-Blade Boron-10-based Neutron Detector for high intensity Neutron Reflectometry at ESS, JINST 12 P03013 (2017) (arxiv: 1701.07623)

Gamma-ray Sensitivity

10^{-6}

10^{-9}

No matter if He3 or B-10
(Solid Dominates)

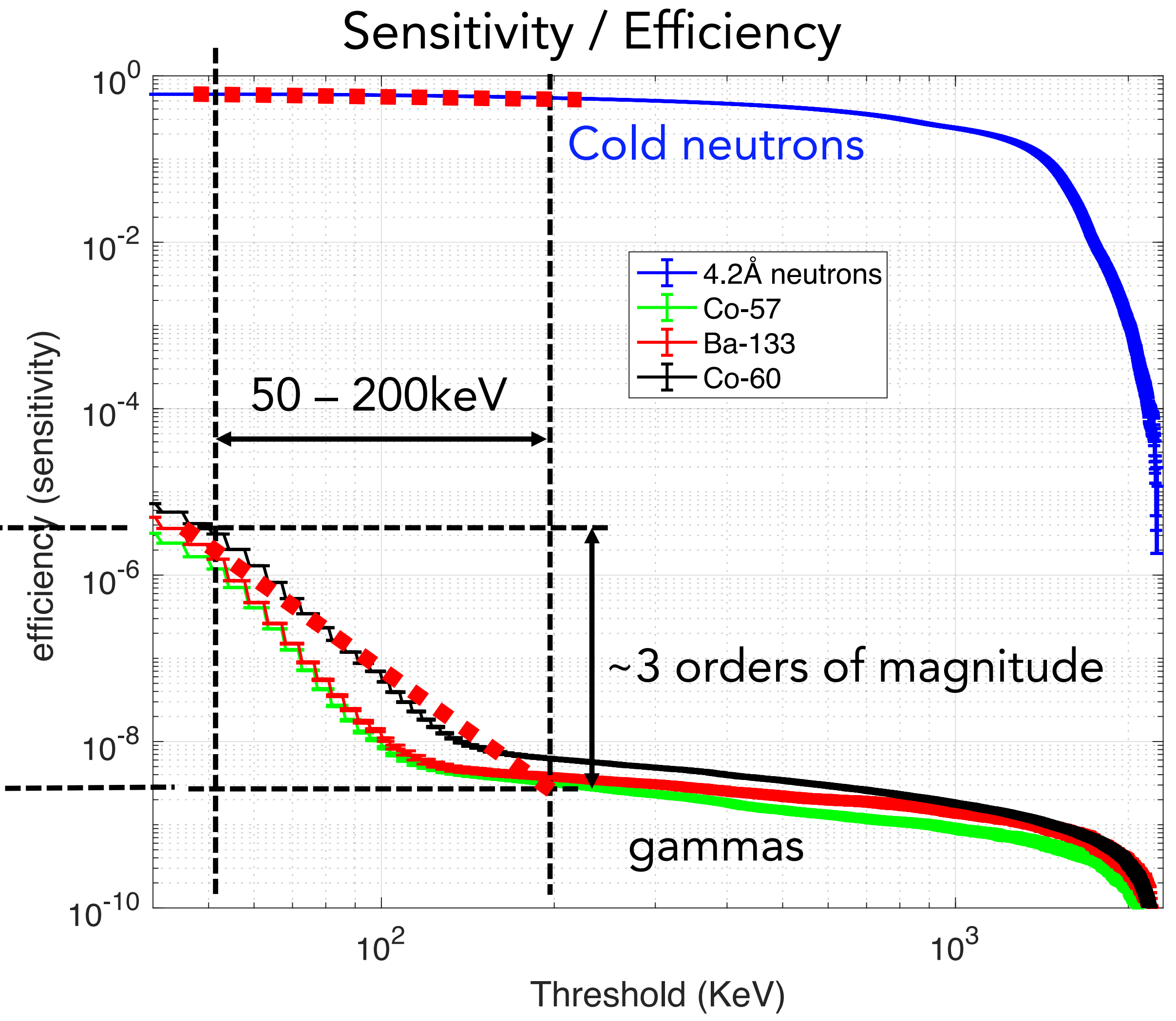

F. Piscitelli et al., The Multi-Blade Boron-10-based Neutron Detector for high intensity Neutron Reflectometry at ESS, JINST 12 P03013 (2017) (arxiv: 1701.07623)

FAST NEUTRON BACKGROUND

BACKGROUND: fast neutrons

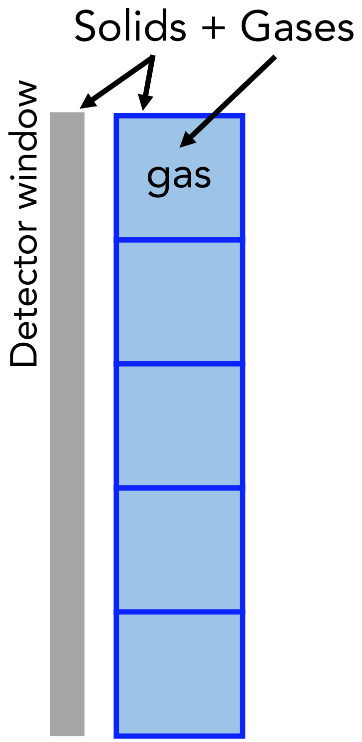

BACKGROUND: fast neutrons

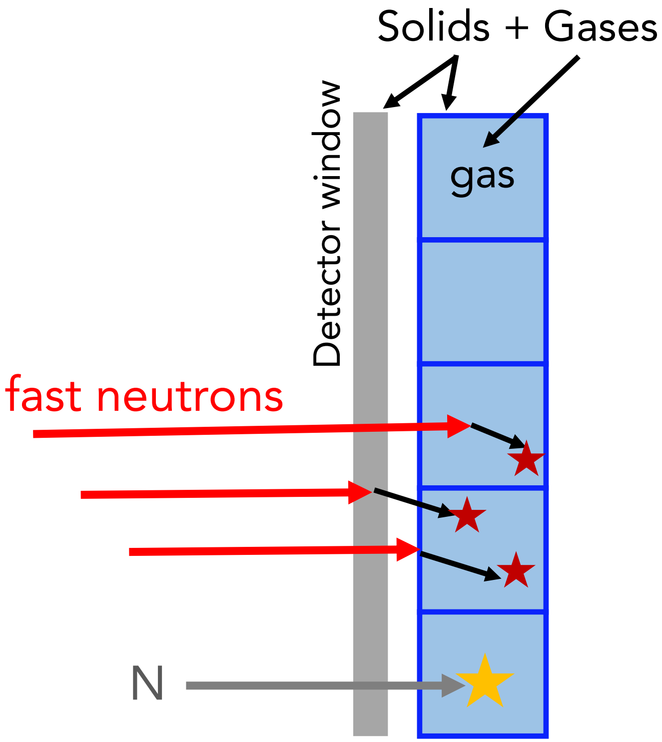

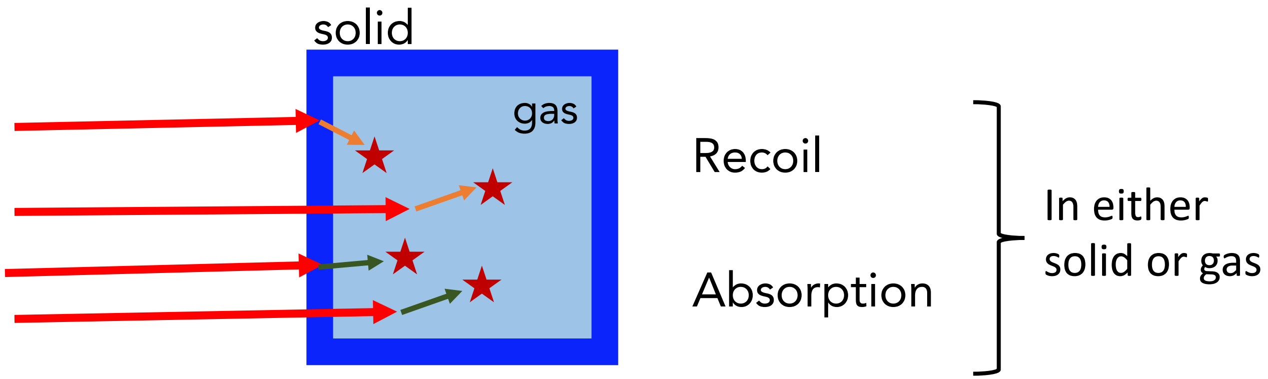

BACKGROUND: fast neutrons

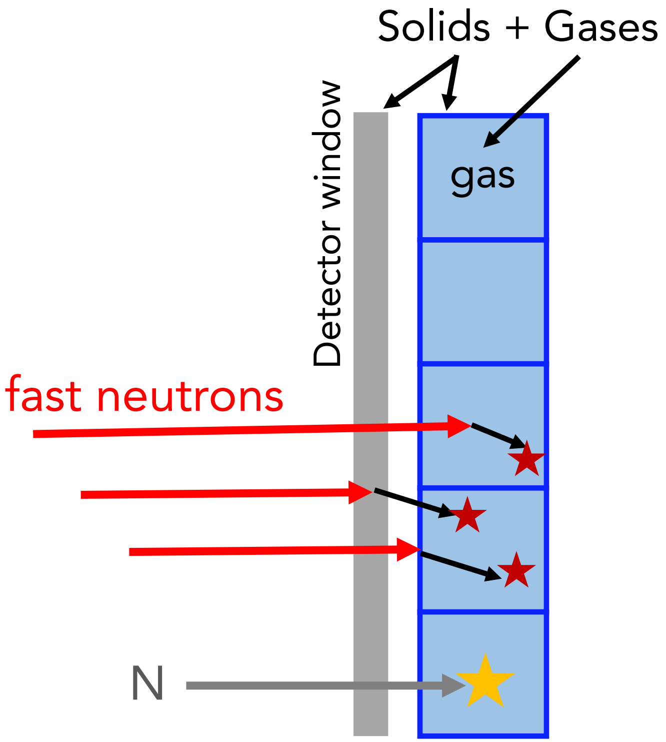

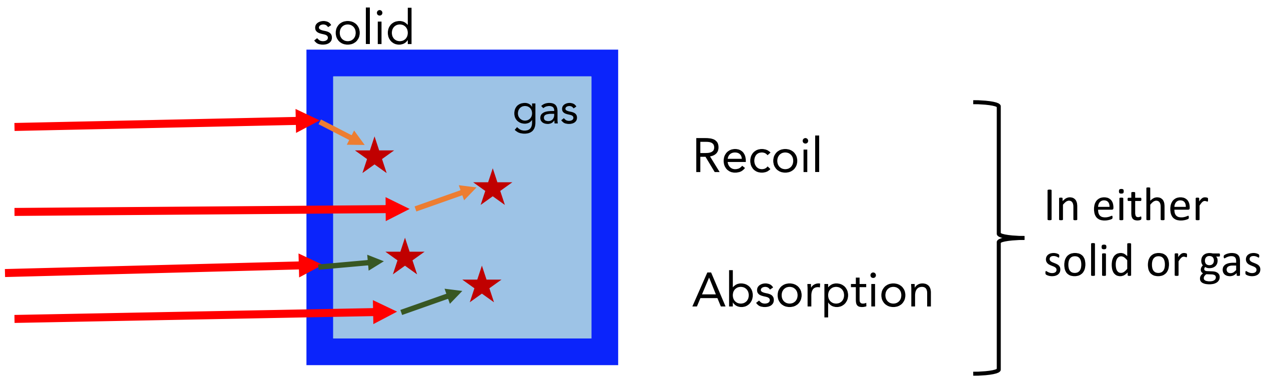

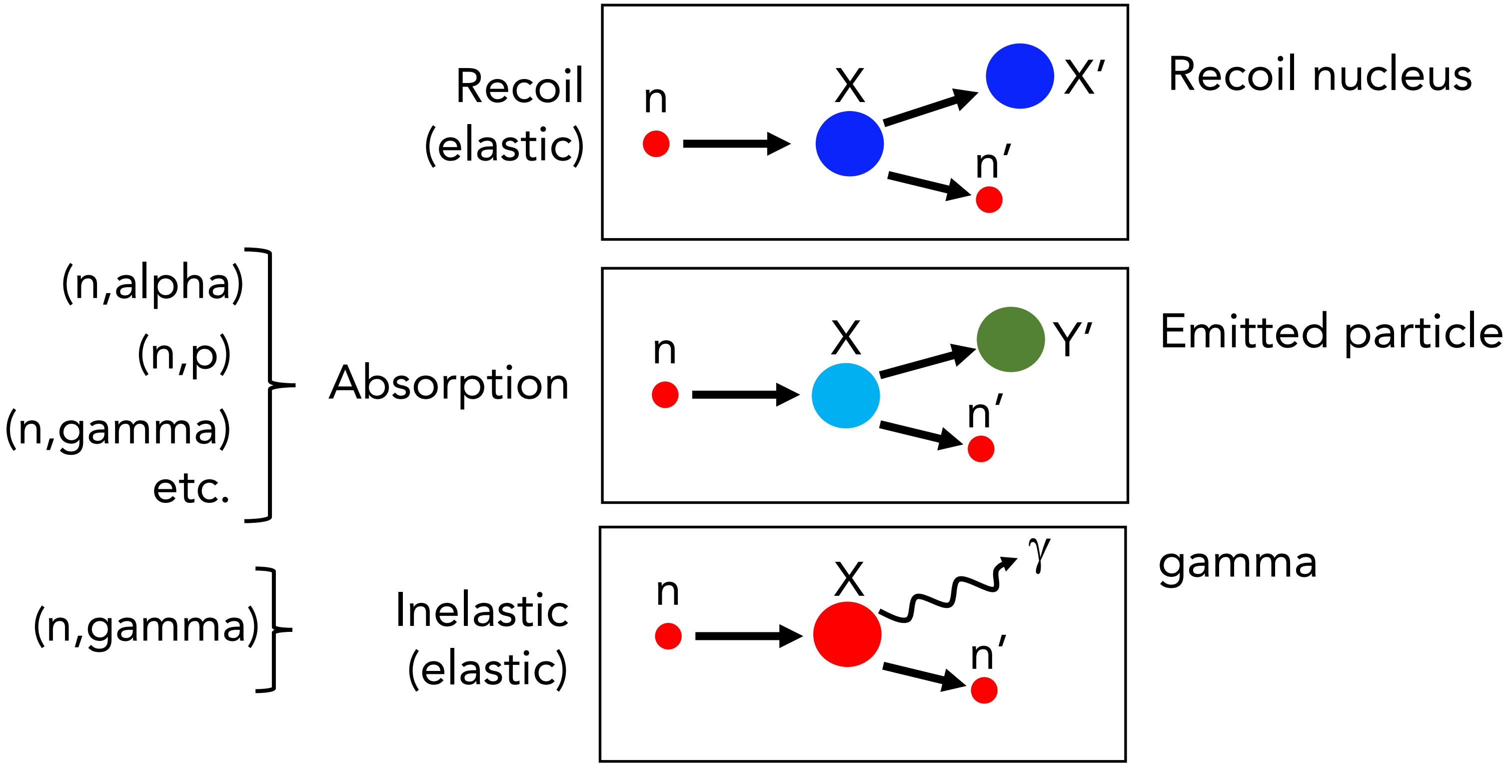

BACKGROUND: fast neutrons

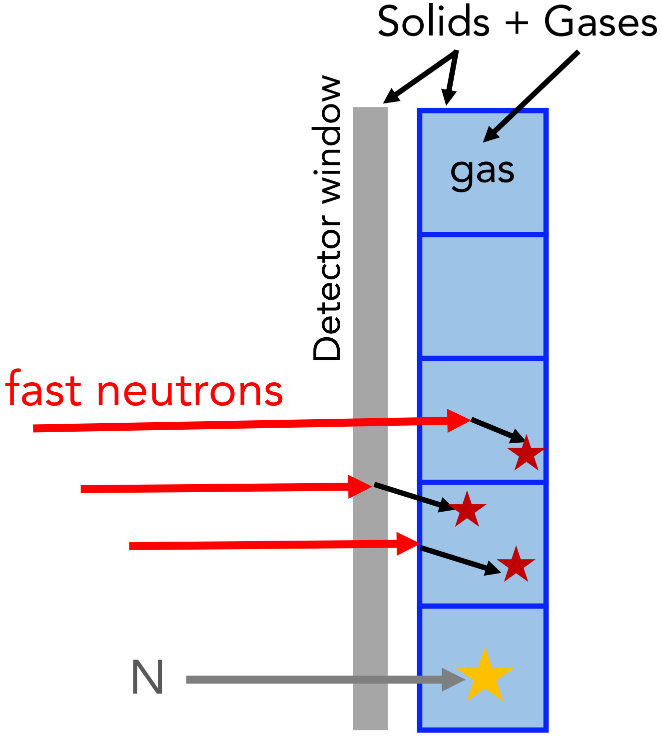

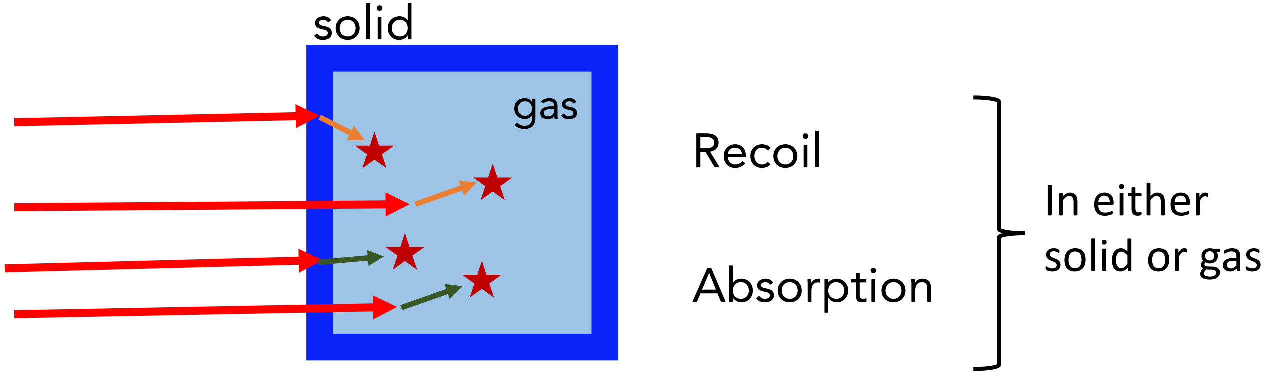

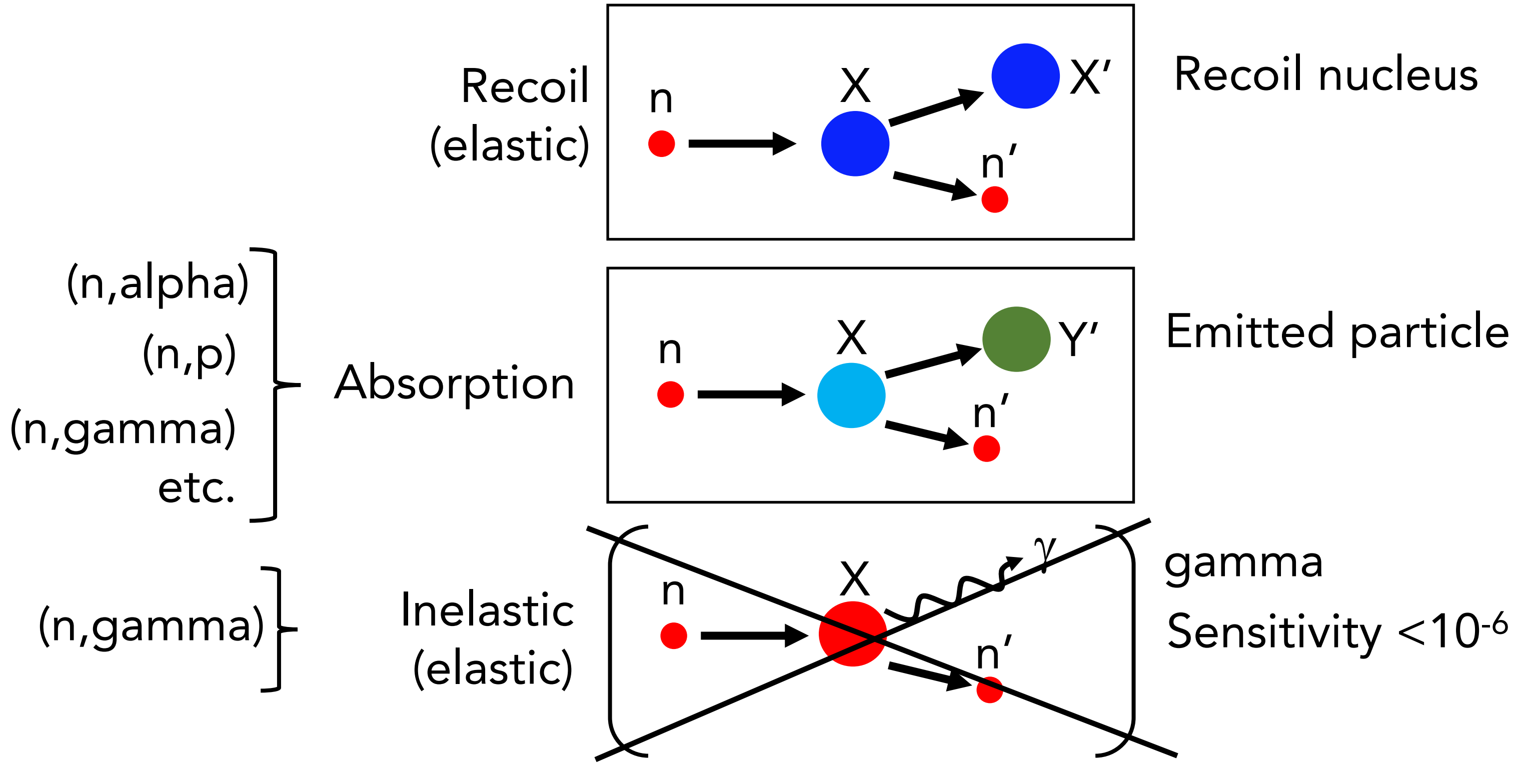

BACKGROUND: fast neutrons

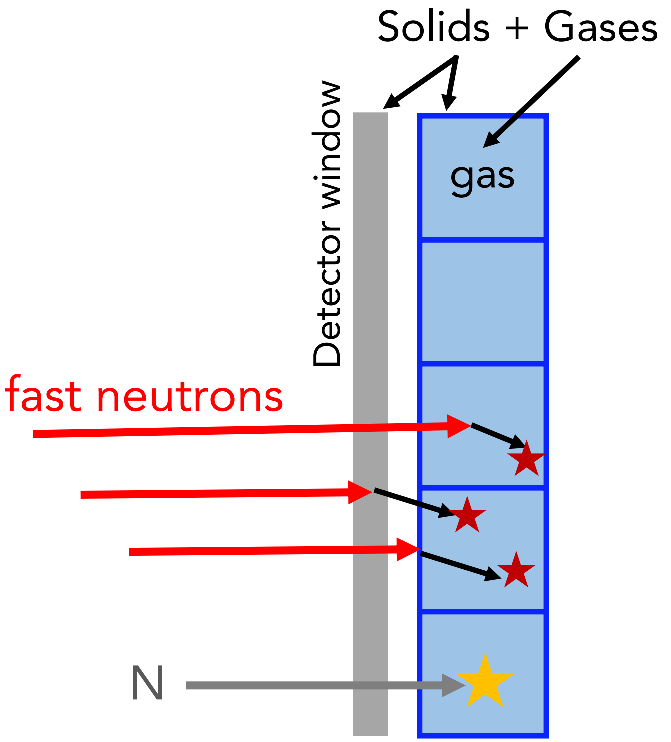

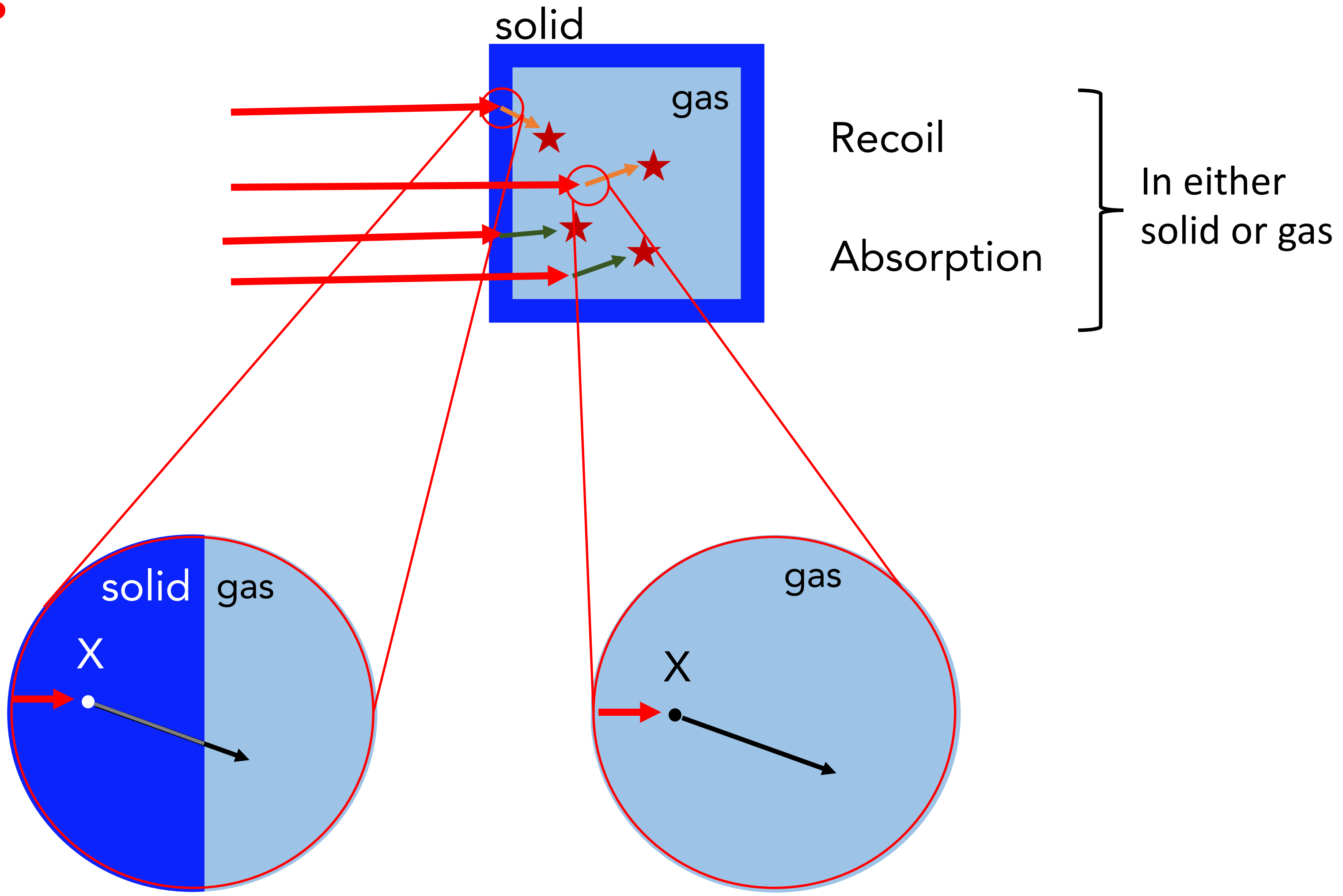

particle in the walls can only result in a signal if the particle reaches the gas

particles interacting with the gas are guaranteed to generate a signal

Solid vs Gas

BACKGROUND: fast neutrons

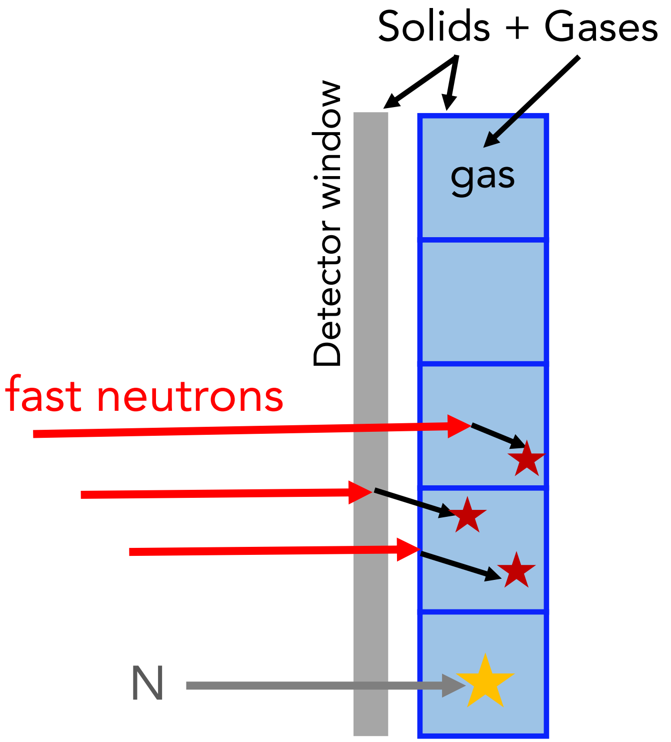

Gas dominates

Gas = x100 Solid

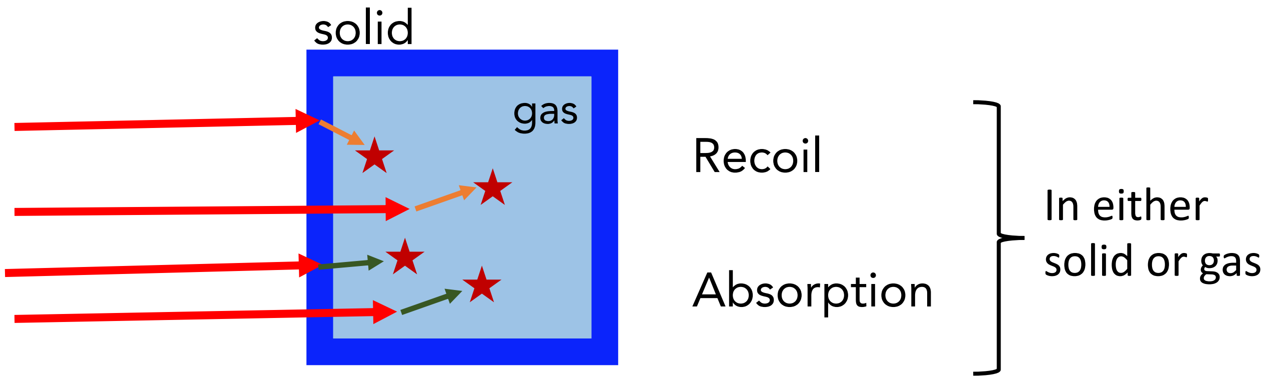

Solid vs Gas

True for both He-3 and B-10

Probability to generate an event

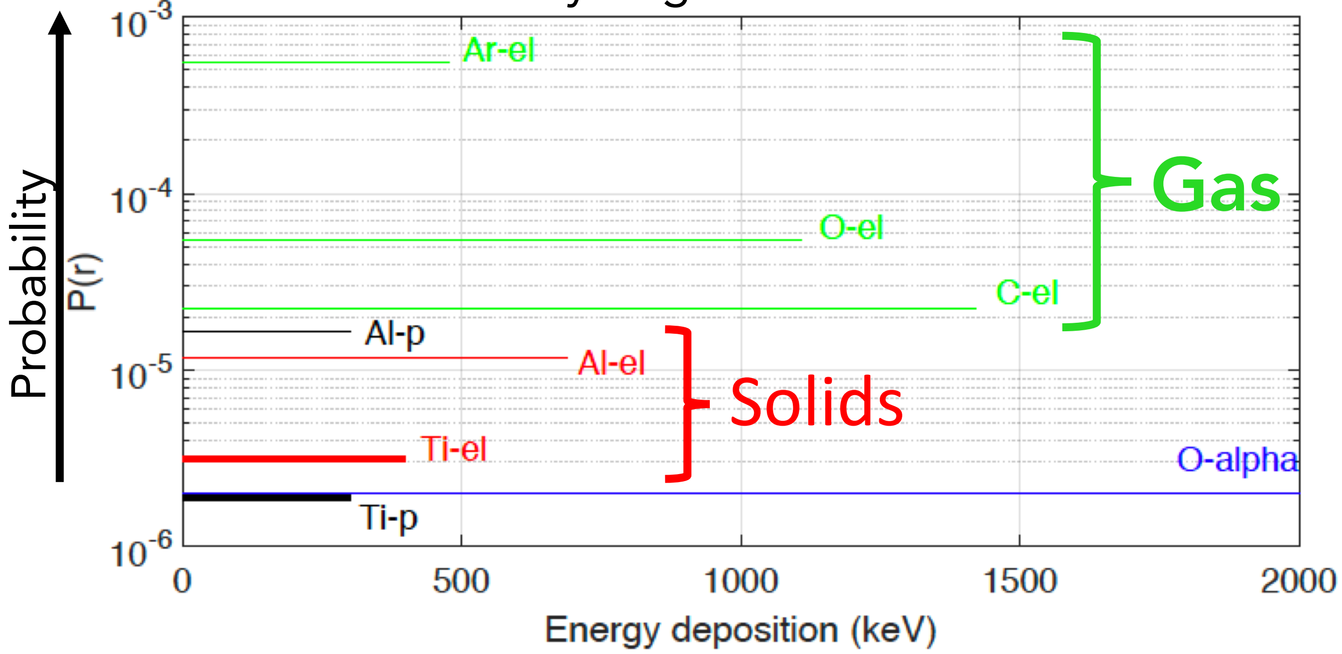

BACKGROUND: fast neutrons

Gas is main component, then He-3 differs from B-10 …

Gas dominates

Recoil on He-3

He-3 detector

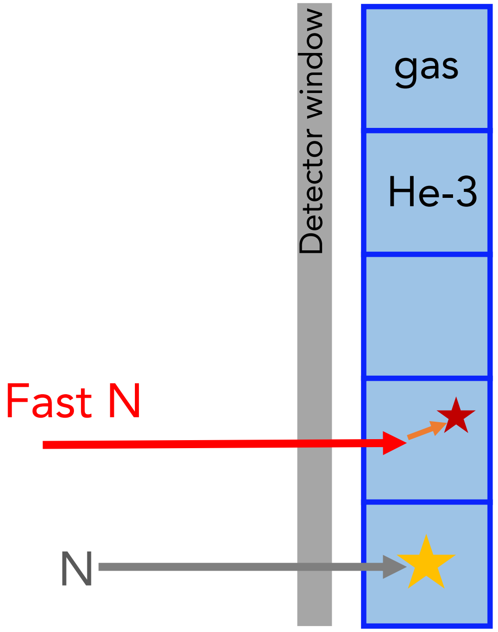

Window+(conversion+detection)

Recoil on Argon

B-10 detector

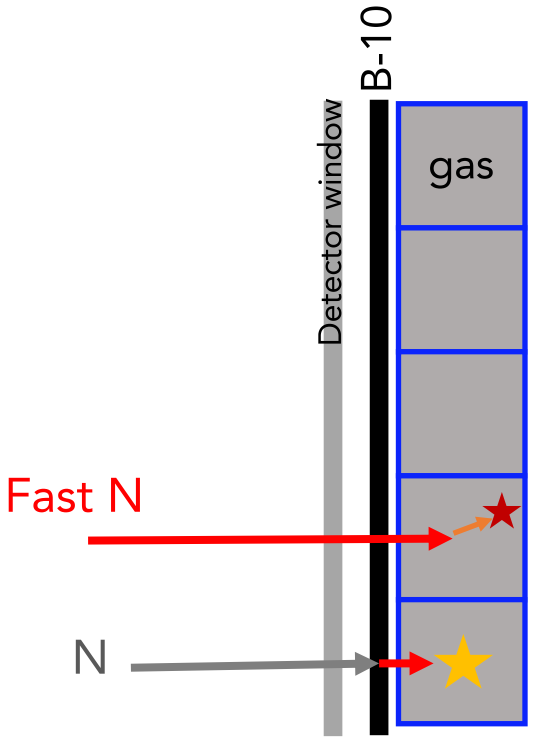

Window+conversion+detection

BACKGROUND: fast neutrons

Gas is main component, then He-3 differs from B-10 …

Gas dominates

Recoil on He-3

He-3 detector

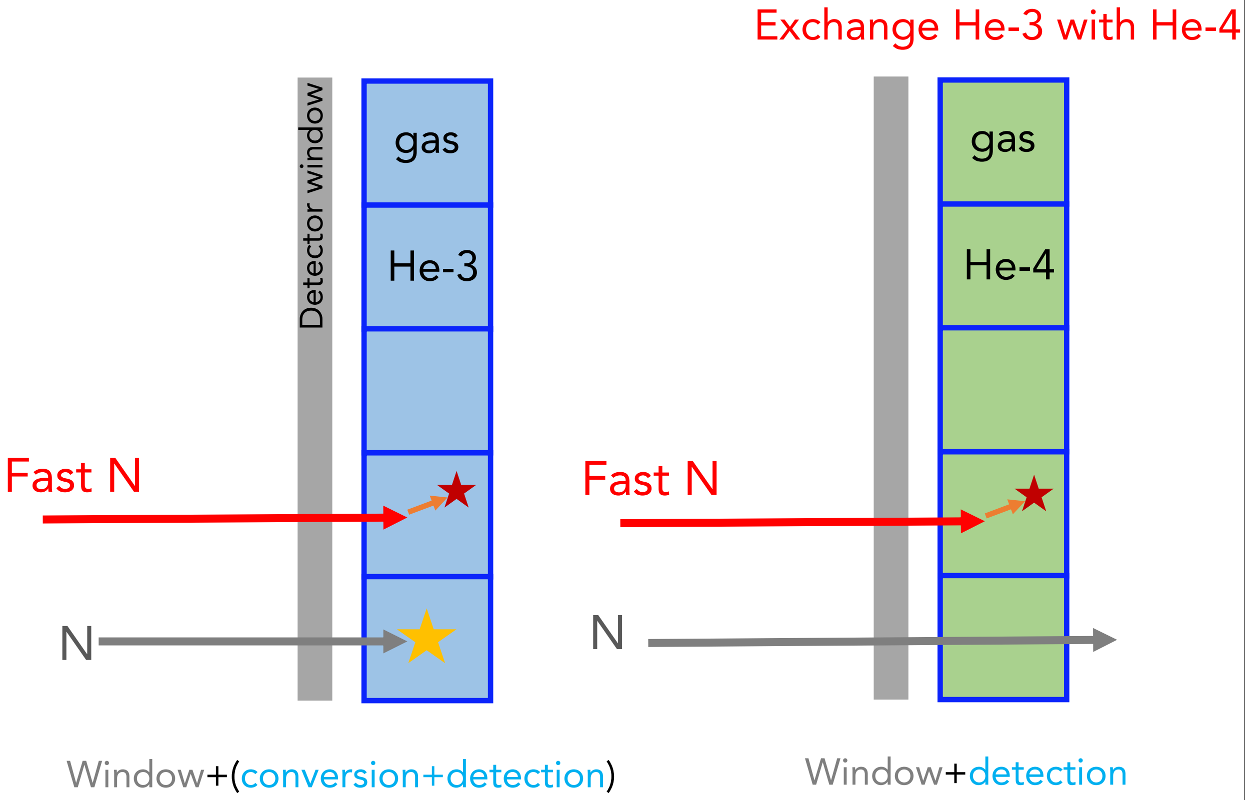

Recoil on Argon

B-10 detector

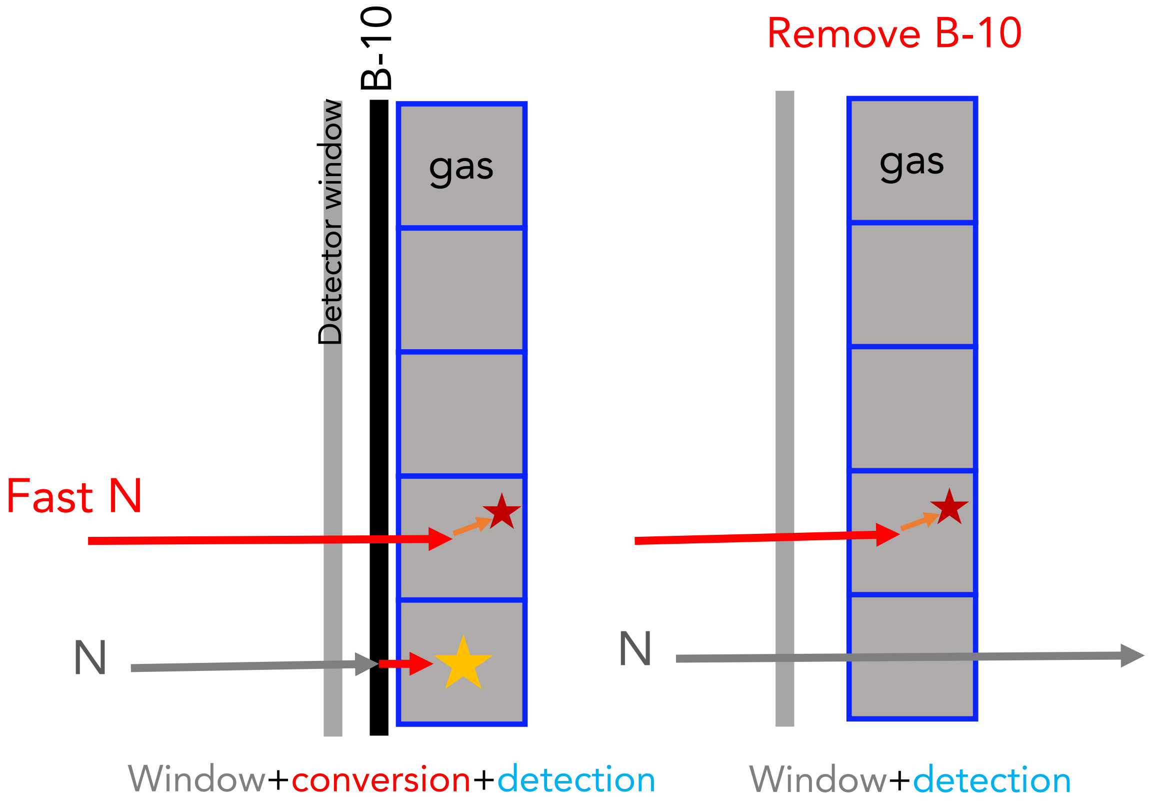

BACKGROUND: fast neutrons

Gas is main component, then He-3 differs from B-10 …

Gas dominates

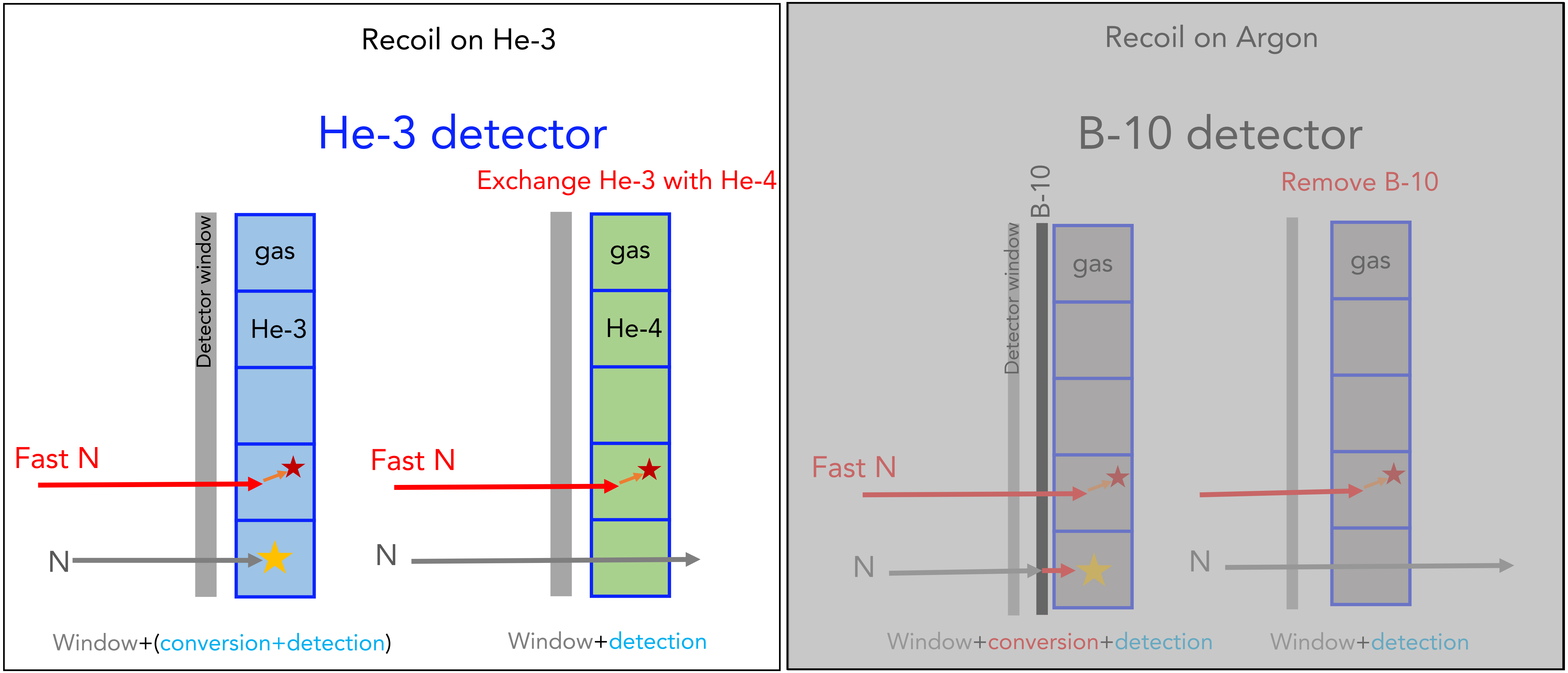

BACKGROUND: fast neutrons in He-3 detectors

*Thanks to Toshiba/Canon Electron Tubes & Devices Co. LTD for the He-4 tubes.

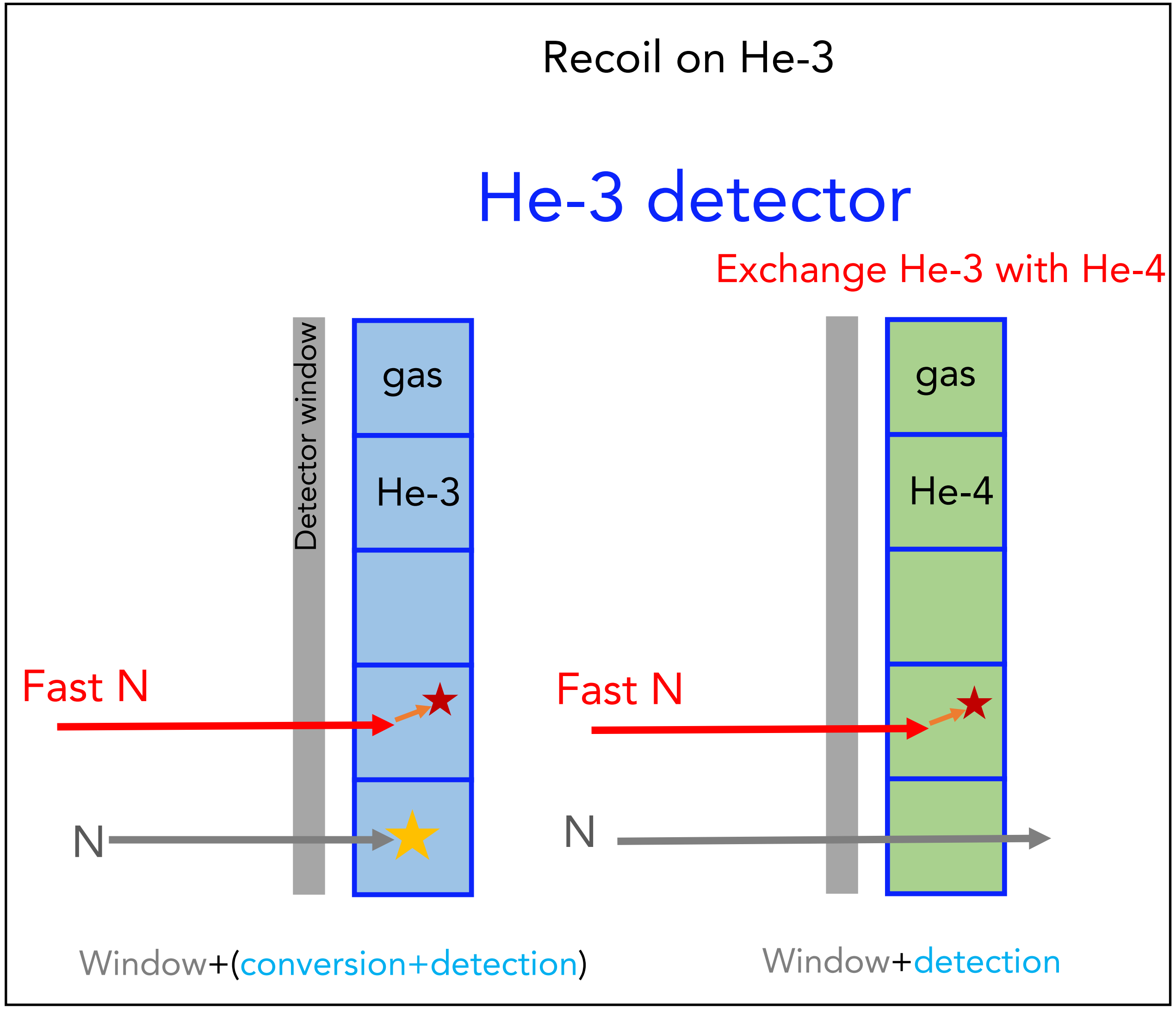

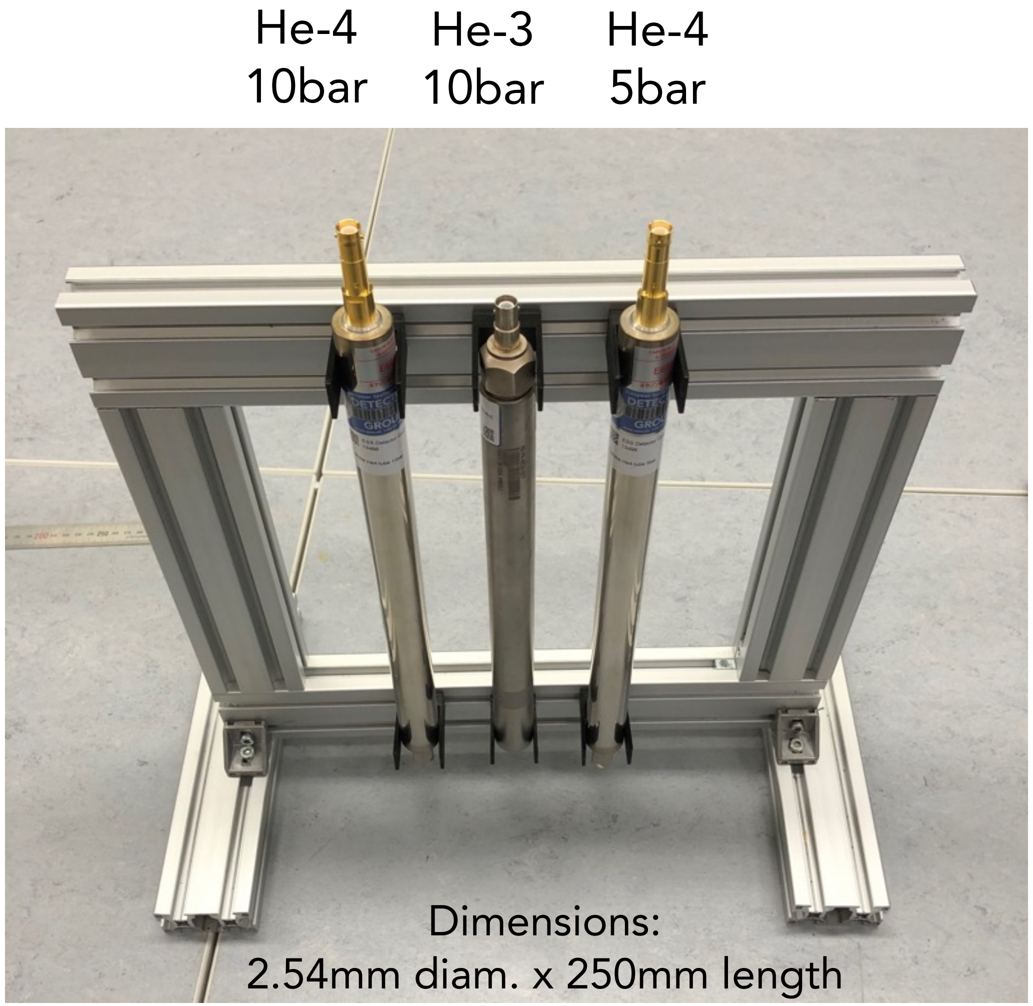

F. Piscitelli et al., Verification of He-3 proportional counters fast neutron sensitivity through a comparison with He-4 detectors, sub. to EPJ Plus (2020) (arxiv: 2002.08153)

BACKGROUND: fast neutrons in He-3 detectors

Exchanging He-3 with He-4 is a good approximation to evaluate the sensitivity of He-3 to fast n

He-3

Recoil

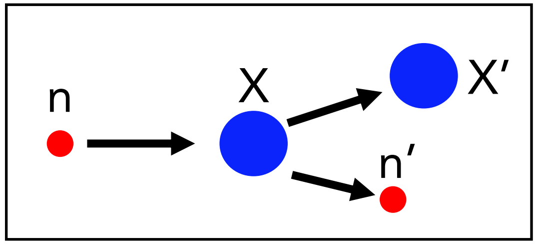

Absorption

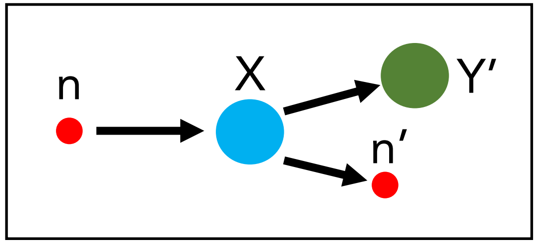

(n,p)

He-4

Recoil

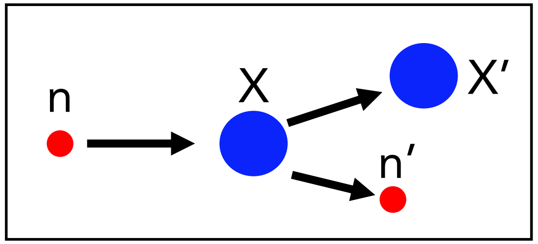

F. Piscitelli et al., Verification of He-3 proportional counters fast neutron sensitivity through a comparison with He-4 detectors, sub. to EPJ Plus (2020) (arxiv: 2002.08153)

BACKGROUND: fast neutrons in He-3 detectors

Exchanging He-3 with He-4 is a good approximation to evaluate the sensitivity of He-3 to fast n

- 1 Similar total cross-section: σ(He-3) ~ σ(He-4)

He-3

Recoil

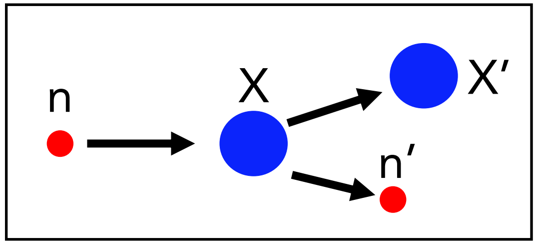

Absorption

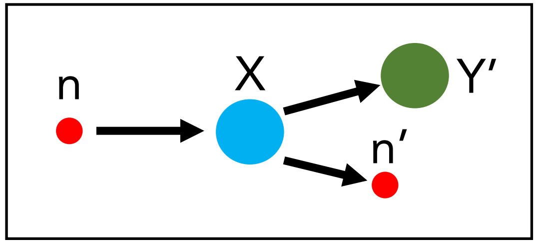

(n,p)

He-4

Recoil

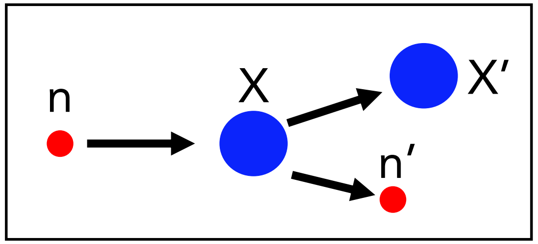

F. Piscitelli et al., Verification of He-3 proportional counters fast neutron sensitivity through a comparison with He-4 detectors, sub. to EPJ Plus (2020) (arxiv: 2002.08153)

BACKGROUND: fast neutrons in He-3 detectors

Exchanging He-3 with He-4 is a good approximation to evaluate the sensitivity of He-3 to fast n

He-3

Recoil

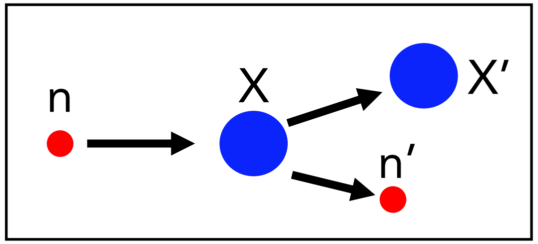

Absorption

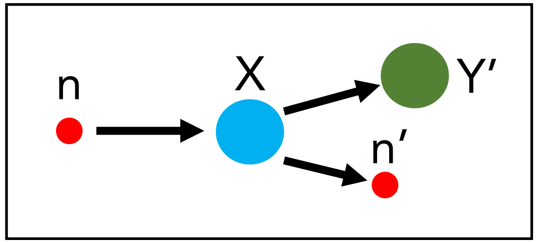

(n,p)

- 1 Similar total cross-section: σ(He-3) ~ σ(He-4)
- 2 Almost identical energy deposition ion gas: $He\text{-}3^{++}$ in He-3 ~ $He\text{-}4^{++}$ in He-4

He-4

Recoil

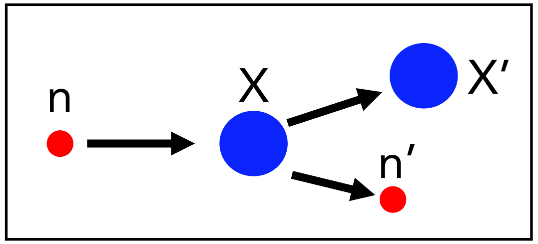

F. Piscitelli et al., Verification of He-3 proportional counters fast neutron sensitivity through a comparison with He-4 detectors, sub. to EPJ Plus (2020) (arxiv: 2002.08153)

BACKGROUND: fast neutrons in He-3 detectors

Exchanging He-3 with He-4 is a good approximation to evaluate the sensitivity of He-3 to fast n

He-3

Recoil

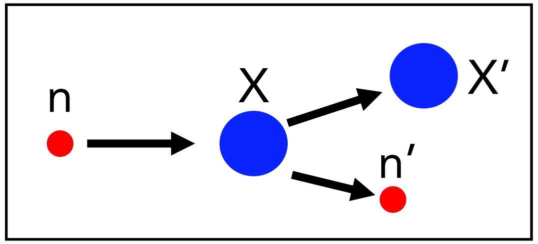

Absorption

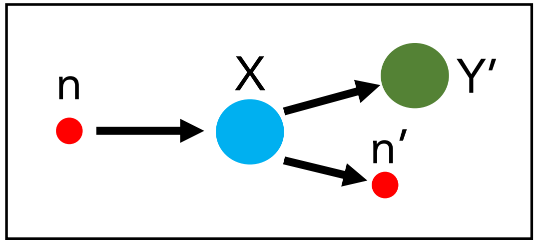

(n,p)

- 1 Similar total cross-section:
  σ(He-3) ~ σ(He-4)
- 2 Almost identical energy deposition ion gas:
  $He\text{-}3^{++}$ in He-3 ~ $He\text{-}4^{++}$ in He-4
- 3 If mono-energetic beam E_i

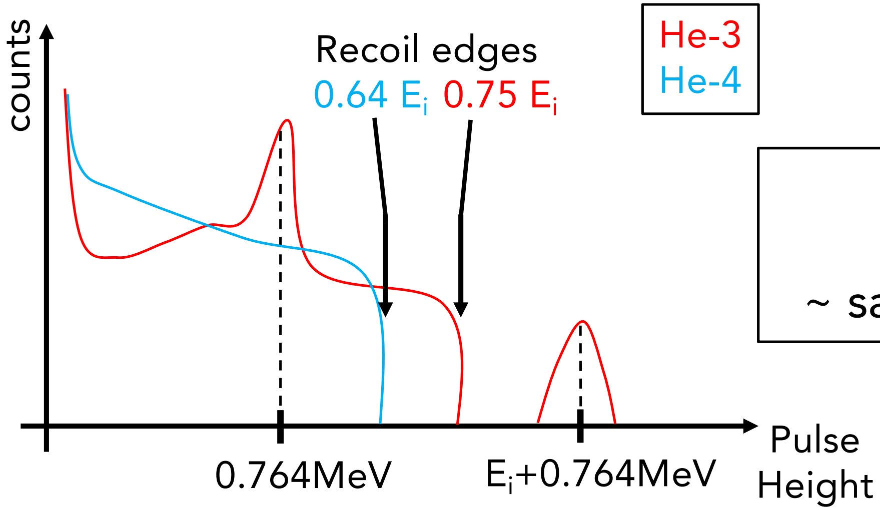

Different PHS
but
~ same number of events !

He-4

Recoil

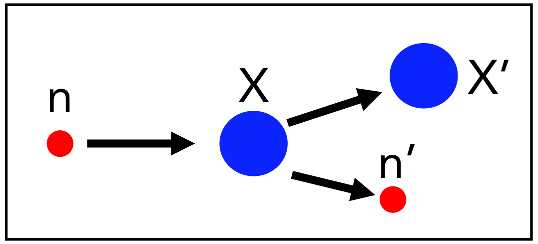

F. Piscitelli et al., Verification of He-3 proportional counters fast neutron sensitivity through a comparison with He-4 detectors, sub. to EPJ Plus (2020) (arxiv: 2002.08153)

Pulse Height Spectrum - PHS

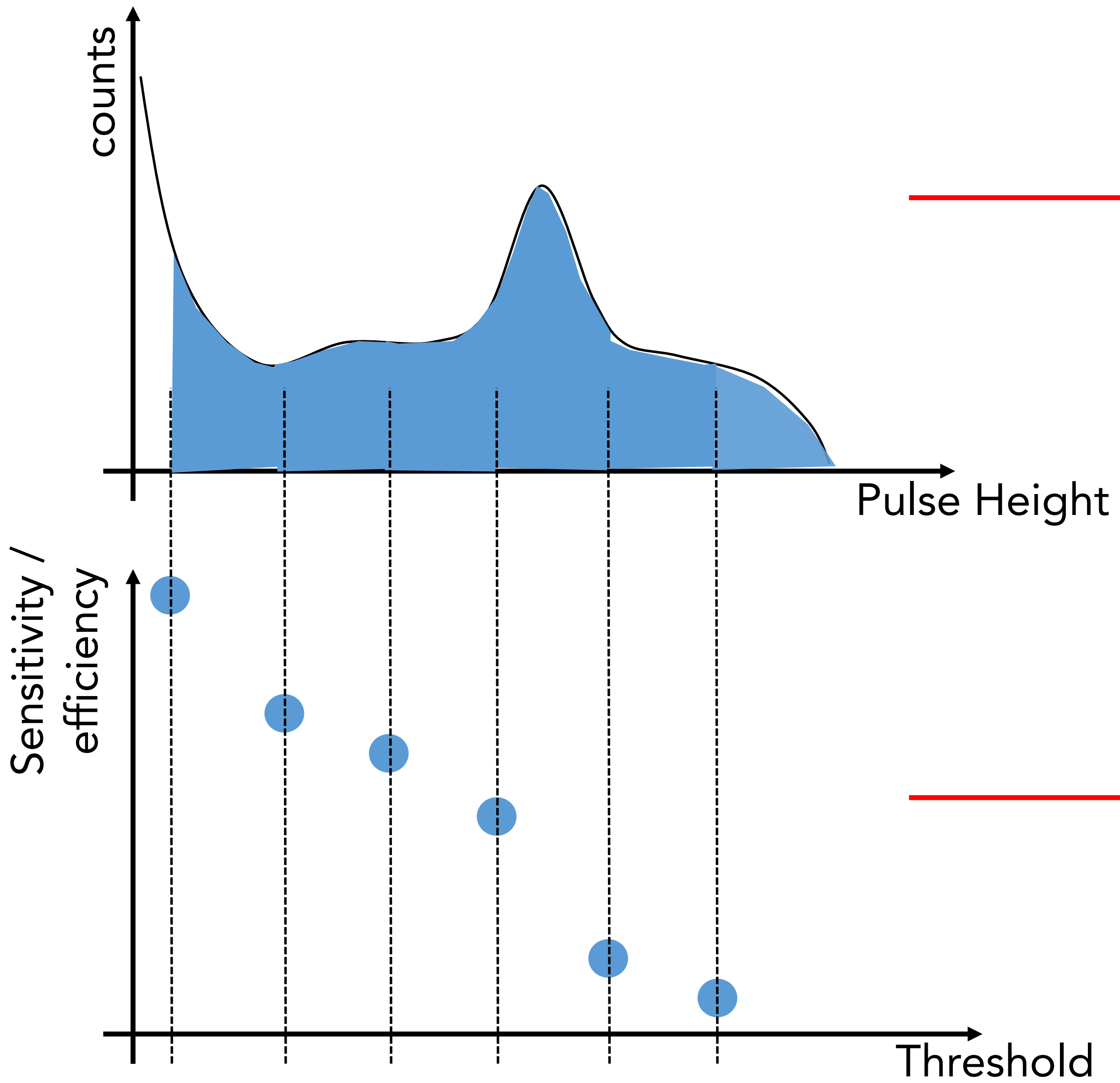

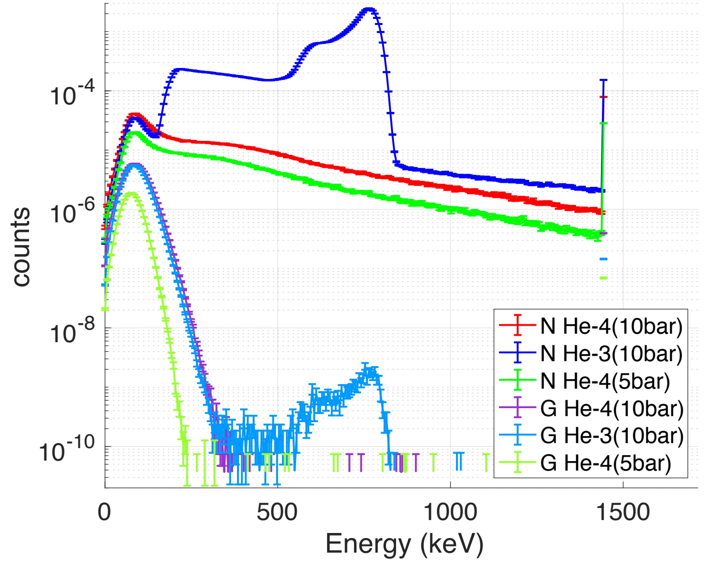

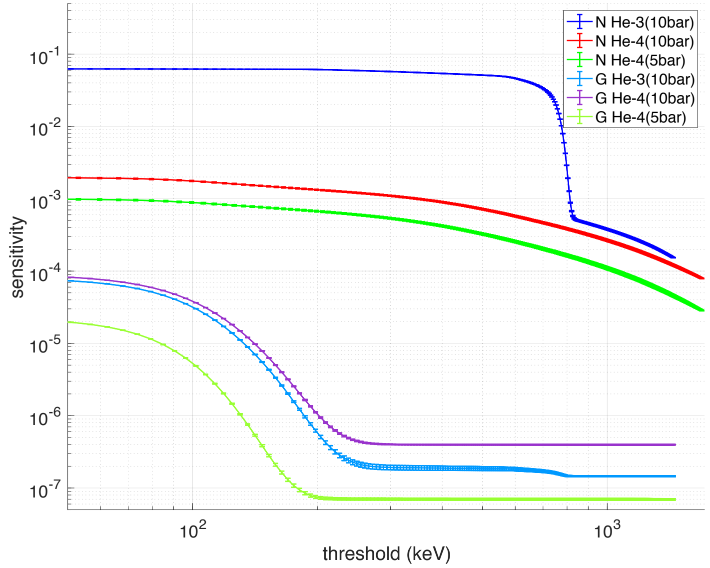

F. Piscitelli et al., Verification of He-3 proportional counters fast neutron sensitivity through a comparison with He-4 detectors, sub. to EPJ Plus (2020) (arxiv: 2002.08153)

Sensitivity / Efficiency

Pulse Height Spectrum - PHS

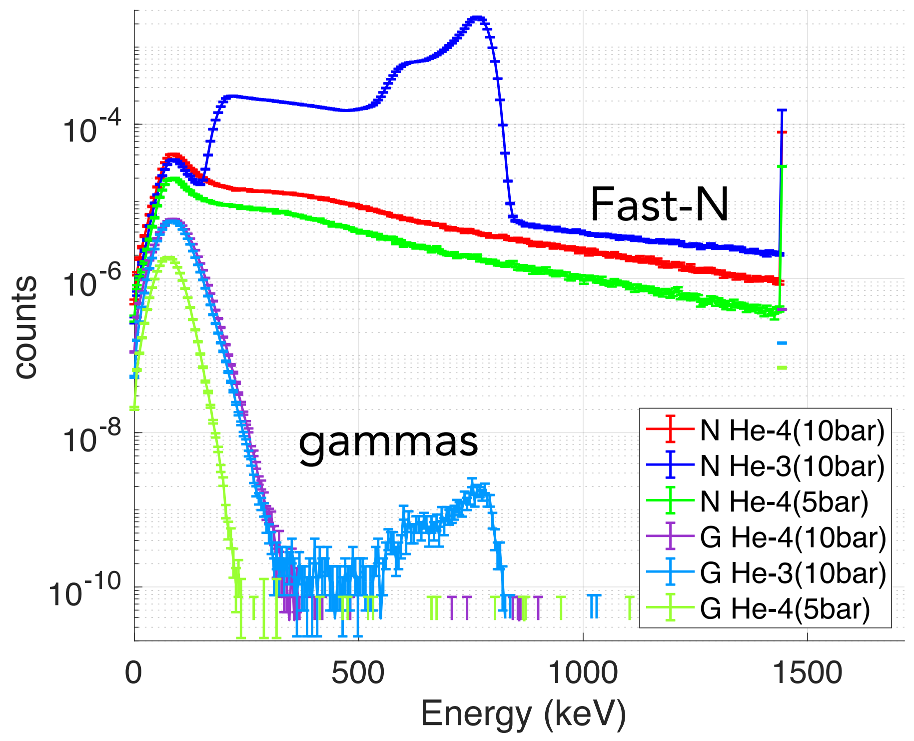

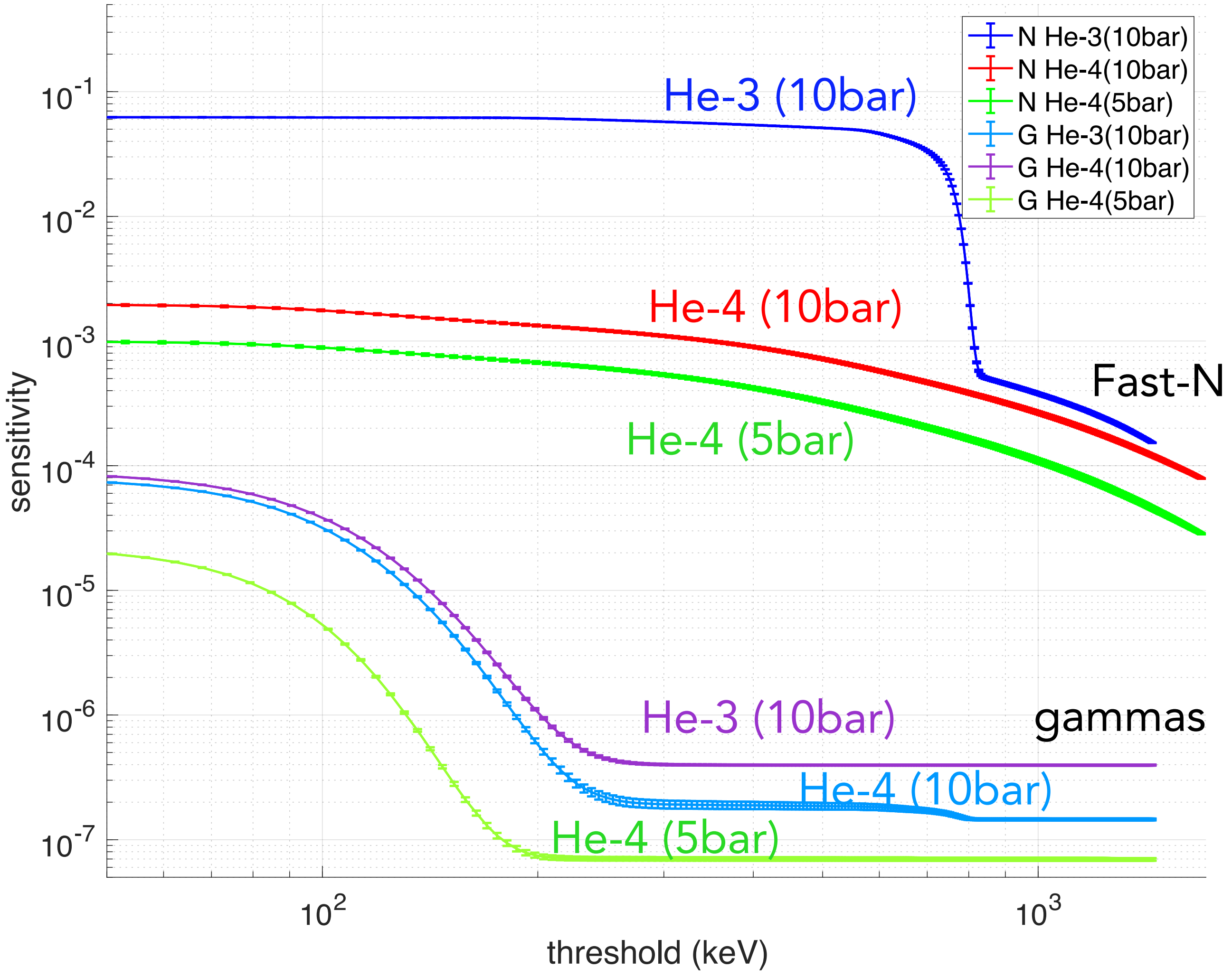

F. Piscitelli et al., Verification of He-3 proportional counters fast neutron sensitivity through a comparison with He-4 detectors, sub. to EPJ Plus (2020) (arxiv: 2002.08153)

Sensitivity / Efficiency

Fast Neutron Sensitivity

He-3

10^{-3}

Difference between He3 or B-10
(Gas Dominates)

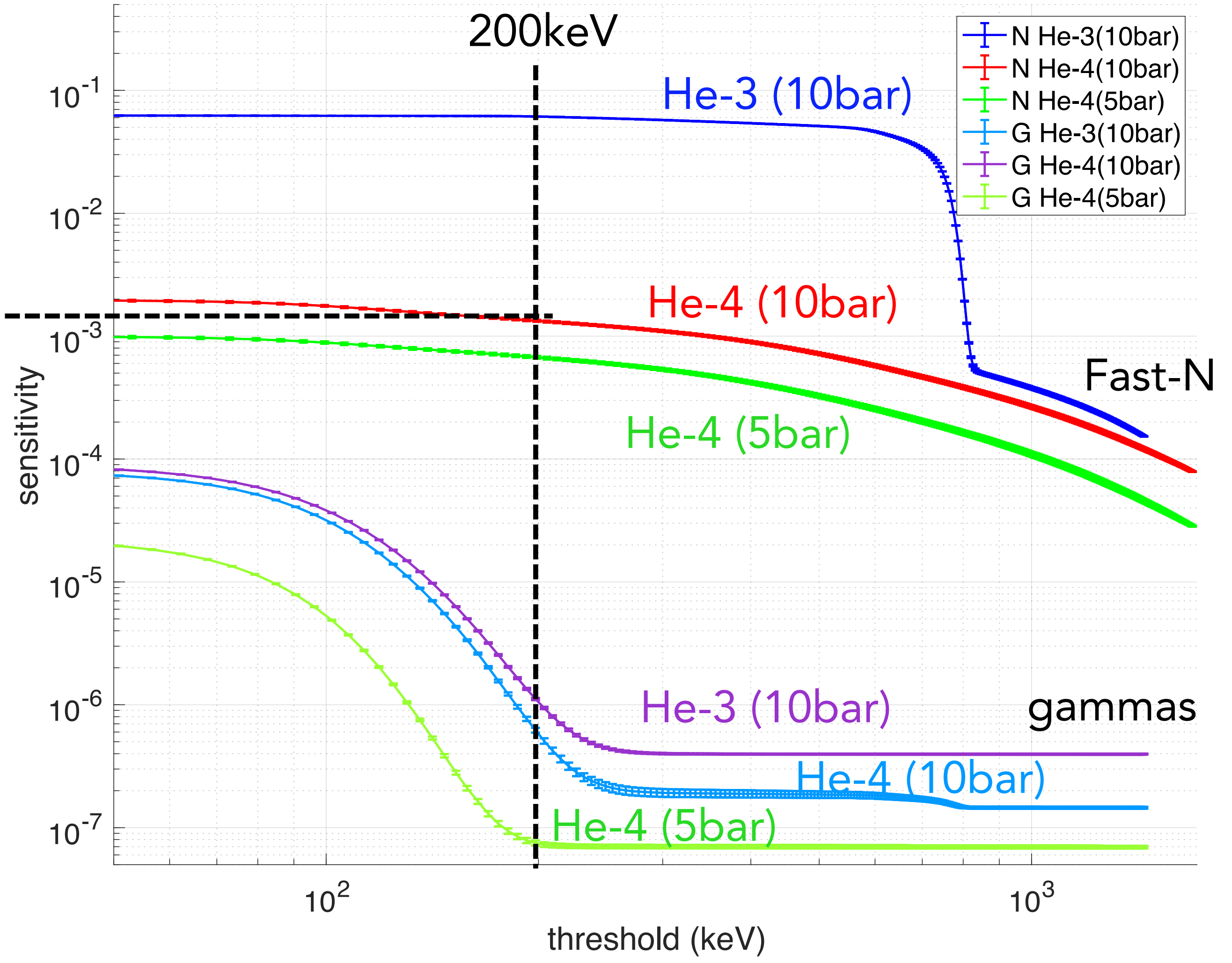

F. Piscitelli et al., Verification of He-3 proportional counters fast neutron sensitivity through a comparison with He-4 detectors, sub. to EPJ Plus (2020) (arxiv: 2002.08153)

Sensitivity / Efficiency

Fast Neutron Sensitivity

He-3

10^{-3}

Difference between He3 or B-10
(Gas Dominates)

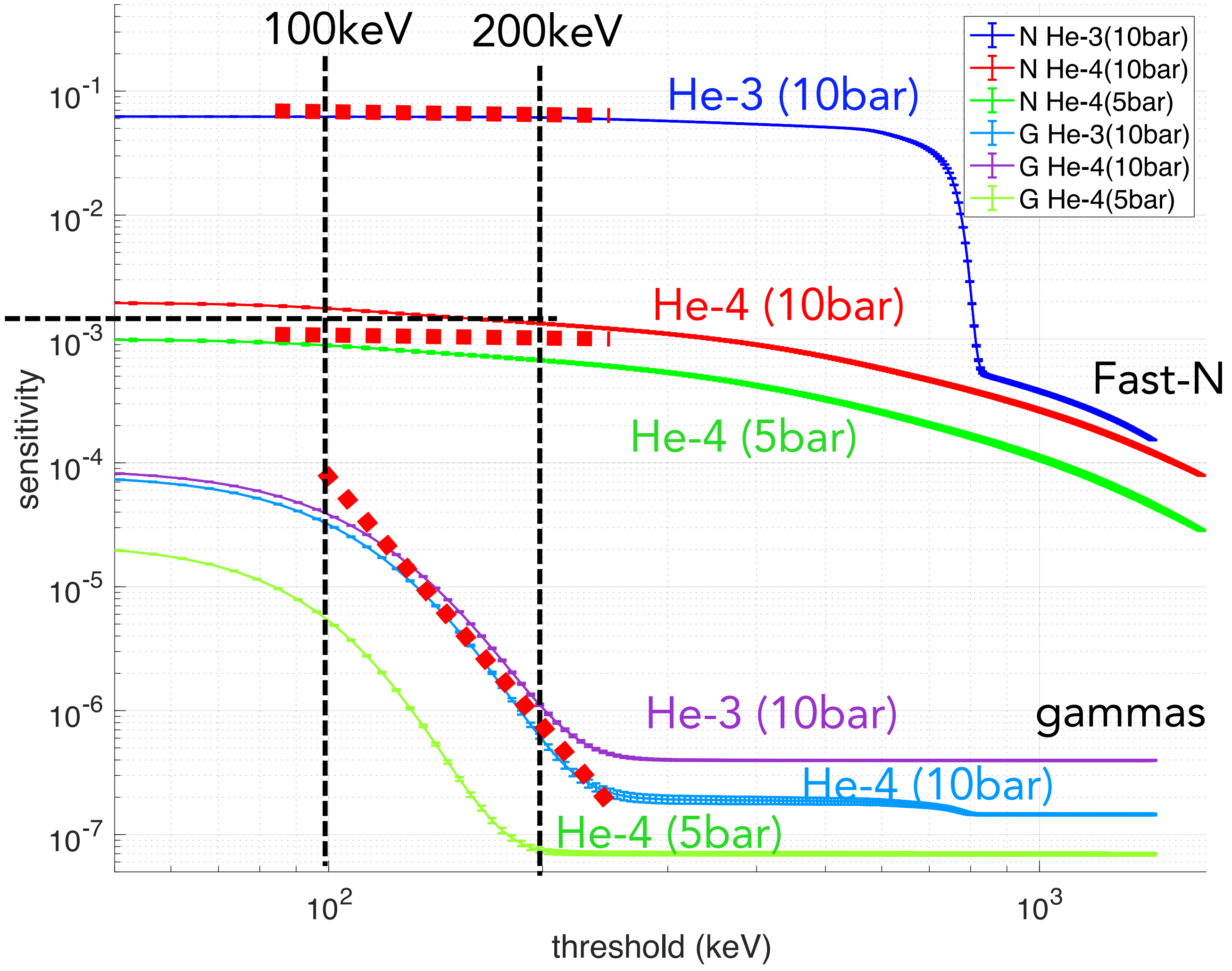

F. Piscitelli et al., Verification of He-3 proportional counters fast neutron sensitivity through a comparison with He-4 detectors, sub. to EPJ Plus (2020) (arxiv: 2002.08153)

Sensitivity / Efficiency

Fast Neutron Sensitivity

He-3

10^{-3}

Difference between He3 or B-10
(Gas Dominates)

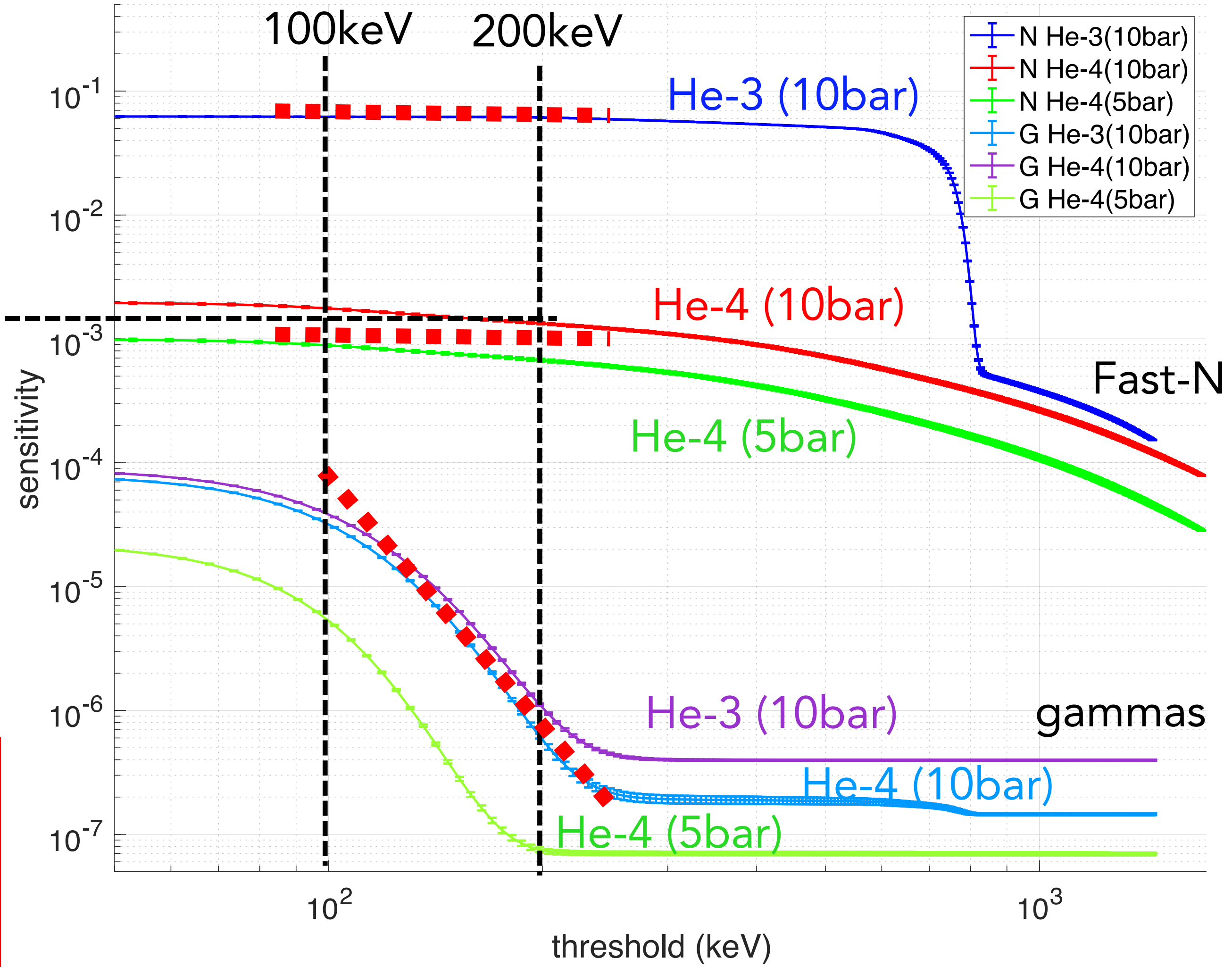

NOTE:
high pressure He-3 detectors,
little gain in thermal n efficiency with
drastic increase of fast n sensitivity!
S/B matters!

F. Piscitelli et al., Verification of He-3 proportional counters fast neutron sensitivity through a comparison with He-4 detectors, sub. to EPJ Plus (2020) (arxiv: 2002.08153)

BACKGROUND: fast neutrons

Gas is main component, then He-3 differs from B-10 …

Gas dominates

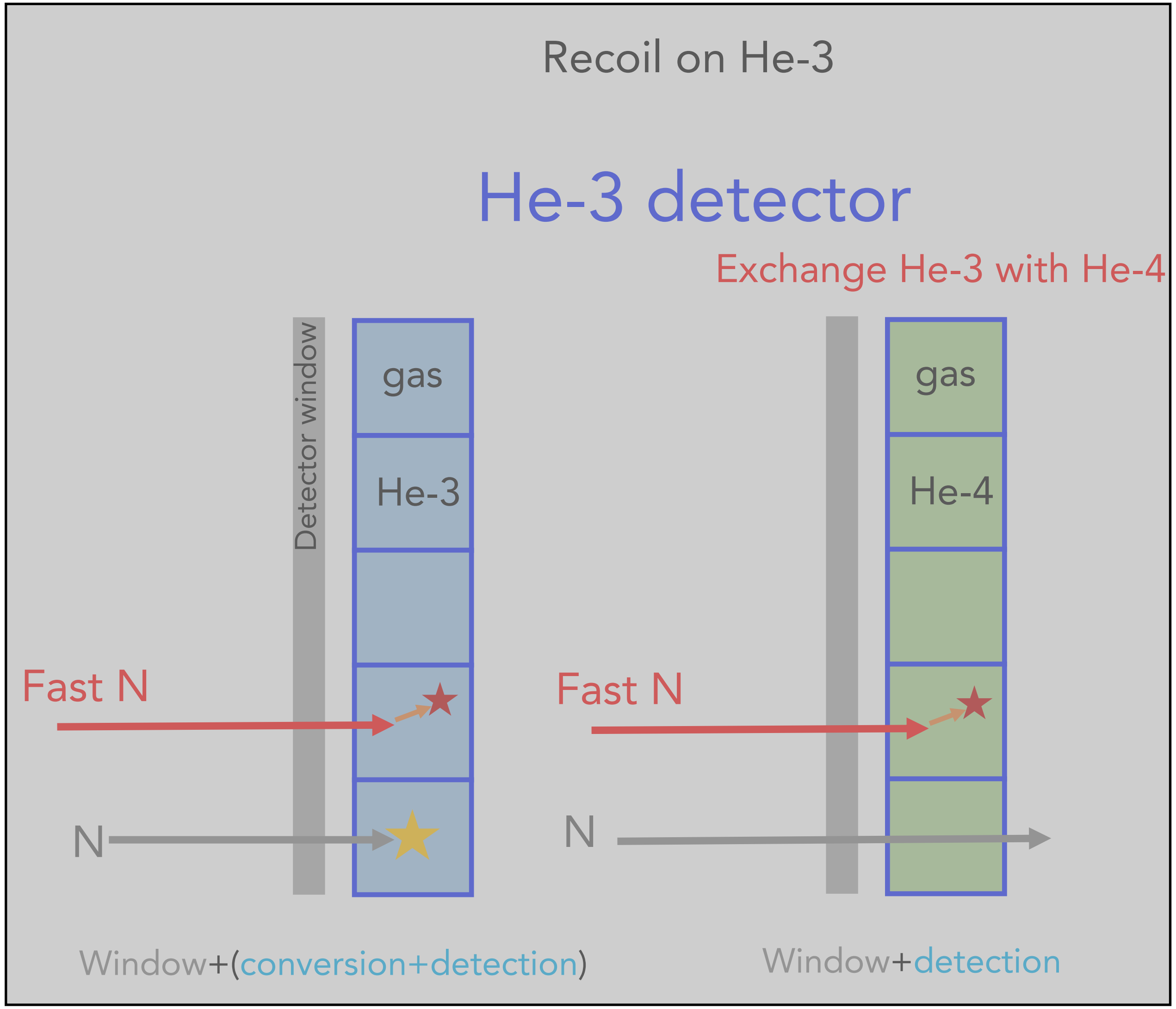

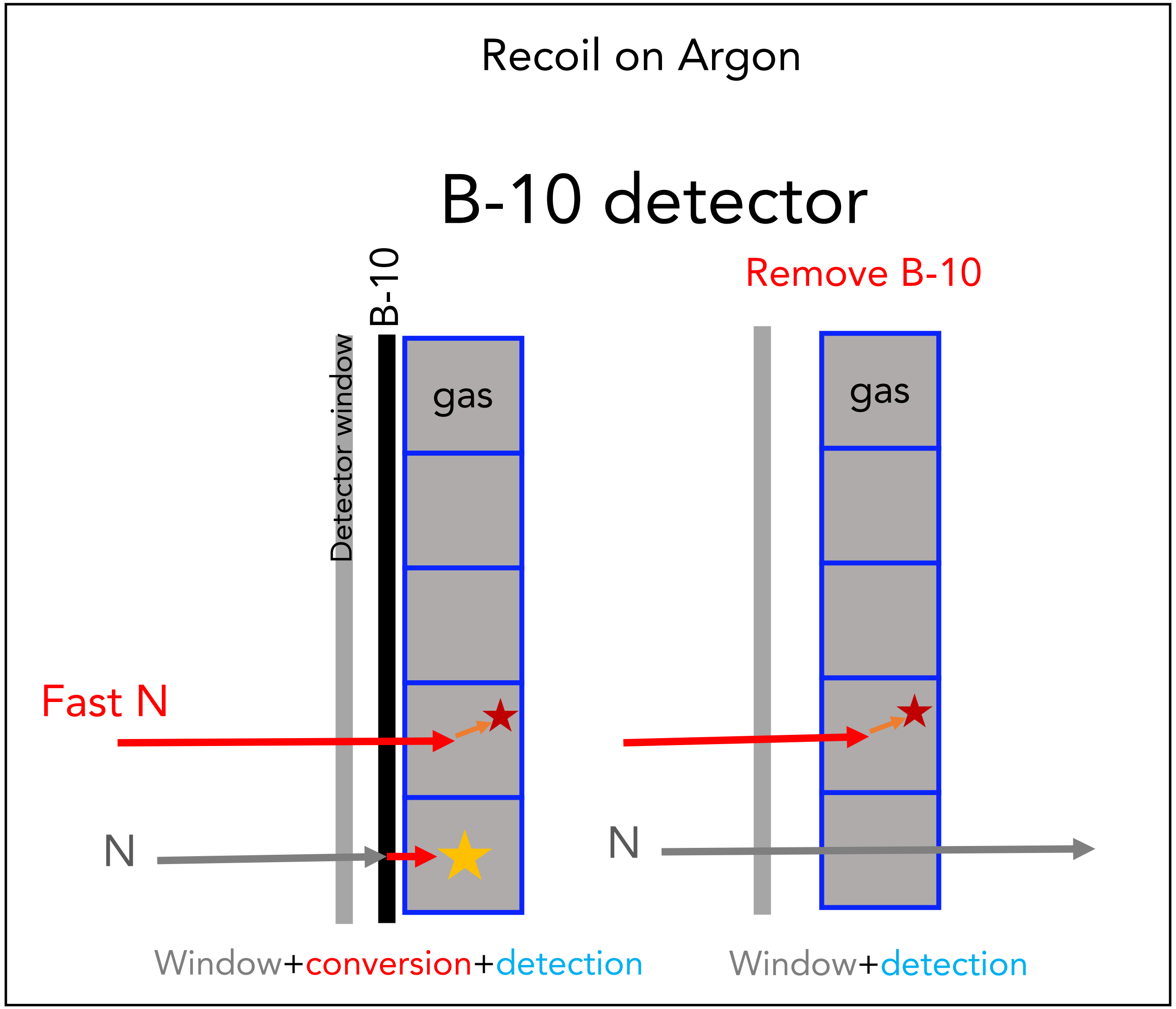

BACKGROUND: fast neutrons in B-10 detectors

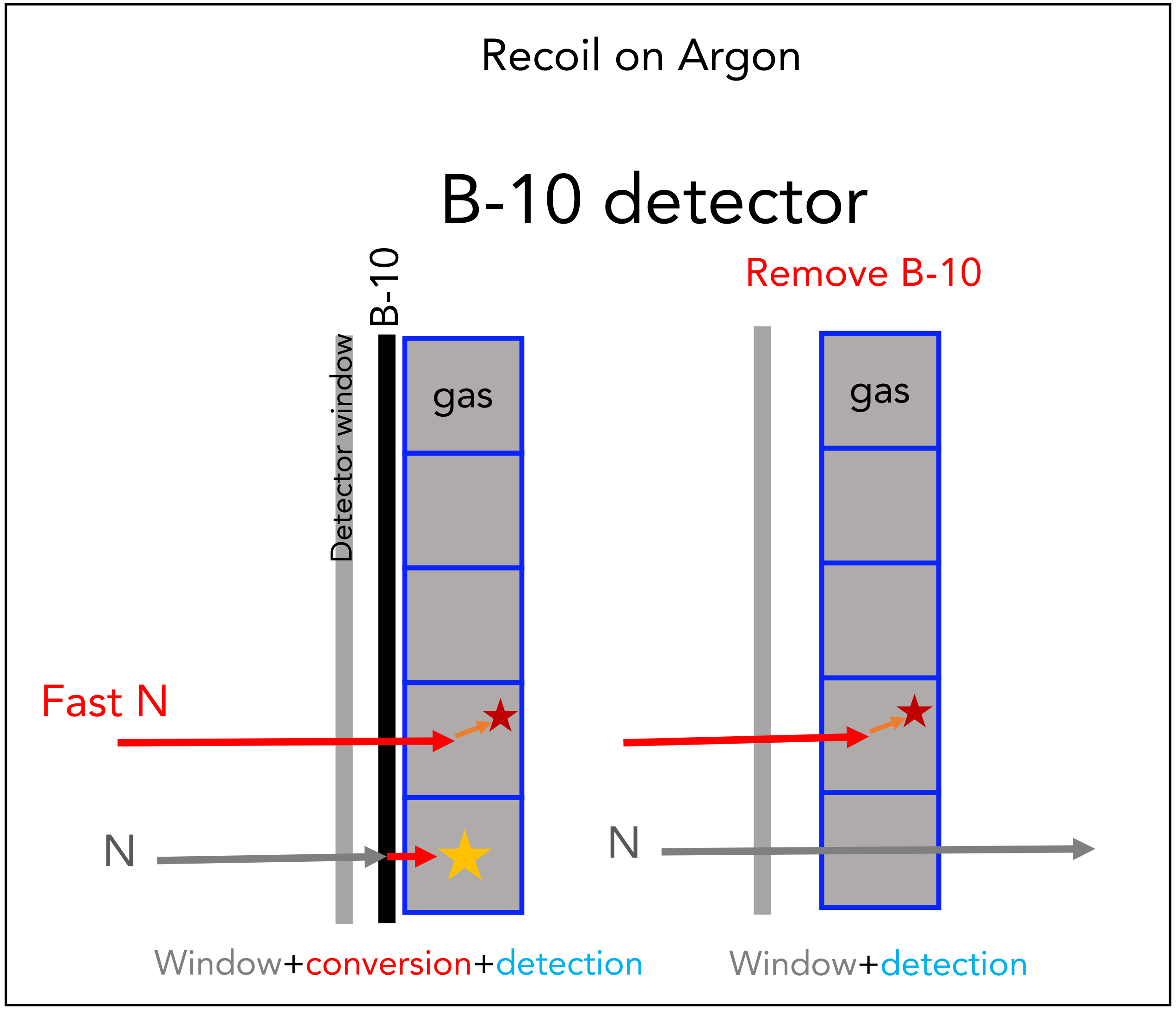

BACKGROUND: fast neutrons in B-10 detectors

Gas dominates

Gas = x100 Solid

Compared Titanium, Aluminum, Copper, Kapton

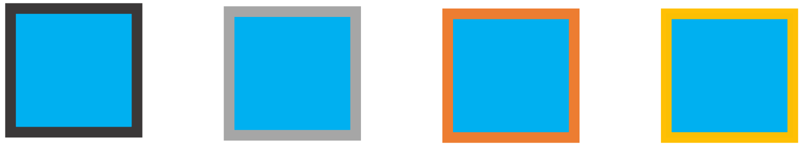

Experimentally (+simulations) proved -> no difference!

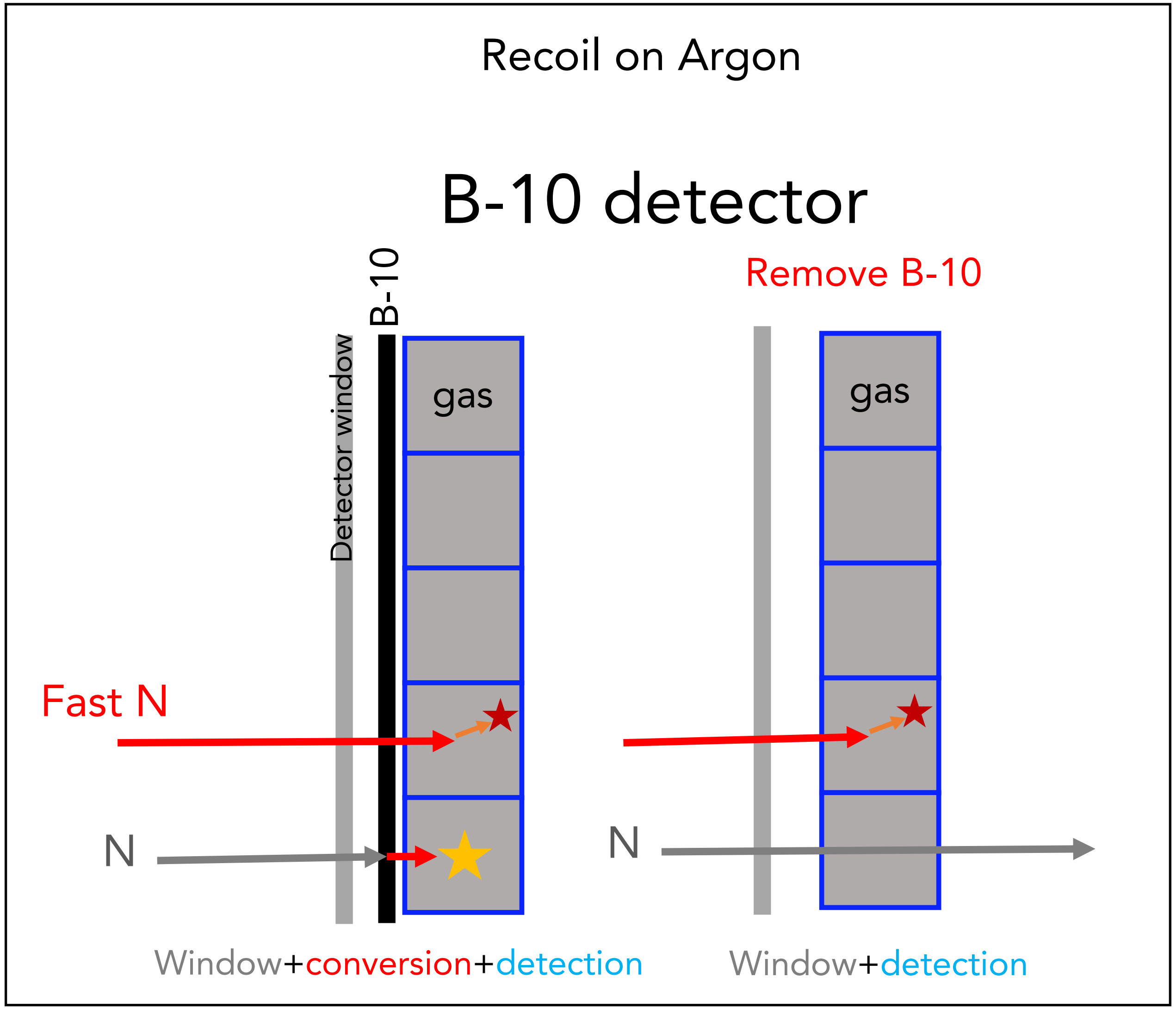

G. Mauri et al., Fast neutron sensitivity of neutron detectors based on Boron-10 converter layers, JINST 13 P03004 (2018) (arxiv: 1712.05614)

Pulse Height Spectrum - PHS

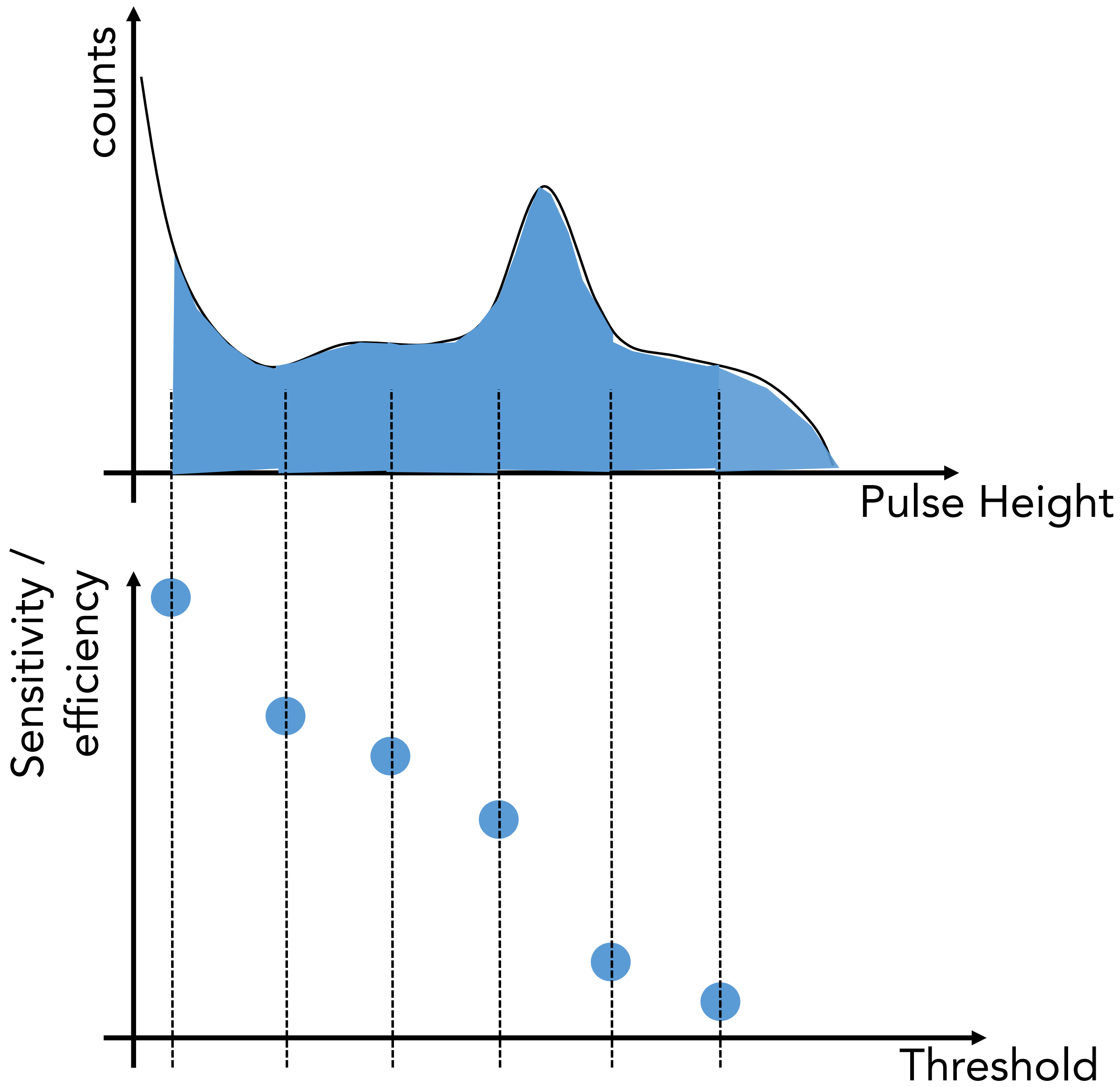

G. Mauri et al., Fast neutron sensitivity of neutron detectors based on Boron-10 converter layers, JINST 13 P03004 (2018) (arxiv: 1712.05614)

BACKGROUND: fast neutrons in B-10 detectors

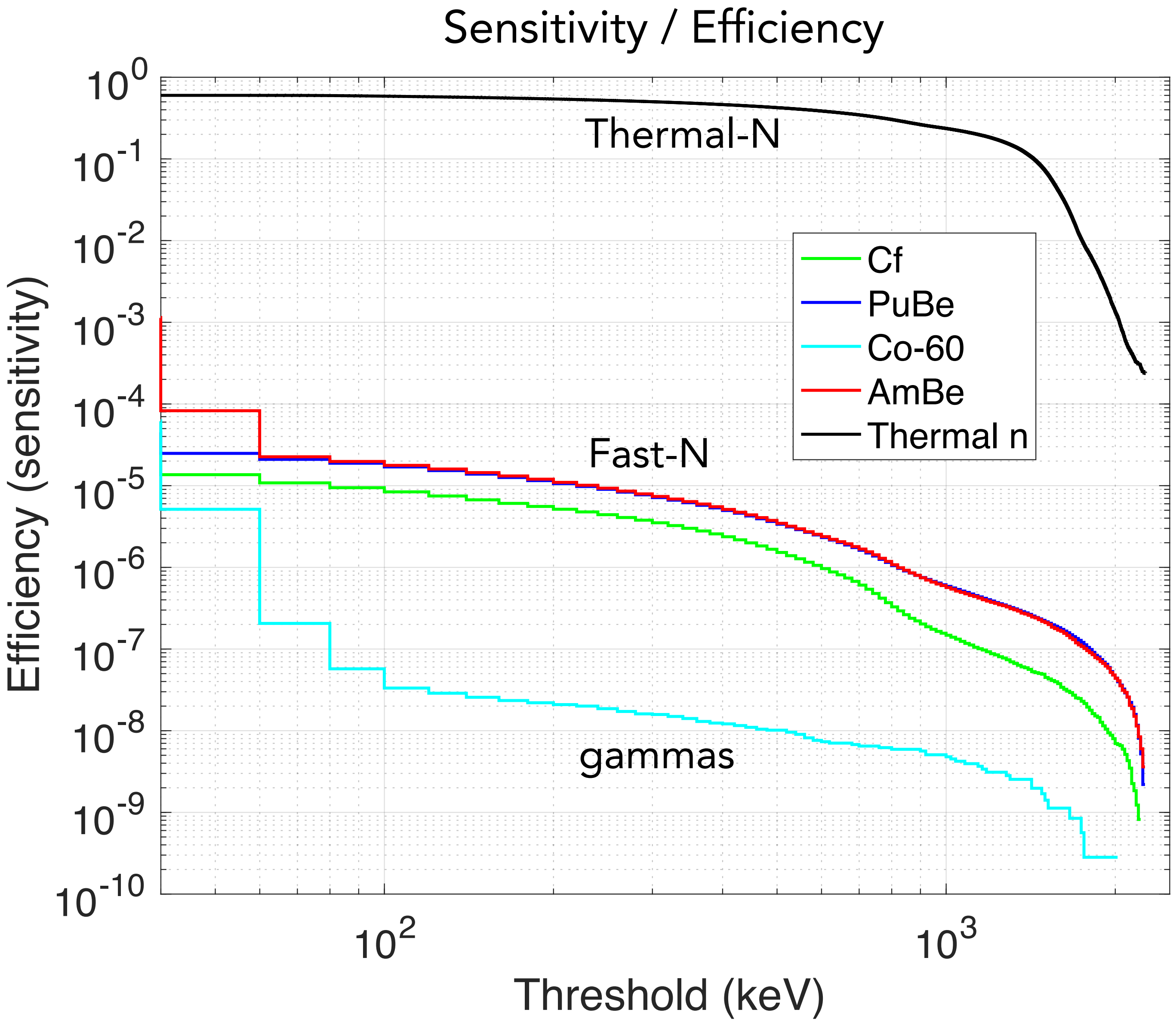

G. Mauri et al., Fast neutron sensitivity of neutron detectors based on Boron-10 converter layers, JINST 13 P03004 (2018) (arxiv: 1712.05614)

BACKGROUND: fast neutrons in B-10 detectors

Fast Neutron Sensitivity

B-10

10^{-5}

Difference between He3 or B-10
(Gas Dominates)

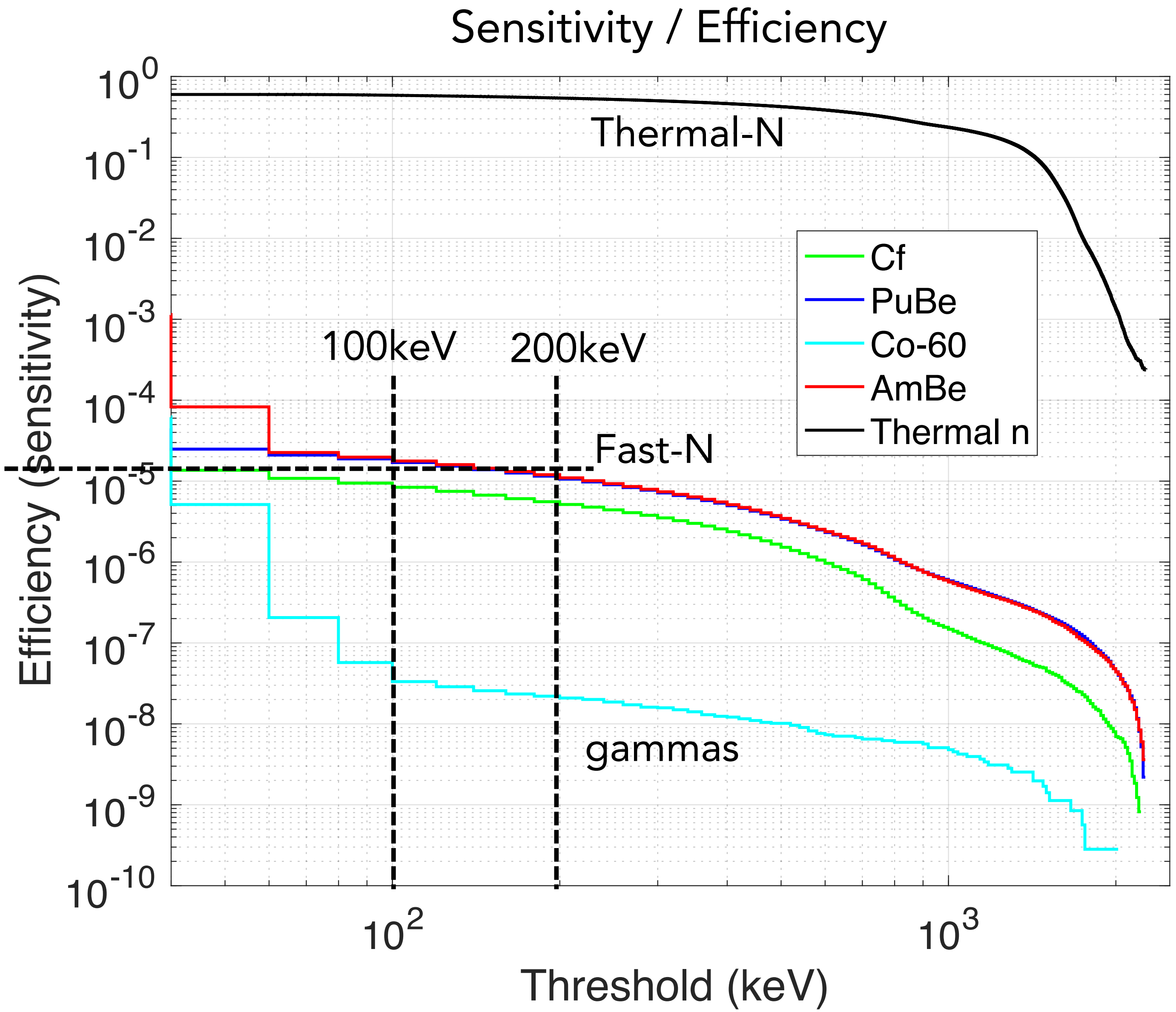

G. Mauri et al., Fast neutron sensitivity of neutron detectors based on Boron-10 converter layers, JINST 13 P03004 (2018) (arxiv: 1712.05614)

BACKGROUND DUE TO SCATTERED NEUTRONS

BACKGROUND: scattering

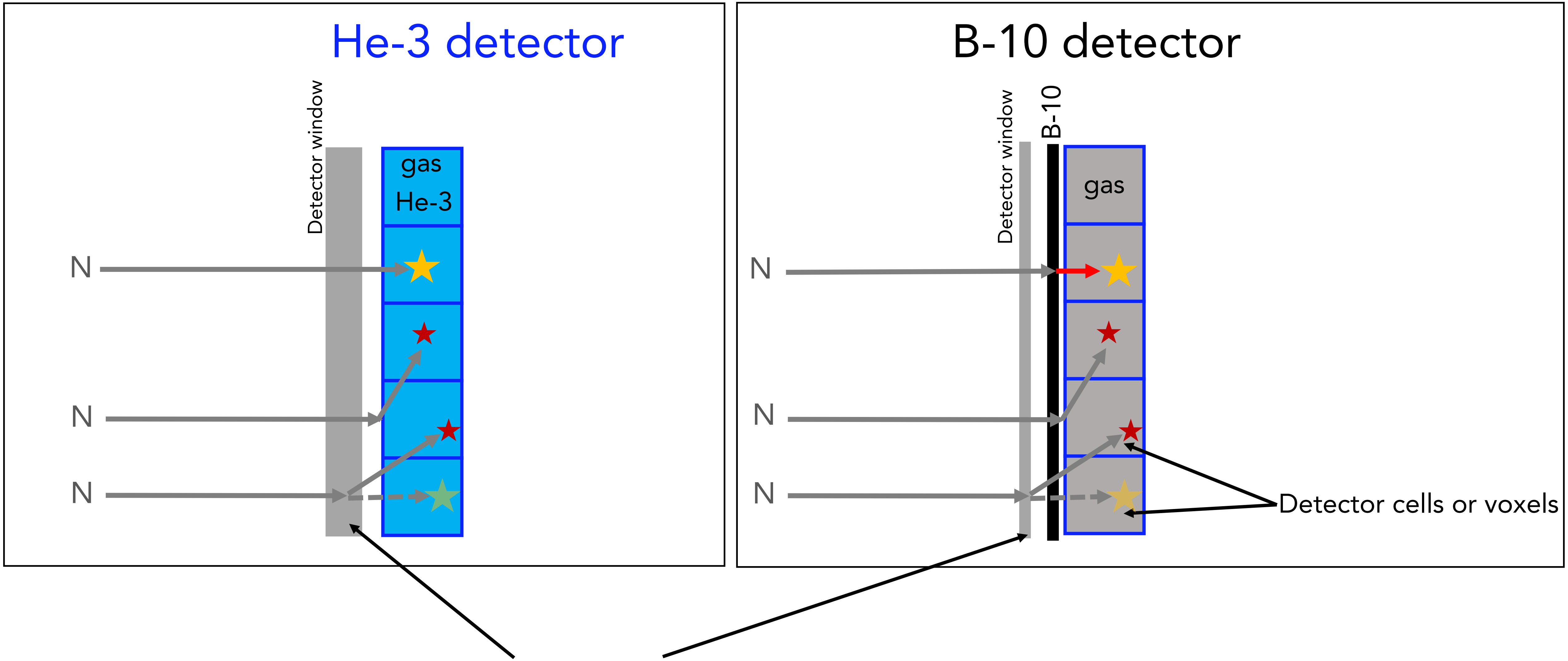

- Scattering at the detector window: B10 has generally thinner windows due to lower pressure
- Scattering at other parts of the detector

BACKGROUND: scattering

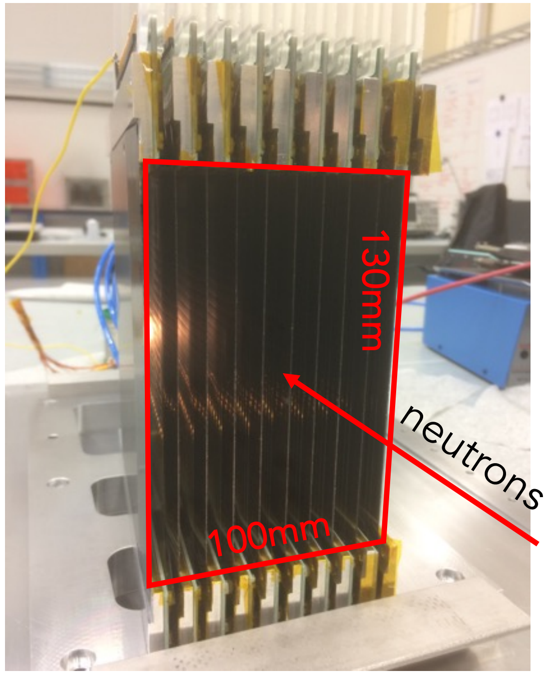

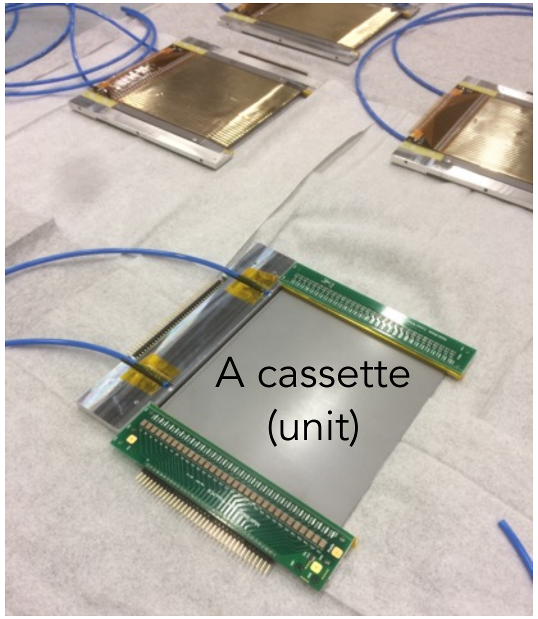

^{10}B-detector for reflectometers:
Estia and FREIA

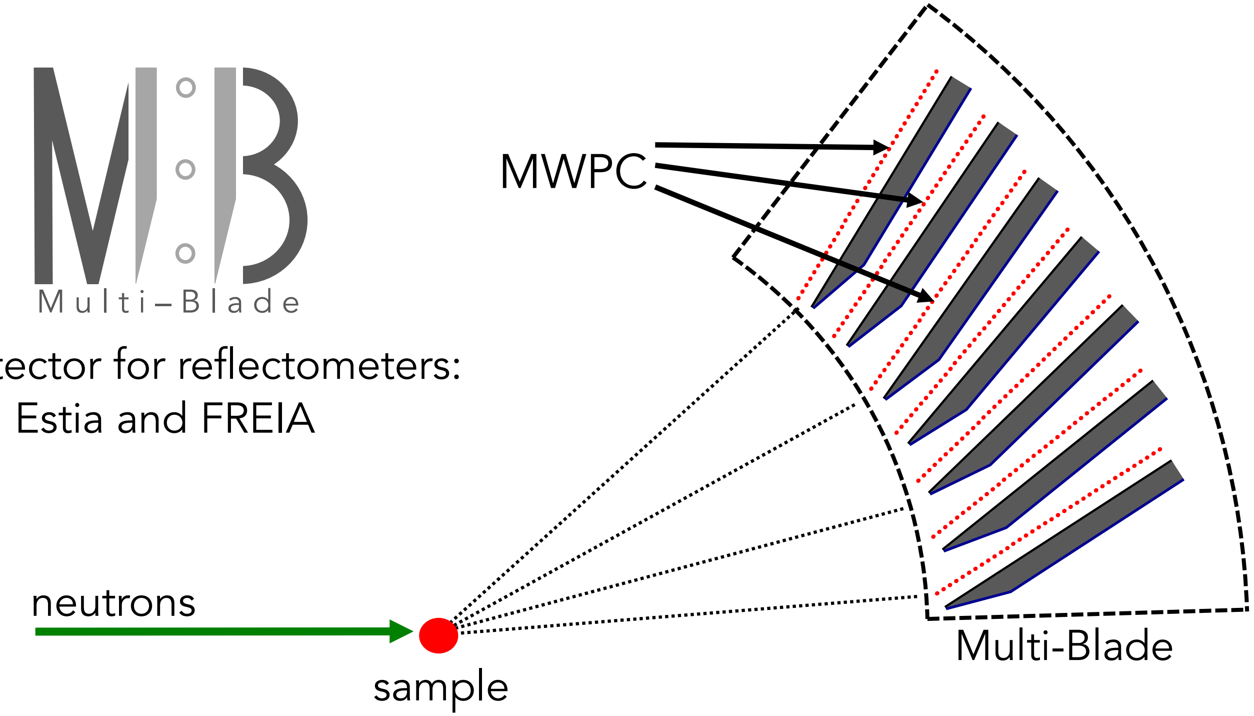

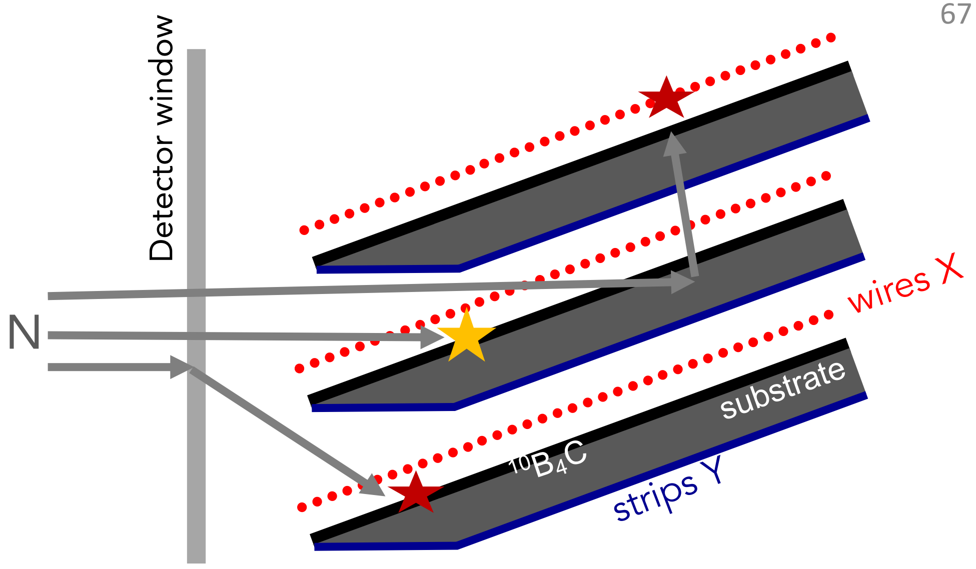

G. Mauri et al., The Multi-Blade Boron-10-based neutron detector performance using a focusing reflectometer, (2020) (arxiv: 2001:02965). Accepted for publ. in JINST.

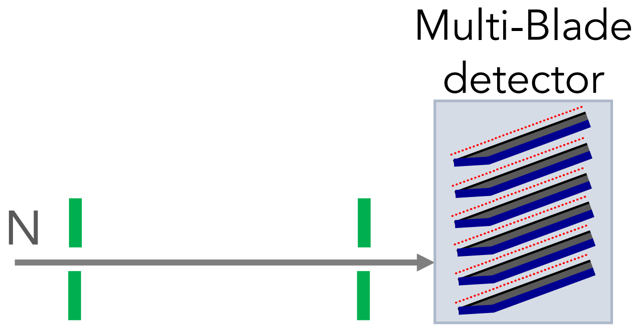

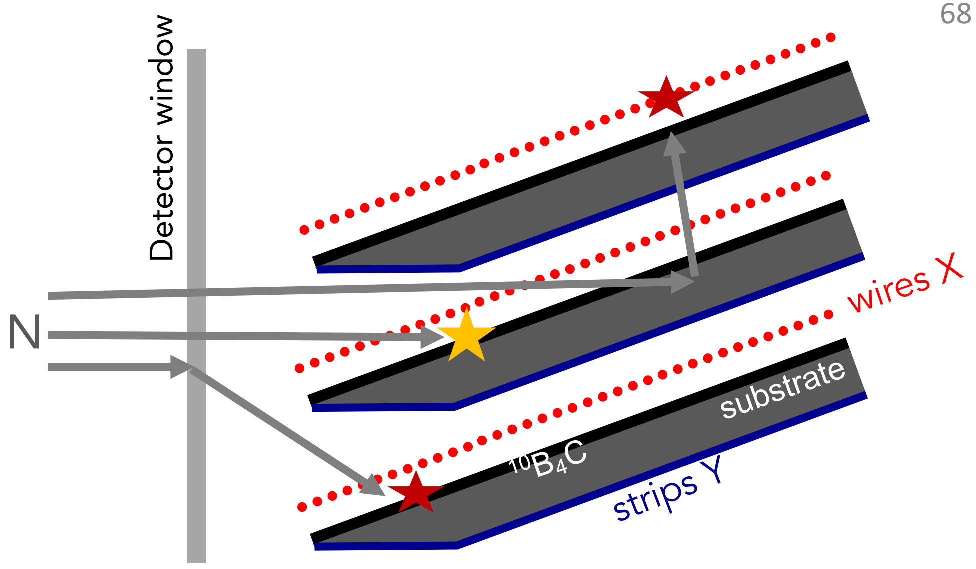

G. Mauri et al., The Multi-Blade Boron-10-based neutron detector performance using a focusing reflectometer, (2020) (arxiv: 2001:02965). Accepted for publ. in JINST.

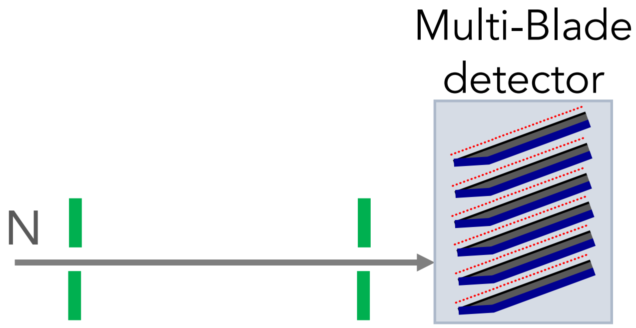

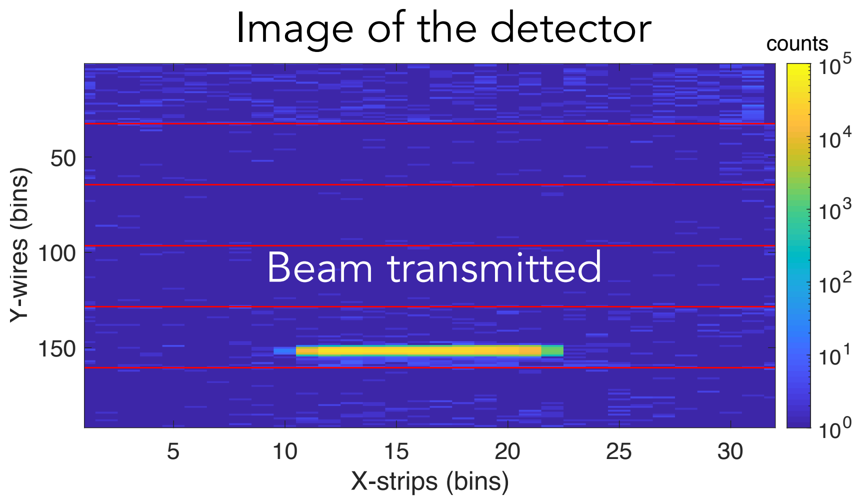

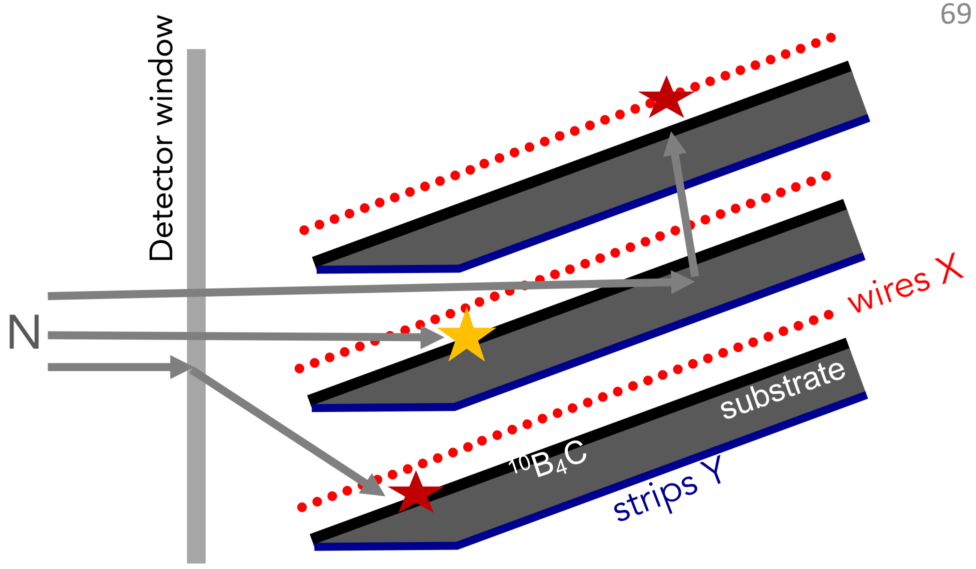

G. Mauri et al., The Multi-Blade Boron-10-based neutron detector performance using a focusing reflectometer, (2020) (arxiv: 2001:02965). Accepted for publ. in JINST.

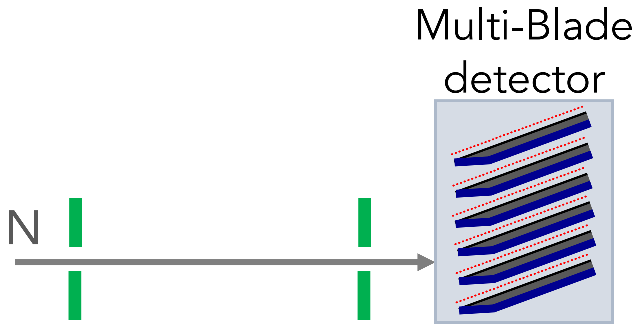
Multi-Blade
detector
N

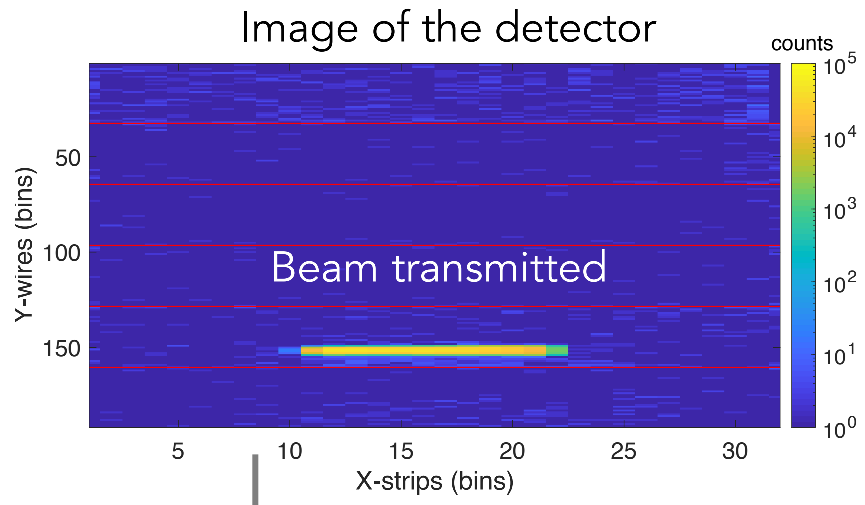
Image of the detector
counts
Beam transmitted
Y-wires (bins)
X-strips (bins)

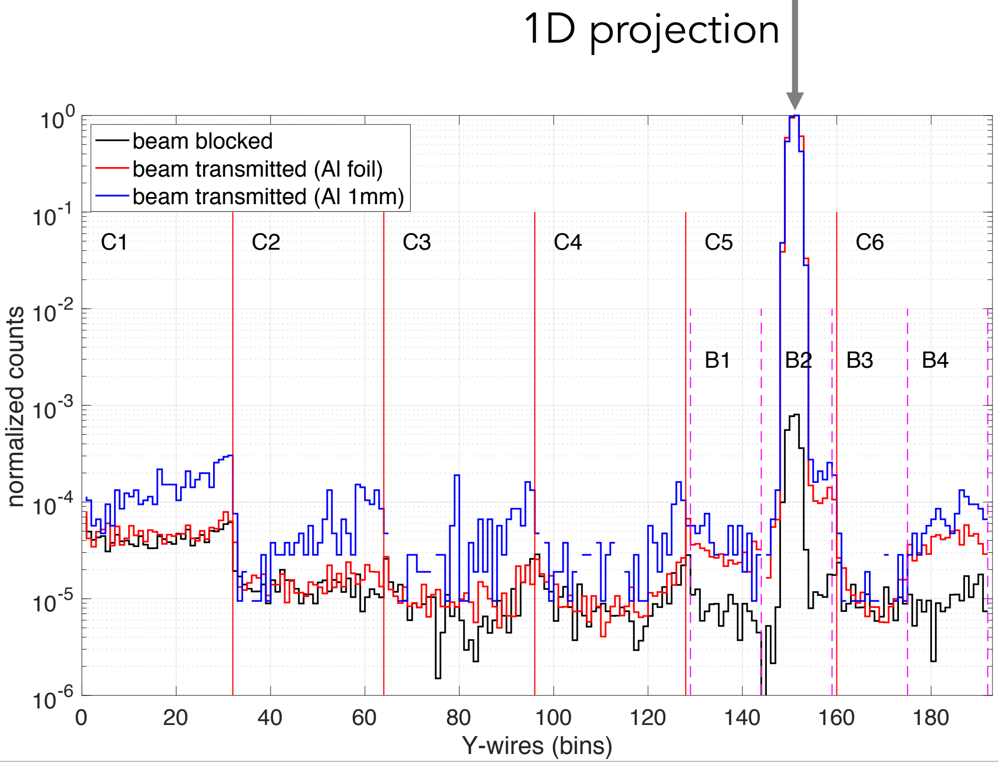
1D projection
beam blocked
beam transmitted (Al foil)
beam transmitted (Al 1mm)
C1
C2
C3
C4
C5
C6
B1
B2
B3
B4
normalized counts
Y-wires (bins)

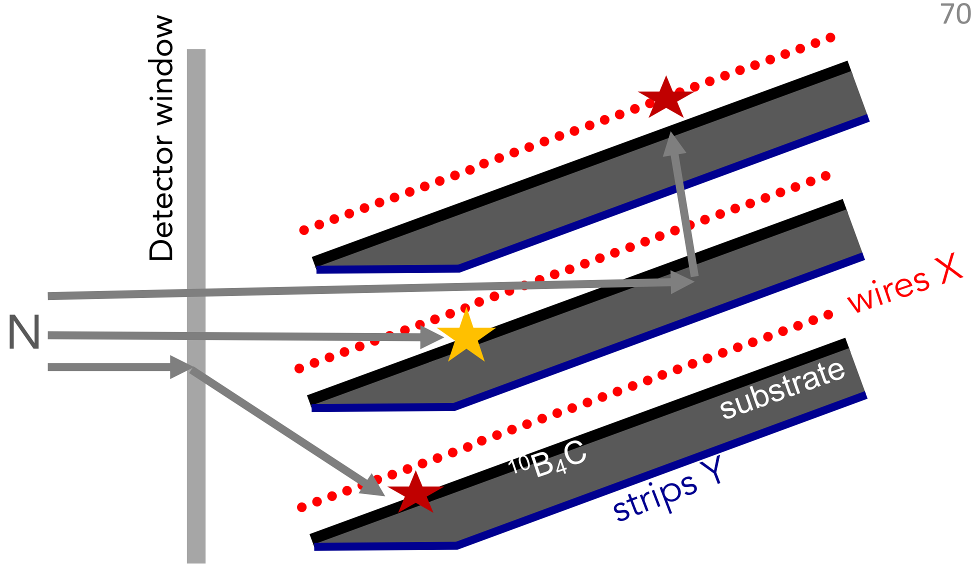
Detector window
N
wires X
substrate
$^{10}B_4C$
strips Y

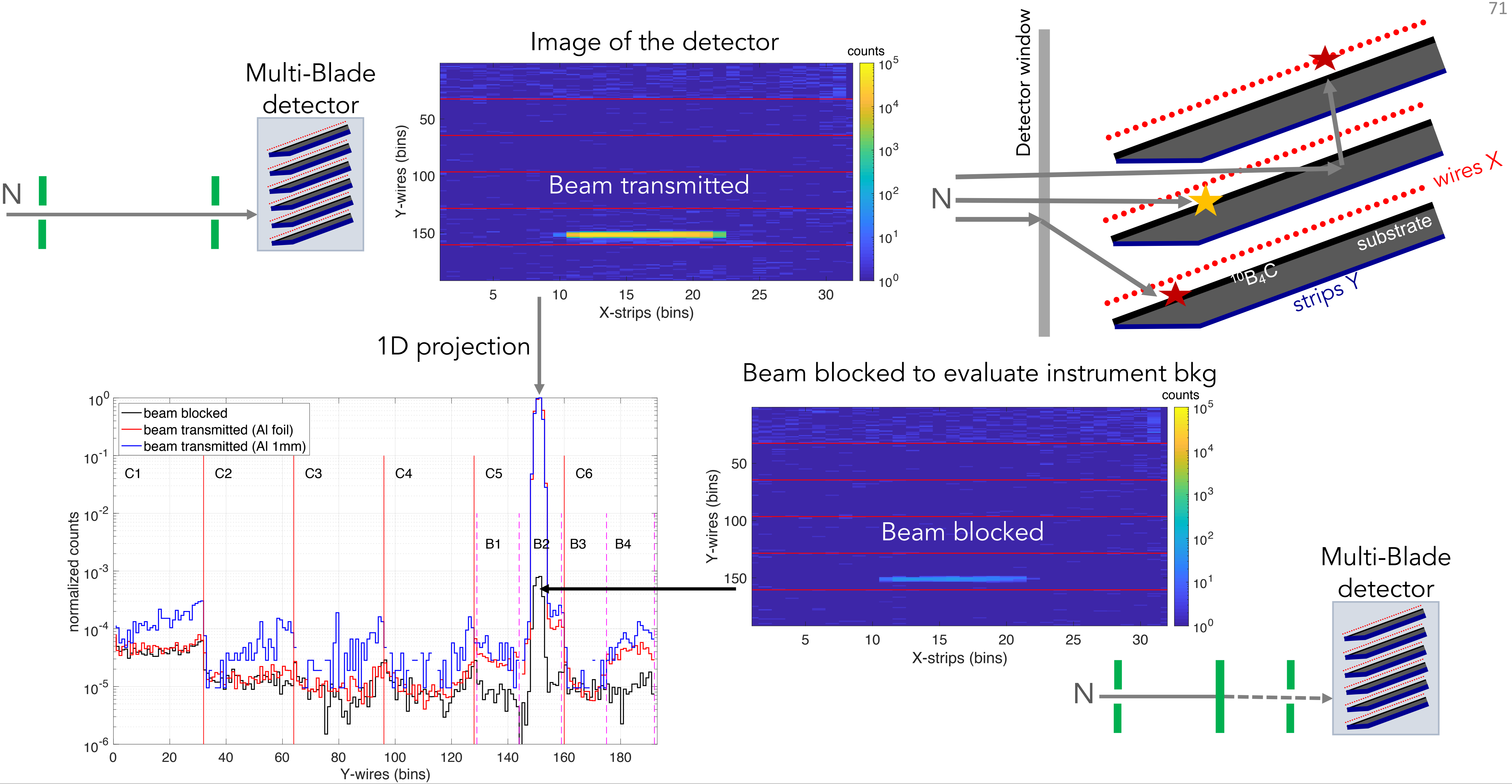

G. Mauri et al., The Multi-Blade Boron-10-based neutron detector performance using a focusing reflectometer, (2020) (arxiv: 2001:02965). Accepted for publ. in JINST.

Multi-Blade detector

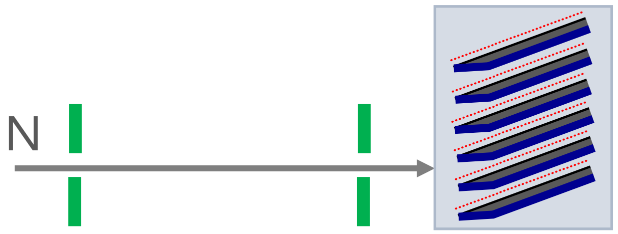

Image of the detector

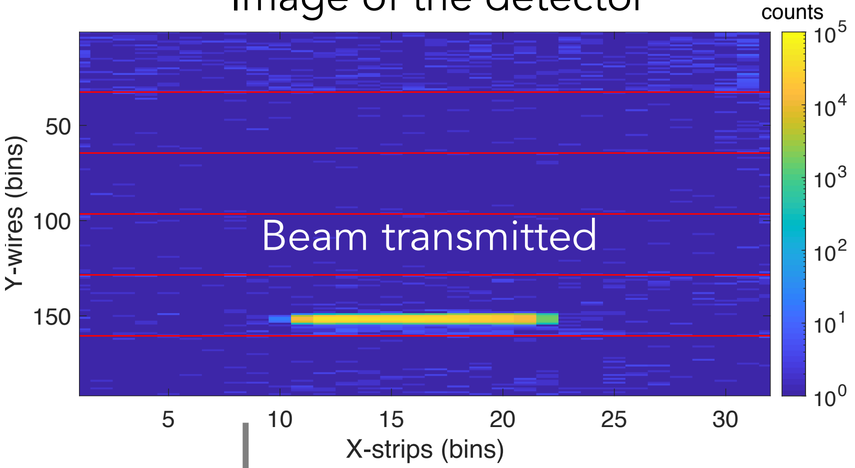

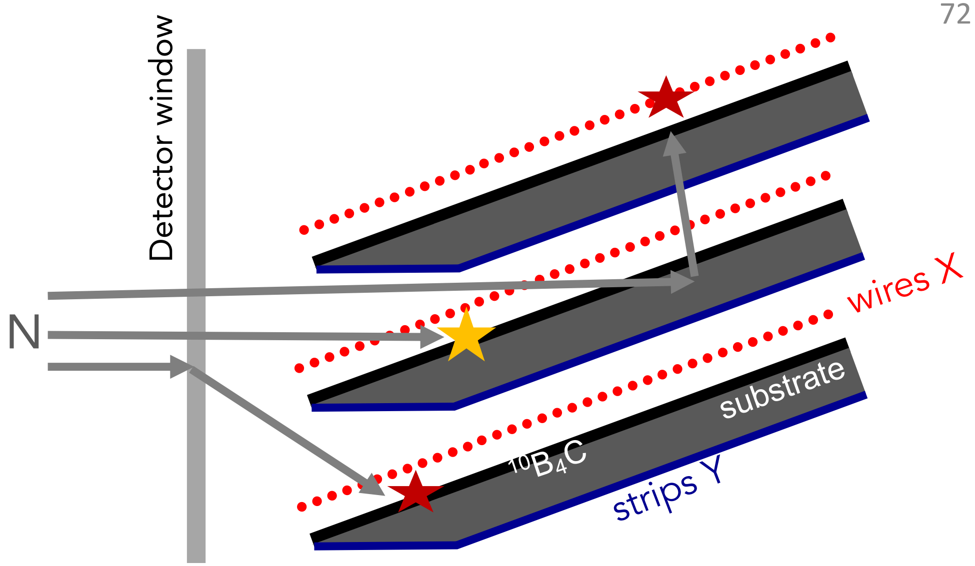

1D projection

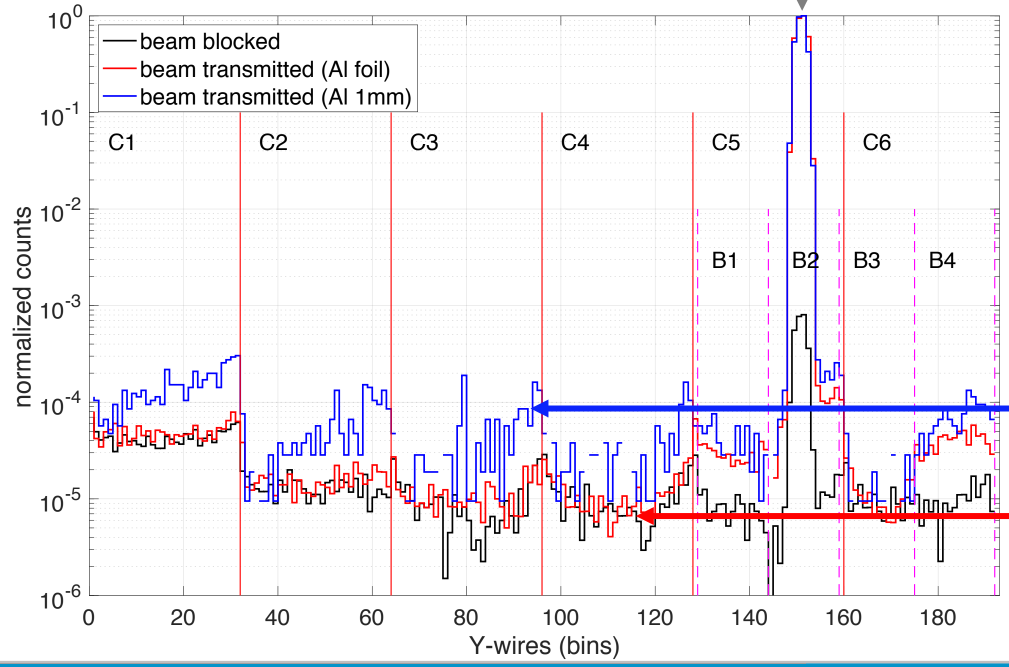

DETECTOR WINDOW

1mm Aluminium

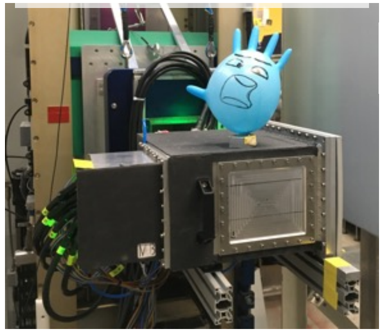

50um Aluminium foil

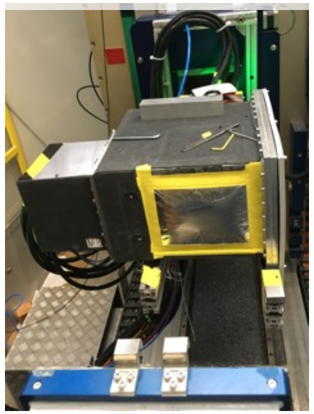

G. Mauri et al., The Multi-Blade Boron-10-based neutron detector performance using a focusing reflectometer, (2020) (arxiv: 2001:02965). Accepted for publ. in JINST.

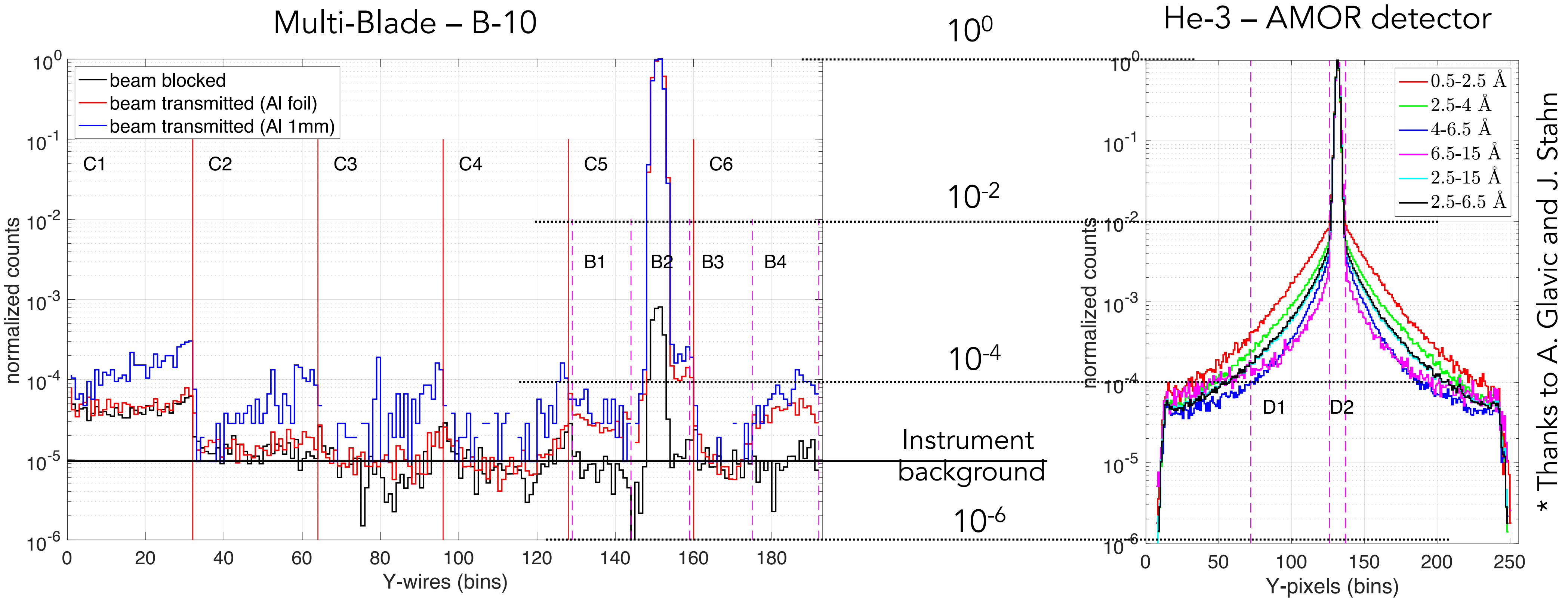

G. Mauri et al., The Multi-Blade Boron-10-based neutron detector performance using a focusing reflectometer, (2020) (arxiv: 2001:02965). Accepted for publ. in JINST.

Multi-Blade – B-10

He-3 – AMOR detector

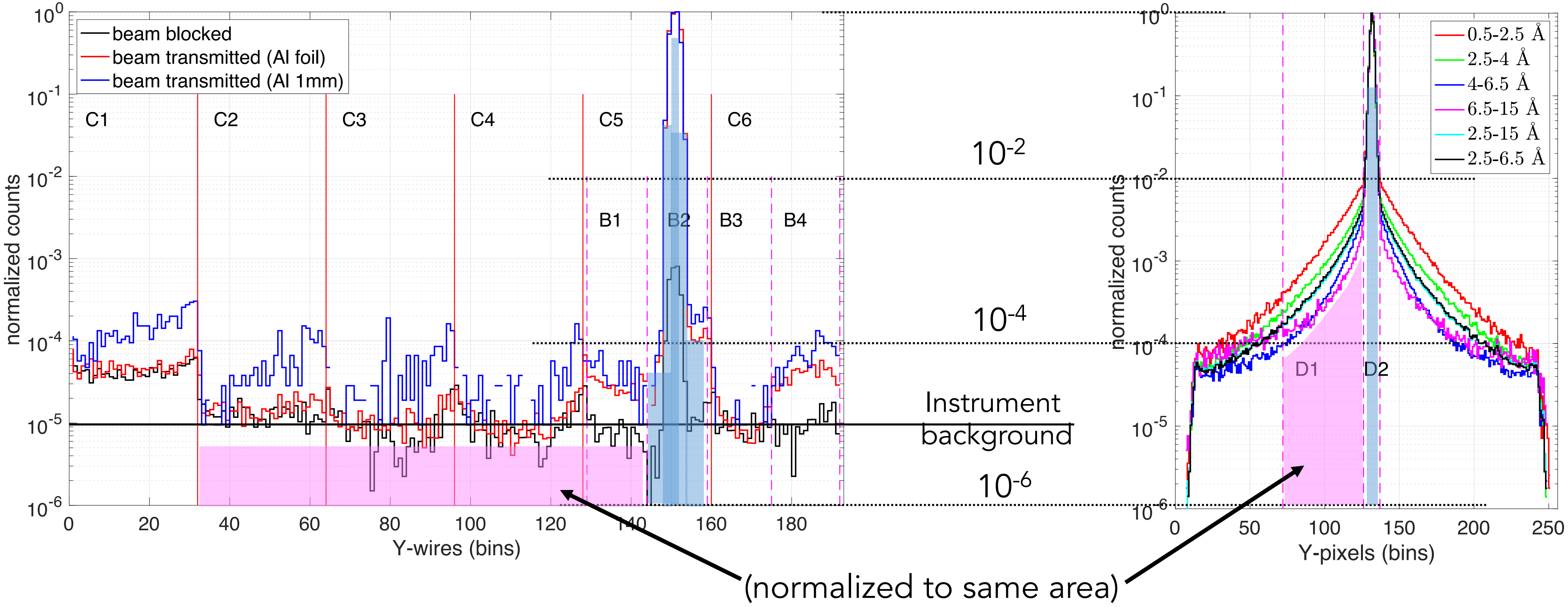

* Thanks to A. Glavic and J. Stahn

Figure-of-Merit ∝ Signal-to-Background

$$FoM = \frac{D2}{D1}$$

G. Mauri et al., The Multi-Blade Boron-10-based neutron detector performance using a focusing reflectometer, (2020) (arxiv: 2001:02965). Accepted for publ. in JINST.

Multi-Blade – B-10 | He-3 – AMOR detector

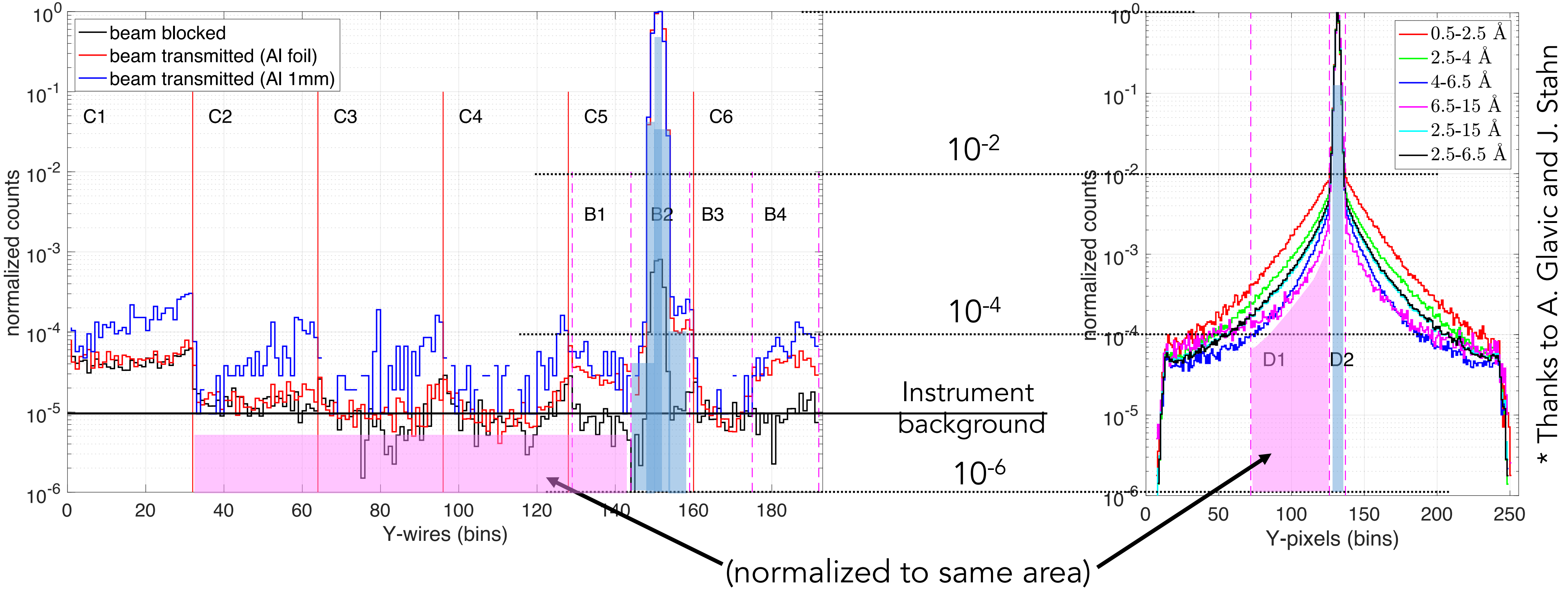

Detector	FoM (2.5-15Å)
He-3 (a few mm Al window)	4000
Multi-Blade B10 – Al 1mm window	73000
Multi-Blade B10 – Al foil window	211000

x20 x50

Figure-of-Merit ∝ Signal-to-Background

$$FoM = \frac{D2}{D1}$$

G. Mauri et al., The Multi-Blade Boron-10-based neutron detector performance using a focusing reflectometer, (2020) (arxiv: 2001:02965). Accepted for publ. in JINST.

Conclusions

Conclusions

- 1 @ESS 23 Hz/m^2 cosmic thermal neutrons and 1 Hz/m^2 with shielding

Conclusions

- 1 @ESS 23 Hz/m^2 cosmic thermal neutrons and 1 Hz/m^2 with shielding

- 2 Aluminium foil as a detector window reduces x50 the background generated by scattered neutrons

Conclusions

(*results are general and applicable for any facility)

- 1 @ESS 23 Hz/m^2 cosmic thermal neutrons and 1 Hz/m^2 with shielding

- 2 Aluminium foil as a detector window reduces x50 the background generated by scattered neutrons

- 3

Boron-10		Helium-3
0.5 – 0.8	Thermal N Efficiency	0.6 - 1
10^{-5}	Fast neutron sensitivity (gas dominates)	10^{-3}
10^{-6} - 10^{-9}	Gamma-ray sensitivity (solid dominates)	10^{-6} - 10^{-9}

Highly affected by a small variation of the threshold

References

Gamma-ray sensitivity

- A. Khaplanov et al., Investigation of gamma-ray sensitivity of neutron detectors based on thin converter films, JINST 8 P10025 (2013) (arxiv: 1306:6247)
- F. Piscitelli et al., The Multi-Blade Boron-10-based Neutron Detector for high intensity Neutron Reflectometry at ESS, JINST 12 P03013 (2017) (arxiv: 1701.07623)

Fast neutron sensitivity

- F. Piscitelli et al., Verification of He-3 proportional counters fast neutron sensitivity through a comparison with He-4 detectors, sub. to EPJ Plus (2020) (arxiv: 2002.08153)
- G. Mauri et al., Fast neutron sensitivity for 3He detectors and comparison with Boron-10 based neutron detectors, EPJ TI 6, no. 1, p. 3, (2019) (arxiv: 1902:09870)
- G. Mauri et al., Fast neutron sensitivity of neutron detectors based on Boron-10 converter layers, JINST 13 P03004 (2018) (arxiv: 1712.05614)

Scattered Neutron Background

- G. Mauri et al., The Multi-Blade Boron-10-based neutron detector performance using a focusing reflectometer, Accepted for publ. in JINST (2020) (arxiv: 2001:02965).
- F. Piscitelli et al., Characterization of the Multi-Blade 10B-based detector at the CRISP reflectometer at ISIS, JINST 13 P05009 (2018) (arxiv: 1803.09589)
- G. Galgoczi et al., Investigation of neutron scattering in the Multi-Blade detector with GEANT4 simulations, JINST 13 P12031 (2018) (arxiv: 1810:06241)
- E. Rossi, Master. thesis, Characterisation of the Spatial Resolution and the Gamma-ray Discrimination of Helium-3 Proportional Counters (2015) (arxiv: 1702:06501)
- J. Birch et al., Investigation of background in large-area neutron detectors due to alpha emission from impurities in aluminium, JINST 10, P10019 (2015) (arxiv: 1507:00607)
- J. Birch et al., In-beam test of the Boron-10 Multi-Grid neutron detector at the IN6 Time-of-Flight spectrometer at the ILL, J. Phys. Conf. Ser. 528:1, 012040 (2014)

BACKUP SLIDES

He3 detector

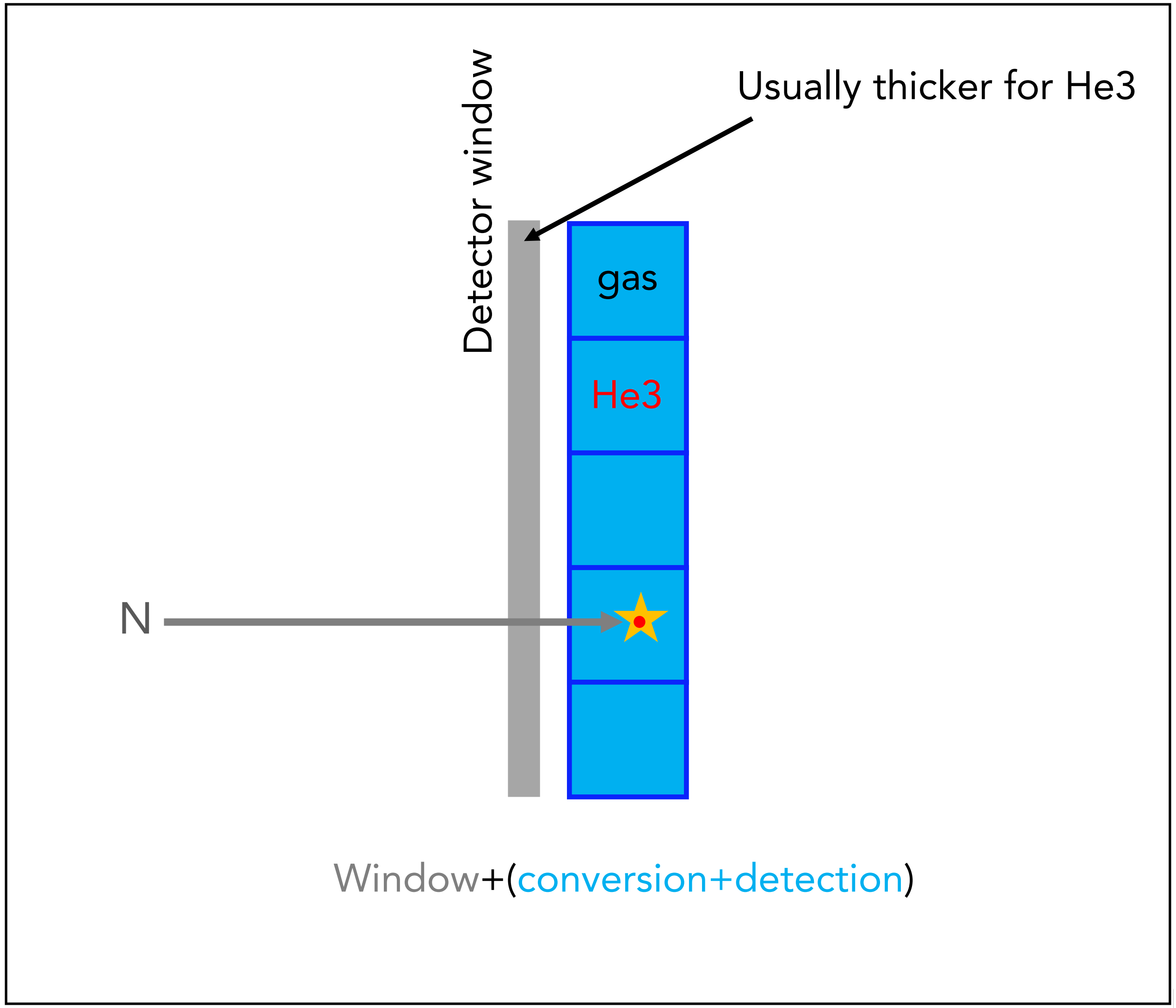

$$n + {}^{3}He \rightarrow p(0.57\,\text{MeV}) + {}^{3}H(0.19\,\text{MeV})$$

B10 detector

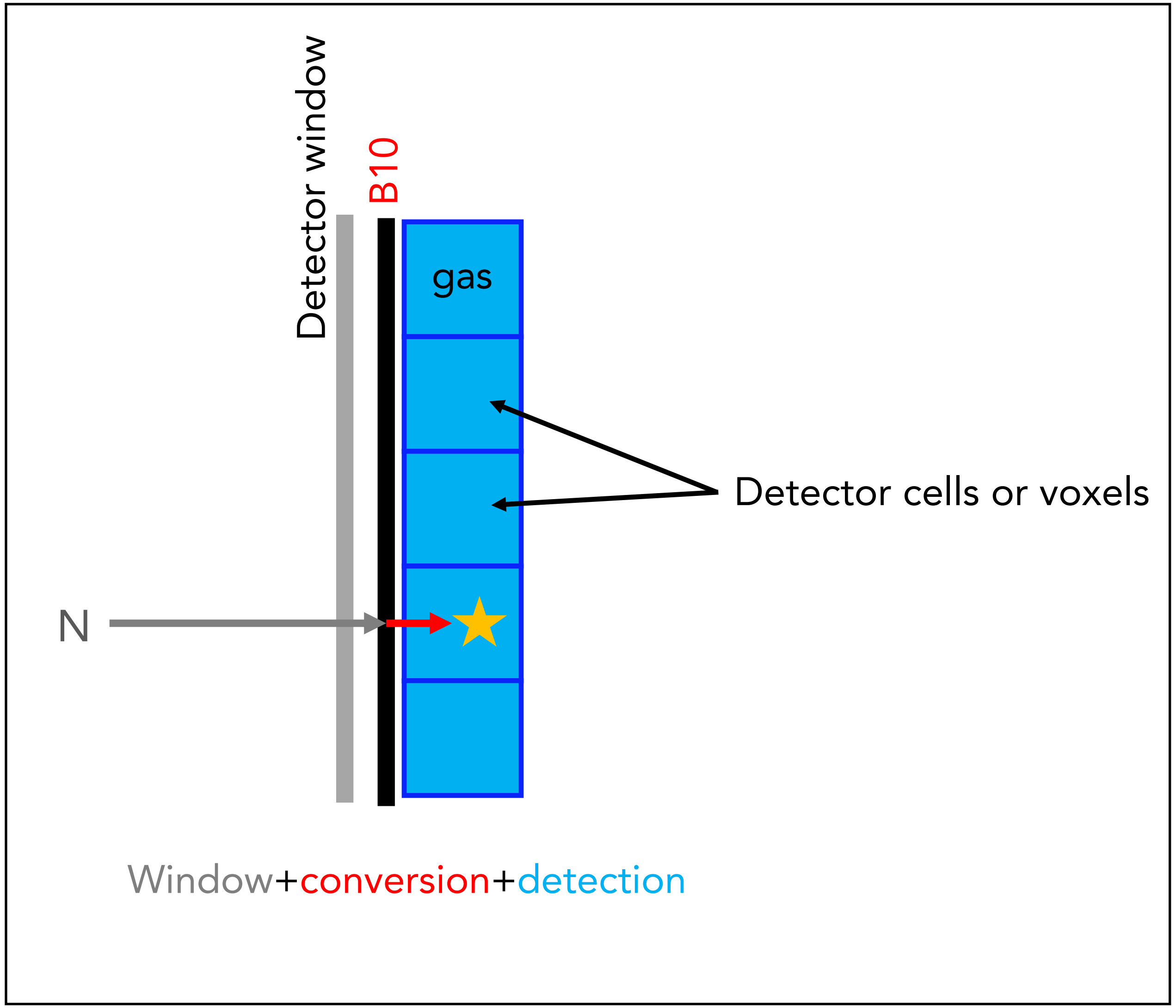

$$n + {}^{10}B \xrightarrow{94\%} {}^{7}Li(0.84\,\text{MeV}) + {}^{4}He(1.47\,\text{MeV}) + \gamma(0.48\,\text{MeV})$$
$$\xrightarrow{6\%} {}^{7}Li(1.02\,\text{MeV}) + {}^{4}He(1.78\,\text{MeV})$$

BACKGROUND DUE TO SCATTERED NEUTRONS

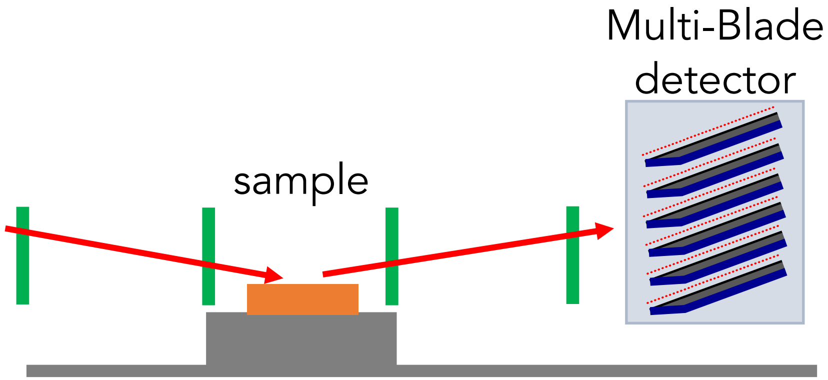

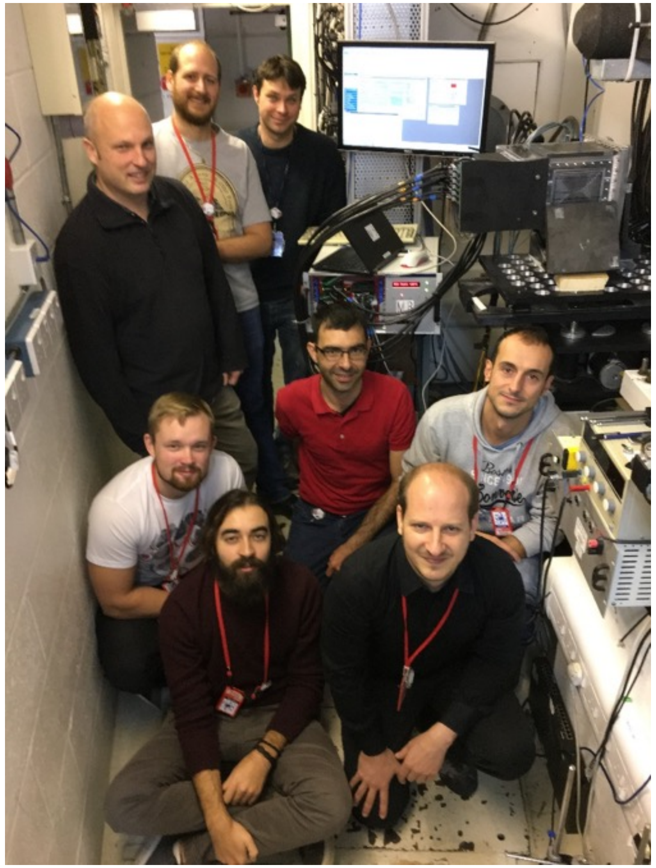

detector area

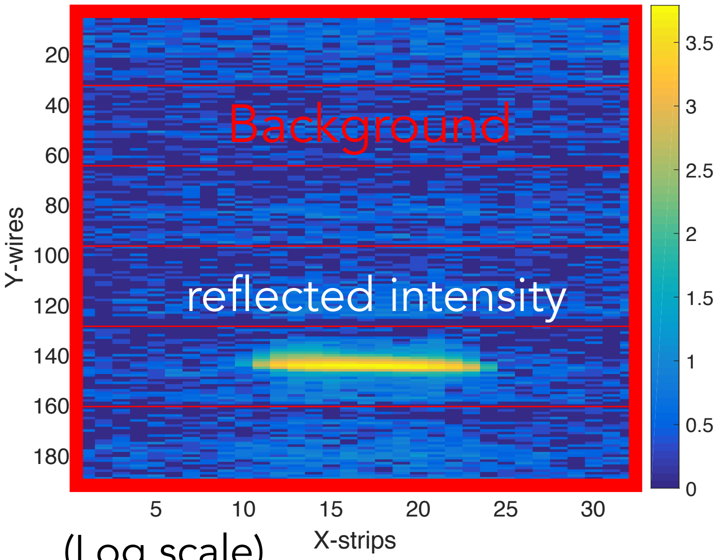

detector ToF

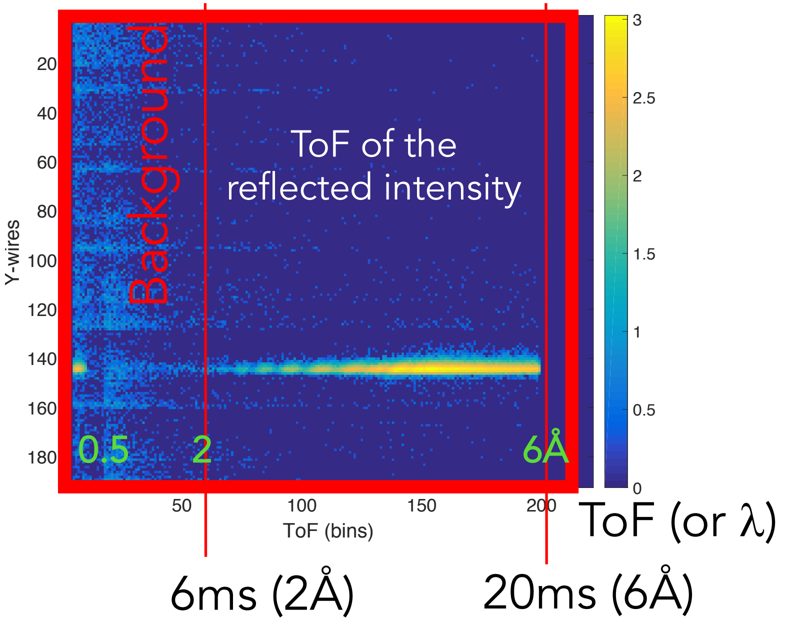

Science & Technology Facilities Council ISIS

October 2017 - CRISP reflectometer @ ISIS

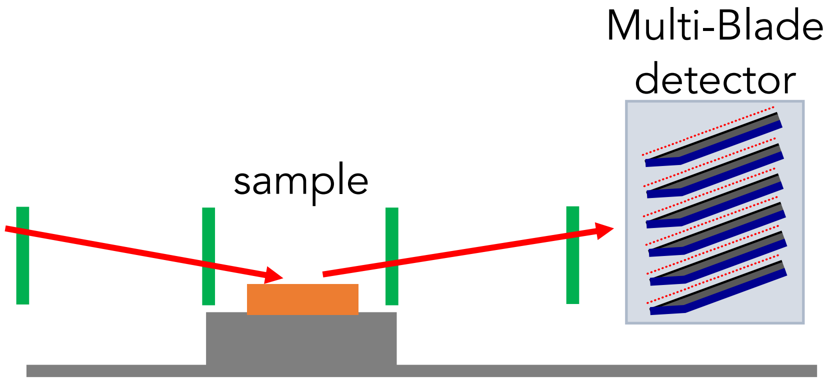
Multi-Blade
detector
sample

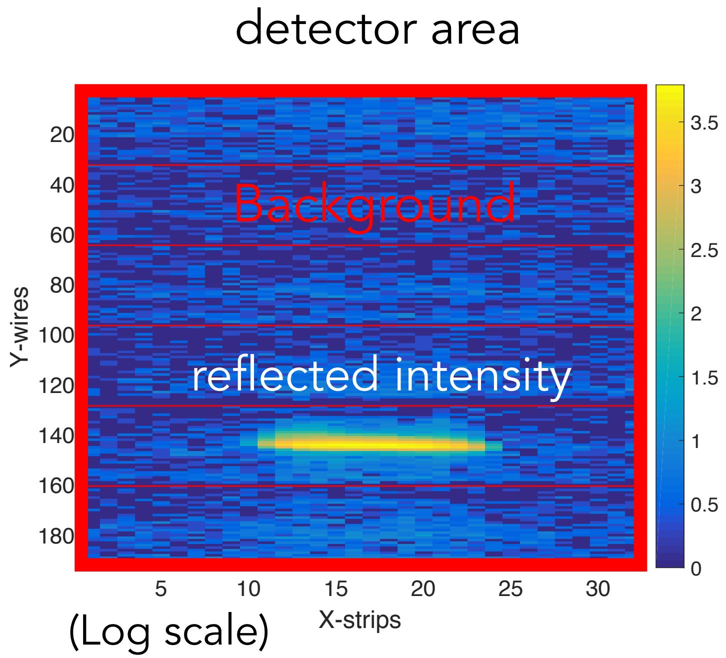
detector area
Background
reflected intensity
Y-wires
X-strips
(Log scale)

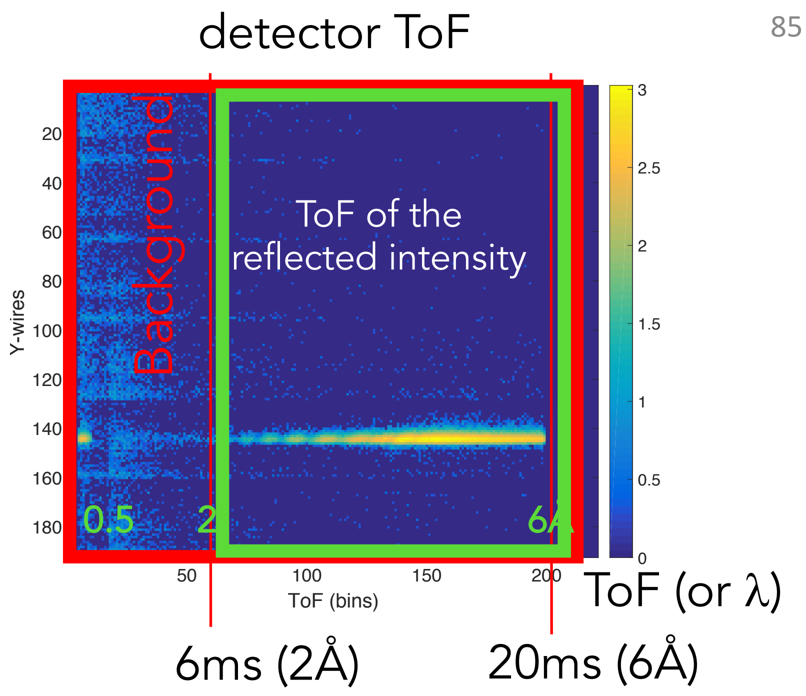
detector ToF
Background
ToF of the
reflected intensity
0.5
2
6Å
Y-wires
ToF (bins)
ToF (or λ)
6ms (2Å)
20ms (6Å)

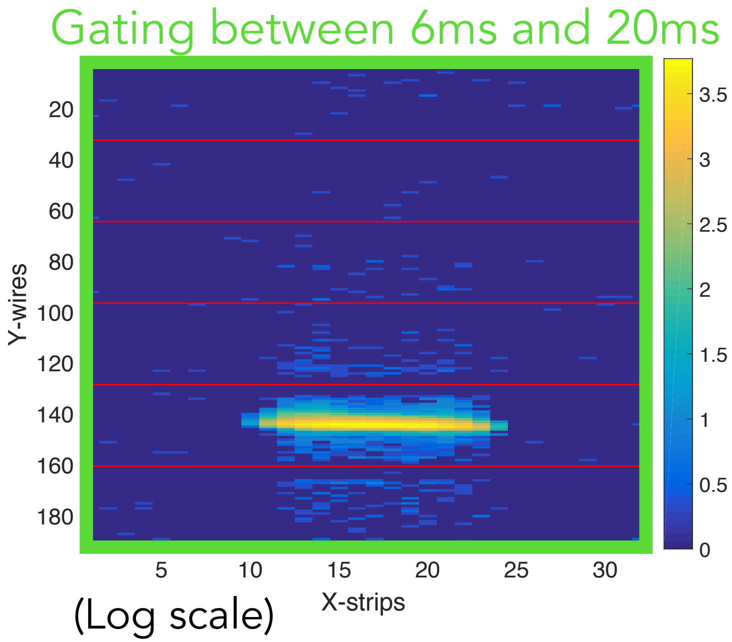
Gating between 6ms and 20ms
Y-wires
X-strips
(Log scale)

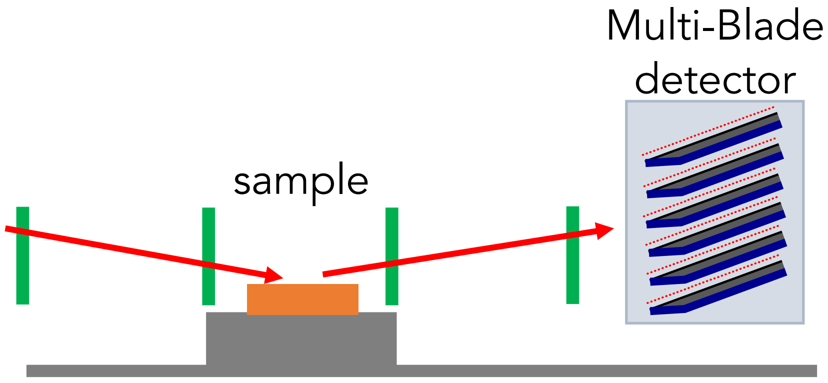

detector area

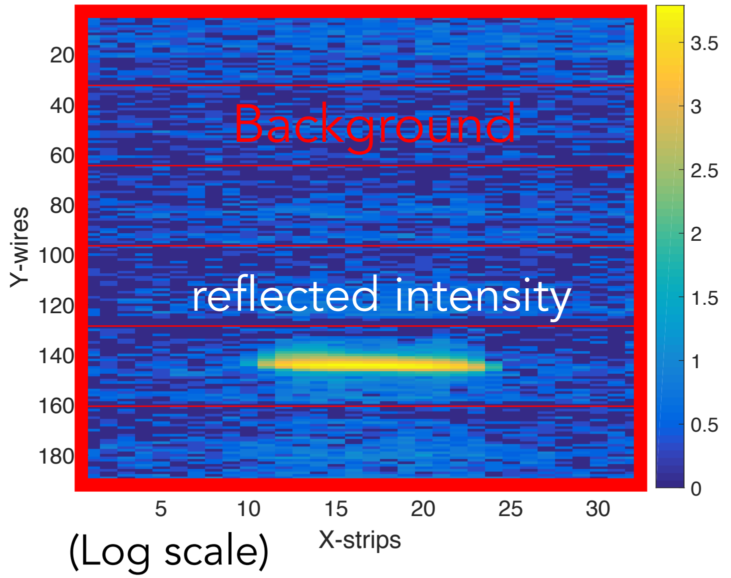

detector ToF

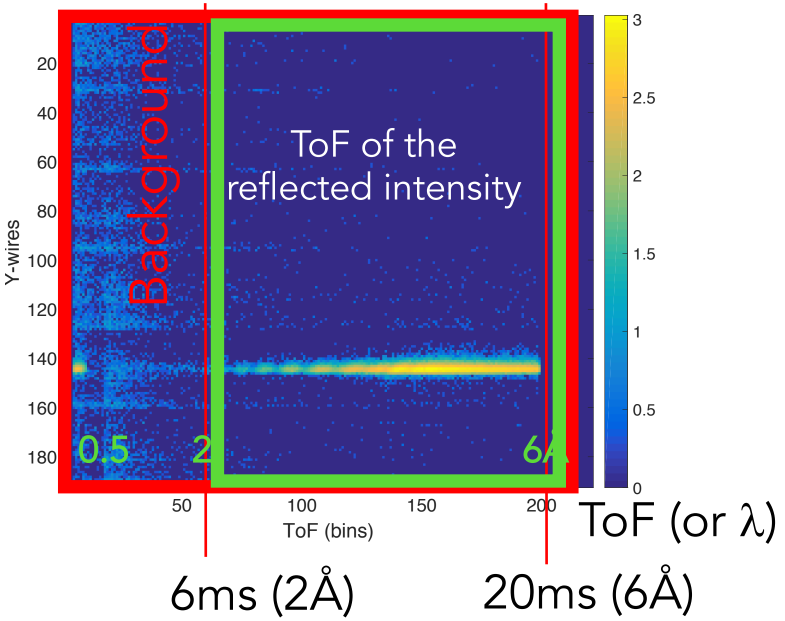

Projection over Y-axis

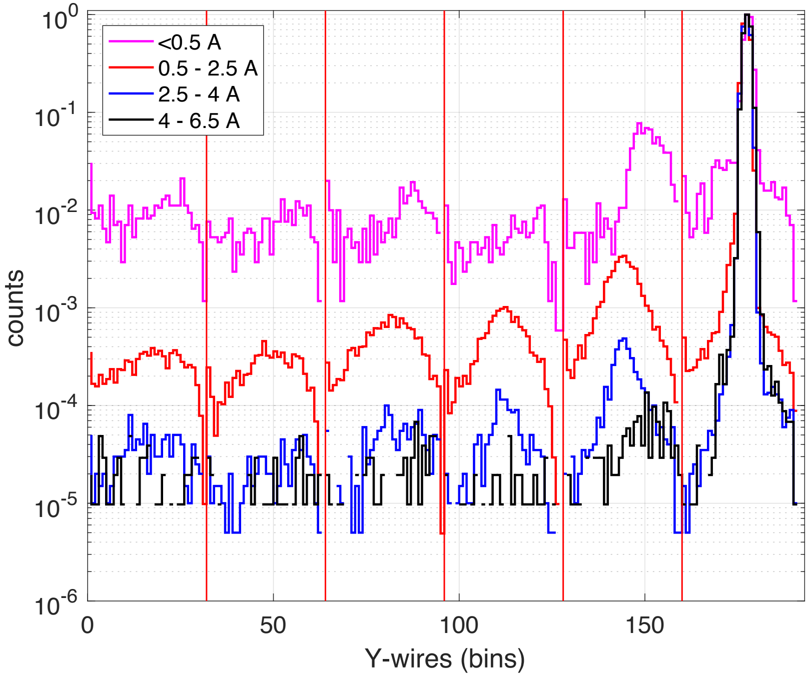

Gating between 6ms and 20ms

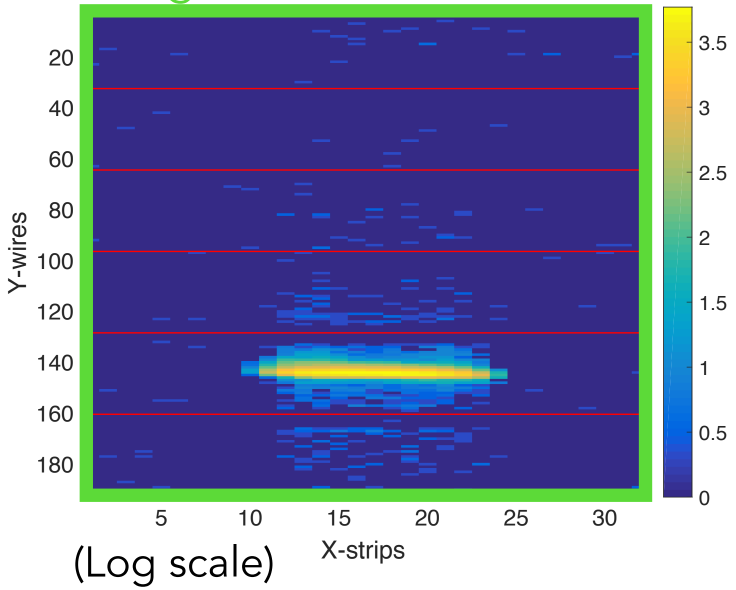

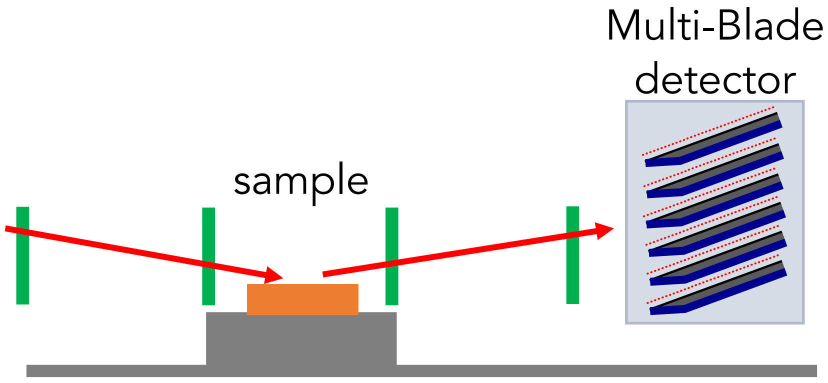
Multi-Blade
detector
sample

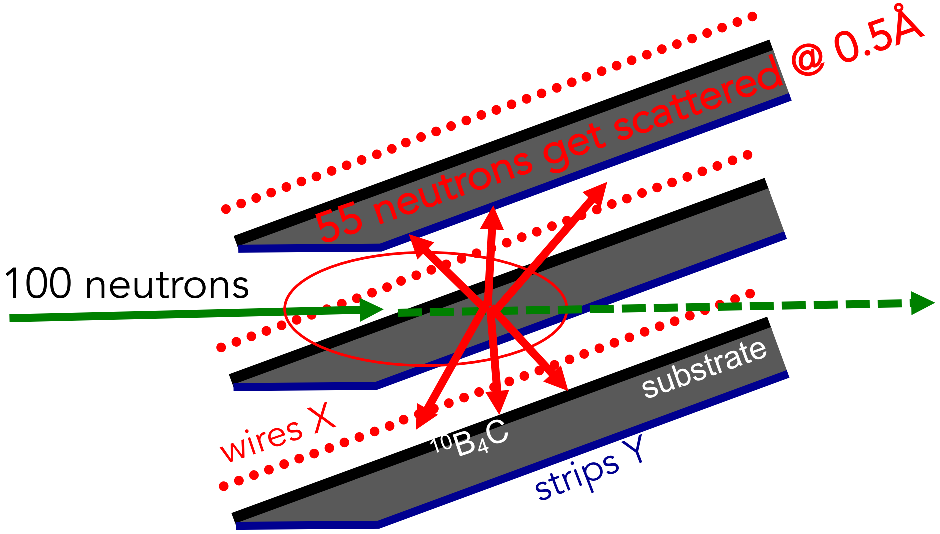
55 neutrons get scattered @ 0.5Å
100 neutrons
substrate
wires X
$^{10}B_4C$
strips Y

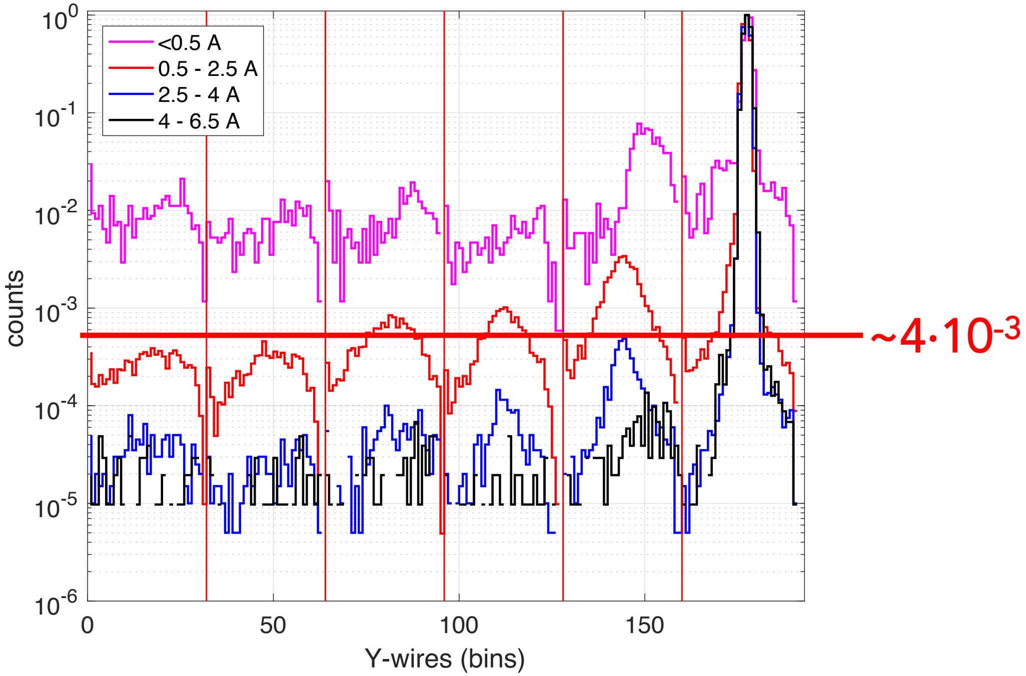
<0.5 A
0.5 - 2.5 A
2.5 - 4 A
4 - 6.5 A
~4·10^{-3}
counts
Y-wires (bins)

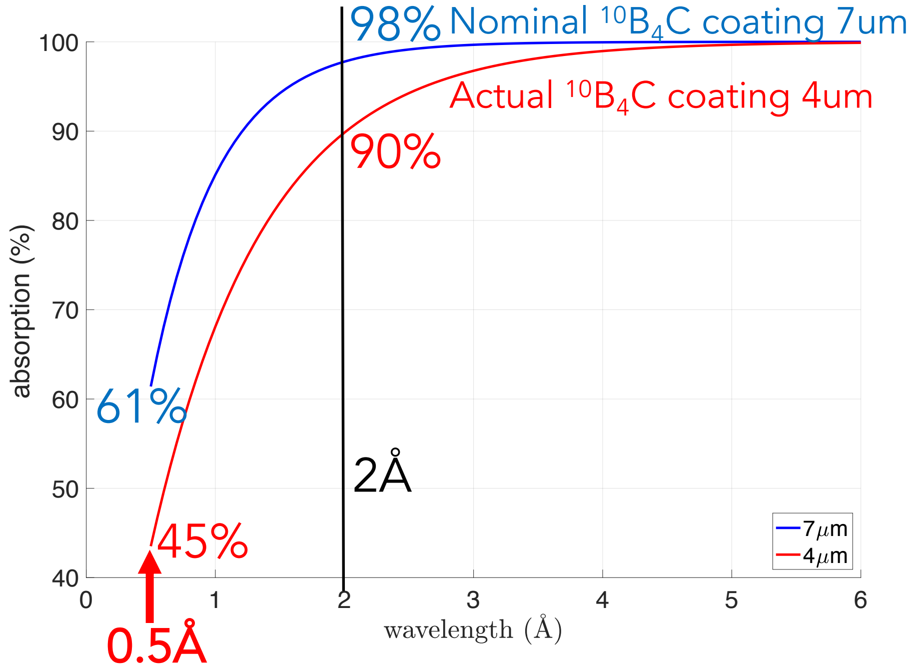
98% Nominal $^{10}B_4C$ coating 7um
Actual $^{10}B_4C$ coating 4um
90%
61%
45%
2Å
0.5Å
absorption (%)
wavelength (Å)
7μm
4μm

PAUL SCHERRER INSTITUT PSI

November 2018 - AMOR reflectometer @ PSI

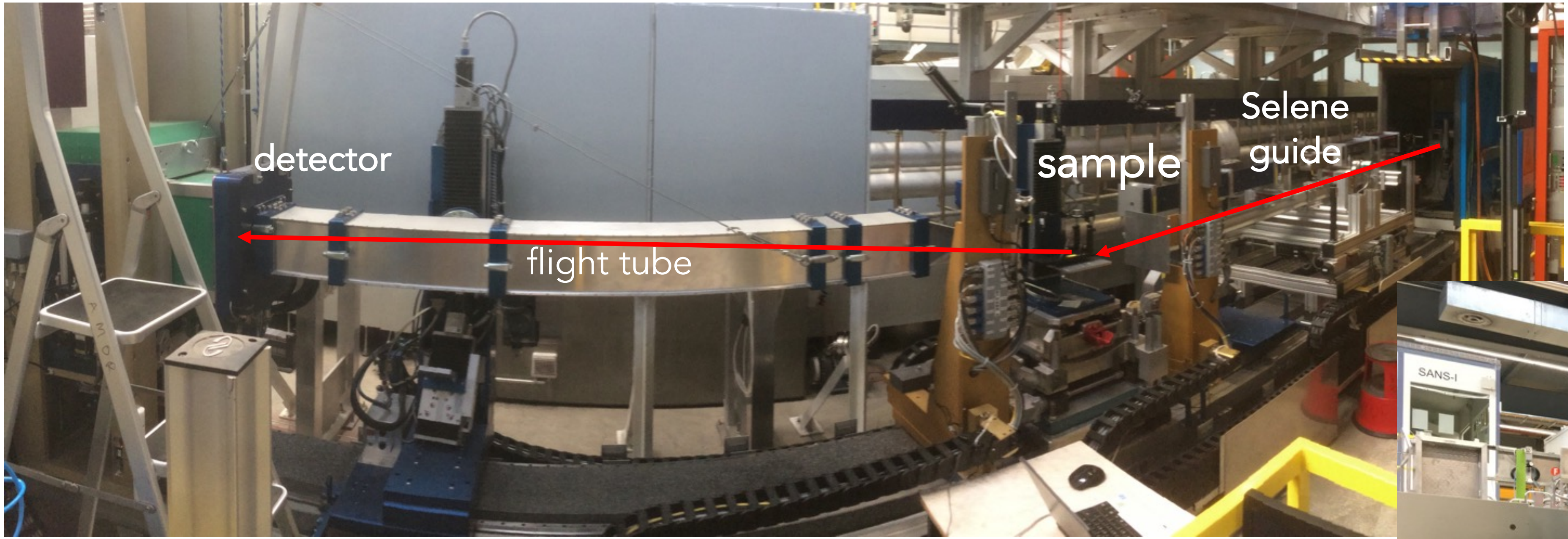

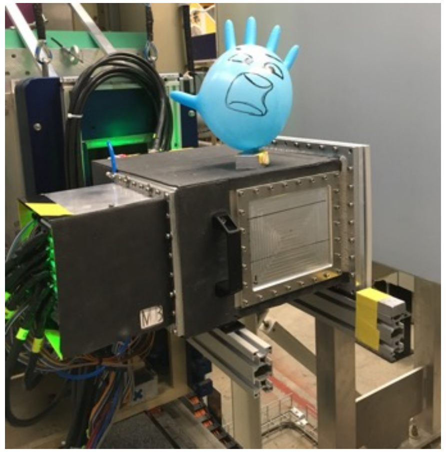

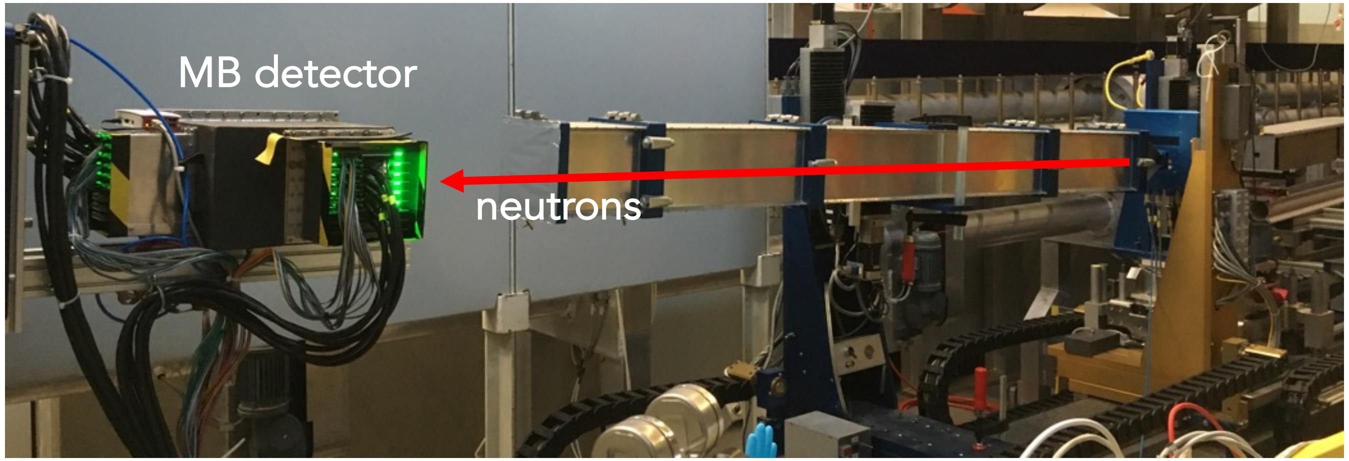

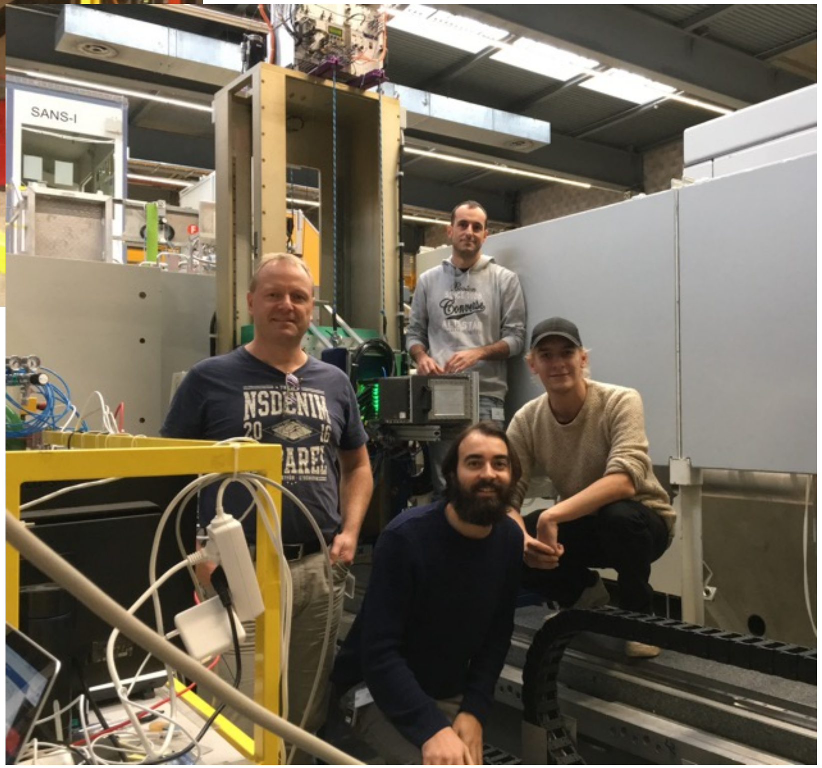

WP5 Data Acquisition software chain has been developed during BrightnESS (WP5 - i.e. DMSC/Data) and tested @ AMOR

PAUL SCHERRER INSTITUT PSI

November 2018 - AMOR reflectometer @ PSI

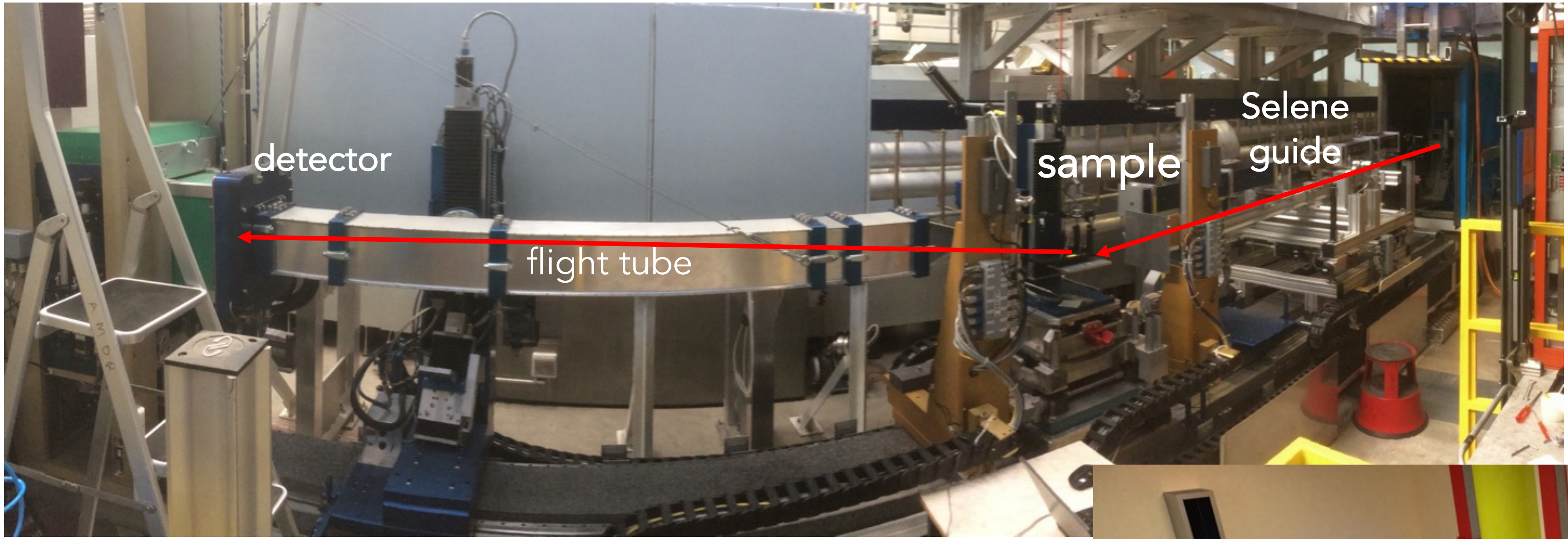

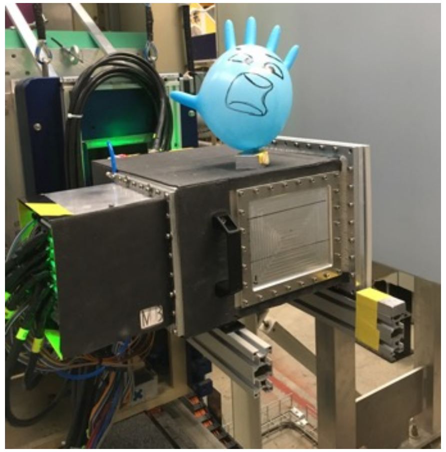

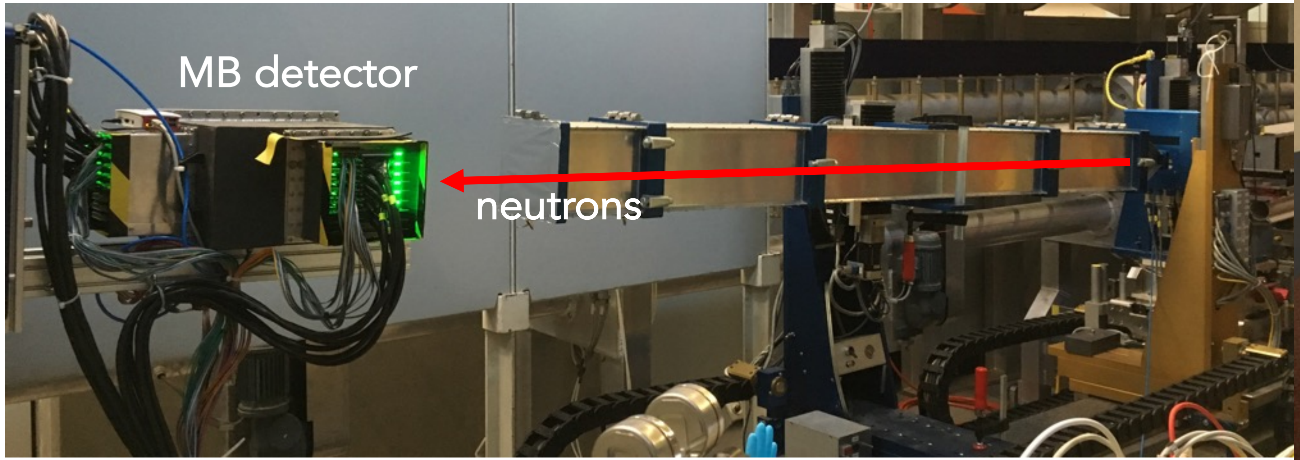

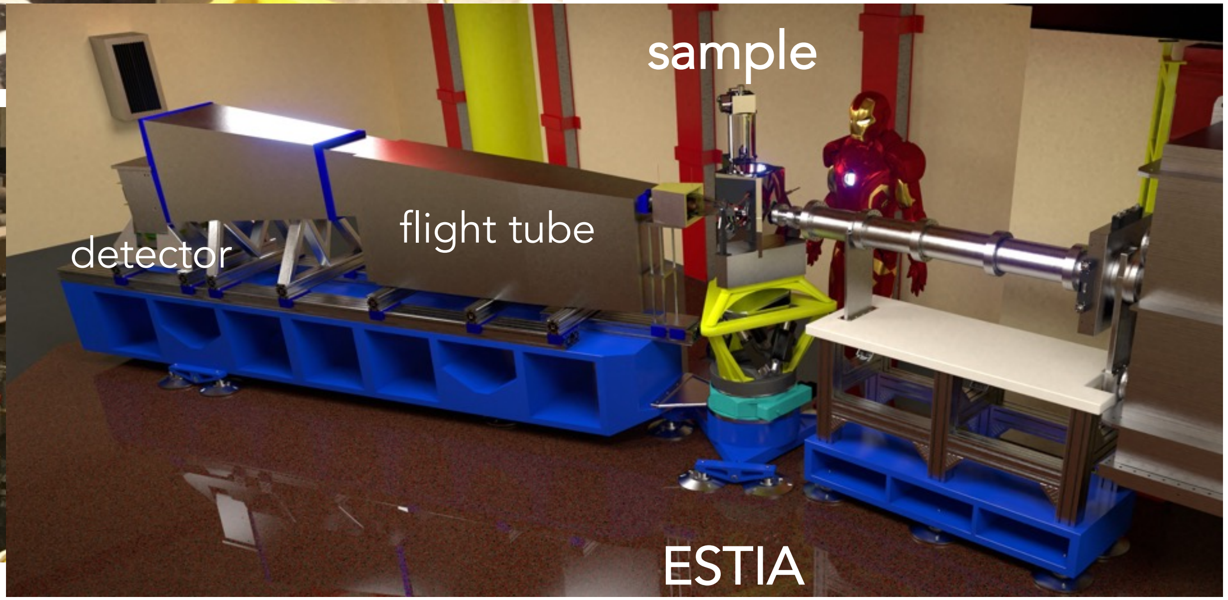

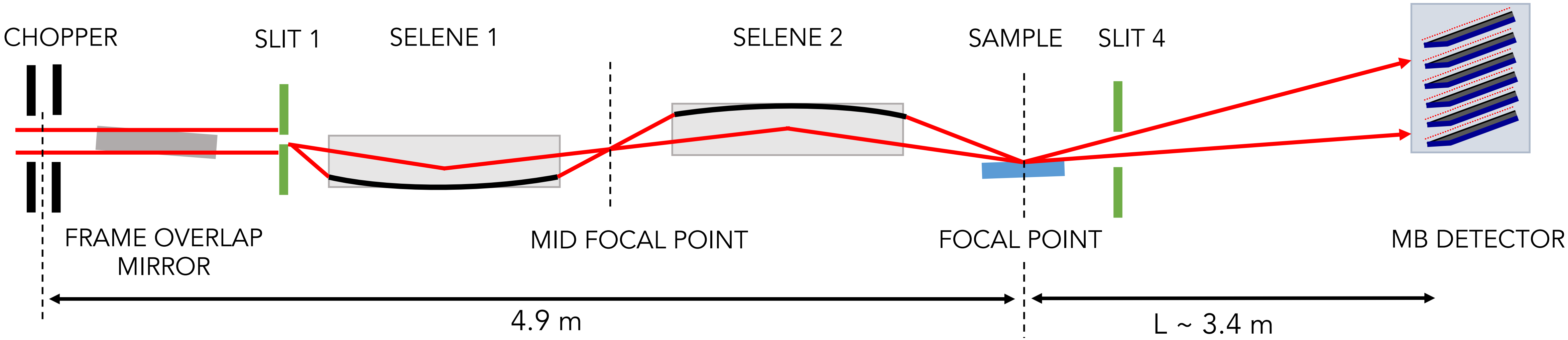
CHOPPER
SLIT 1
SELENE 1
SELENE 2
SAMPLE
SLIT 4
FRAME OVERLAP
MIRROR
MID FOCAL POINT
FOCAL POINT
MB DETECTOR
4.9 m
L ~ 3.4 m


Selene
guide
sample
flight tube
Multi-Blade

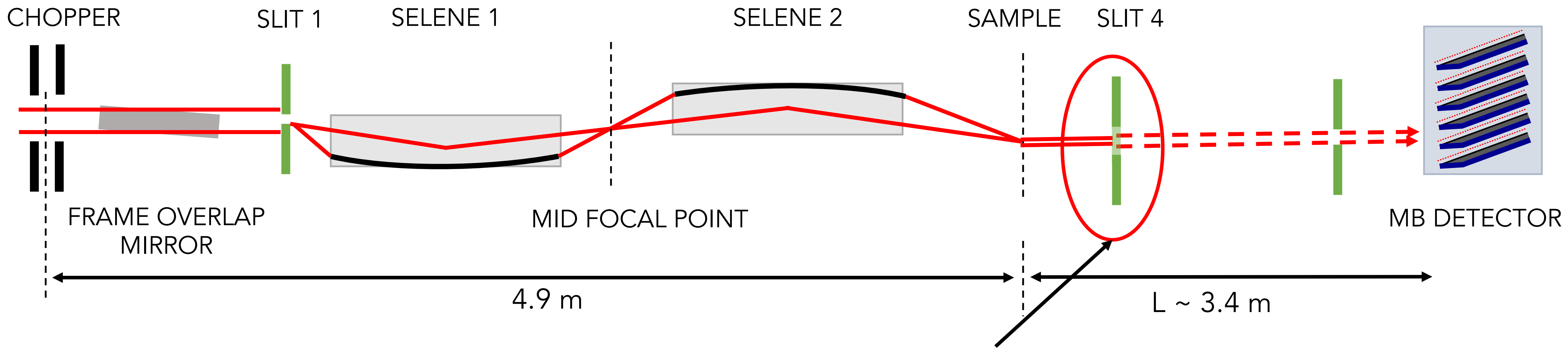

Cd slit to block the beam far from the detector with shutter open

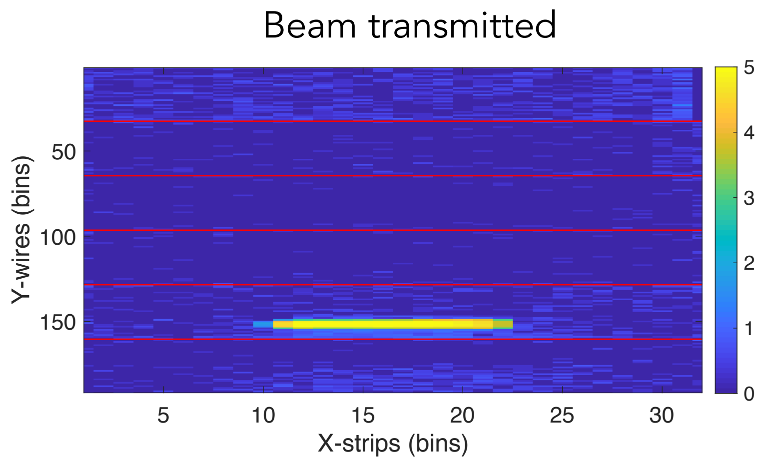

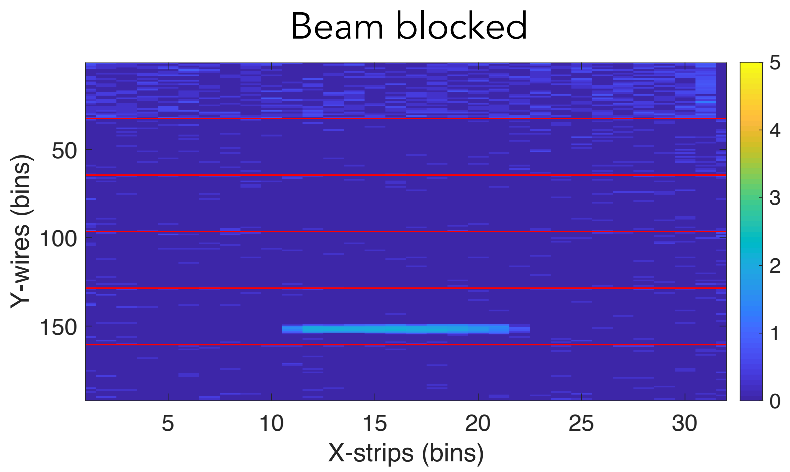

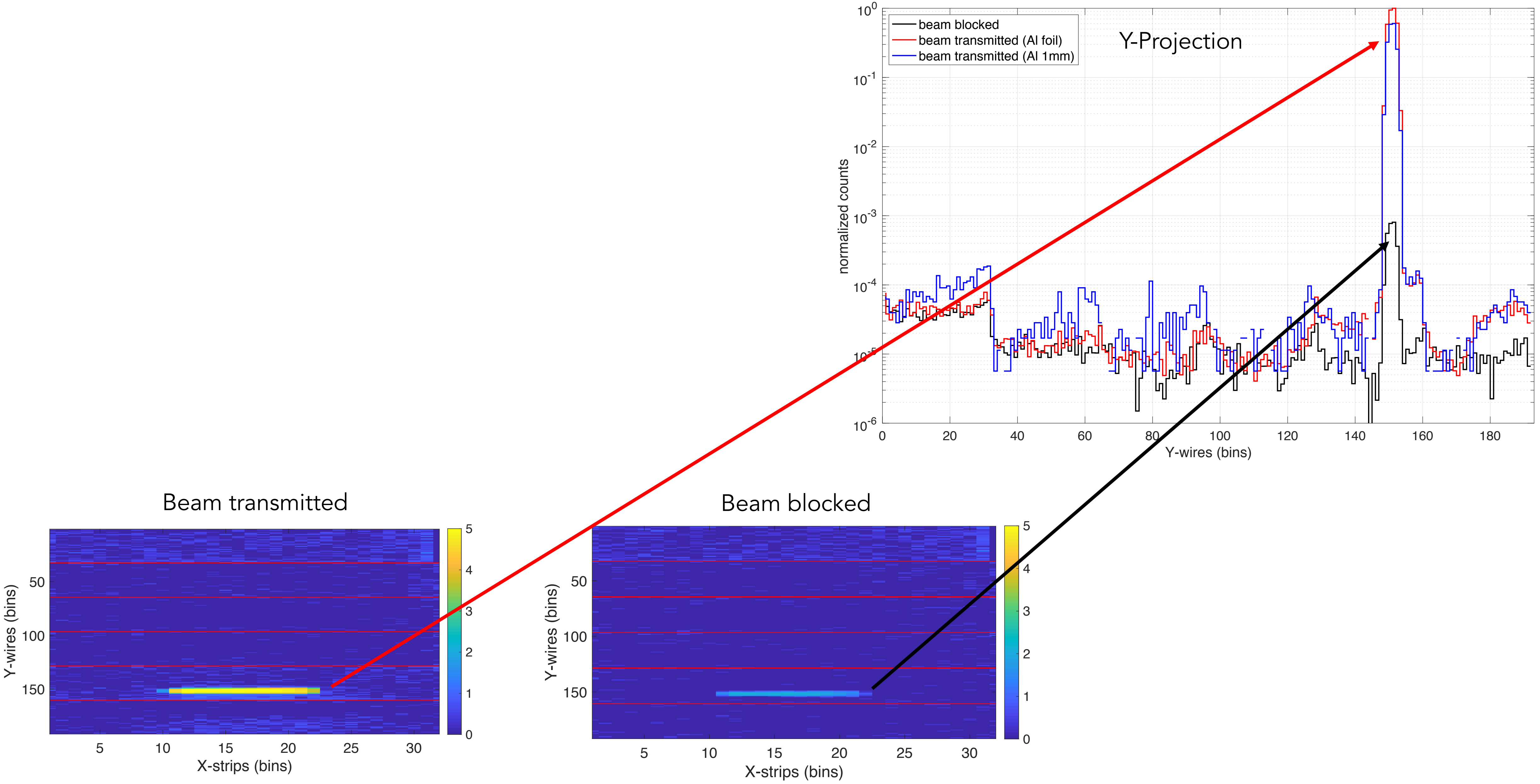

Y-Projection
beam blocked
beam transmitted (Al foil)
beam transmitted (Al 1mm)
normalized counts
Y-wires (bins)
Beam transmitted
Beam blocked
Y-wires (bins)
X-strips (bins)

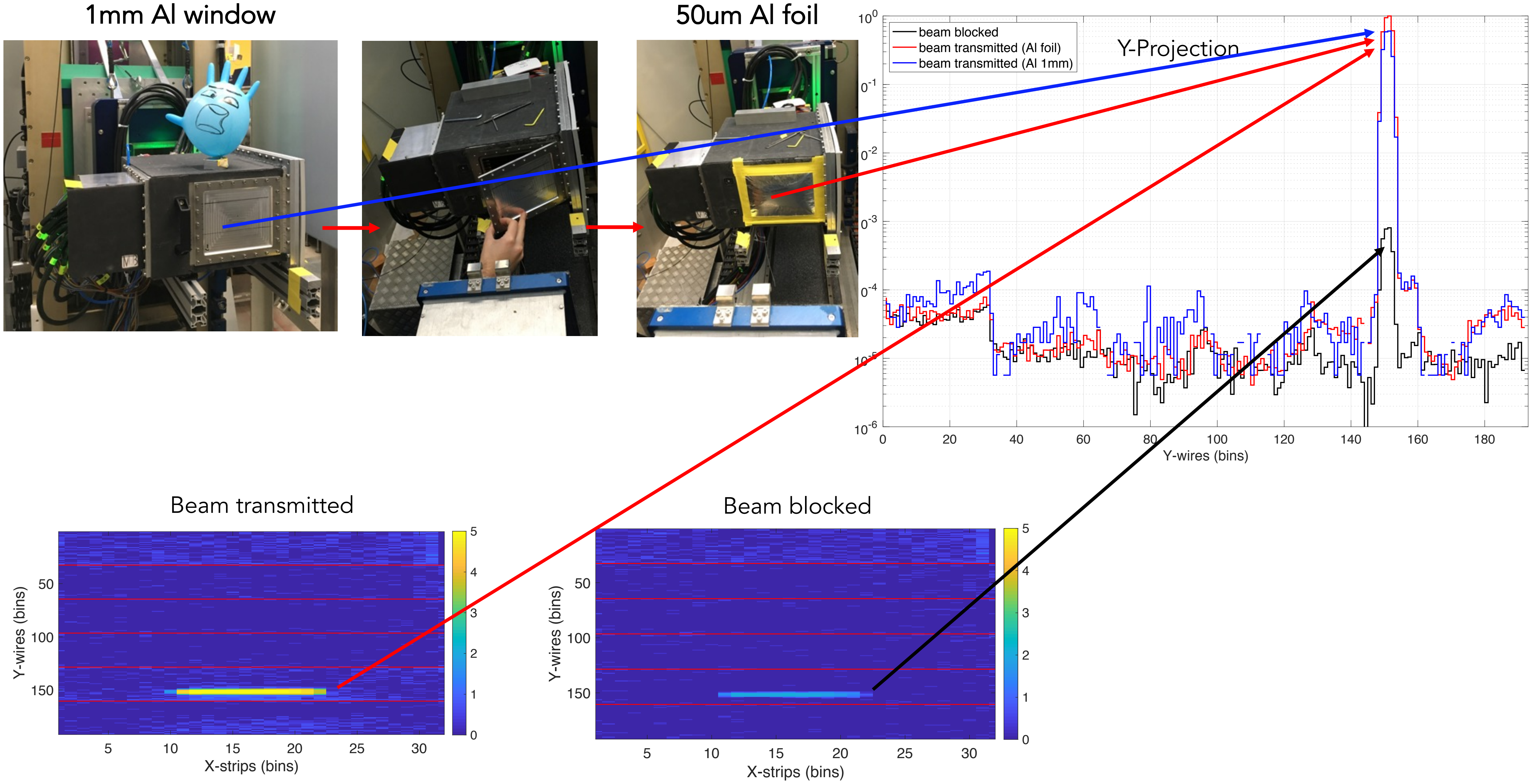
1mm Al window
50um Al foil
Y-Projection
beam blocked
beam transmitted (Al foil)
beam transmitted (Al 1mm)
Y-wires (bins)
Beam transmitted
Beam blocked
Y-wires (bins)
X-strips (bins)

1mm window ~ 10^{-4}

Foil window ~ $3 \cdot 10^{-5}$

Instrument background ~ $2 \cdot 10^{-5}$

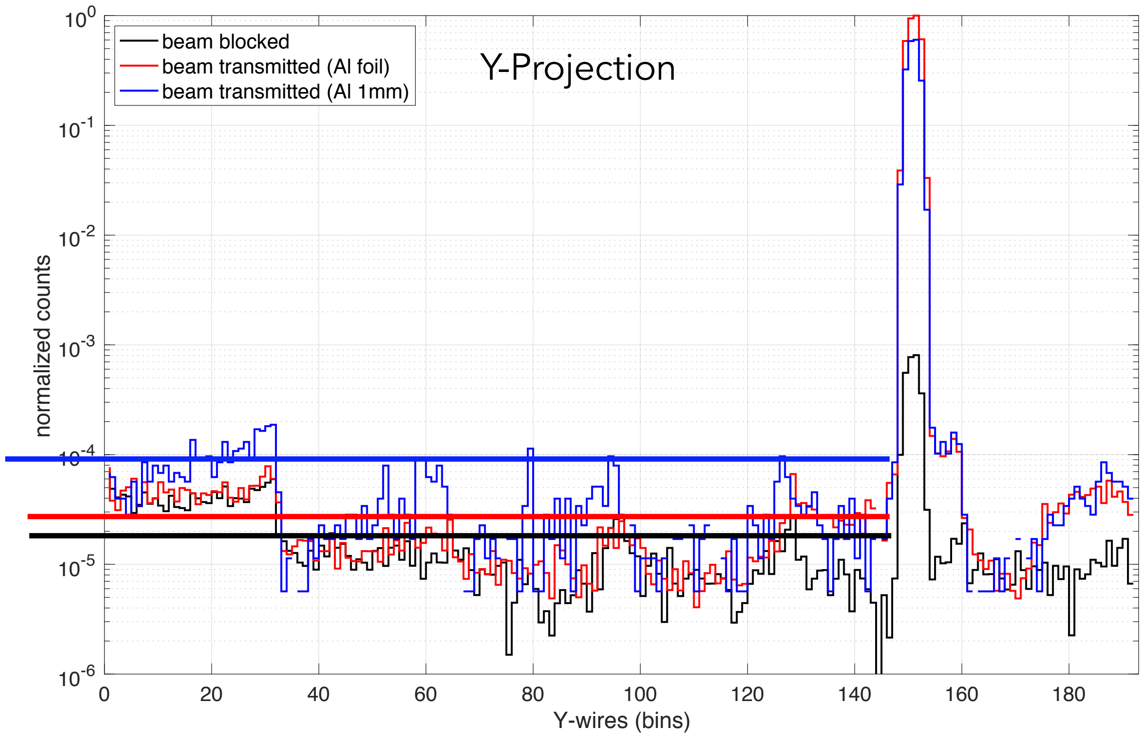

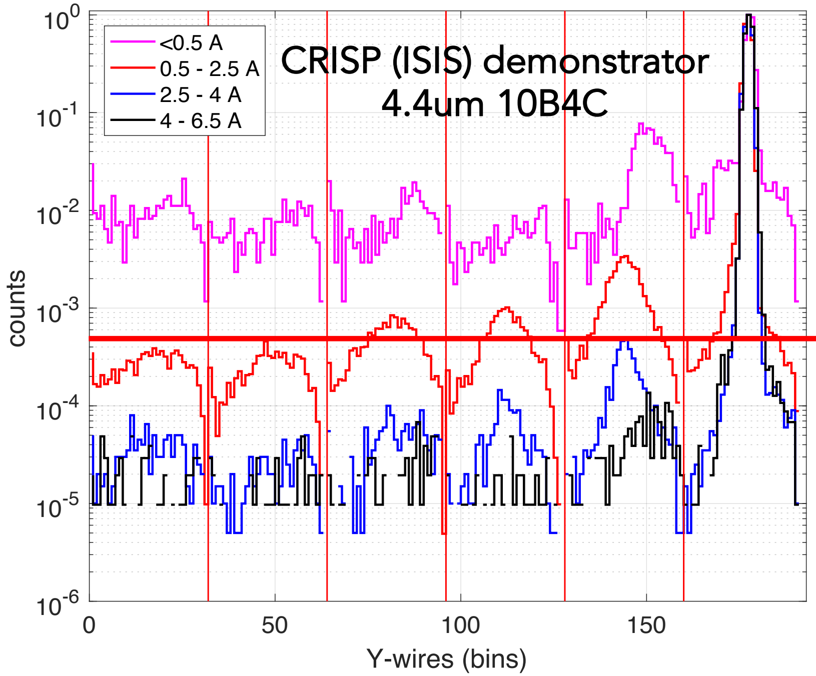

~4·10^{-3}

~ 3·10^{-5}

~ 2·10^{-5}

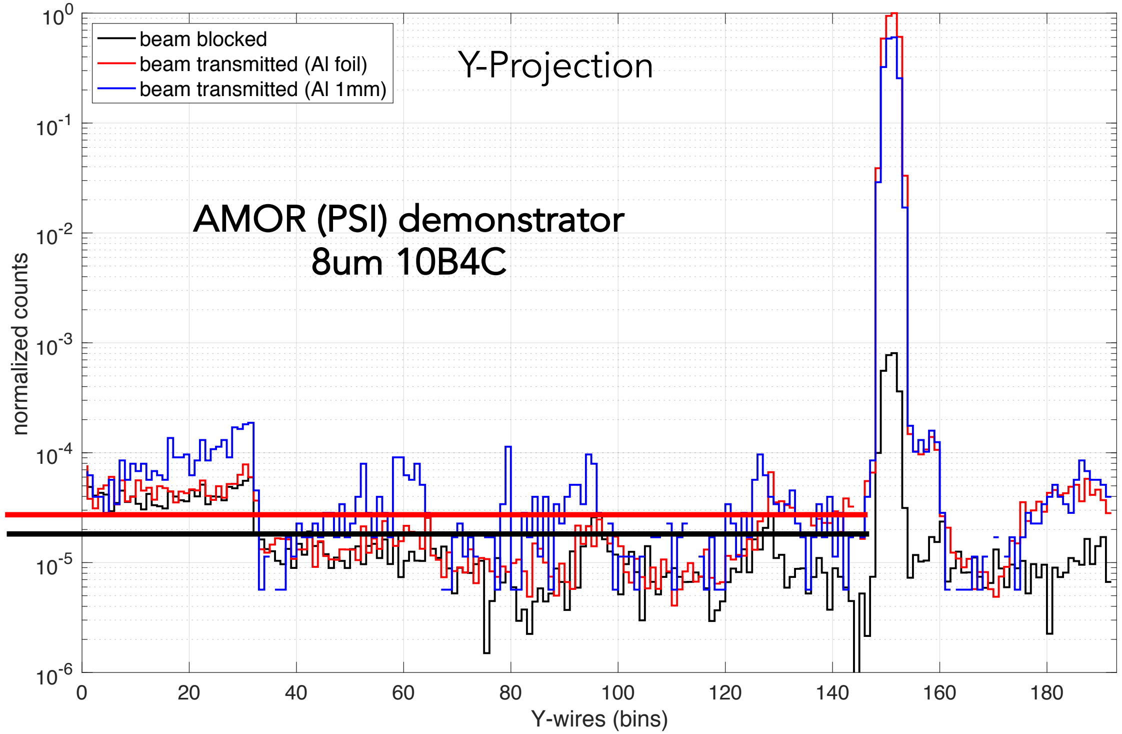

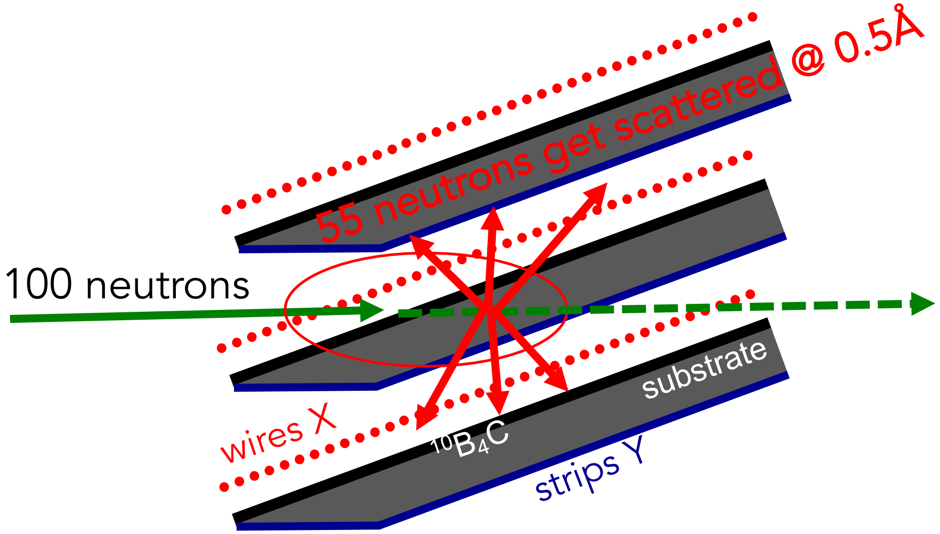

Problem Solved!

Multi-Blade - B10 | He3 – AMOR detector

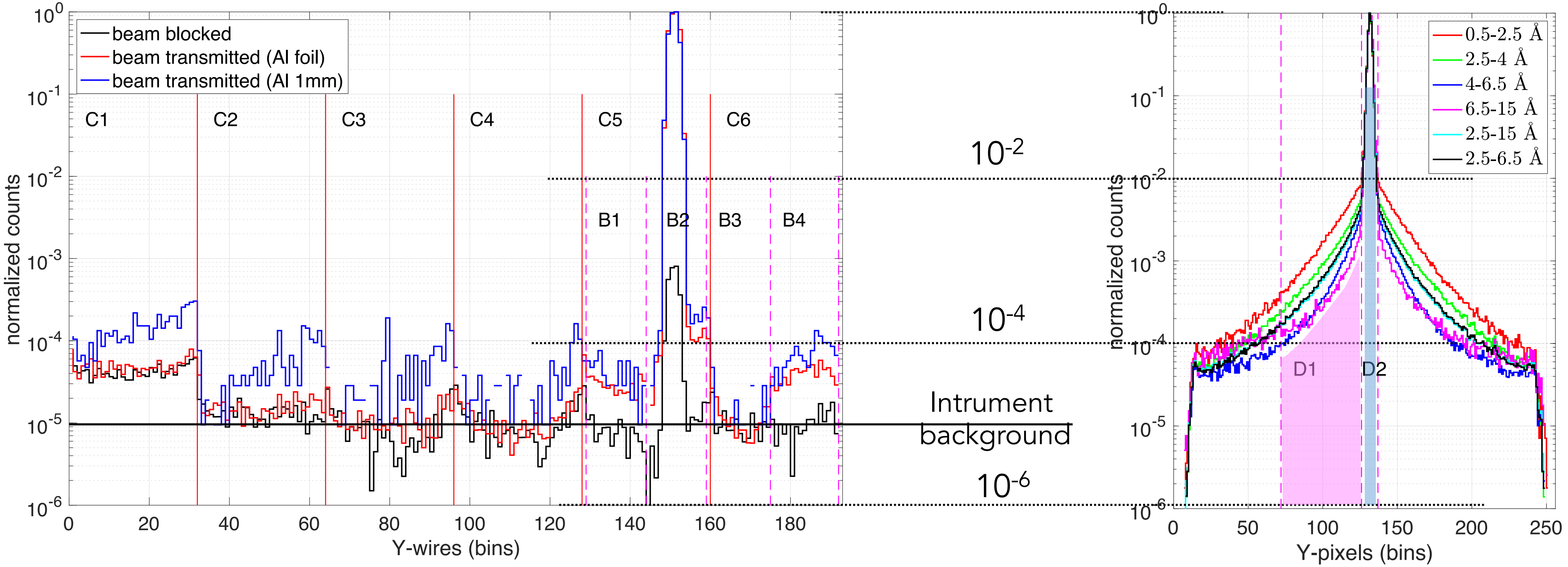

FoM ($\times 10^4$)	wavelength range (Å)					
	0.5-2.5	2.5-4	4-6.5	2.5-6.5	6.5-15	2.5-15
MB@AMOR (>7.5μm coating)						
1mm Al window	n/a	7.3	8.0	7.4	7.2	7.3
Al foil window	n/a	22.6	47.7	40.5	11.3	21.1
He3@AMOR	0.1	0.2	0.5	0.3	0.8	0.4

$$FoM = \frac{D2}{D1}$$

(normlized to same area)

Foil ~ x3 ~ 1mm window ~ x20 ~ He3
Foil ~ x60 ~ He3

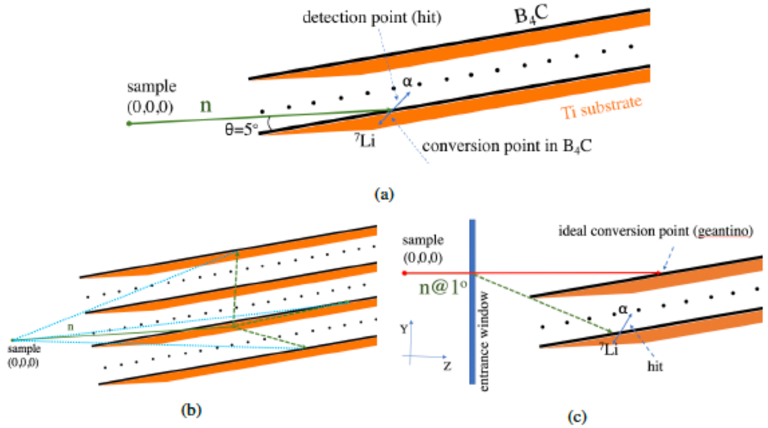

Figure 4. (a) Difference between conversion and detection point. (b) A neutron traversing the first converter layer (solid green) can scatter in the blade material and finally get converted away from the first crossing point (dashed green). This leads to the miscalculation of the distance between sample and detection point (dashed blue). (c) Similarly for a scattered neutron on the detector window. The latter is 1° inclined with respect to the vertical axis. The projection of the detection point on the converter layer is not displayed here for view simplification.

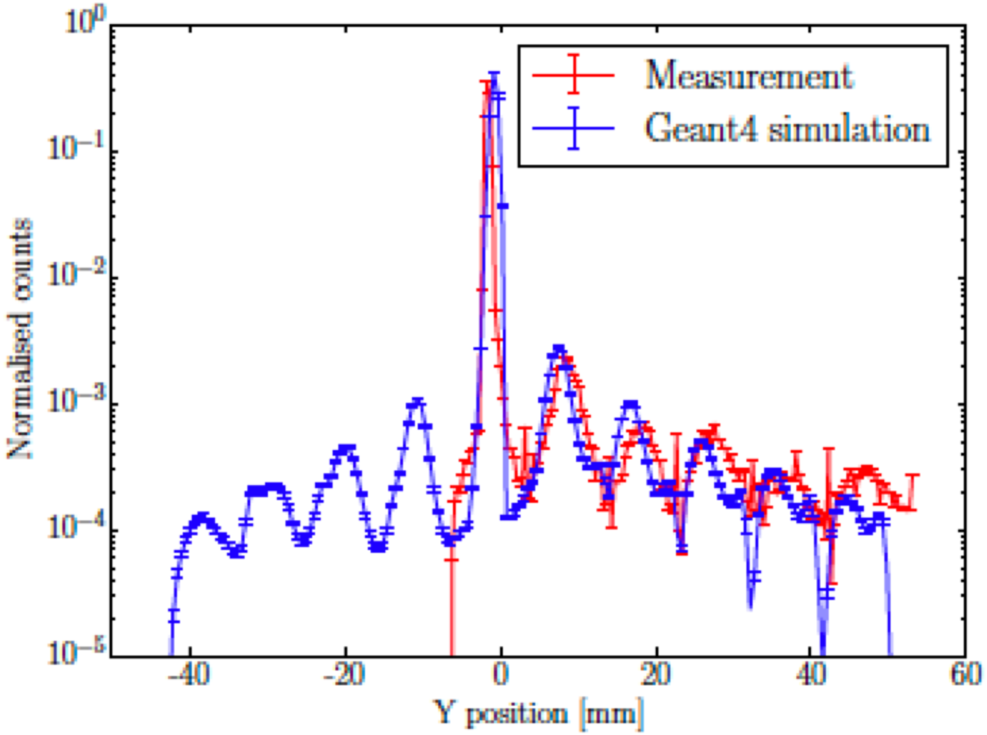

Figure 6. Comparison of Y-position of detected neutrons in measurements taken at CRISP [33] and the results of the simulation (this work). Reproduced from [33]. CC BY 4.0.

FAST NEUTRON BACKGROUND

THEORY

Cross-sections

- ^{3}He
  - ^{3}He recoil (elastic scattering): $^3\mathrm{He} + n \rightarrow {}^3\mathrm{He}' + n'$ $\quad (E_{R\,max} = 0.75\,E_i)$
  - (n,p): $^3\mathrm{He} + n \rightarrow {}^1\mathrm{H} + {}^3\mathrm{H} + 0.764\,MeV$
  - (n,d): $^3\mathrm{He} + n \rightarrow {}^2\mathrm{H} + {}^2\mathrm{H} - 3.27\,MeV$
  - (n,γ) γ-rays

- ^{4}He
  - ^{4}He recoil (elastic scattering): $^4\mathrm{He} + n \rightarrow {}^4\mathrm{He}' + n'$ $\quad (E_{R\,max} = 0.64\,E_i)$

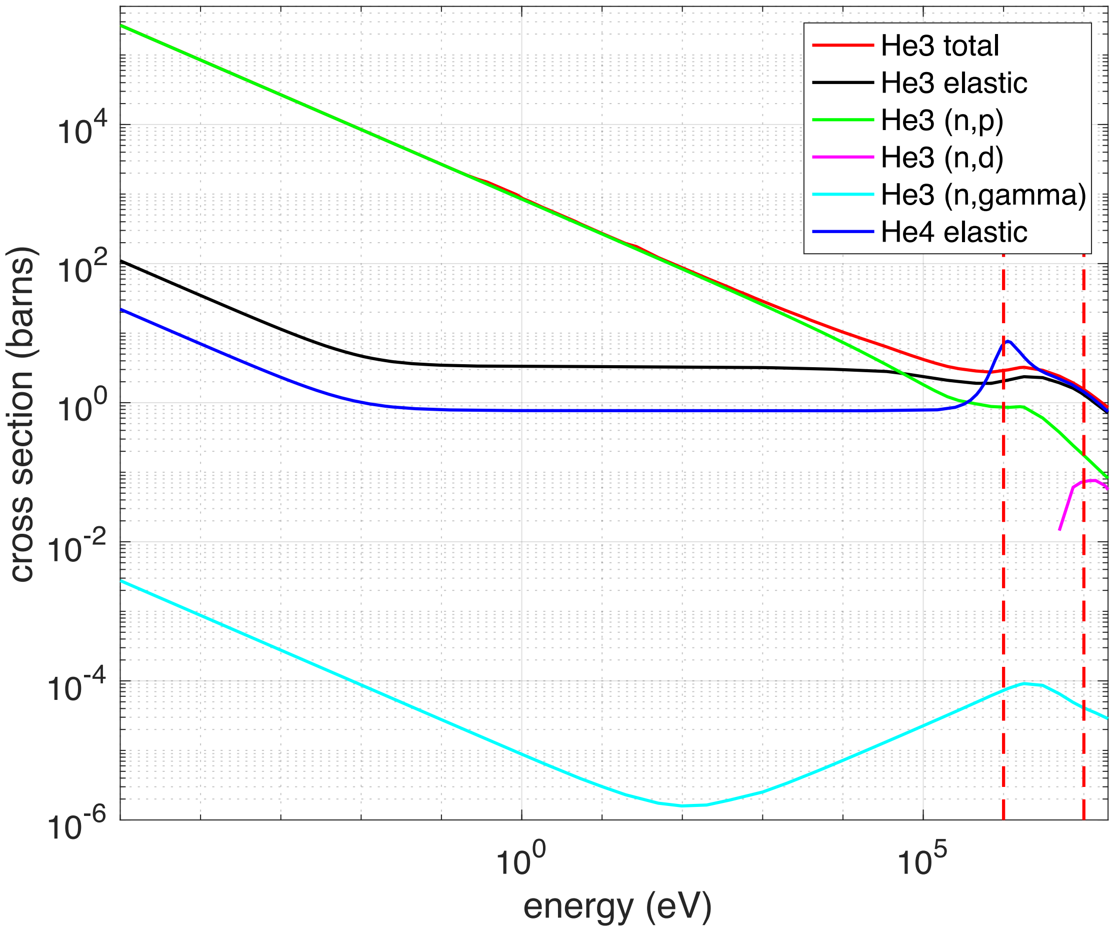

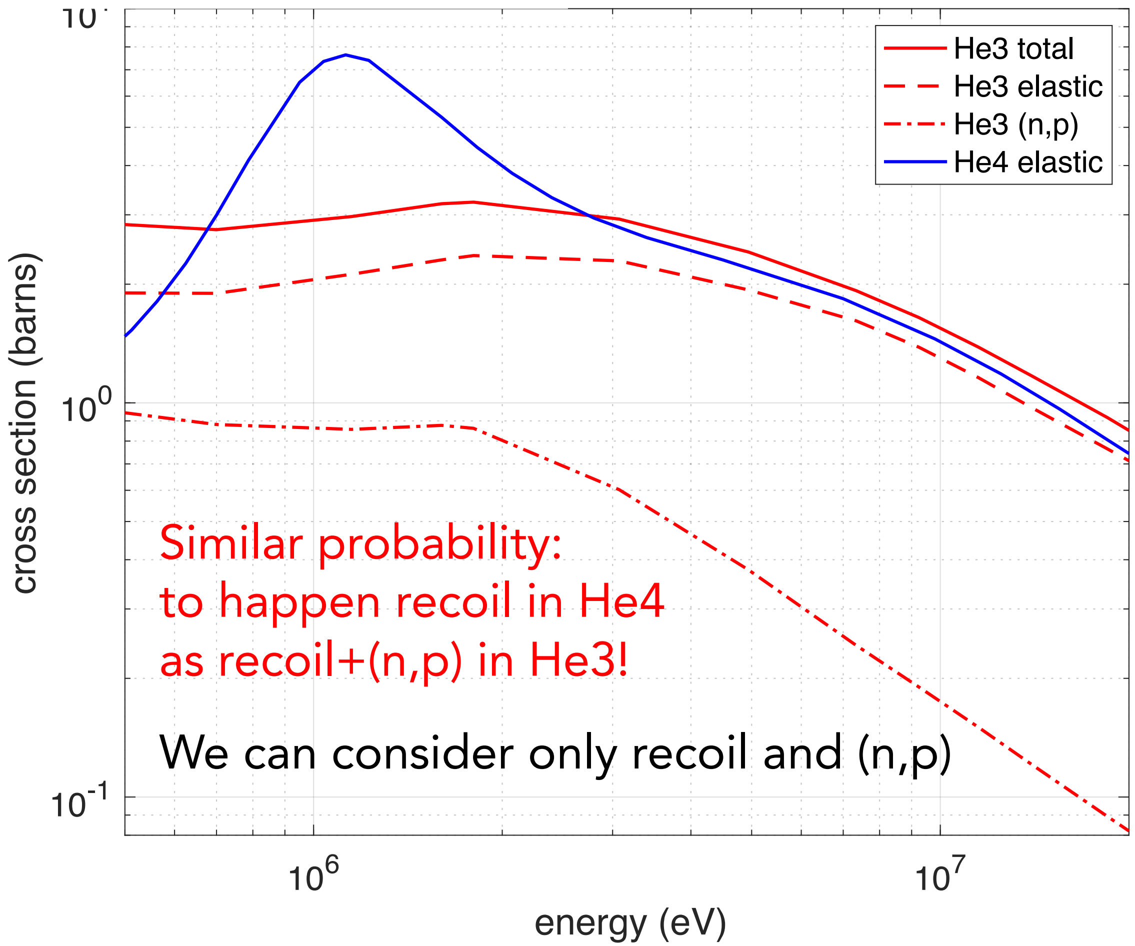

THEORY

Macro corss-sect
And Probability

Same number density for He3 and He4 -> n = 2.43e19 1/cm^3 @ 1 bar

Mass density: He4 0.00016 g/cm3 and He3 0.00012 g/cm3 @ 1bar

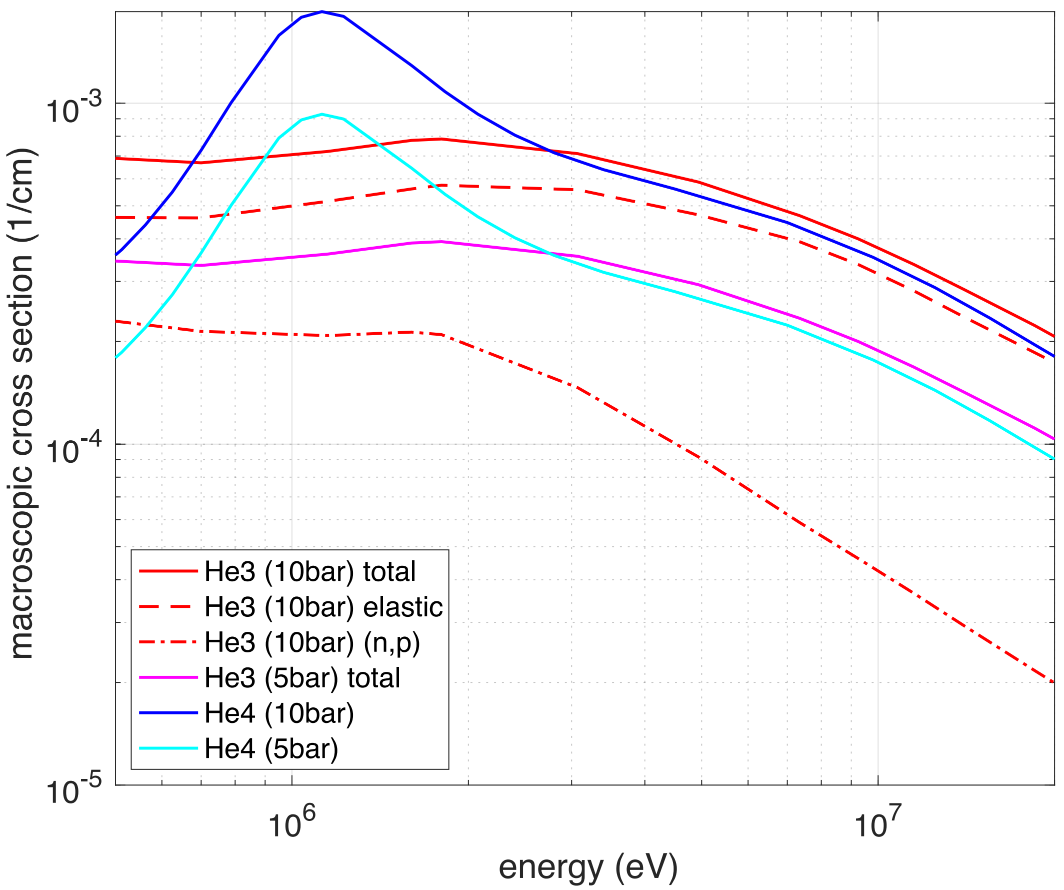

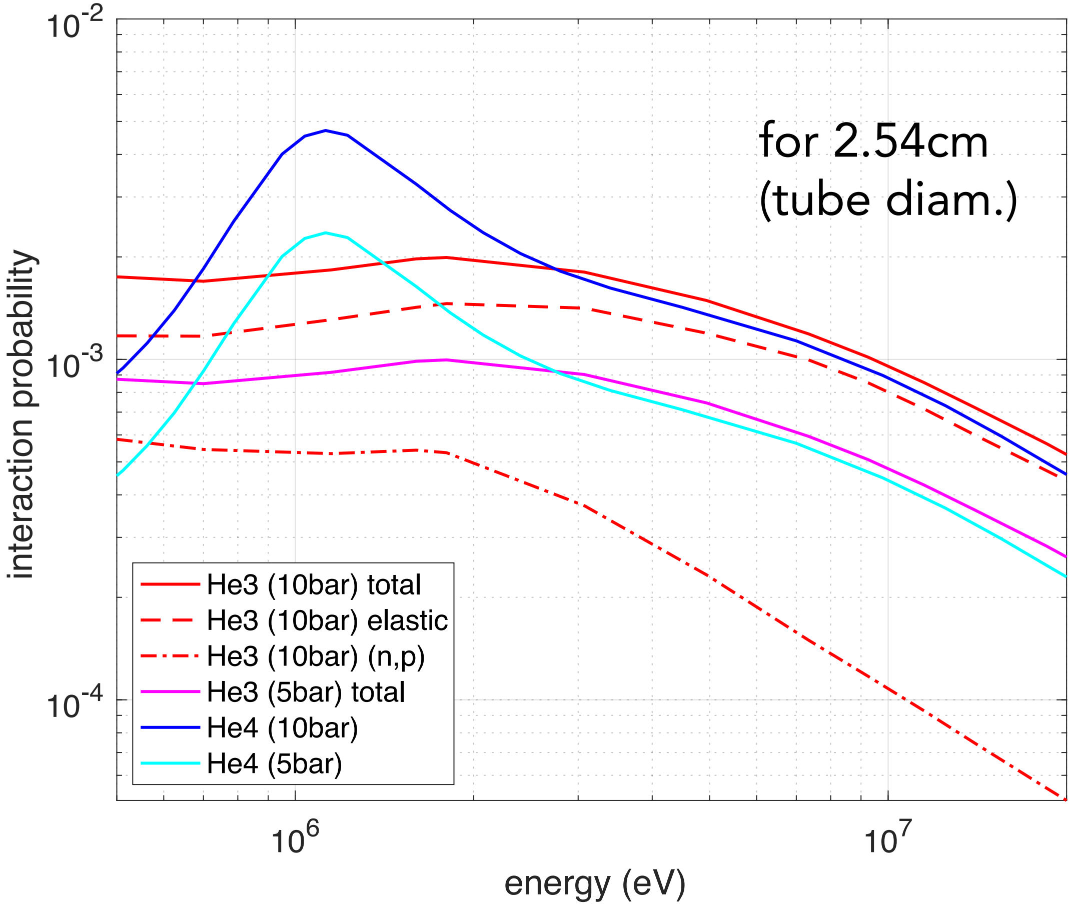

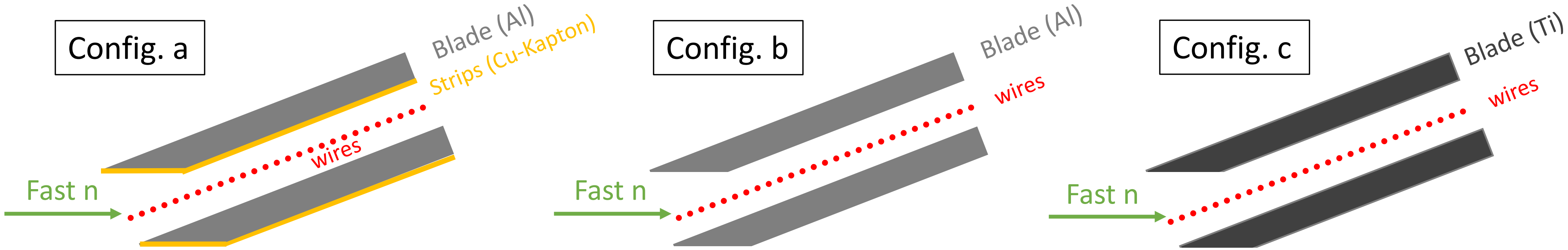

SCATTERING INTERACTION

ELASTIC

$n + X \rightarrow X + n$

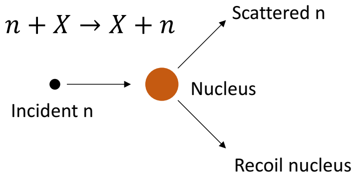

INELASTIC

$n + X \rightarrow X^{*} + n'$

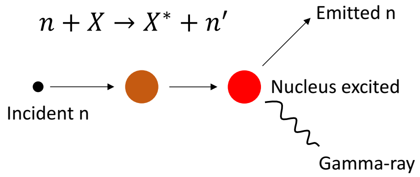

ABSORPTION INTERACTION

$n + X \rightarrow Y + y$

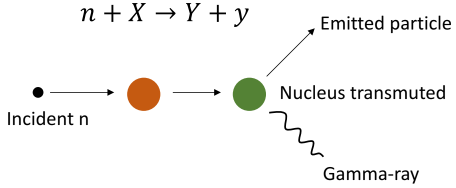

Set-up and Methodology. Background Measurements @ CRISP reflectometer

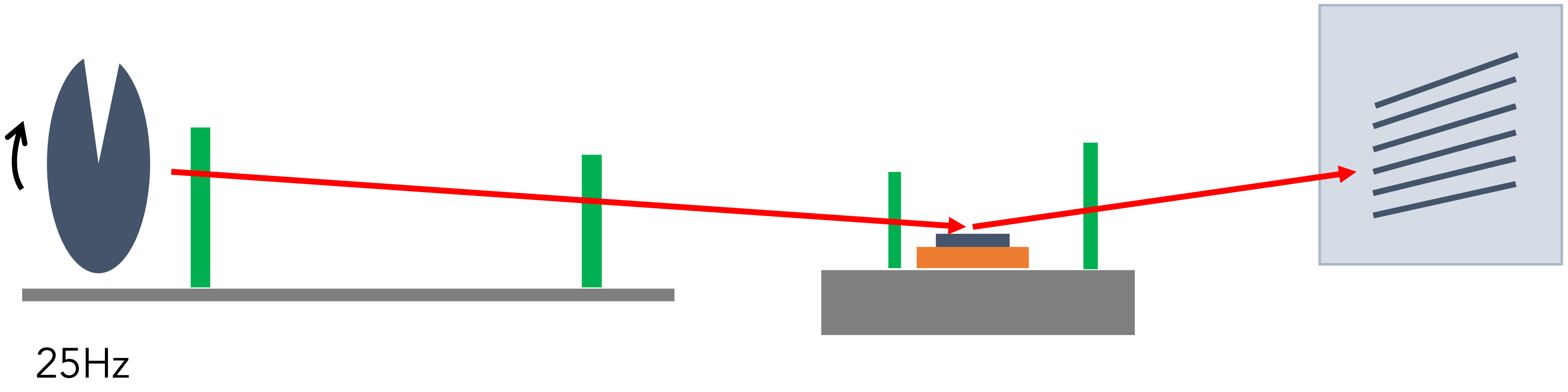

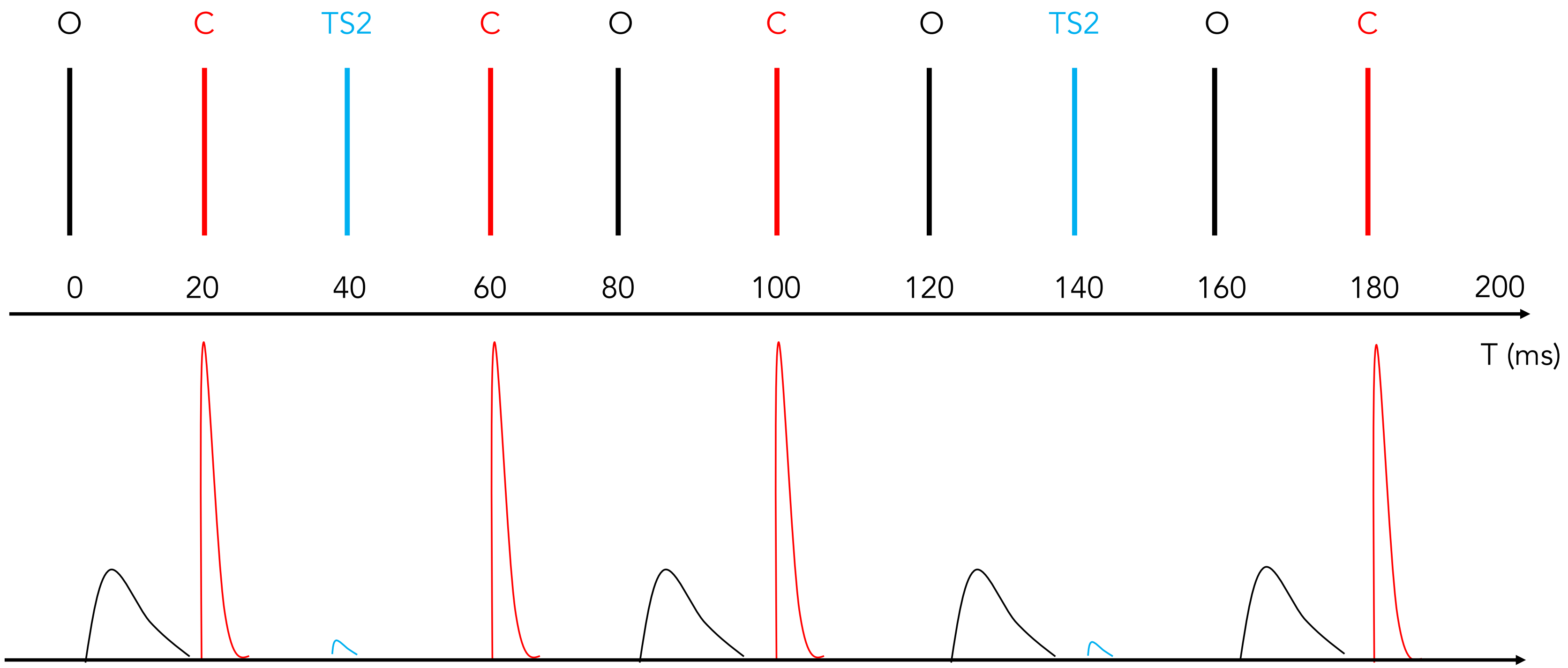

Spectrum sketch scenarios:

1. O: chopper in phase with the proton pulse. Beam passes through the chopper

2. C: chopper not in phase with the proton pulse. Neutron beam hits the chopper

3. TS2: 1 every 5 pulse is sent to Target Station 2

Measurements & Calculation. Background Measurements @ CRISP reflectometer

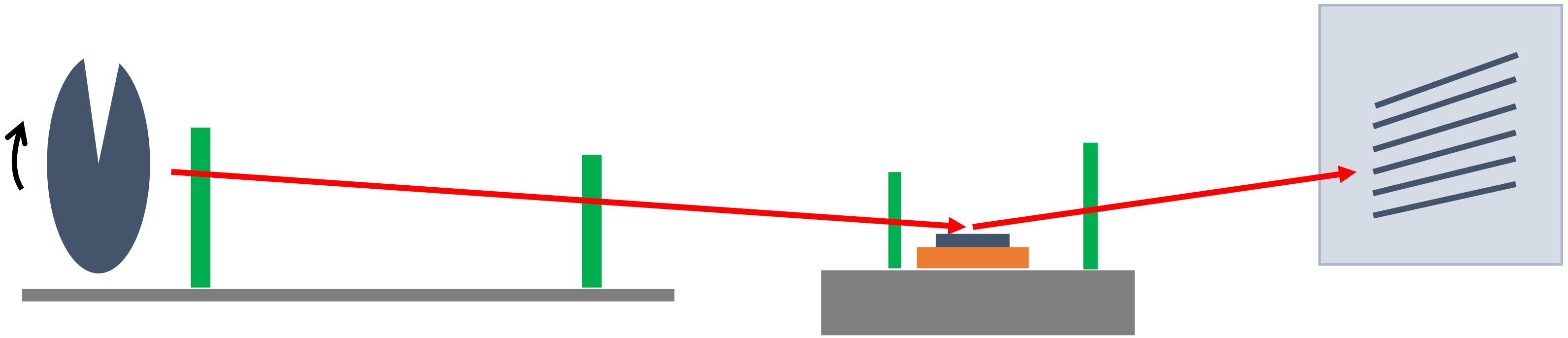

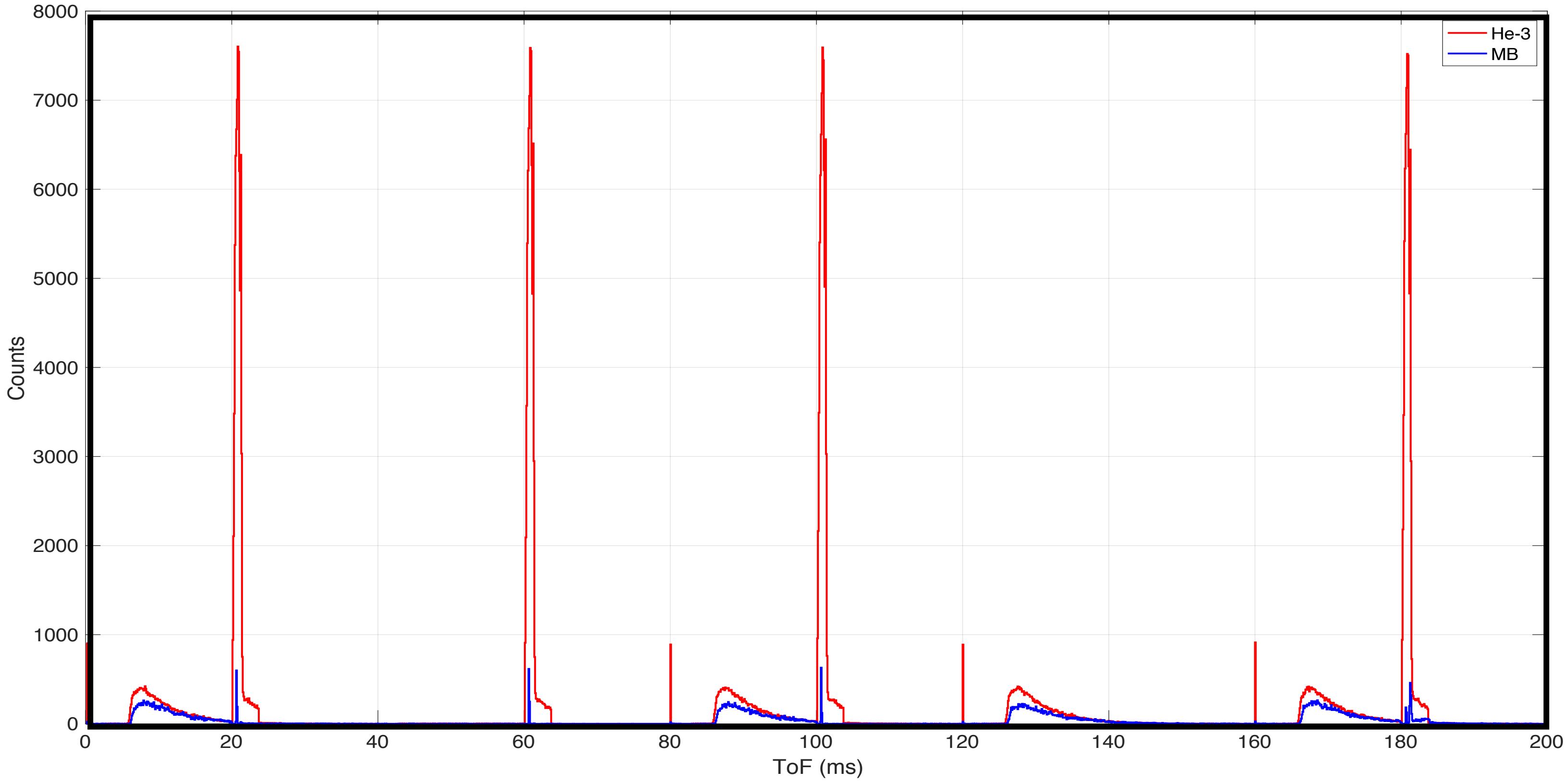

Spectrum region of interest:

1. (T): Φ total flux integrated in the full spectrum t = 0-200 ms

2. (O): Φ_{tn} thermal flux integrated in t = 120-160 ms

3. (C): Φ_{p} background flux integrated in t = 100-105 ms

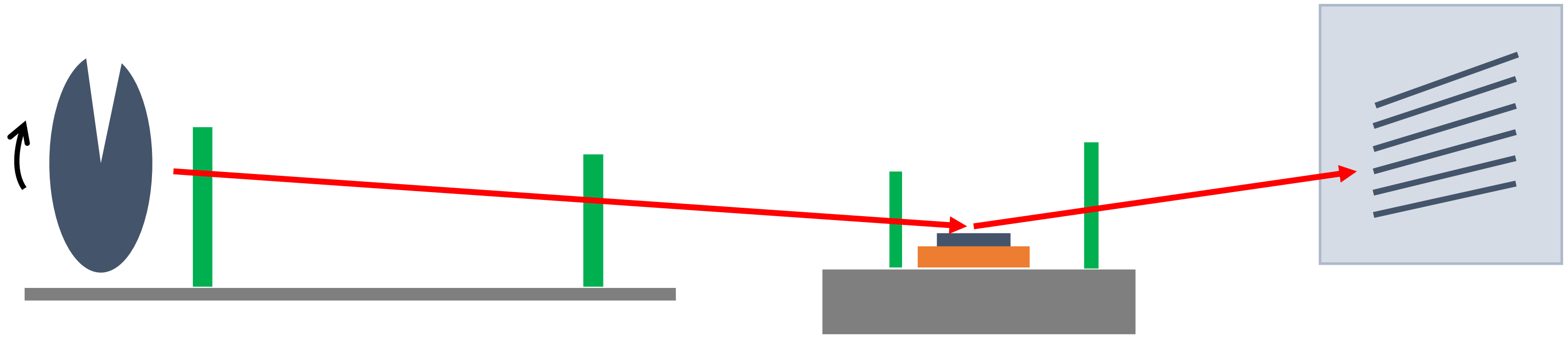

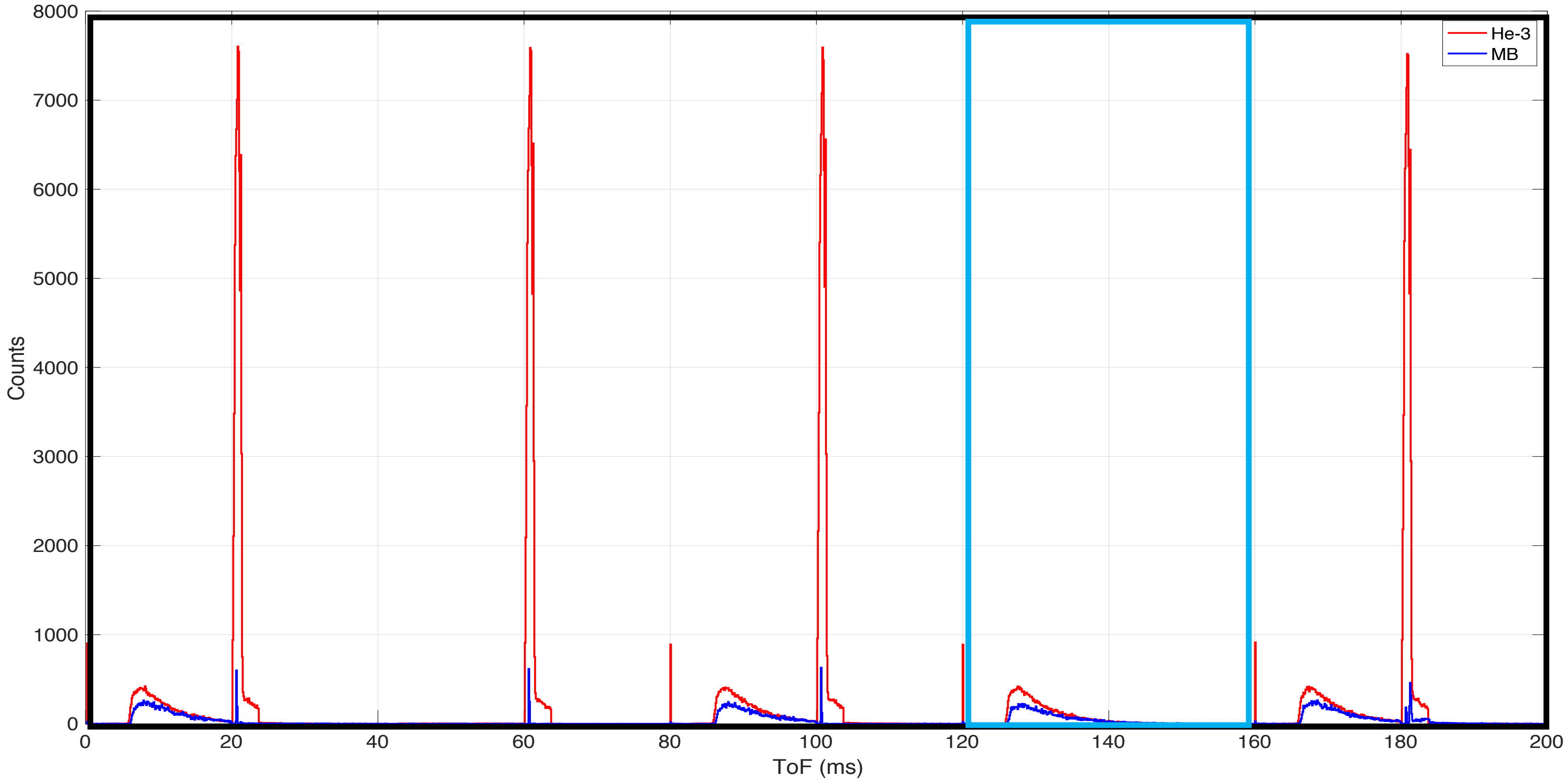

Spectrum region of interest:

1. (T): $\mathbf{\Phi}$ total flux integrated in the full spectrum t = 0-200 ms
2. (O): $\mathbf{\Phi}_{tn}$ thermal flux integrated in t = 120-160 ms
3. (C): $\mathbf{\Phi}_{p}$ background flux integrated in t = 100-105 ms

Measurements & Calculation. Background Measurements @ CRISP reflectometer

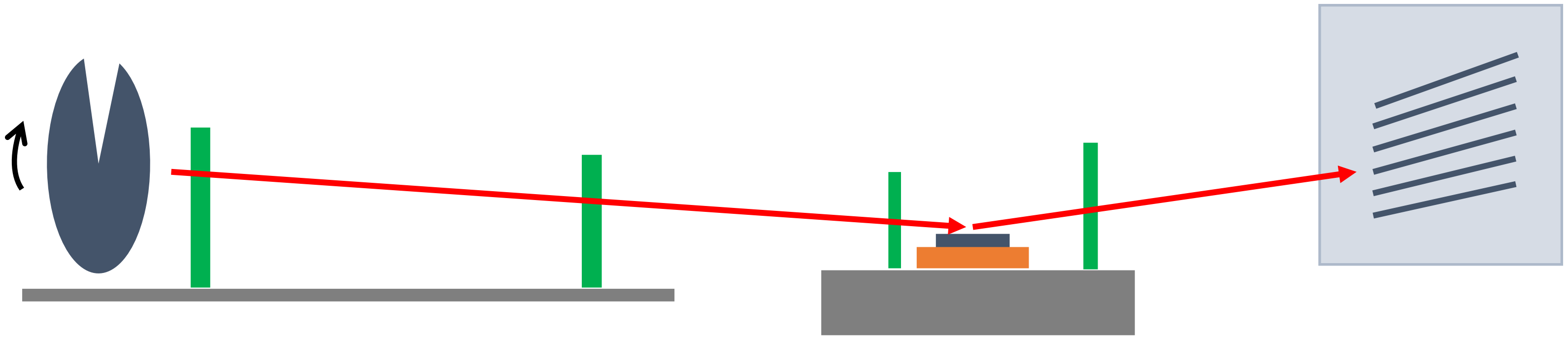

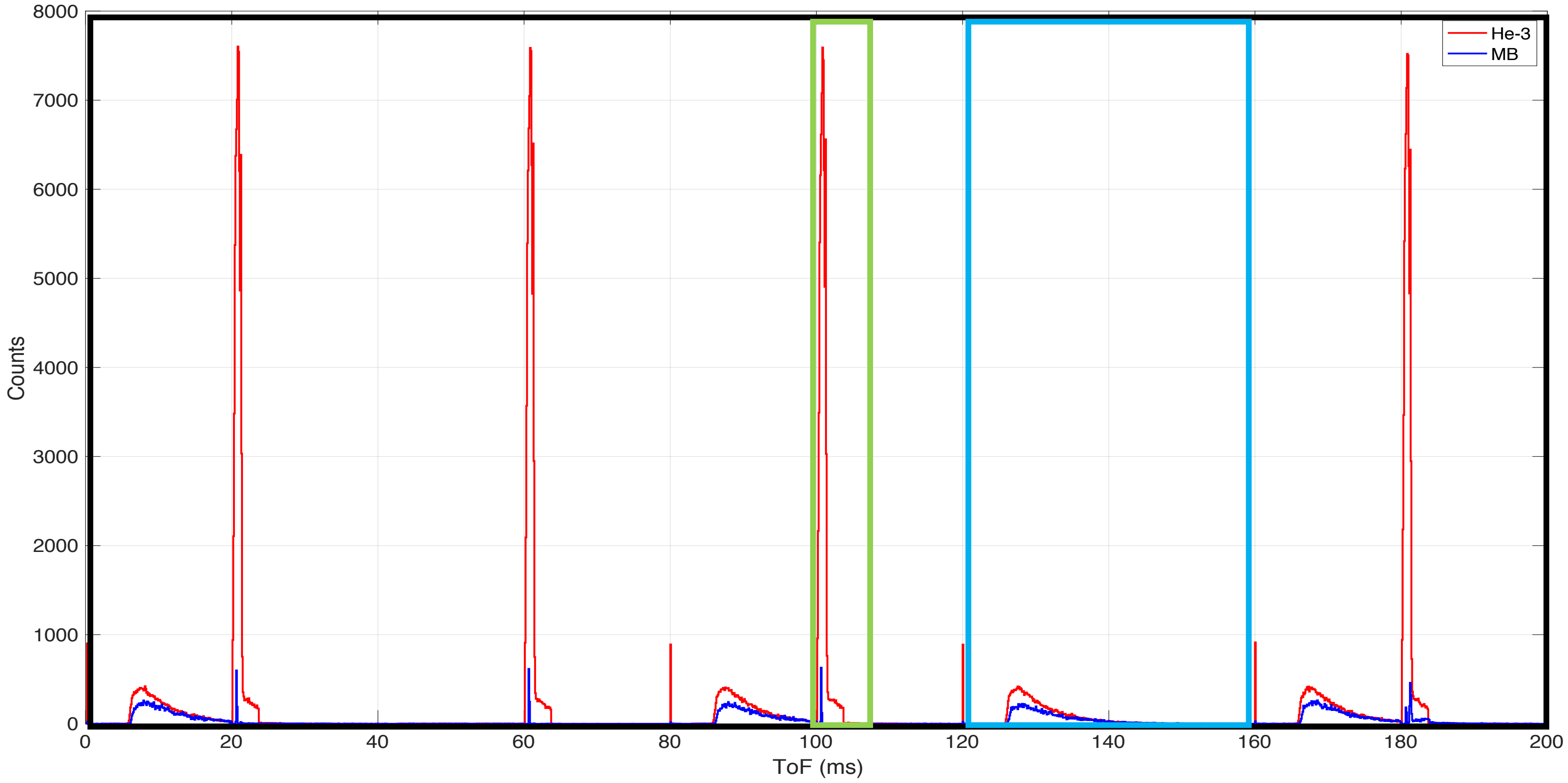

Spectrum region of interest:

1. (T): Φ total flux integrated in the full spectrum t = 0-200 ms
2. (O): Φ_{tn} thermal flux integrated in t = 120-160 ms
3. (C): Φ_{p} background flux integrated in t = 100-105 ms

Measurements & Calculation. Background Measurements @ CRISP reflectometer

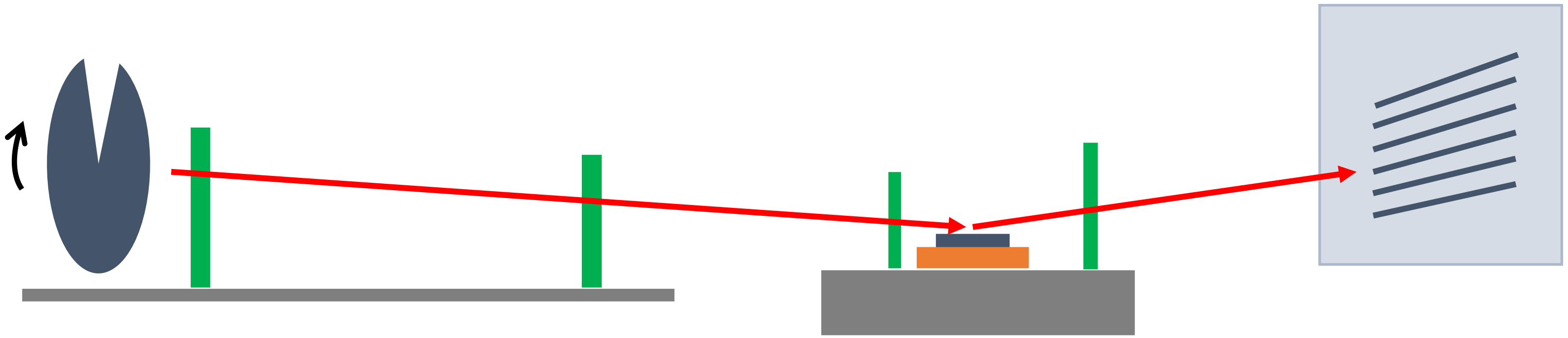

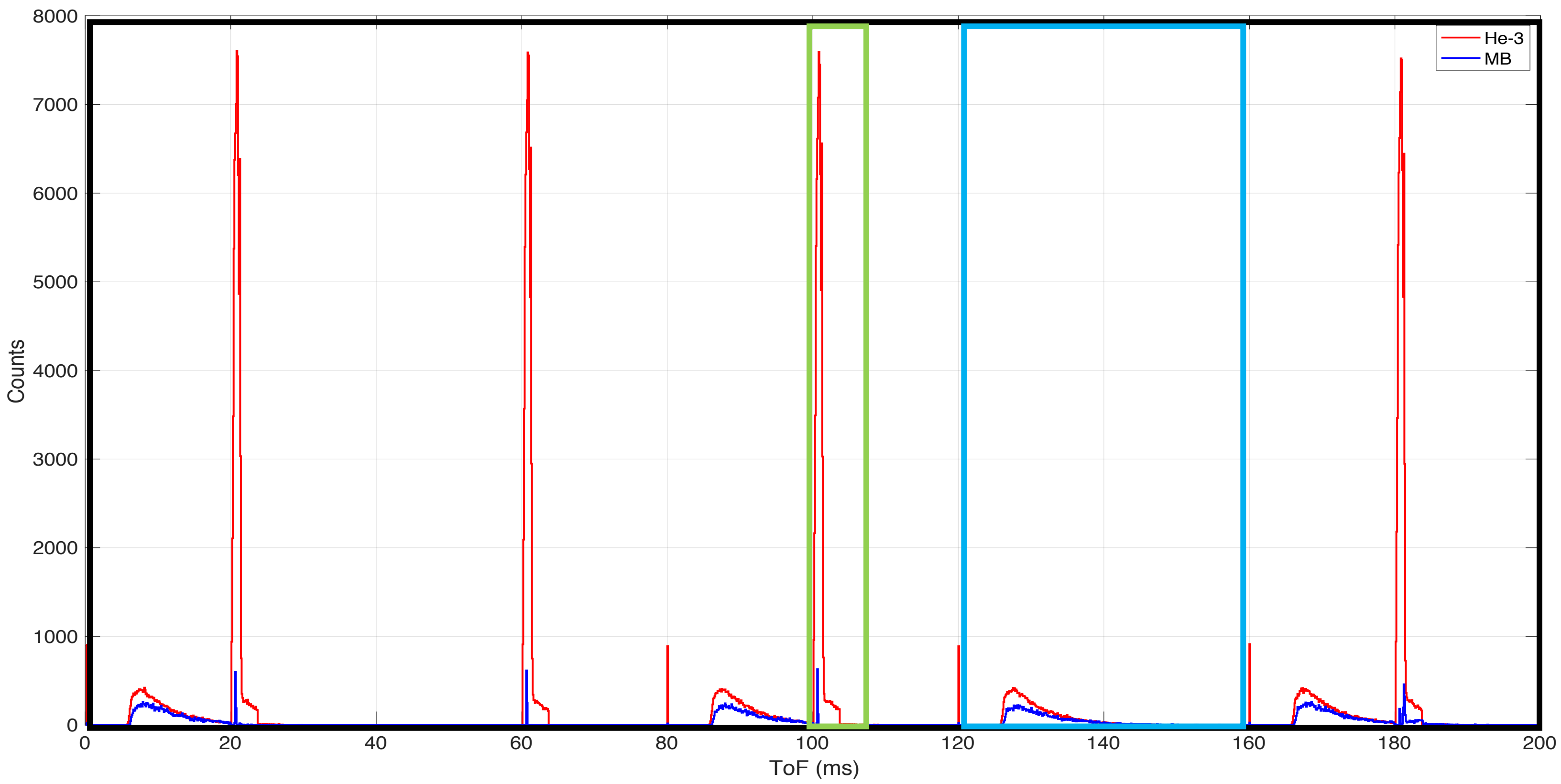

Indirect calculation

$$\Phi_i^{MB} : \epsilon_i^{MB} = \Phi_i^{He} : \epsilon_i^{He}$$

$$\epsilon_i^{He} = \frac{\Phi_i^{He} * \epsilon_i^{MB}}{\Phi_i^{MB}}$$

Calculated fast neutron flux

$$\Phi_{fn} = \frac{\Phi - (4 * \Phi_{tn})}{4} \sim \Phi_p$$

Measurements & Calculation. Background Measurements @ CRISP reflectometer

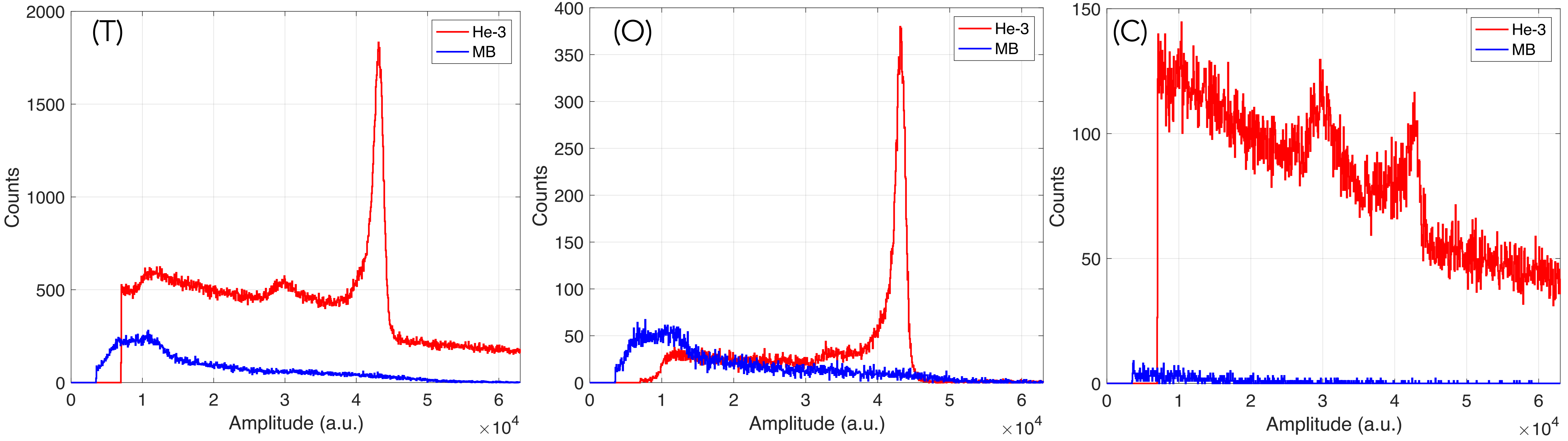

	Φ	Φ_{tn}	Φ_p	Φ_{fn}
MB	$6.6\cdot10^4 \pm 250$	$1.56\cdot10^4 \pm 120$	870 ± 30	900 ± 140
^{3}He	$3.95\cdot10^5 \pm 600$	$2.45\cdot10^4 \pm 150$	$7.38\cdot10^4 \pm 300$	$7.4\cdot10^4 \pm 200$

$$\epsilon_{tn}^{He} = 0.94 \pm 0.09$$

$$\epsilon_{fn}^{He} = 1.2 \cdot 10^{-3} \pm 6 \cdot 10^{-4}$$

GAMMA-RAY BACKGROUND

Source	*x*- or *γ*-ray, keV	intensity, %
^{133}Ba	31	96.1
	35	17.3
	81	32.9
	276	7.2
	303	18.3
	356	62.0
	384	9.8
^{60}Co	1173	99.8
	1332	100
^{137}Cs	32	5.6
	662	85.1

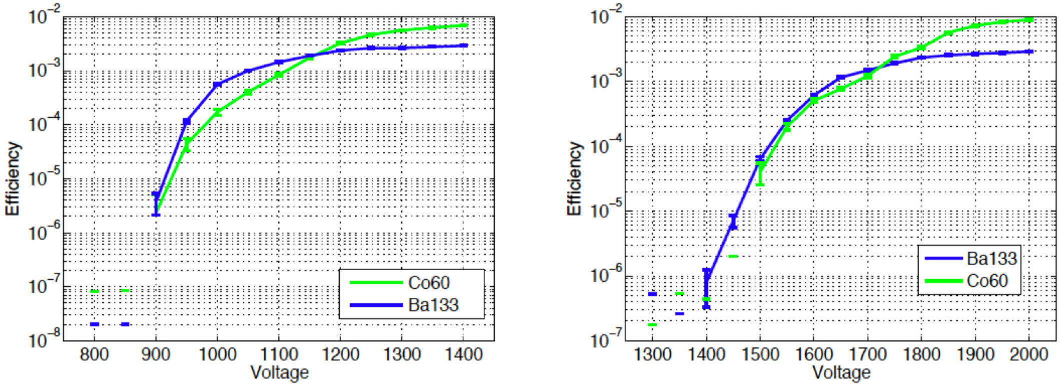

Figure 7: Plateau measurements with the Multi-Grid ^{10}B detector (left) and a Multi-Tube ^{3}He detector (right) with ^{133}Ba (200 kBq) and ^{60}Co (25 kBq) γ-ray sources. Detection efficiency per tube is shown. The nominal operating voltages are 850V and 1350V respectively. The disconnected points at the left ends of the curves are upper limits, where no statistically-significant counts could be detected over background.

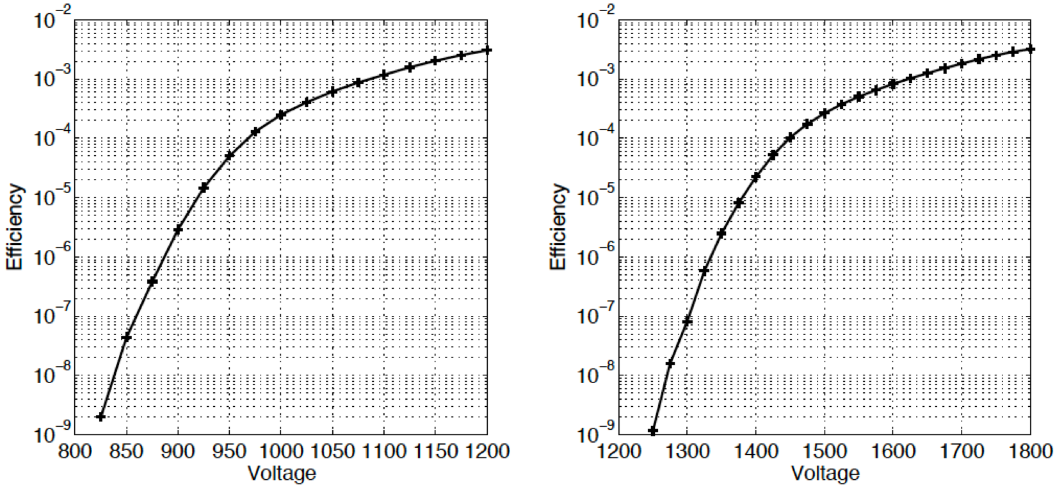

Figure 8: Plateau measurement with the Multi-Grid ^{10}B detector (left) and a Multi-Tube ^{3}He detector (right) with a 164 MBq ^{137}Cs source.

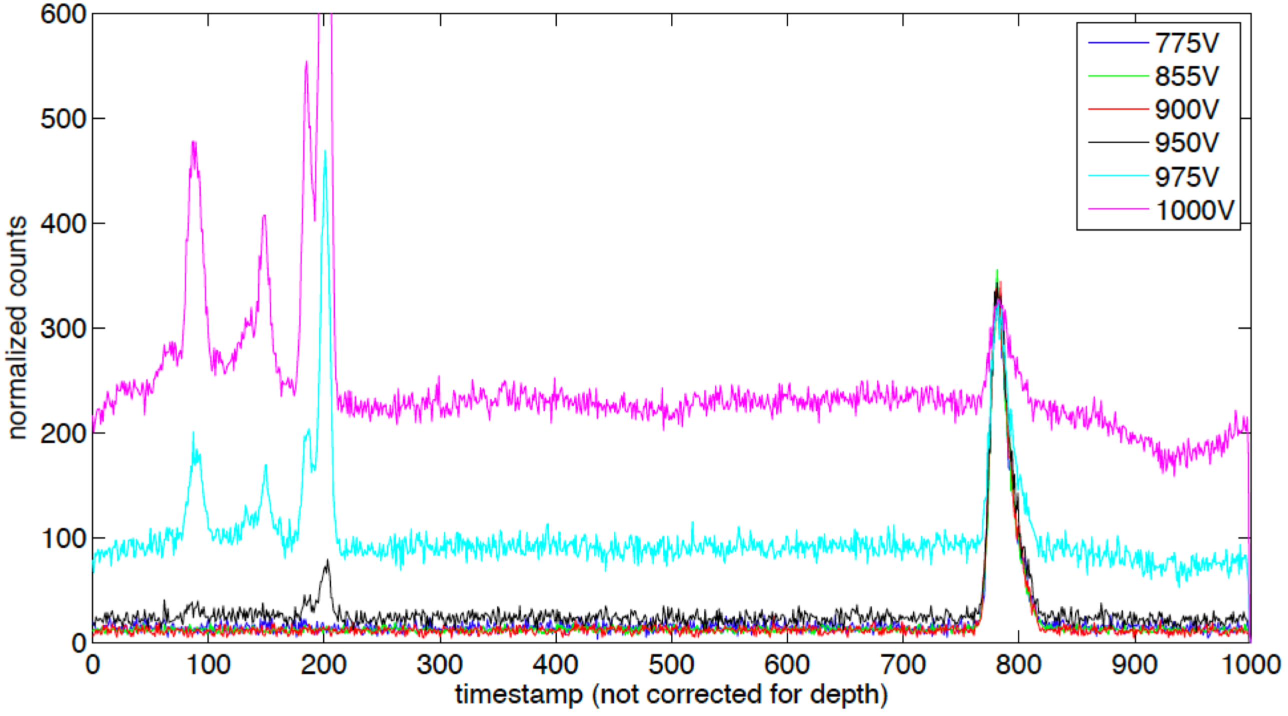

Figure 10: Time spectrum of the ^{10}B prototype for a range of bias voltages. No evidence of the γ-peaks is visible until the voltage reaches 950V. The peak at the channel numbers 770-810 is the elastic neutron peak. Note that no timing correction for the depth of the detector was performed here, since it cannot be done in a consistent way for both γ and n at the same time – and here we are interested in γ – therefore the neutron peak appears wider than it normally would.

JINST
PUBLISHED BY IOP PUBLISHING FOR SISSA MEDIALAB
RECEIVED: *June 27, 2013*
REVISED: *September 27, 2013*
ACCEPTED: *October 21, 2013*
PUBLISHED: *October 28, 2013*

Investigation of gamma-ray sensitivity of neutron detectors based on thin converter films

A. Khaplanov,[a,b,1] F. Piscitelli,[b,c] J.-C. Buffet,[b] J.-F. Clergeau,[b] J. Correa,[b] P. van Esch,[b] M. Ferraton,[b] B. Guerard[b] and R. Hall-Wilton[a]

[a] *European Spallation Source, P.O Box 176, SE-22100 Lund, Sweden*
[b] *Institute Laue Langevin, Rue Jules Horowitz, FR-38042 Grenoble, France*
[c] *University of Perugia, Piazza Università 1, 06123 Perugia, Italy*

E-mail: Anton.Khaplanov@esss.se

ABSTRACT: Currently, many detector technologies for thermal neutron detection are in development in order to lower the demand for the rare ^{3}He gas. Gas detectors with solid thin film neutron converters readout by gas proportional counter method have been proposed as an appropriate choice for applications where large area coverage is necessary. In this paper, we investigate the probability for γ-rays to generate a false count in a neutron measurement. Simulated results are compared to measurement with ^{10}B thin film prototypes and a ^{3}He detector. It is demonstrated that equal γ-ray rejection to that of ^{3}He tubes is achieved with the new technology. The arguments and results presented here are also applicable to gas detectors with converters other than solid ^{10}B layers, such as ^{6}Li layers and $^{10}BF_3$ gas.

KEYWORDS: Gaseous detectors; Neutron detectors (cold, thermal, fast neutrons); Detector modelling and simulations I (interaction of radiation with matter, interaction of photons with matter, interaction of hadrons with matter, etc)

ARXIV EPRINT: 1306.6247

[1] Corresponding author.

doi:10.1088/1748-0221/8/10/P10025

2013 JINST 8 P10025

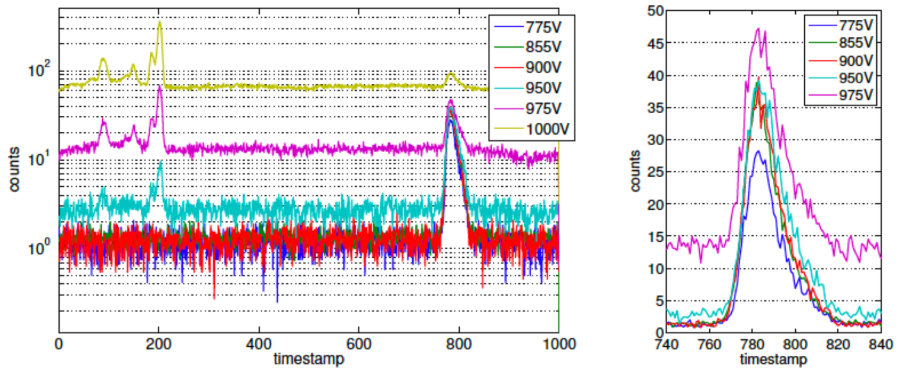

Figure 10. *Left:* time spectrum of the ^{10}B prototype for a range of bias voltages. No evidence of the γ-peaks is visible until the voltage reaches 950 V. The peak at the channel numbers 770–810 is the elastic neutron peak. *Right:* detail of the neutron peak in linear scale. Note the reduced height of the peak at the lowest voltage is due to reduced neutron efficiency. No timing correction for the depth of the detector was performed here, since it cannot be done in a consistent way for both γ and n at the same time — and here we are interested in γ — therefore the neutron peak appears wider than it normally would.

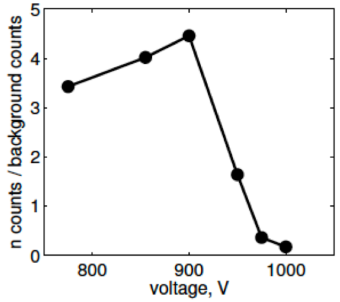

Figure 11. Evolution of the ratio of the neutron signal in the elastic peak to background corresponding to the largest γ peak.

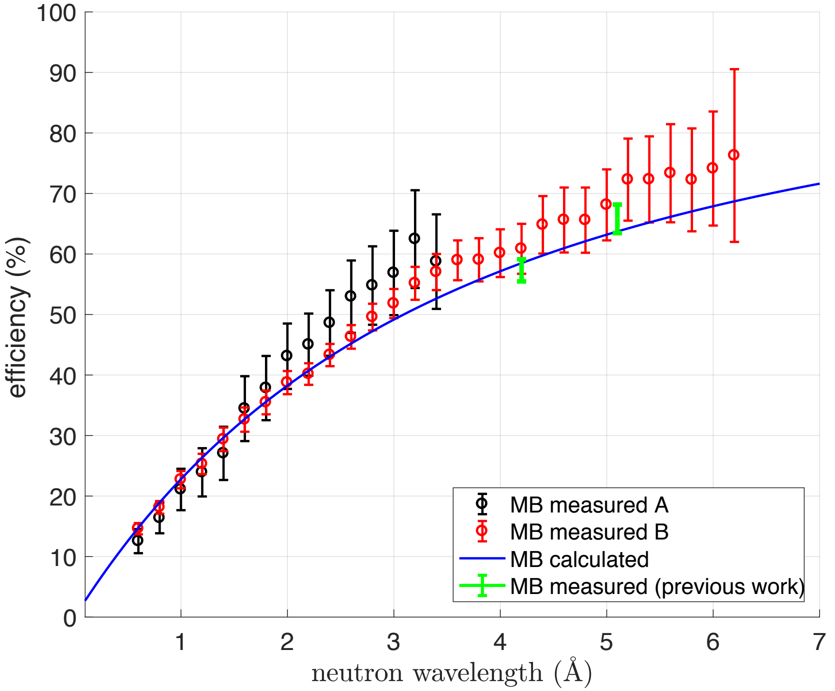
100
90
80
70
60
50
40
30
20
10
0
efficiency (%)
1
2
3
4
5
6
7
neutron wavelength (Å)
MB measured A
MB measured B
MB calculated
MB measured (previous work)